NUREG/IA-0001

International Agreement Report

Assessment of TRAC-PD2 Using SUPER CANNON and HDR Experimental Data

Office of Nuclear Regulatory Research
U.S. Nuclear Regulatory Commission
Washington, D.C. 20555

August 1986

NOTICE

This report was prepared under an international cooperative agreement for the exchange of technical information. Neither the United States Government nor any agency thereof, or any of their employees, makes any warranty, expressed or implied, or assumes any legal liability or responsibility for any third party's use, or the results of such use, of any information, apparatus product or process disclosed in this report, or represents that its use by such third party would not infringe privately owned rights.

Available from

Superintendent of Documents
U.S. Government Printing Office
P.O. Box 37082
Washington, D.C. 20013-7082

and

National Technical Information Service
Springfield, VA 22161

NUREG/IA-0001

International Agreement Report

Assessment of TRAC-PD2 Using SUPER CANNON and HDR Experimental Data

Prepared by
U. Neumann

Kraftwerk Union
Hammerbacherstr. 12+14
Postfach 3220
8520 Erlangen, The Federal Republic of Germany

Office of Nuclear Regulatory Research
U.S. Nuclear Regulatory Commission
Washington, D.C. 20555

August 1986

Prepared as part of
The Agreement on Research Participation and Technical Exchange
Between the United States Nuclear Regulatory Commission (USNRC)
and the Federal Minister for Research and Technology of the Federal
Republic of Germany (BMFT) in USNRC Thermal Hydraulic Research
Programs and BMFT Thermal Hydraulic Research Programs

NOTICE

This report documents work performed under the sponsorship of the Kraftwerk Union in the Federal Republic of Germany. The information in this report has been provided to the USNRC under the terms of an information exchange agreement between the United States and the Federal Republic of Germany (Technical Exchange and Cooperation Arrangement Between the United States Nuclear Regulatory Commission and the Bundesminister Fuer Forschung und Technologie of the Federal Republic of Germany in the field of reactor safety research and development, April 30, 1981). The Kraftwerk Union has consented to the publication of this report as a USNRC document in order that it may receive the widest possible circulation among the reactor safety community. Neither the United States Government nor the Kraftwerk Union or any agency thereof, or any of their employees, makes any warranty, expressed or implied, or assumes any legal liability of responsibility for any third party's use, or the results of such use, of any information, apparatus, product or process disclosed in this report, or represents that its use by such third party would not infringe privately owned rights.

ABSTRACT

This report assesses the predictive capabilities of the Transient Reactor Analysis Code (TRAC-PD2) using data from the SUPER CANON and HEISS DAMPF REACTOR (HDR) experimental facilities. The report is divided into three parts. Part I is the TRAC-PD2 assessment using SUPER CANON data. Part II is the TRAC-PD2 assessment using HDR data. Part III provides recommendations for the user using the combined assessment results. In general, it is shown that the TRAC-PD2 predictions were in good agreement with the actual test pressures and and mass flow rates for both these tests. TRAC-PD2 provided considerably better results than TRAC-P1A. This was particularly true with regard to sound velocity predictions which play a significant role whenever the speed of pressure relief waves must be determined.

TABLE OF CONTENTS

		Page
ABSTRACT		iii
PART I:	TRAC-PD2 RECALCULATION OF THE SUPER CANON EXPERIMENT	
1.	Introduction	2
2.	Recalculation of the Results from Los Alamos	2
3.	TRAC-PD2 Calculation with 120 Zones	4
4.	Computer Time and Computer Costs	6
	References	8
PART II:	PARAMETRIC STUDY OF TRAC-PD2 USING THE HDR TEST RESULTS	
1.	Introduction	3
2.	Parameter study for the HDR tests	3
2.1	HDR 1/3 initial calculation	4
2.2	HDR 2/3 automatic boiler connection	5
2.3	HDR 3/3 automatic boiler connection with nozzle	7
2.4	HDR 4/5 and HDR 5/4	8
3.	Discussion of the Results	9
4.	References	10

PART III: RECOMMENDATION FOR THE APPLICATION OF TRAC-PD2 TO SHORT TERM TRANSIENTS

		Page
1.	Introduction	3
2.	Automatic Calculation of Pressure Loss Coefficients for Contraction or Enlargement	4
3.	Parameter Study on HDR Tests	9
3.1	HDR 1/3 Initial Test Calculation	16
3.2	HDR 2/3 Automatic Vessel Junction	23
3.3	HDR 3/3 Automatic Vessel Junction with Nozzle	29
3.4	HDR 4/5 Vessel Junction	35
3.5	HDR 5/4 Vessel Junction without Loss Coefficient	41
3.6	HDR 6/5 Vessel Junction with Bypass in Blowdown Nozzle	47
3.7	Summary of the Results from HDR Computations	53
4.	TRAC Components	54
4.1	Trip Data	54
4.2	BREAK	55
4.3	TEE	56
4.4	STEAM GENERATOR	57
4.5	VESSEL	60
4.6	PUMP	63
5.	General TRAC Instructions	65
	References	66

PART I: TRAC-PD2 RECALCULATION OF THE SUPER CANON EXPERIMENT

Part I

Translated By: TECHTRAN Corporation
P.O. Box 729
Glen Burnie, MD 21061

This page intentionally left blank.

1. Introduction

Recalculations of various tests with the old TRAC-P1A version showed that the pressure relief process proceeded 1.5 times faster than would have been expected from experimental results.

For this reason the SUPER CANON EXPERIMENT was the first to be recalculated with the new TRAC-PD2 version.

This involves a horizontal pipe (Fig. 1.1) which is filled with subcooled water. The rupture opening time, which is less than 1 msec, is attained by igniting a small explosive charge which destroys the rupture disk at the end of the pipe.

For the recalculations carried out with the TRAC-PD2 program, the following conditions were taken as the basis:

Initial pressure	150 bar
Initial temperature	300°C
Initial steam content	x = 0

Rupture opening area, full cross-section

Outlet pressure decreases to instantaneous critical pressure

Seven computer runs are carried out, in which the effects of discretization and time step width are determined.The calculated sound velocities are compared with the theoretical tabular values. In addition, the computation costs and computer time are discussed as a function of the precision of the results.

2. Recalculation of the Results from LOS ALAMOS

During the TRAC workshop held from 2/3 to 2/7/80 at LOS ALAMOS, Mr. Hughes carried out a simple calculation of the SUPER CANON EXPERIMENTS with the TRAC-PD2 version. The results were brought to the meeting in the form of a plot figure (Fig. 2.1). With the first three calculations, an attempt was therefore made to complete this curve after the fact. Handwritten documents

from Mr. Hughes provided the following geometric input data for the pipe:

Length L	4.0 m (divided up to 20 zones of 0.2 m each)
Diameter D	0.1 m

From Figure 2.1 the sound velocity with L = 3.9 m (length from the open end to the midpoint of zone 20) and the transit time which can be read off (curve Z 20) T = 0.00349 sec is calculated at w = 1117.4 m/sec. At 150 bar and 300°C, the homogeneous, isentropic sound velocity is $w_{hom,\ isentr.}$ = 952.37 m/sec. The deviation from this value is approximately 17.3% and can be regarded as quite acceptable. Table 2.1 gives the recalculations with their input data and results.

TABLE 2.1 RESULTS OF THE RECALCULATIONS

	TRAC	Zones	T	w	Deviation in % from $w_{hom,\ isentr.}$	Figure
LOS ALAMOS	PD2	20	-	1117.	17.3	2.1
1st recalculation	PD2	20	2×10^{-4}	1274.	33.7	2.2-2.4
2nd recalculation	PD2	20	1×10^{-4}	1181.	24.0	2.5-2.6
3rd recalculation	PD2	20	1×10^{-5}	1048.	10.0	2.7-2.9

Since the time step for the calculation for LOS ALAMOS is not known, from the comparisation of the results it can only be assumed that it must be less than 1×10^{-4}. The results from Table 2.1 indicate that, as the maximum time step decreases in size, the sound velocity coincides better and better with the tabular value. This relationship is verified by the fact that the TRAC program per se uses a completely implicit procedure which calculates the time step width ΔT from the following equation:

$$\Delta T = \left| \frac{\Delta x}{v} \right| \qquad 2.1$$

where Δx is the zone length and v is the mixture velocity. In an explicit procedure, however, the time step is also affected by the sound velocity so

that the following equation results:

$$\Delta T = \left| \frac{\Delta x}{v + w} \right| \qquad 2.2$$

where w is the sound velocity. A comparison of the two equations shows that sound velocity is indirectly taken into account by an artificial reduction in the size of the time step and thus the calculation lead to better results. This leads to the conclusion that in the transient region the time step width should never be allowed to exceed 1×10^{-4} in order to ensure that the sound velocity will not deviate by more than 25% from the actual value.

Regarding Figures 2.2 to 2.11, it can also be stated that they contain all the curves with which the sound velocities in Table 2.1 were calculated.

Curves 2.4 and 2.9 represent profile plots. They were plotted by Dr. Sueveges using a subroutine in the DEGAS plot program. The pipe length is plotted on the x-axis; here the open end of the pipe is at 4.389 m (on the right in the figure). In the case the profile plots provide instantaneous pictures (snapshots) which depict the pressure variation at a certain point in time (1 msec, 2 msec, 3 msec, 4 msec, etc.) over the length of the pipe.

3. TRAC-PD2 Calculation with 120 Zones

These calculations were carried out in order to consider the effect of discretization and, on the other hand, to verify the dependency of the computation precision on the time step width.

TABLE 3.1 RESULTS OF THE 120 ZONE CALCULATIONS

	TRAC	Zones	T	w	Deviation in % from $w_{hom,isentr.}$	Figure
4th recalculation	PD2	120	1×10^{-4}	1583.	66.3	3.1-3.7
5th recalculation	PD2	120	1×10^{-4}	1174.	23.3	3.8-3.11
6th recalculation	PD2	120	5×10^{-5}	1106.	16.1	3.12-3.17
7th recalculation	PD2	120	1×10^{-5}	1016.	6.68	3.18-3.20

The results summarized in Table 3.1 clearly substantiate the assumption that as the size of the time step width is decreased further, the sound speed coincides better with the tabular value. In this process discretization plays a subordinate role, as is clear from comparing Table 2.1 with Table 3.1 with the same time step width. The smaller zone division provides an improvement in the results of only approximately 1-3%. The most important thing recognized, however, is that, in comparison with the old P1A version, the new TRAC-PD2 version provides almost satisfactory results in the calculation of sound velocity. A comparison of recalculations 4 and 5 shows this quite clearly. Therefore Figures 3.1 to 3.7 each contain one PD2 and one P1A curve as a means of direct comparison.

Figures 3.8 and 3.9 are again profile plots which very clearly show the faster pressure drop in the old TRAC-P1A version.

In addition, Figures 3.14-3.17 contain the results from the SUPER CANON EXPERIMENT and older LECK (leak) calculations [2], which are entered by hand.

Towards the closed end and in the center of the pipe, the deviations from the measured curve (Fig. 3.15 and 3.16) are relatively slight; here both calculations compute the pressure drop too early to the same extent. Only at the open end (Fig. 3.17) is a sharp contrast noted between the LECK and TRAC calculations, to the extent that the TRAC-PD2 curve reflects the measured curve very precisely, while in the first 180 msec the LECK calculation provides a greatly deviating curve plot with an excessively high pressure level.

Figures 3.18-3.20 pertain to the 7th recalculation, which was carried out with a time step of $\Delta T = 1 \times 10^{-5}$ and which provides the best approximation to the actual sound velocity.

4. Computer Time and Computer Costs

Table 4.1 gives the problem time, the computation time and the system seconds for the computation costs as a function of the number of zones and time step widths. The results from Table 2.1 and 3.1 have shown that the precision of the calculations is mainly dependent on the selection of the time step width. Table 4.1 shows that, with the same zone distribution, the computation costs decrease by a factor of f^{T}_{cost} - 7 if the time step is reduced from $\Delta T = 10^{-4}$ sec to $\Delta T = 10^{-5}$ sec. On the other hand, the sound velocity is calculated with fair precision only with a time step of $\Delta T = 10^{-5}$. On the other hand, discretization does not provide significantly better results. When the number of zones is increased by a factor of six, from 20 to 120 zones, the cost factor is approximately $f^{\Delta x}_{cost}$ - 2. One possible conclusion from this would be that an attempt should be made to improve the computation results with greater discretization. This is contradicted, however, by the fact that the storage space of the computer system is not unlimited.

In addition, these limits are reached very quickly with a model in which the vessel components are used, in which case the division of zones just meets the minimum requirements. This means that a true improvement in the computation results can be achieved only with a reduction in the size of the time step width.

In order, however, for the costs to remain within reasonable limits, the time step must be optimized in different periods. The 120 zone calculation which is numbered seven is an example of this.

The TRAC program offers the capability of indicating several time intervals in which the actuating variable is redefined each time. In this case the end of the first time interval is 0.008 sec with a minimum step width of 1×10^{-6} and a maximum step width of 5×10^{-5}. This means that in the highly transient region of the first 8 msec the propagation speed of the pressure relief wave is calculated fairly precisely. In the second time interval, up to 0.2 sec, the time step is set at 1×10^{-4}, and the third time interval up to 0.4 sec the pressure relief process has decayed to such an extent that a time step

of 1×10^{-3} is sufficient. This example shows how important it is to optimize the individual time domains. In this way the calculation cost 10,000 system seconds; if, however, the entire 0.4 sec had been calculated with the step width of 1×10^{-5}, then the costs would probably have risen to more than 100,000 system seconds. For larger calculations it would probably be more worthwhile to start a computer run with a large step width in order to determine the highly transient time intervals for the purpose of then precisely calculating this region in a second run.

Bibliography

1. "TRAC-PD2: An Advanced Best Estimate Computer Program for PWR LOCA Analysis", LOS ALAMOS Scientific Laboratory NUREG/CR-2054

2. Neumann, U., "Recalculation of the SUPER CANON EXPERIMENT Using the LECK Computer Program", KWU Working Report R11/2036/80.

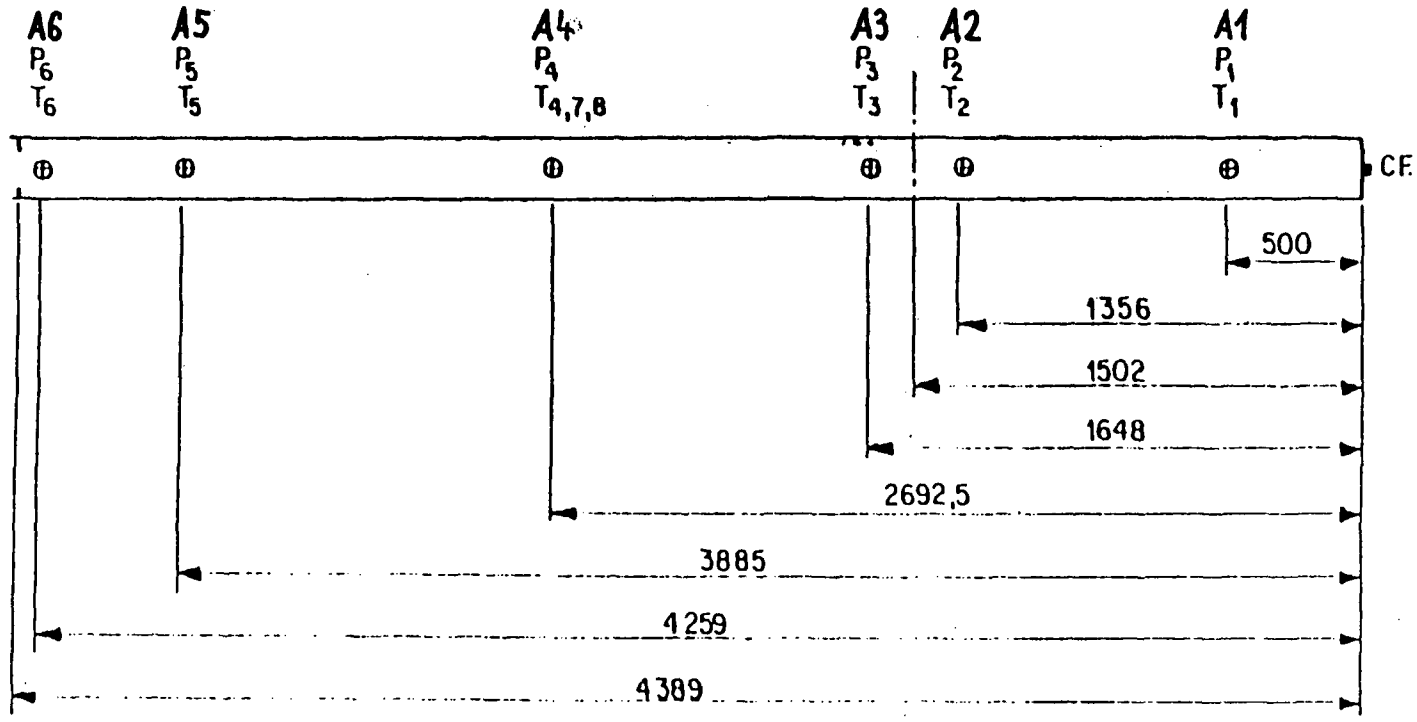

Fig.1: Super_Canon Experiment

Fig. 1.1

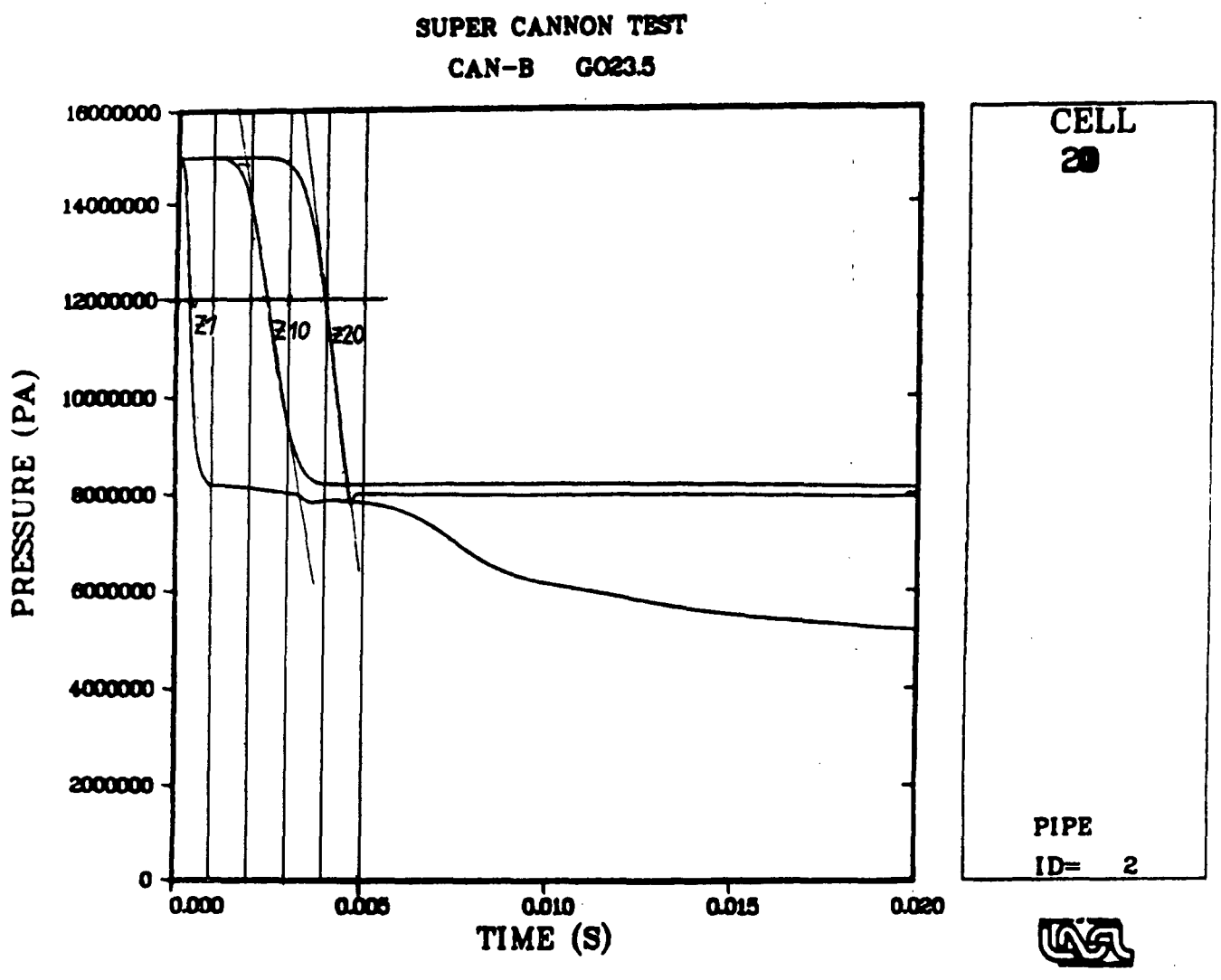

COMPARISON CALCULATION FROM LOS ALAMOS

Fig. 2.1

KWU TRAC - PD2

SUPER CANON EXPERIMENT

COMPARISON WITH LOS ALAMOS

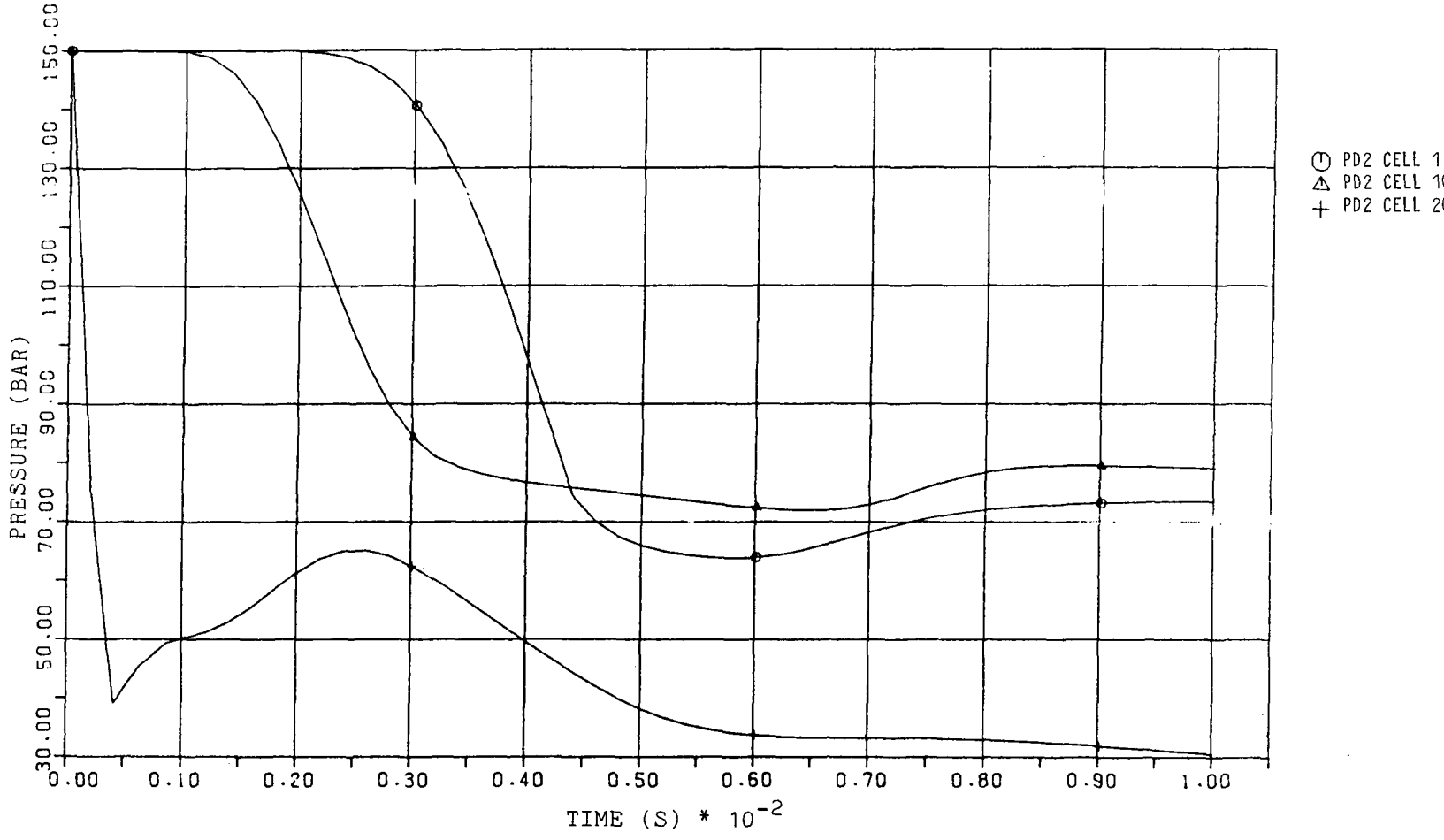

150 BAR / 300 K / 20 CELLS DELT = 1.E-4

Fig. 2.2

KWU TRAC - PD2

SUPER CANON EXPERIMENT

COMPARISON WITH LOS ALAMOS

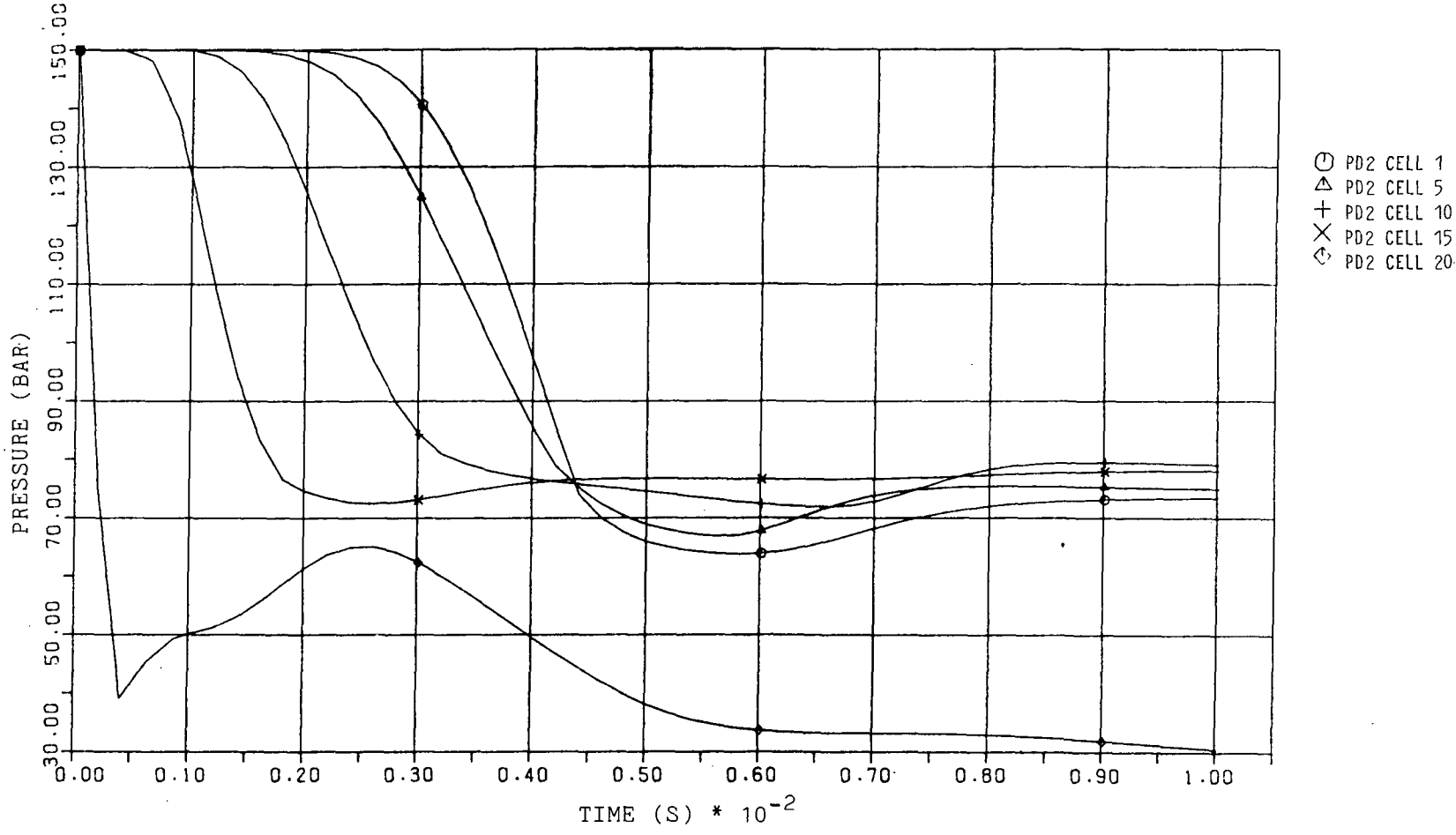

150 BAR / 300 K / 20 CELLS DELT = 1.E-4

Fig. 2.3

KWU TRAC - PD2

SUPER CANON EXPERIMENT

PRESSURE VERSUS AXIAL POSITION

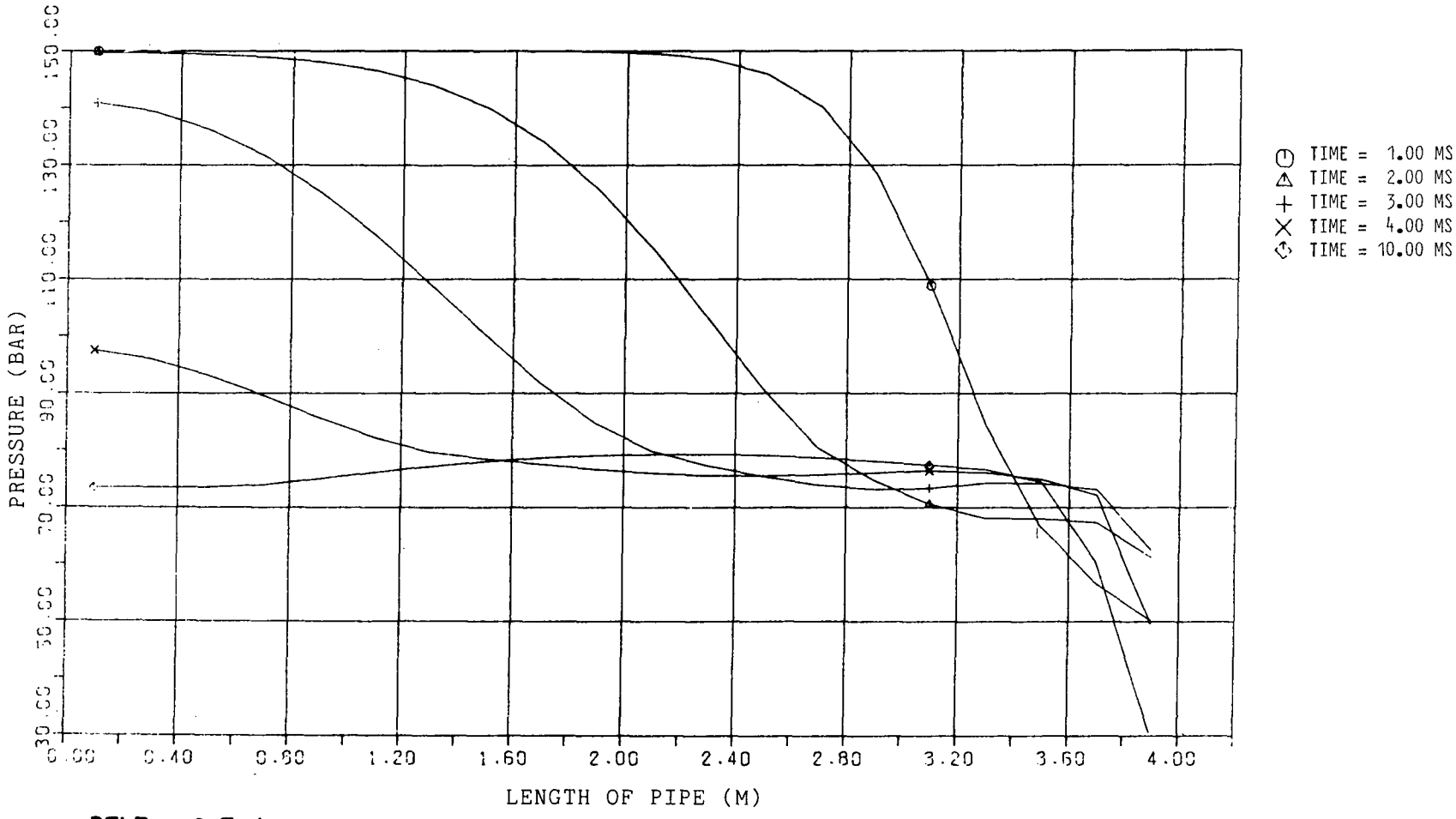

DELT = 2.E-4

Fig. 2.4

KWU TRAC - PD2

SUPER CANON EXPERIMENT

COMPARISON WITH LOS ALAMOS

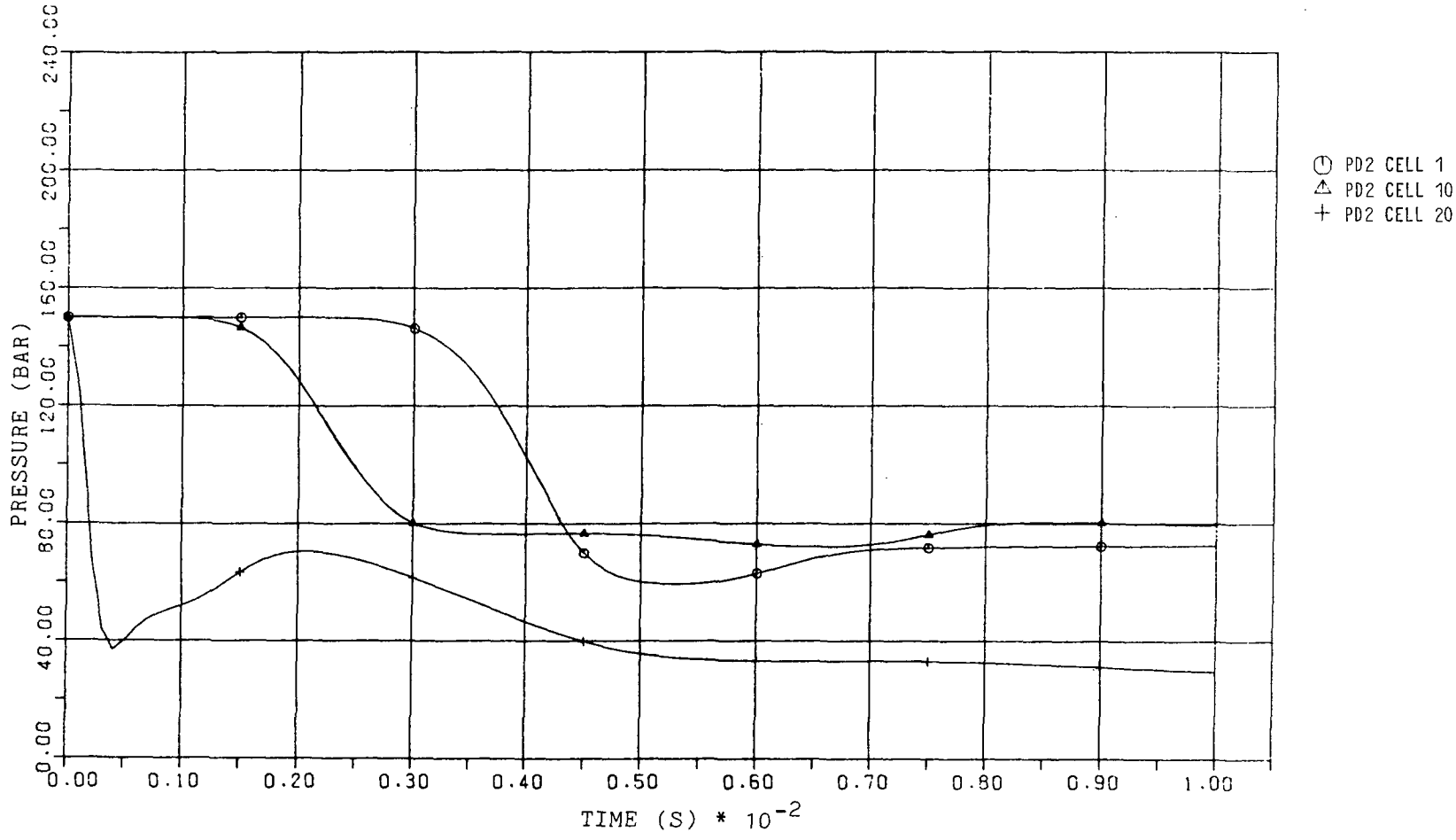

150 BAR / 300 K / 20 CELLS DELT = 1.E-4

Fig. 2.5

KWU TRAC - PD2

SUPER CANON EXPERIMENT

COMPARISON WITH LOS ALAMOS

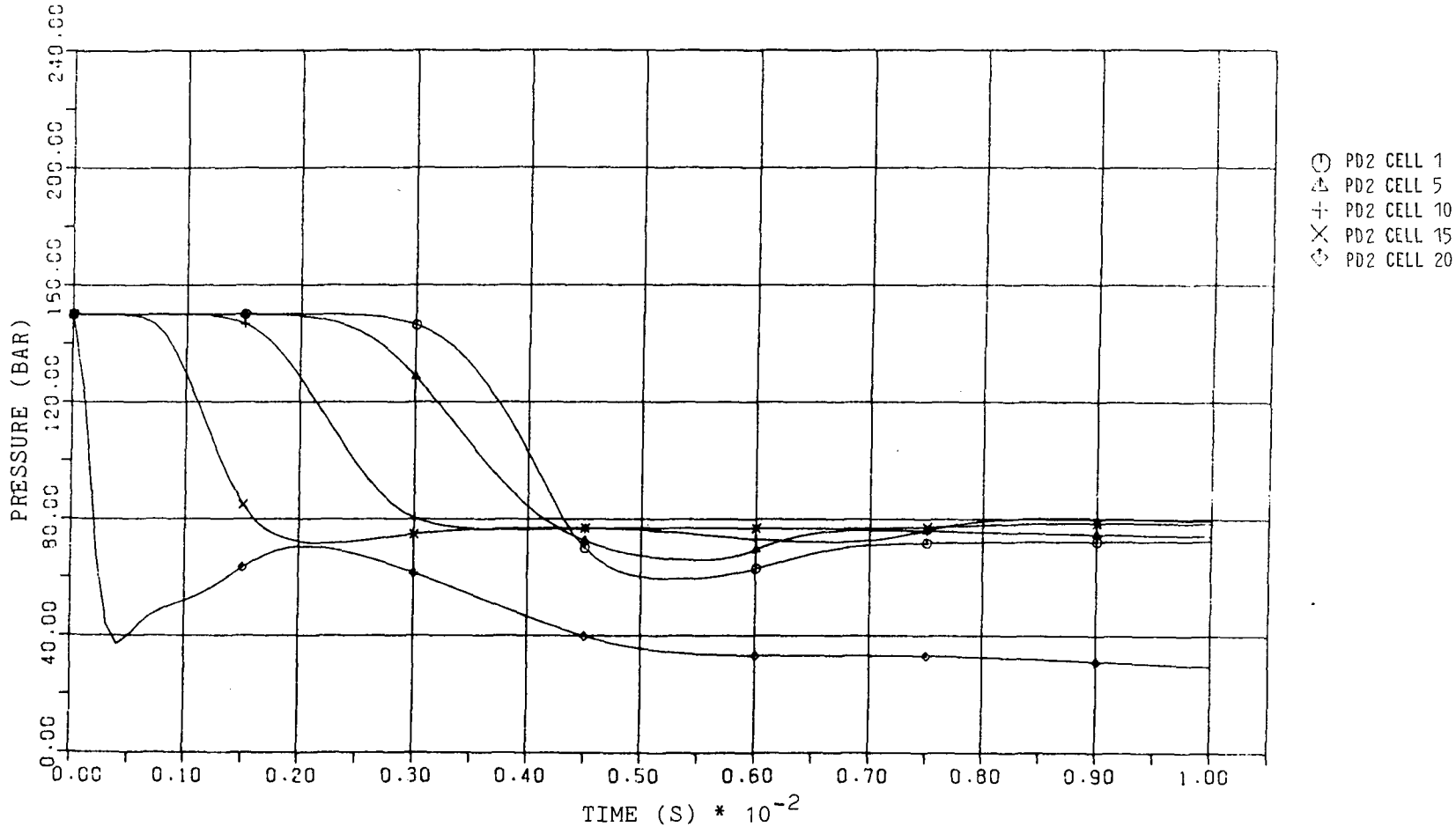

150 BAR / 300 K / 20 CELLS DELT = 1.E-4

Fig. 2.6

KWU TRAC - PD2

SUPER CANON EXPERIMENT

COMPARISON WITH LOS ALAMOS

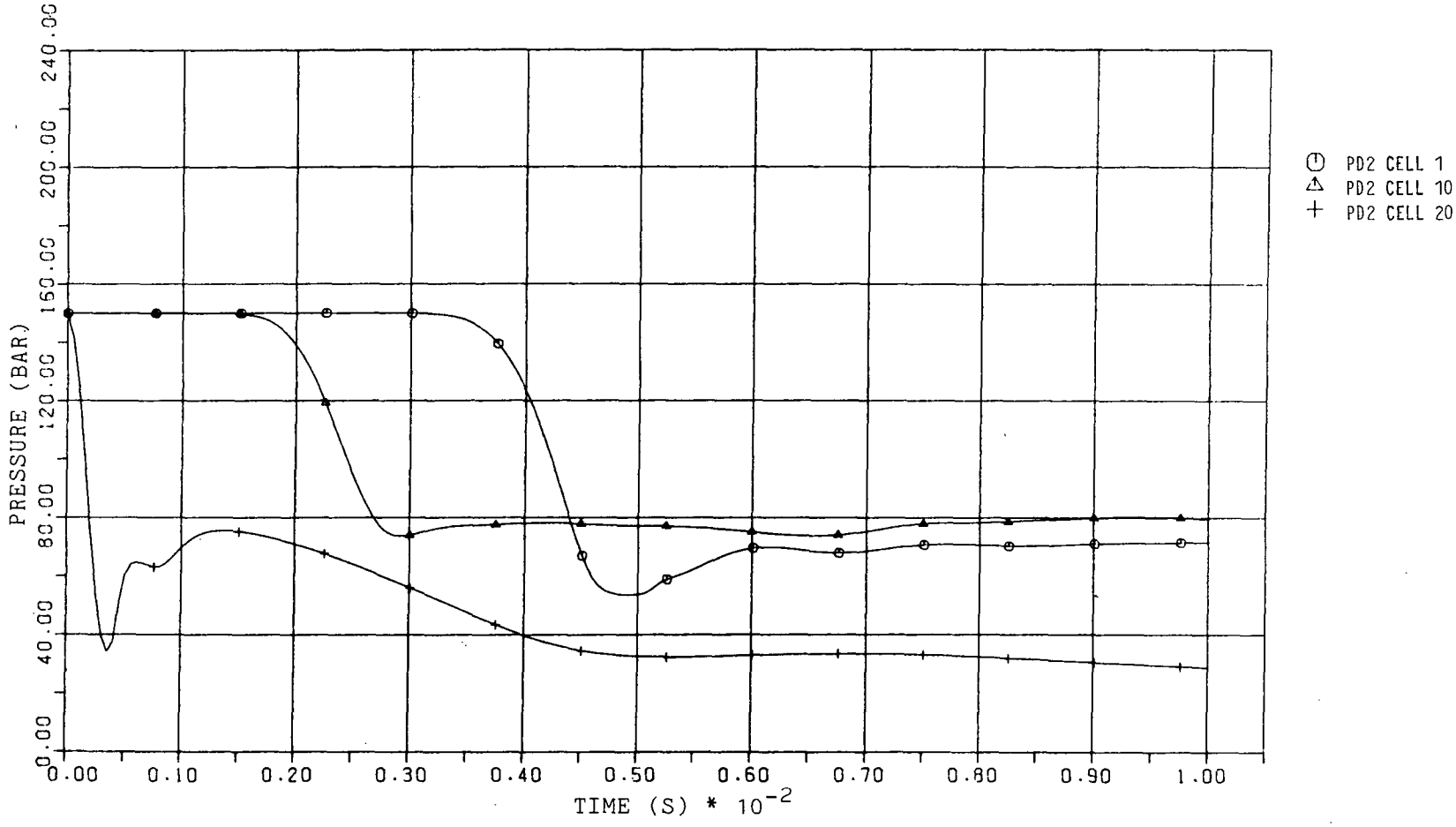

150 BAR / 300 K / 20 CELLS DELT = 1.E-4

Fig. 2.7

KWU TRAC - PD2

SUPER CANON EXPERIMENT

COMPARISON WITH LOS ALAMOS

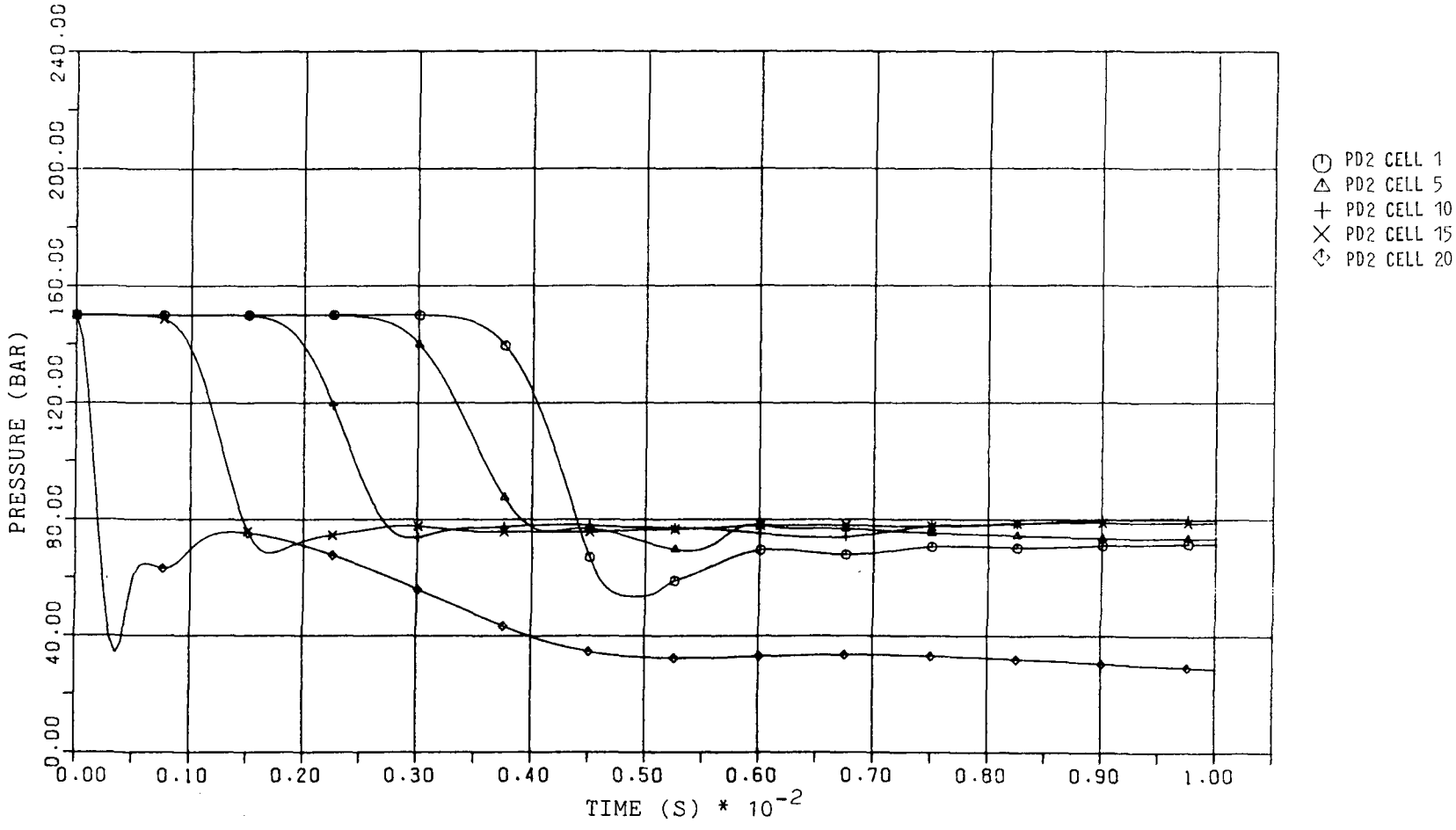

150 BAR / 300 K / 20 CELLS DELT = 1.E-5

Fig. 2.8

KWU TRAC - PD2

SUPER CANON EXPERIMENT

PRESSURE VERSUS AXIAL POSITION

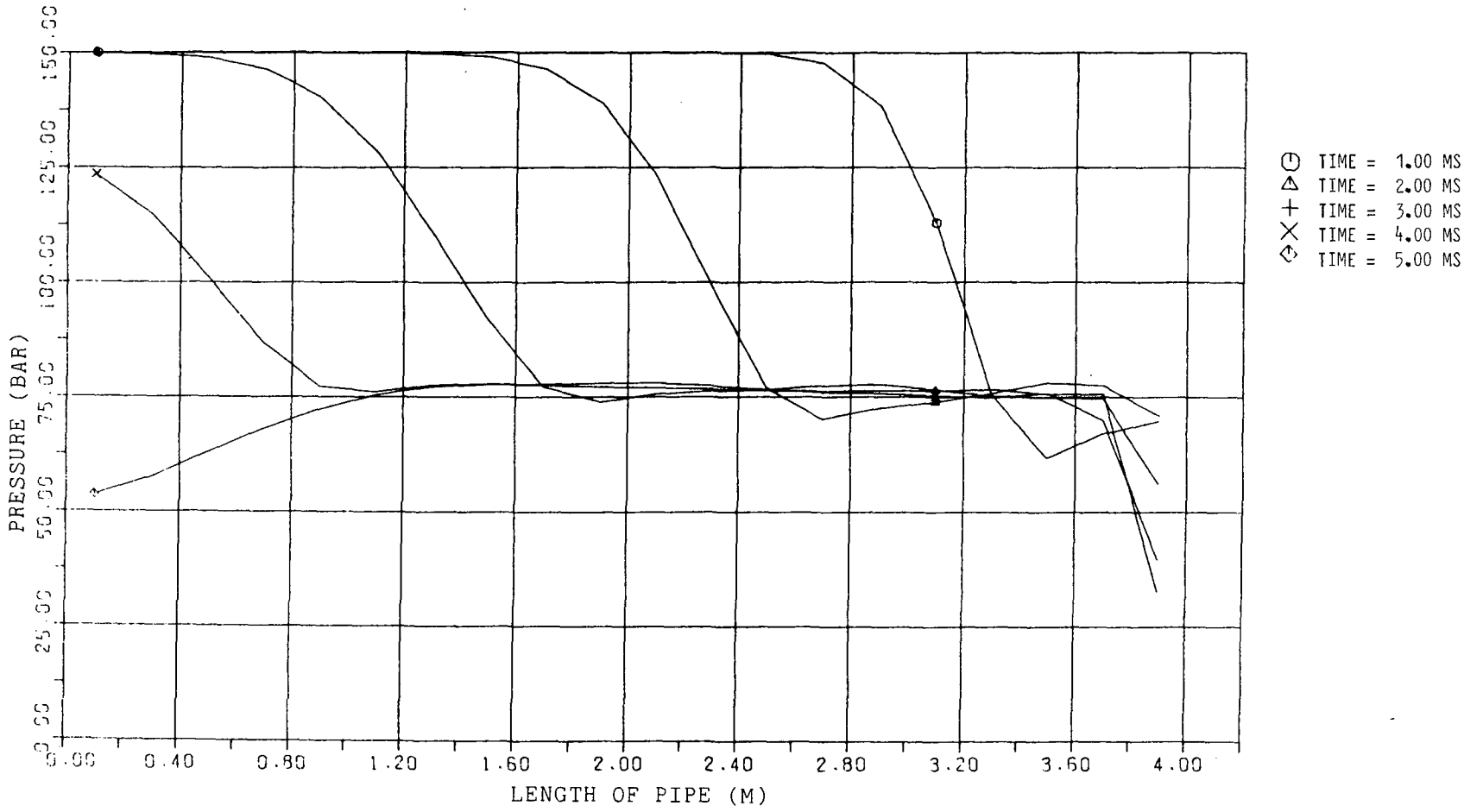

DELT = 1.E-5

Fig. 2.9

KWU

SUPER CANON EXPERIMENT

TRAC - PD2 IN COMPARISON WITH TRAC - P1A

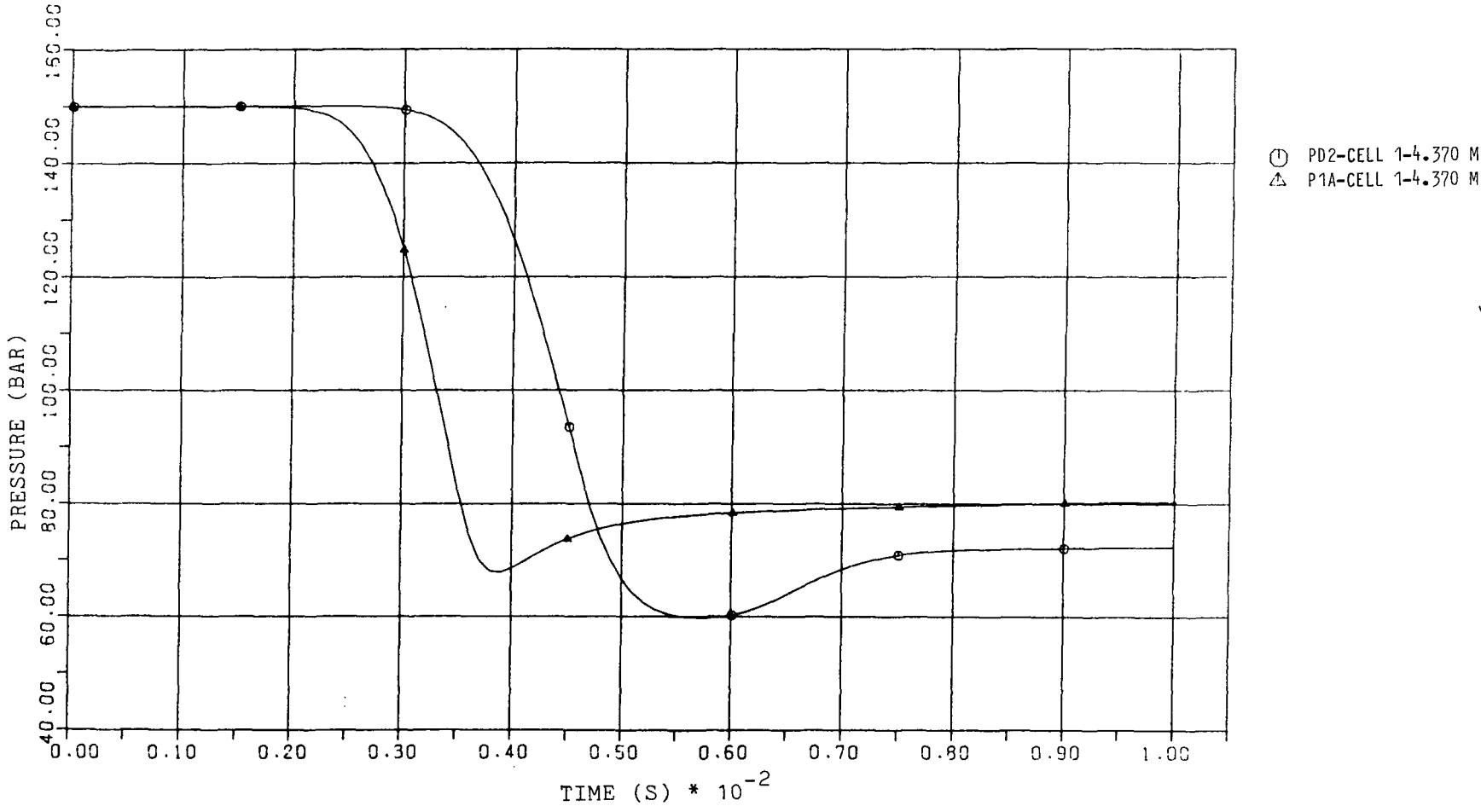

150 BAR / 300 K / 120 CELLS DELT = 1.E-4

Fig. 3.1

KWU

SUPER CANON EXPERIMENT

TRAC - PD2 IN COMPARISON WITH TRAC - P1A

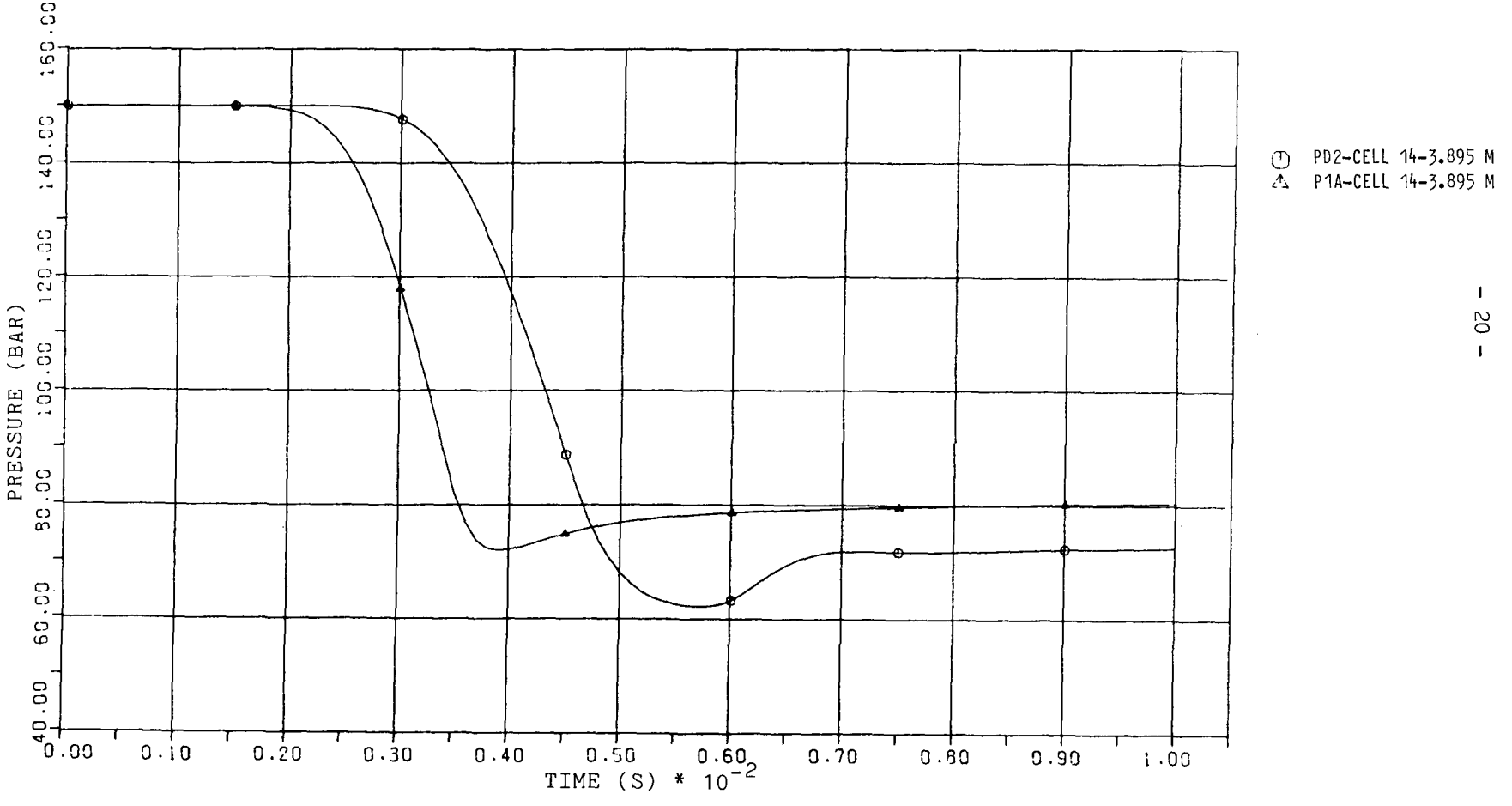

150 BAR / 300 K / 120 CELLS DELT = 1.E-4

Fig. 3.2

KWU

SUPER CANON EXPERIMENT

TRAC - PD2 IN COMPARISON WITH TRAC - P1A

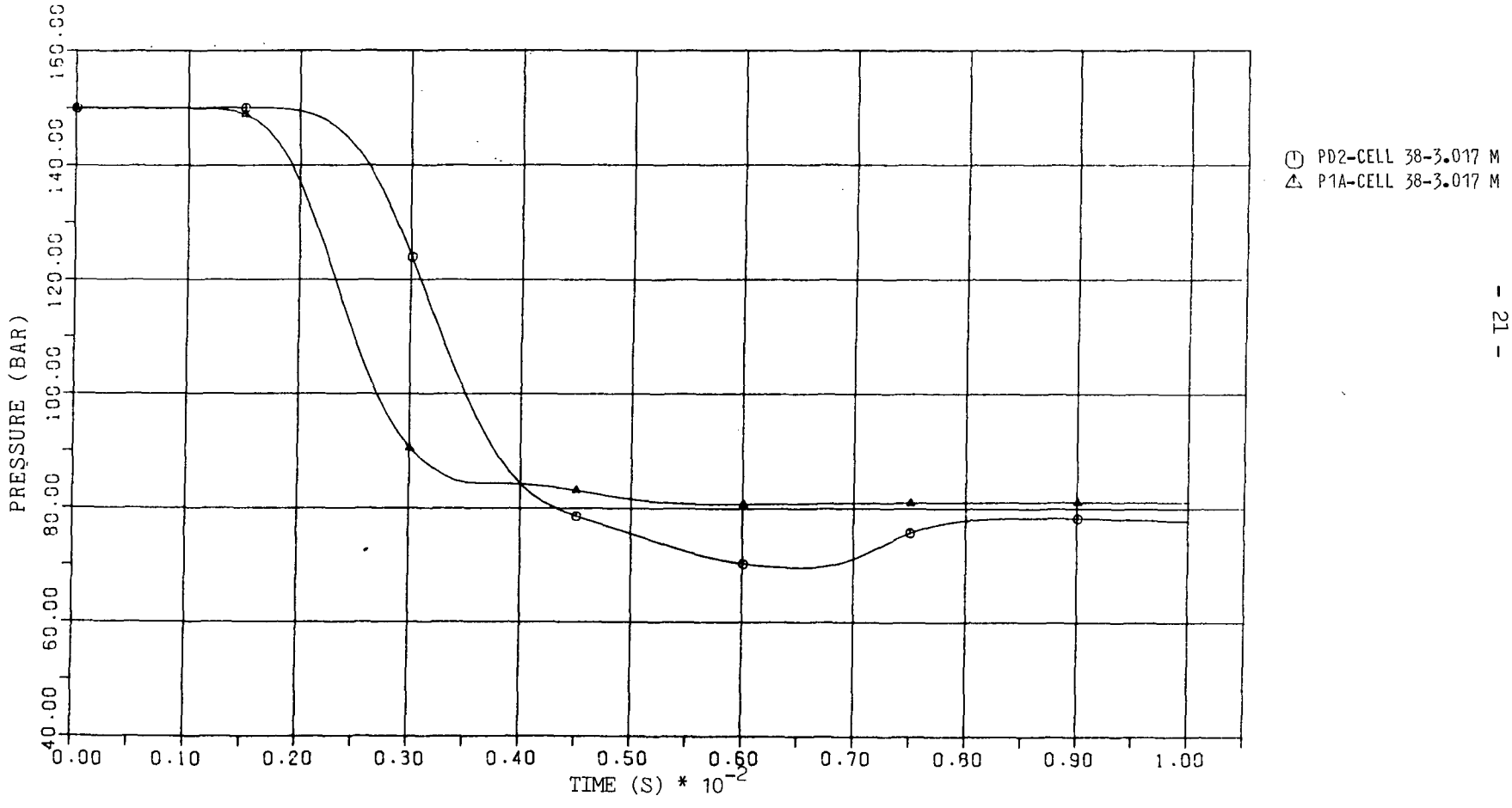

150 BAR / 300 K / 120 CELLS DELT = 1.E-4

Fig. 3.3

KWU

SUPER CANON EXPERIMENT

TRAC - PD2 IN COMPARISON WITH TRAC - P1A

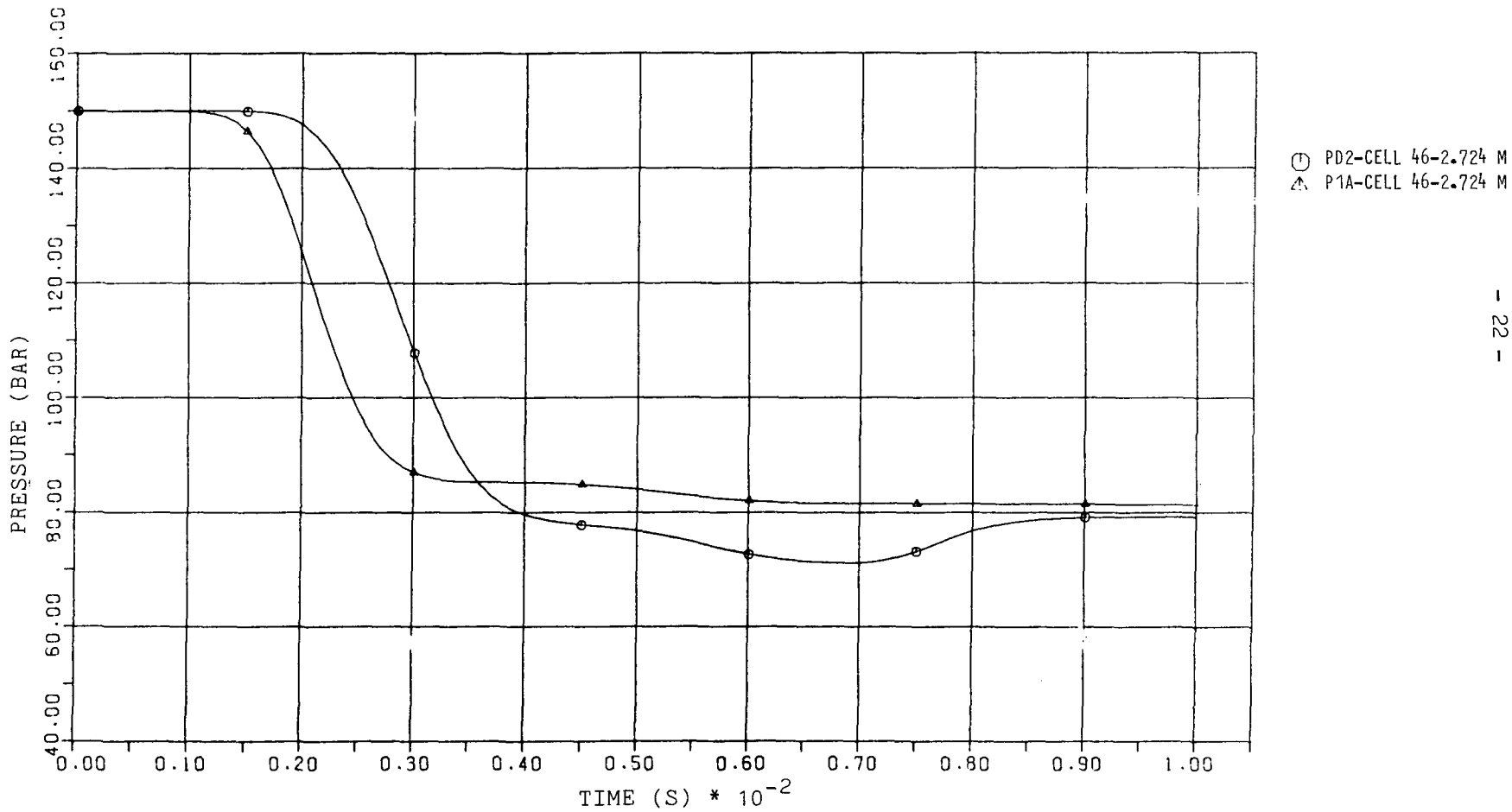

150 BAR / 300 K / 120 CELLS DELT = 1.E-4

Fig. 3.4

KWU

SUPER CANON EXPERIMENT

TRAC - PD2 IN COMPARISON WITH TRAC - P1A

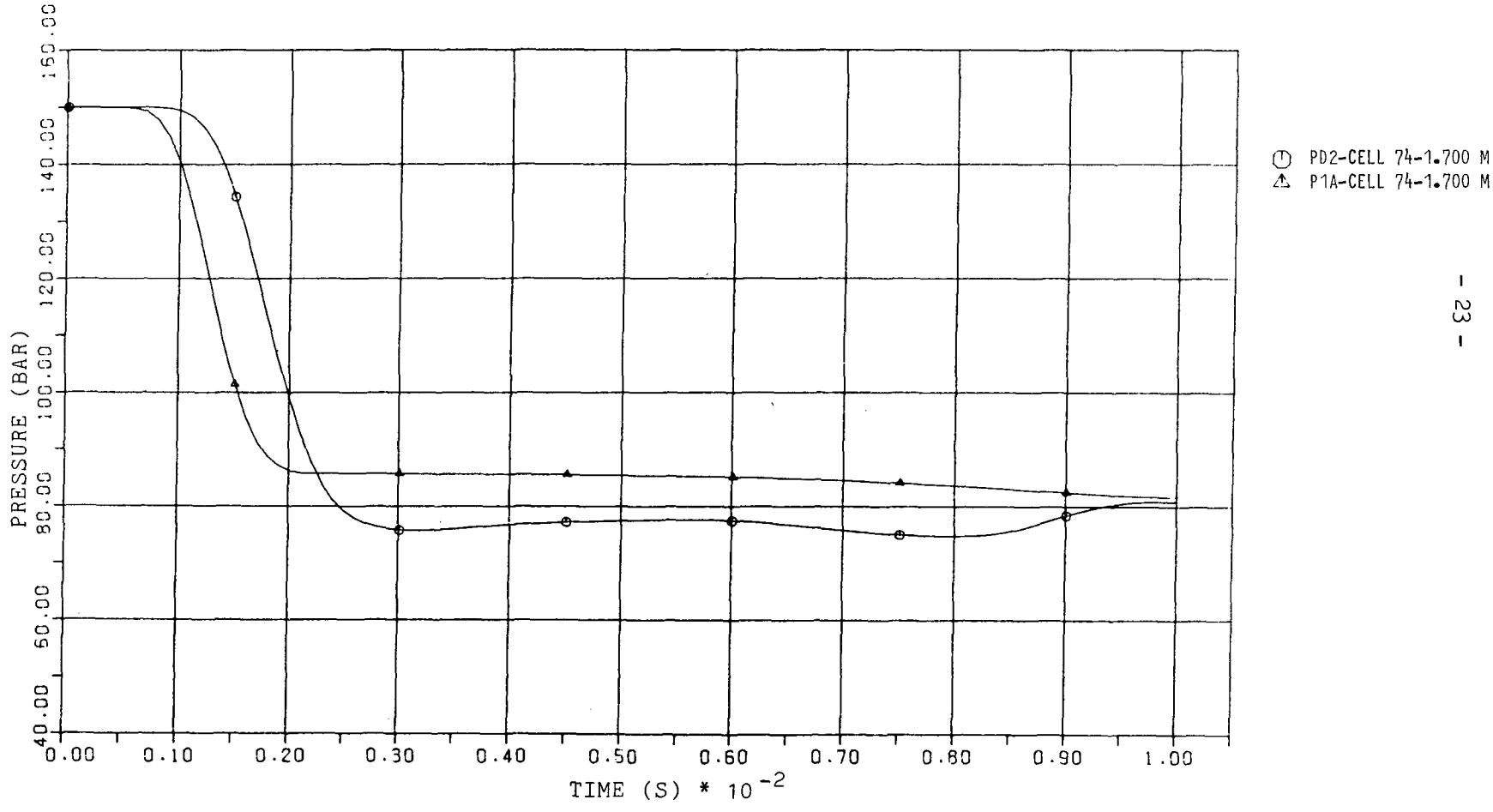

150 BAR / 300 K / 120 CELLS DELT = 1.E-4

Fig. 3.5

KWU

SUPER CANON EXPERIMENT

TRAC - PD2 IN COMPARISON WITH TRAC - P1A

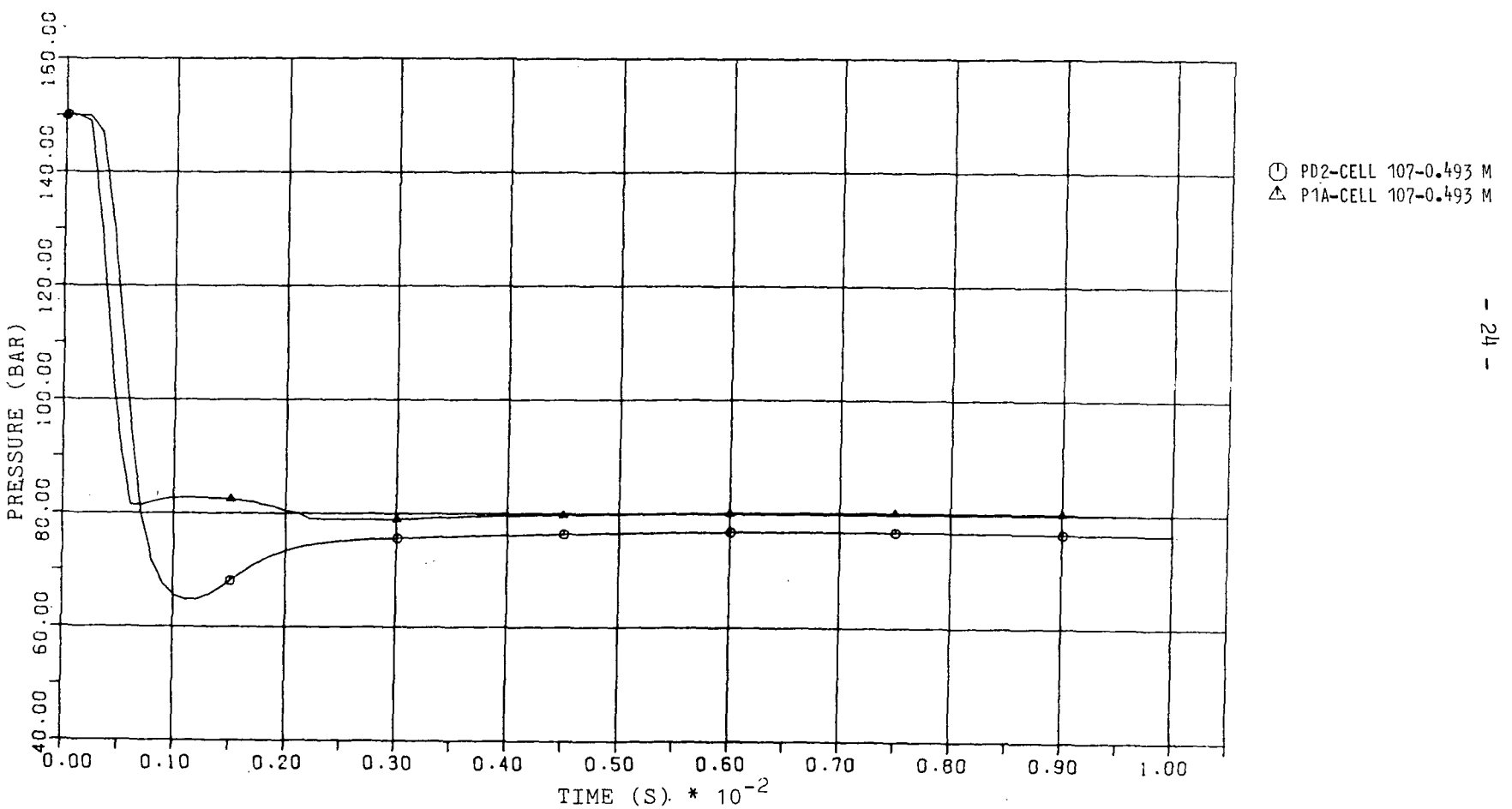

150 BAR / 300 K / 120 CELLS DELT = 1.E-4

Fig. 3.6

KWU

SUPER CANON EXPERIMENT

TRAC - PD2 IN COMPARISON WITH TRAC - P1A

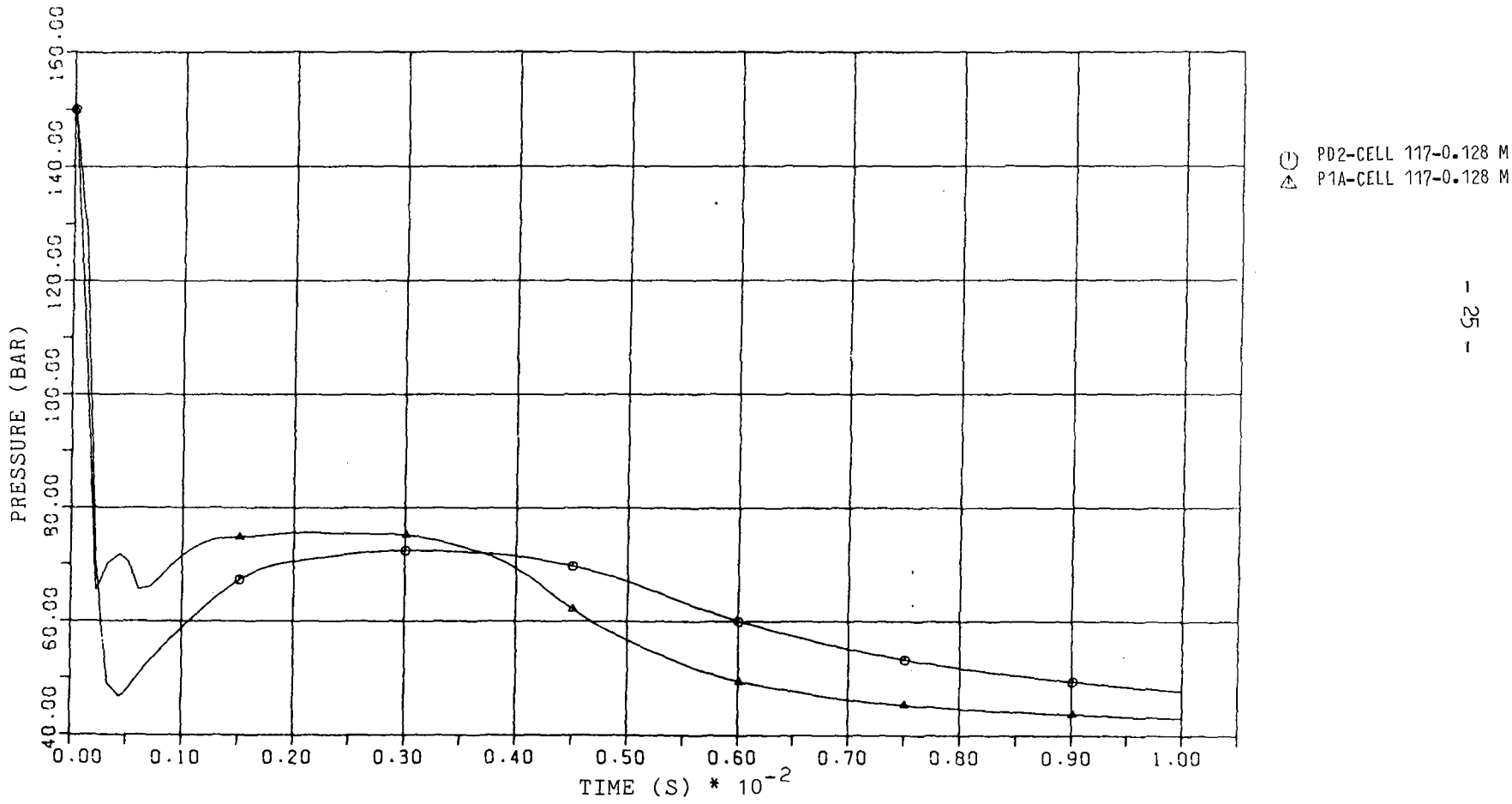

150 BAR / 300 K / 120 CELLS DELT = 1.E-4

Fig. 3.7

KWU TRAC - P1A

SUPER CANON EXPERIMENT

PRESSURE VERSUS AXIAL POSITION

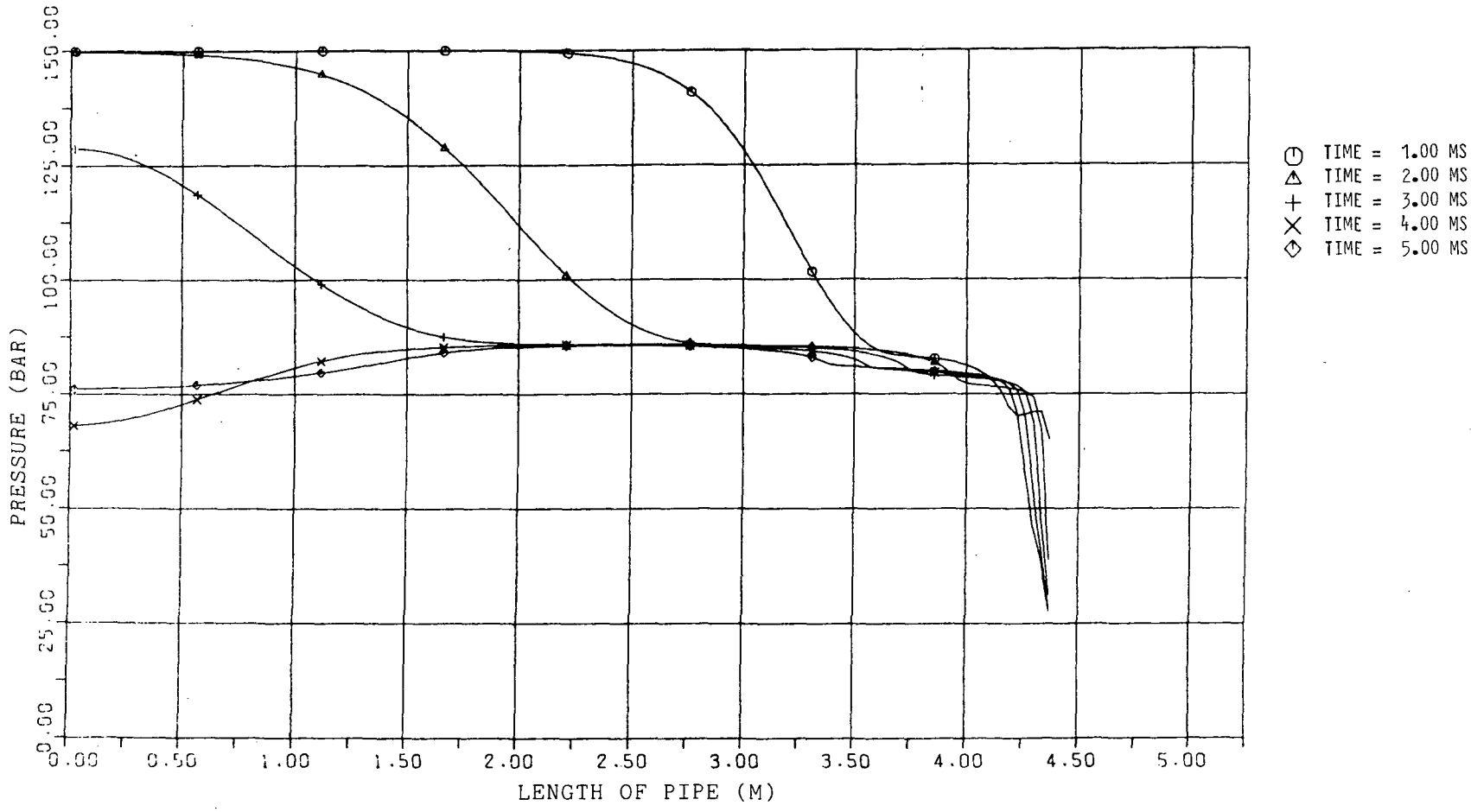

120 CELLS DELT = 1.E-4

Fig. 3.8

KWU TRAC - PD2

SUPER CANON EXPERIMENT

PRESSURE VERSUS AXIAL POSITION

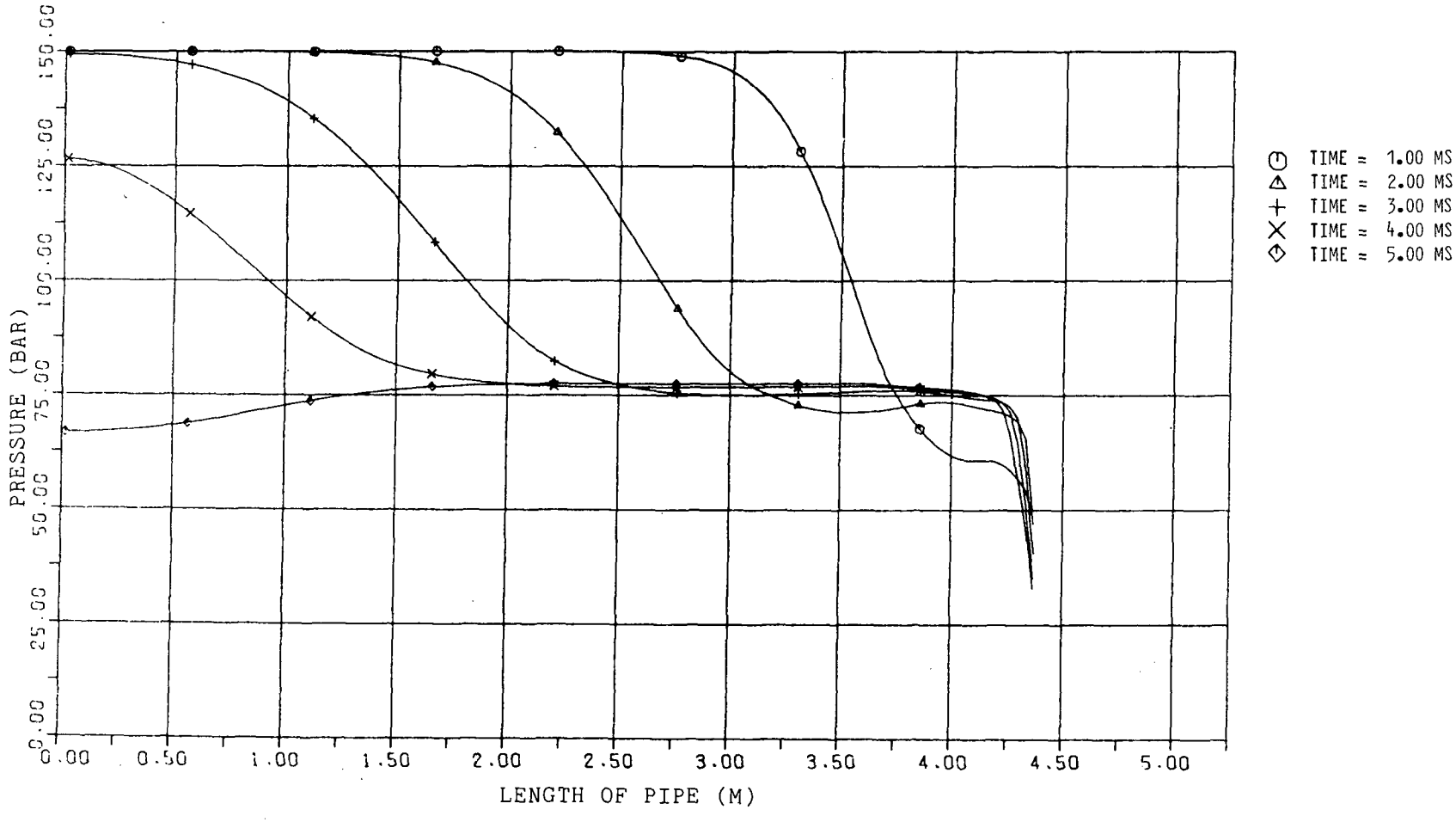

120 CELLS DELT = 1.E-4

Fig. 3.9

KWU TRAC - PD2

SUPER CANON EXPERIMENT

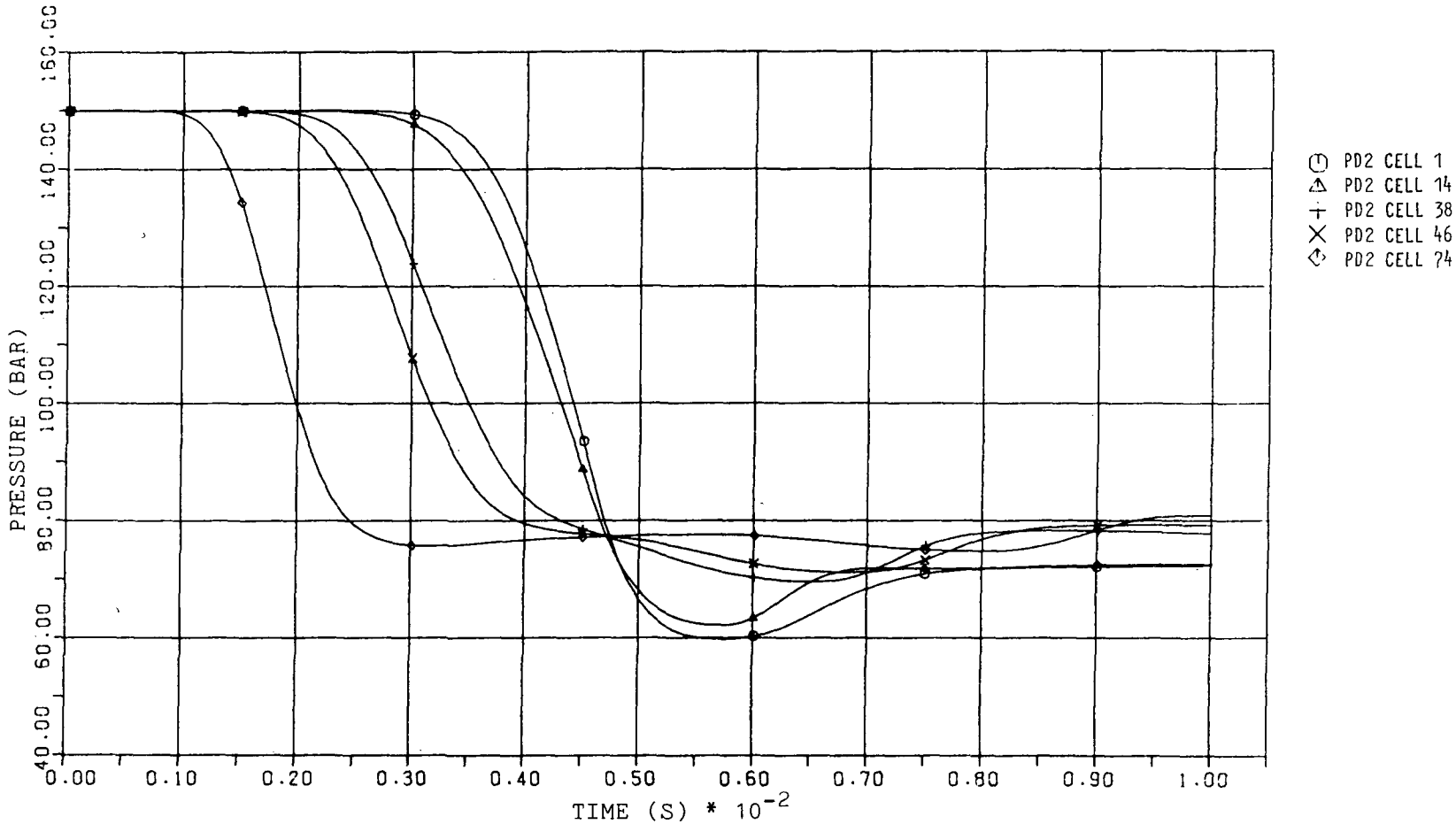

INITIAL CONDITIONS 150 BAR / 300 K

120 CELLS DELT = 1.E-4

Fig. 3.10

KWU TRAC - PD2

SUPER CANON EXPERIMENT

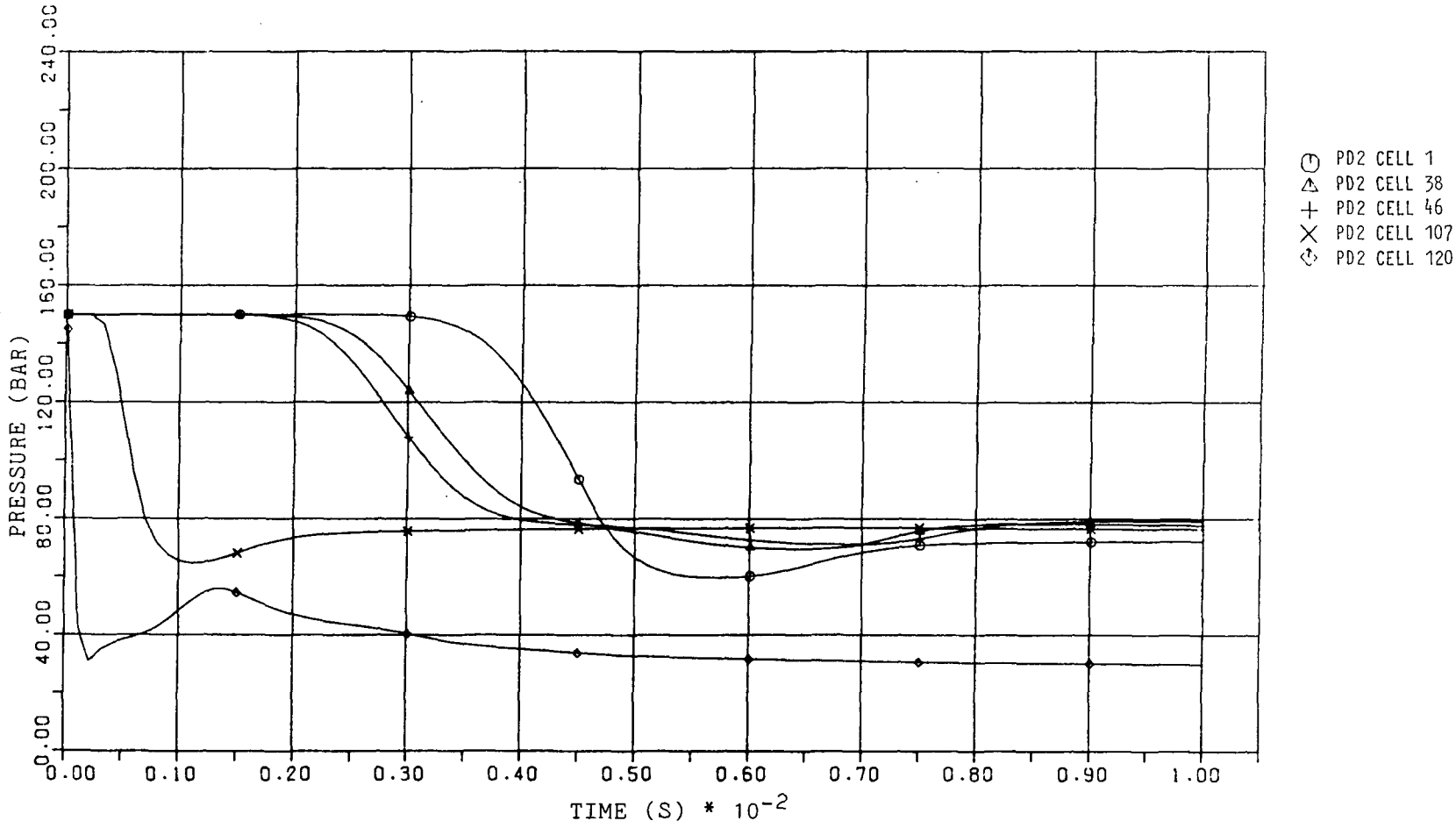

INITIAL CONDITIONS 150 BAR / 300 K

120 CELLS DELT = 1.E-4

Fig. 3.11

KWU TRAC - PD2

SUPER CANON EXPERIMENT

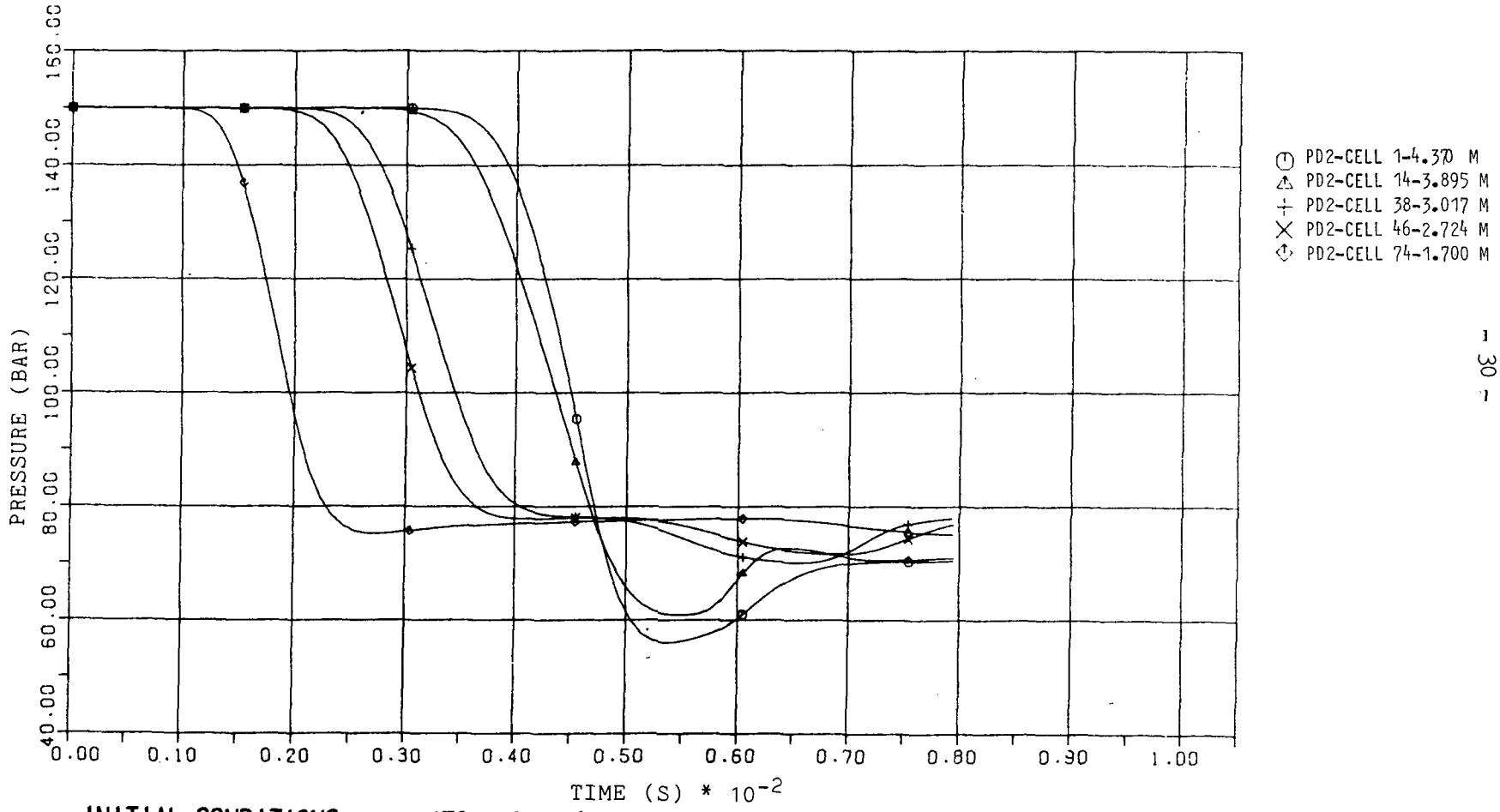

INITIAL CONDITIONS 150 BAR / 300 K

120 CELLS COMPUTATION UNTIL 0.080 SEC

Fig. 3.12

KWU TRAC - PD2

SUPER CANON EXPERIMENT

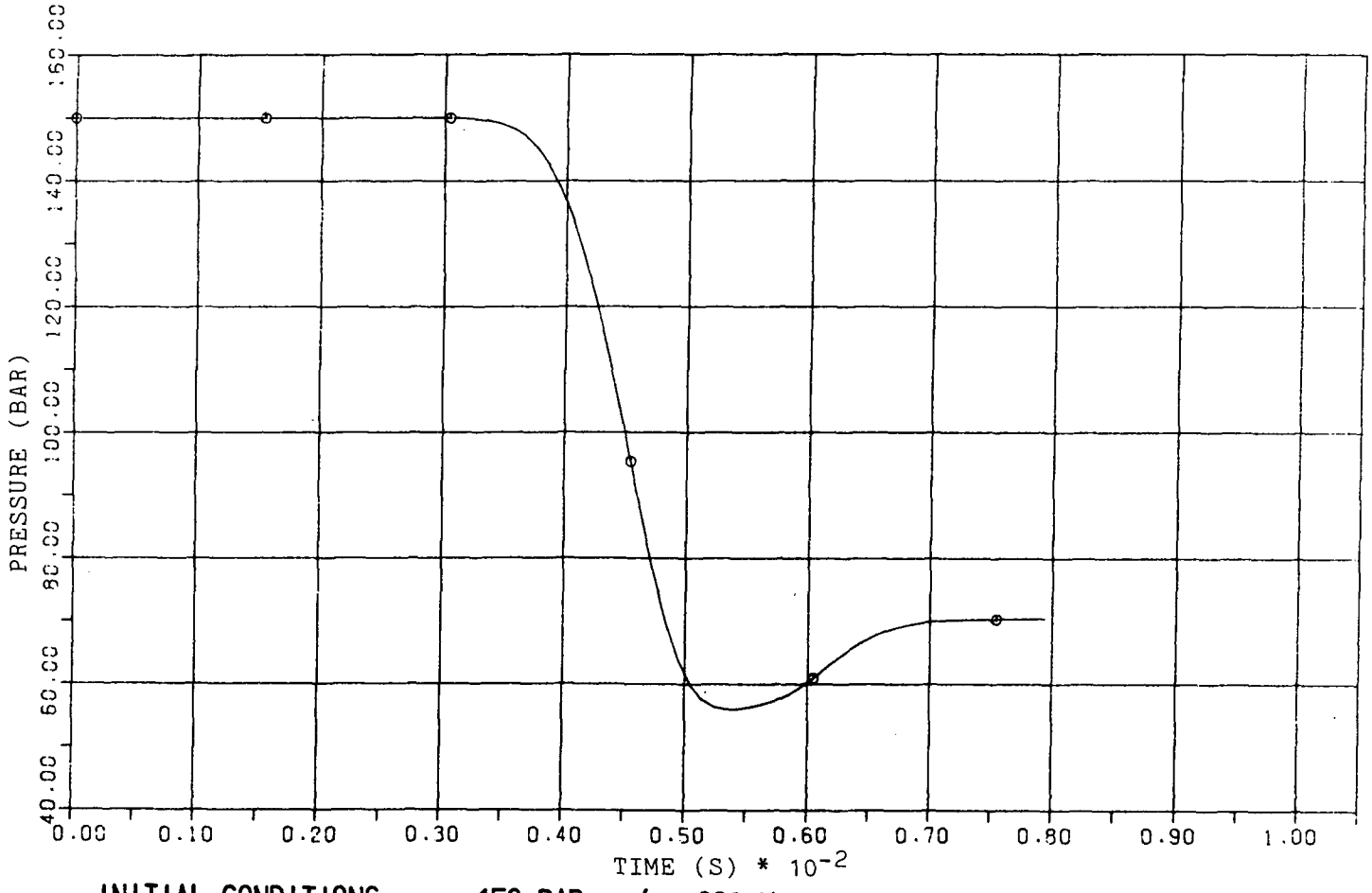

Ⓓ PD2-CELL 1-4.370 M

INITIAL CONDITIONS 150 BAR / 300 K

120 CELLS DELT = 5.E-5 COMPUTATION UNTIL 0.080 SEC

Fig. 3.13

KWU TRAC - PD2

SUPER CANON EXPERIMENT

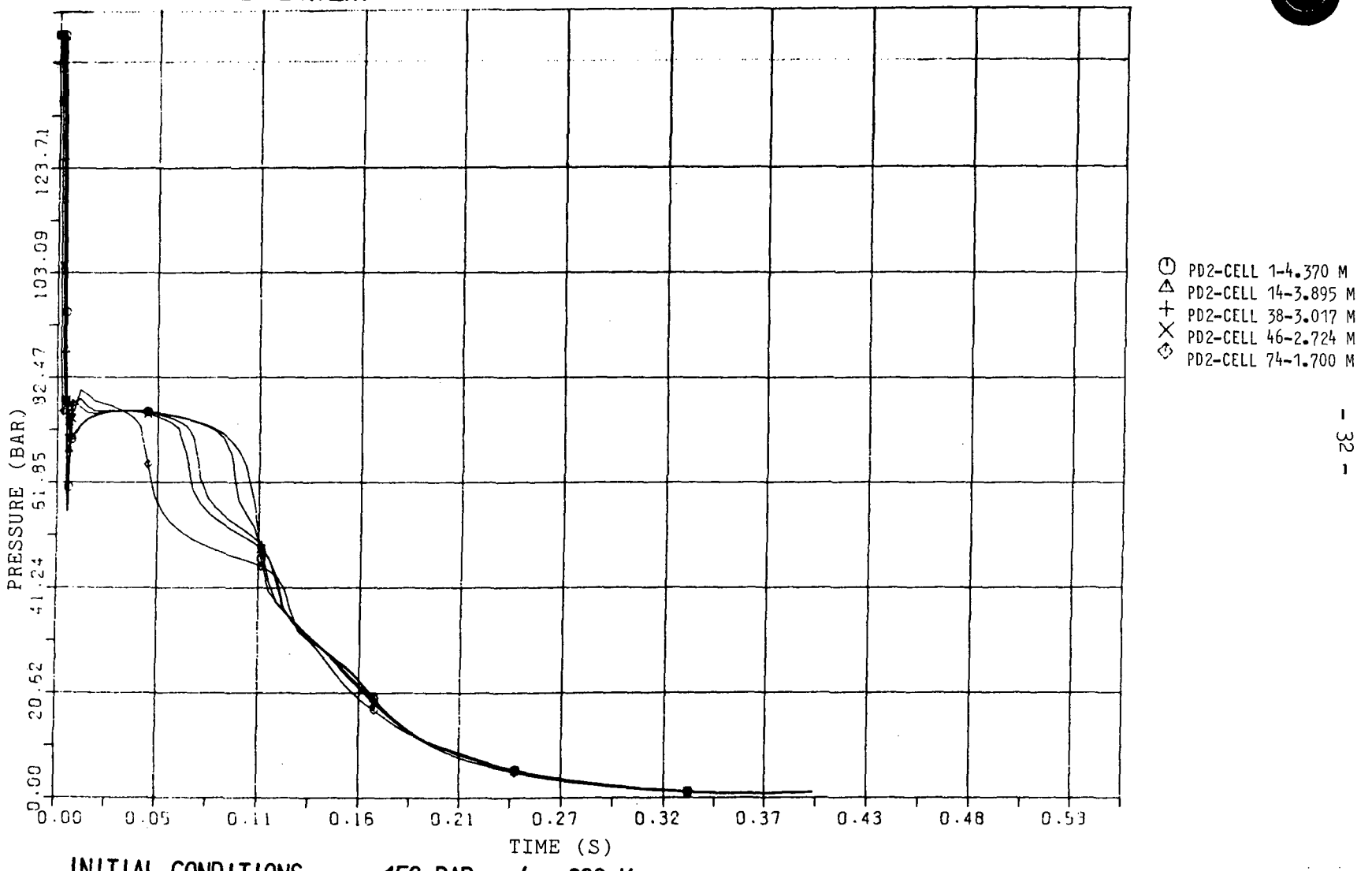

INITIAL CONDITIONS 150 BAR / 300 K

120 CELLS COMPUTATION UNTIL 0.4 SEC

Fig. 3.14

KWU TRAC - PD2

SUPER CANON EXPERIMENT

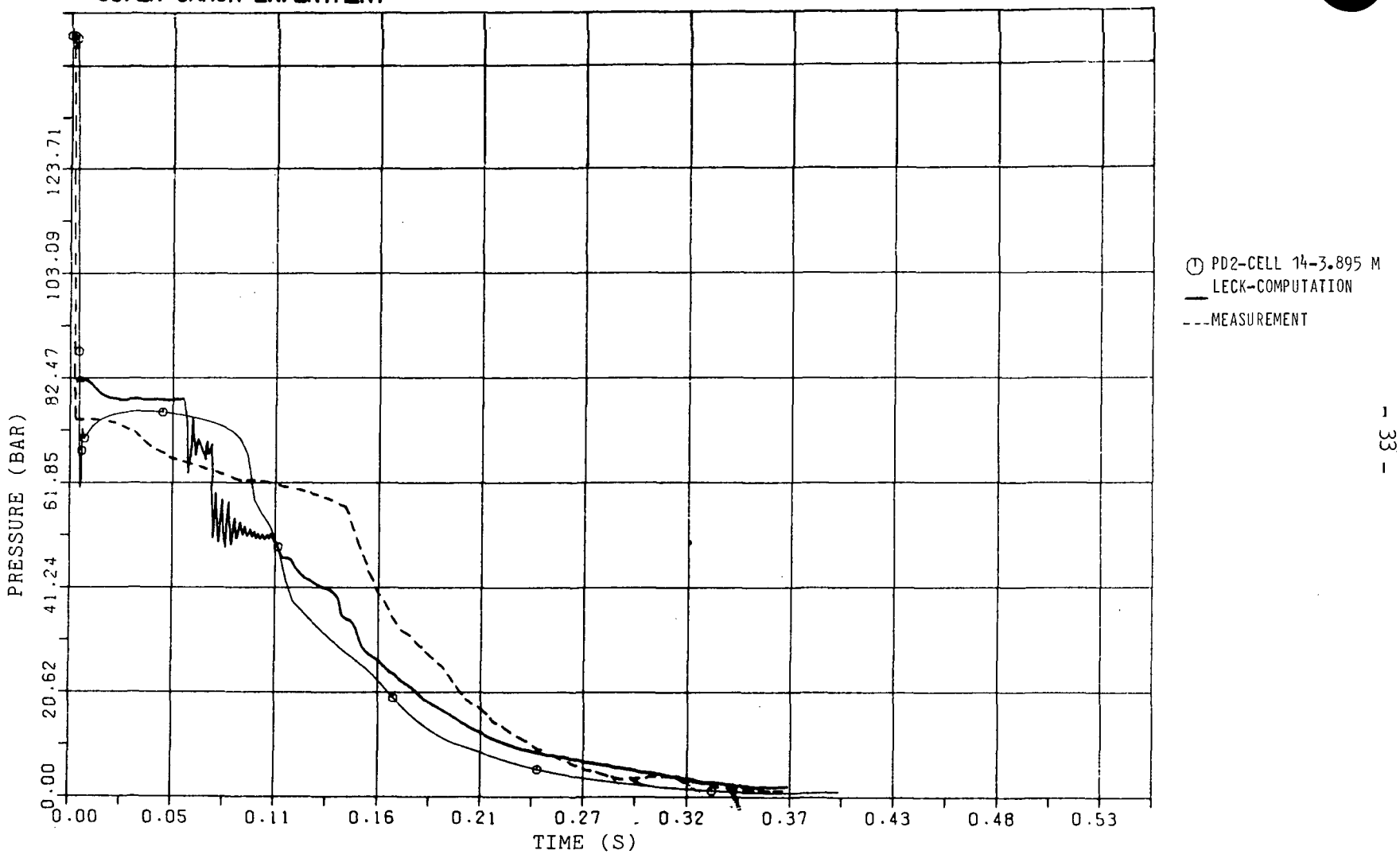

INITIAL CONDITIONS 150 BAR / 300 K

120 CELLS COMPUTATION UNTIL 0.4 SEC

Fig. 3.15

KWU TRAC - PD2

SUPER CANON EXPERIMENT

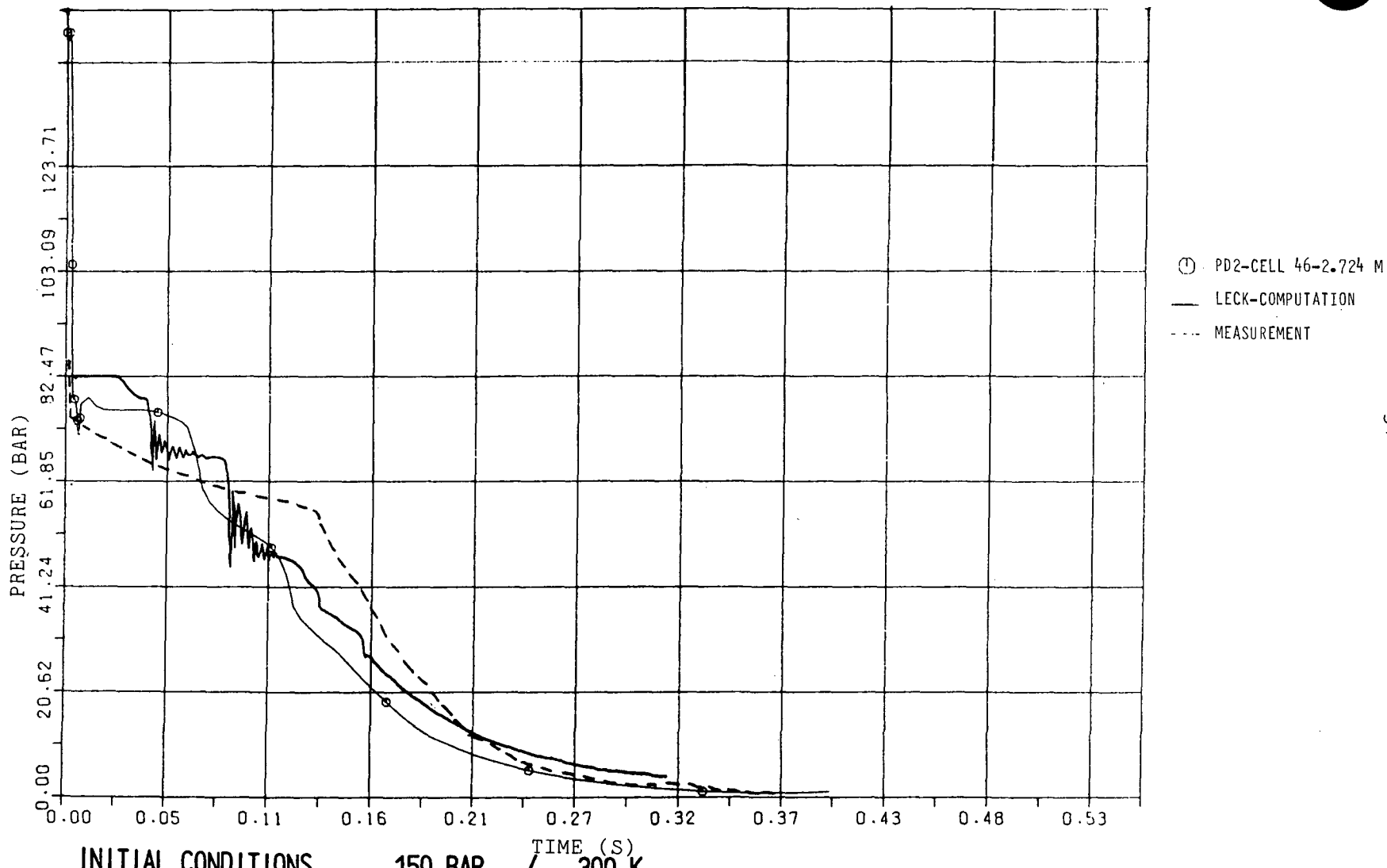

INITIAL CONDITIONS 150 BAR / 300 K

120 CELLS COMPUTATION UNTIL 0.4 SEC

Fig. 3.16

KWU TRAC - PD2

SUPER CANON EXPERIMENT

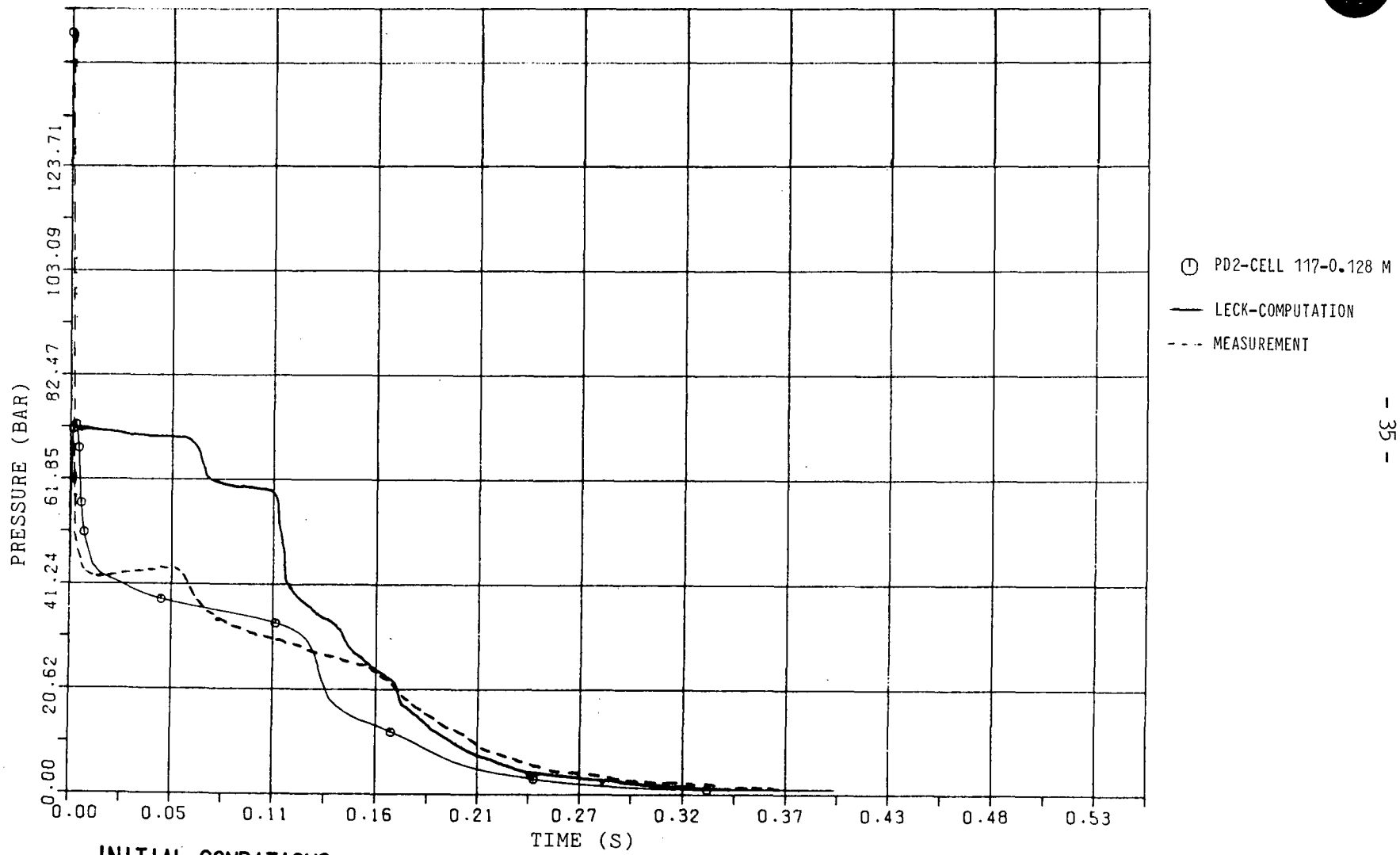

INITIAL CONDITIONS 150 BAR / 300 K

120 CELLS COMPUTATION UNTIL 0.4 SEC

Fig. 3.17

KWU TRAC - PD2

SUPER CANON EXPERIMENT

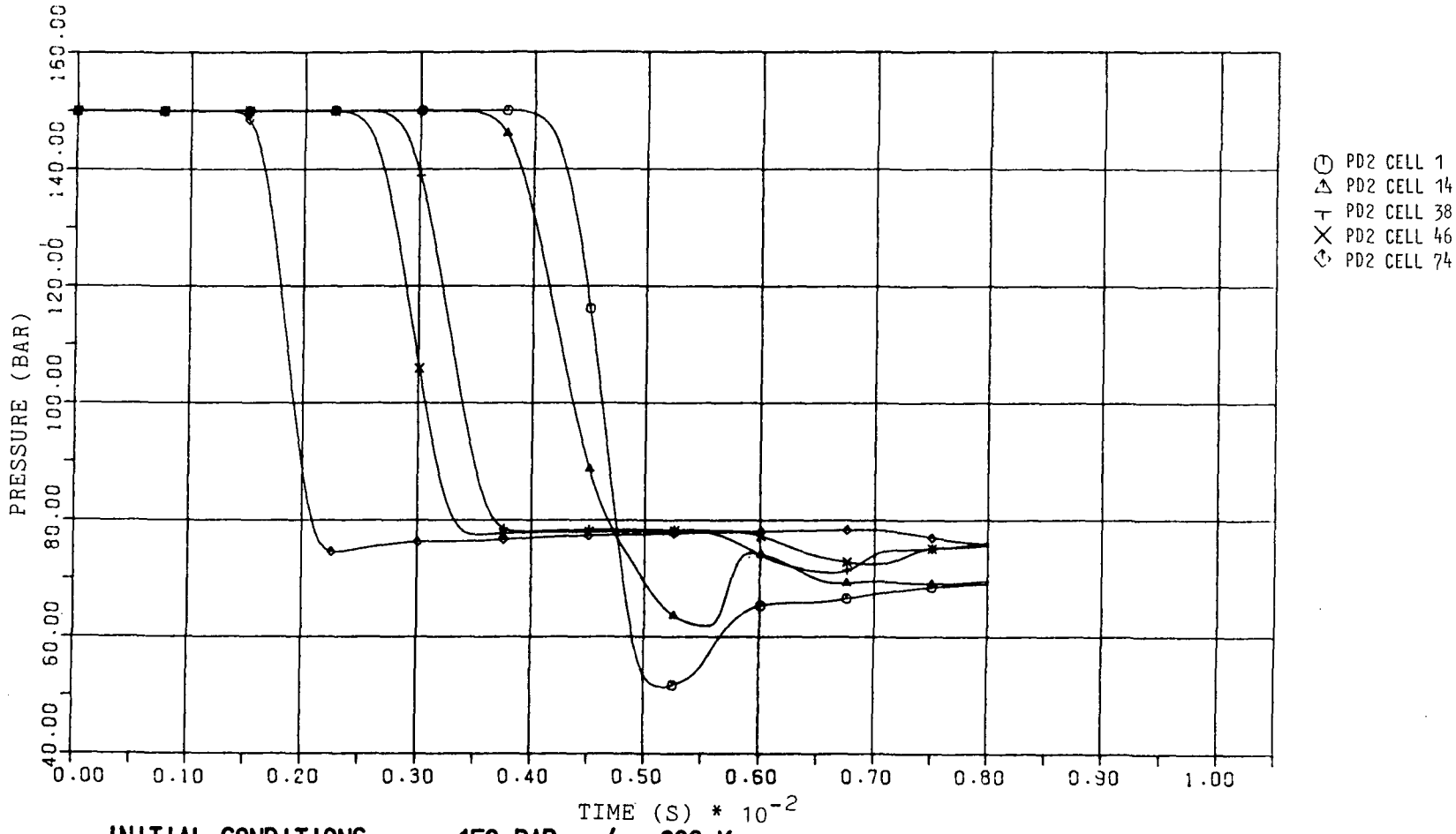

INITIAL CONDITIONS 150 BAR / 300 K

120 CELLS DELT = 1.E-5

Fig. 3.18

KWU TRAC - PD2

SUPER CANON EXPERIMENT

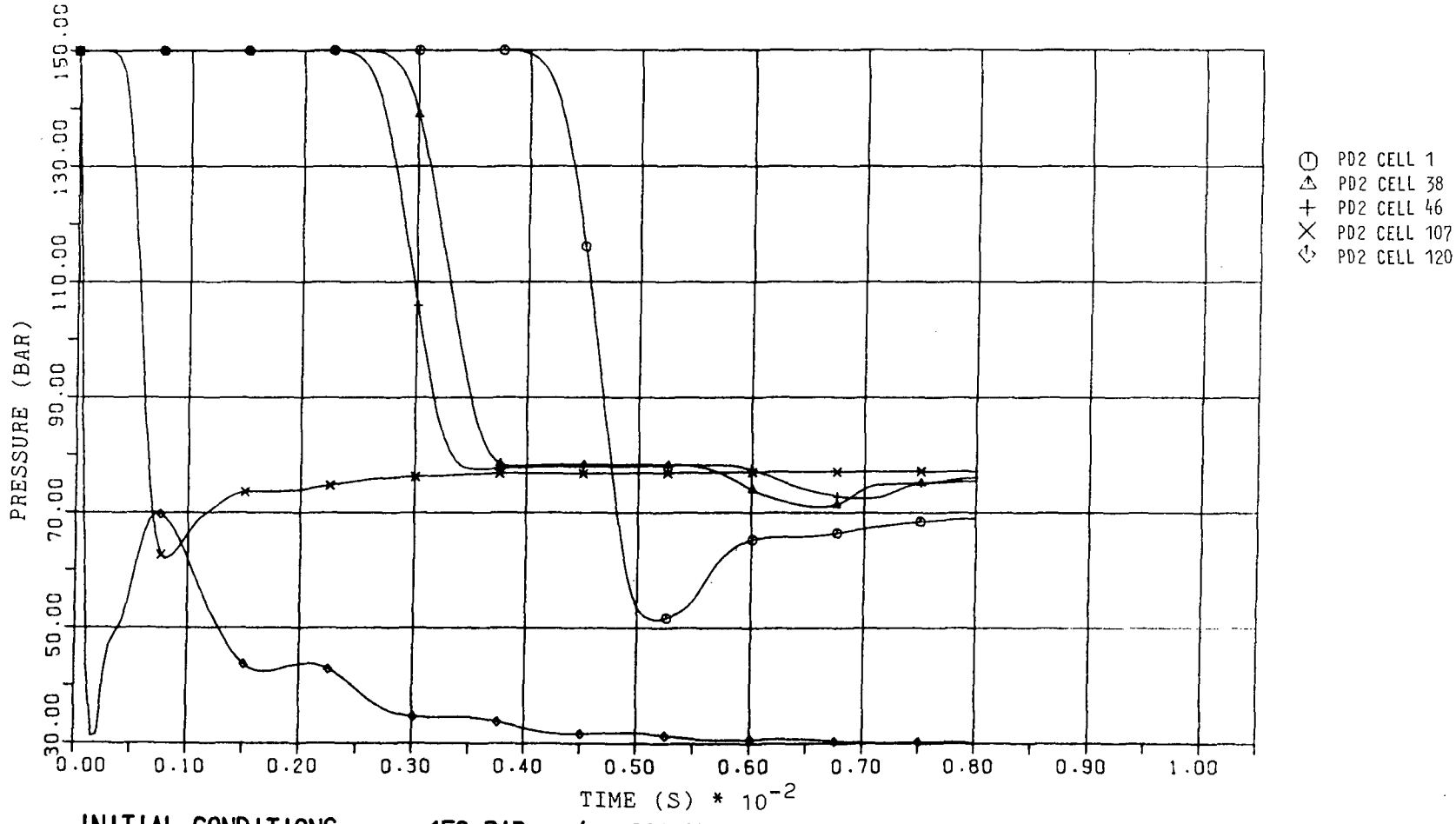

INITIAL CONDITIONS 150 BAR / 300 K

120 CELLS DELT = 1.E-5

Fig. 3.19

KWU TRAC - PD2

SUPER CANON EXPERIMENT

PRESSURE VERSUS AXIAL POSITION

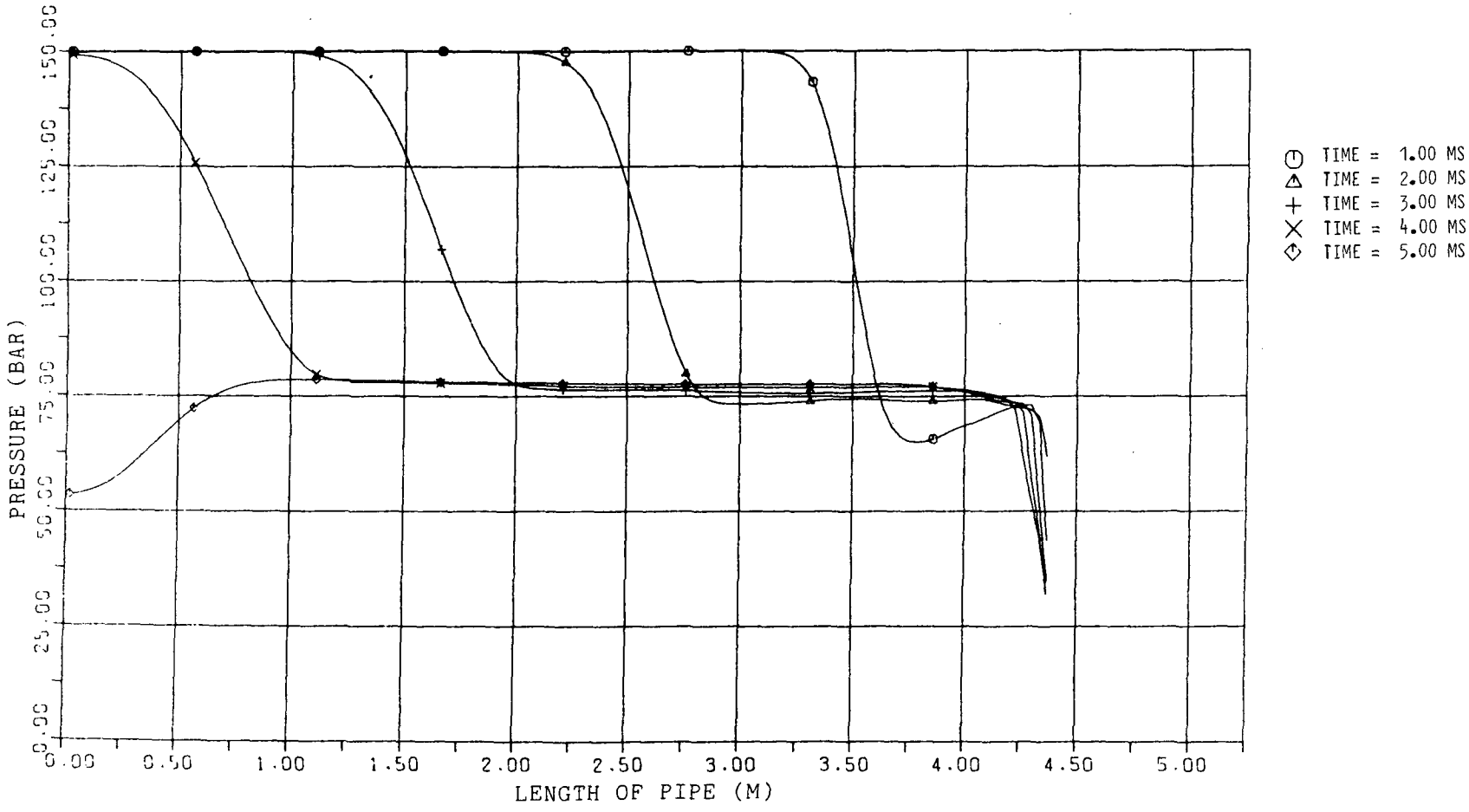

120 CELLS DELT = 1.E-5

Fig. 3.20

KWU TRAC - PD2

SUPER CANON EXPERIMENT

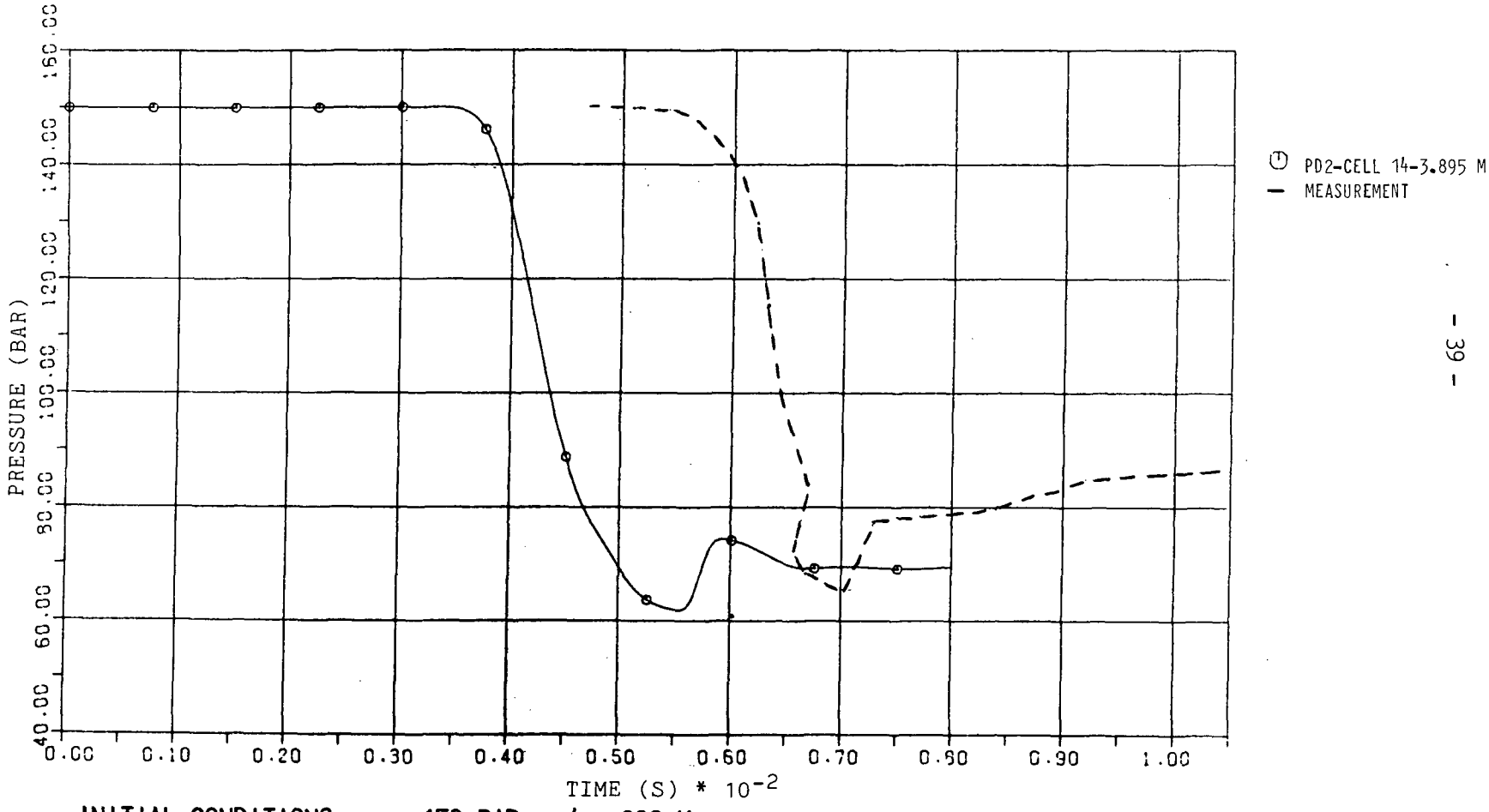

INITIAL CONDITIONS 150 BAR / 300 K

120 CELLS DELT = 1.E-5 COMPUTATION UNTIL 0.080 SEC

Fig. 3.21

COMPUTATION	NUMBER OF CELLS	TIME STEP (S)	PROBLEM TIME INTERVAL (S)	CPA	SYSTEM SECONDS CPU	CORE MEMORY CM	EXTENDED CORE MEMORY EC
1. LOS ALAMOS	20	2.E-4 s	0,010 s	5,317	145,07	3224,14	5188,02
2. LOS ALAMOS	20	1.E-4 s	0,010 s	8,947	256,62	5818,07	8809,08
ΔT-COMPARISON	1	10	1	6,204	7,245	7,507	6,682
3. LOS ALAMOS	20	1.E-5 s	0,010	55,512	1859,1	43679,3	58600,8
4. P1A-CALCULATION	120	1.E-4 s	0,010	36,403	533,2	12056,2	16710,7
5. PD2-CALCULATION	120	1.E-4 s	0,010	38,786	571,8	12930,3	17940,0
ΔT-COMPARISON	120	1.E-4 s	0,008	31,028	457,44	10344,2	14352,0
	1	10	1	7,0828	7,484	7,578	7,297
6. PD2-CALCULATION	120	1.E-5 s	0,008	219,76	3423,4	78395,7	104826,9
7. PD2-CALCULATION	120	5.E-5	0,008				
		1.E-4	0,2				
		1.E-3	0,4	586,59	9310,0	213670,2	284001,7
3. LOS ALAMOS	20	1.E-5 s	0,010s	55,512	1859,1	43679,3	58600,8
THE EFFECT OF THE NODALIZATION	6	1	0,8	4,95	2,3017	2,243	2,234
6. LOS ALAMOS	120	1.E-5 s	0,008 s	219,767	3427,4	78395,7	104726,9
2. LOS ALAMOS	20	1.E-4 s	0,010 s	8,947	256,62	5818,07	8809,08
THE EFFECT OF THE NODALIZATION	6	1	1	4,315	2,228	2,222	2,036
5. PD2-CALCULATION	120	1.E-4 s	0,010 s	38,486	571,8	12930,3	17940,0

able 4.1 COMPARISON OF TIMESTEP, PROBLEM TIME INTERVAL AND COMPUTATION TIME

PART II: PARAMETRIC STUDY OF TRAC-PD2 USING THE HDR TEST RESULTS

Translated By: SCITRAN
1482 East Valley Road
Santa Barbara, CA 93108

Part II

This page intentionally left blank.

1. Introduction /1

Since the computer program TRAC-P1A was first put into operation in March 1979 [1] and the installation in the meantime of the improved version TRAC-PD2 in September 1980, several test follow-up calculations have been conducted for the verification of the program. The information thus gained for the optimization of the computer models will be explained in more detail in the following chapter.

2. Parameter study of the HDR tests /2

Test follow-up calculations are an unavoidable step in the verification of a computer program. For this reason, the HDR/V 31.1 test [3] was subjected to a follow-up calculation with the program version TRAC-PD2 [2] in order to be able to compare the TRAC calculations with the test results. Here, the calculations mentioned in this report were conducted within the framework of a preliminary study in order to investigate the effect of different discretionary steps in the RDB connection (3D - 1D transition resp. coupling) and in the fracture location area (outflow conditions). The individual computer cases are listed in table 2.1. Here, the results of the model modifications explained in the following chapters were referenced to an initial calculation (HDR 1/3) in order to be able to determine the effect of the individual measures clearly. Figure 2.1 presents a schematic total view of the test stand. However, only the RDB and the break nozzle (nozzle A1) are simulated in a model. Figure 2.2 shows the RDB and contains the most importa geometrical dimensions. In the model, RDB is calculated in a gre simplified form since the processes within the boiler are not interest for this study.

In figure 2.3, the models used for the break nozzles orifices are recorded. Additionally, the zone sub most important geometrical data are plotted.

the measurement locations which will be used for comparing the results in figures 2.4 and 2.5.

The subdivision is somewhat finer only in the connection area of the break nozzle in order to still be able to compare the calculated results in this area with the test results.

The information gained from these calculations was utilized in the follow-up calculation of Mr. J. Herterich within the framework of a thesis project [4]. The model used in this work is considerably more detailed in RDB and produced very good results compared to the test results.

2.1 HDR 1/3 initial calculation /3

The results of this calculation are used as a basis for the assessment of the effectiveness of the measures carried out in the continuation of this effort. Figure 2.1.1 shows the model used for this computer case. The RDB (VESSEL) is subdivided into 4 levels, which each consist of 2 radial rings and 4 azimuth segments so that each level includes 8 zones. The break nozzle is connected to zone 5 in level 4. In the model it consists of two pipes (PIPE 1 and PIPE 2). The exact differentiation can be seen in figure 2.3. The surroundings are simulated by a break component (break-boundary condition). The pressure drop is specified and proceeds linearly within 2 ms to 1 bar.

In figures 2.4 and 2.5 the calculation results from the 5 calculations are plotted in comparison with the data curves.

In the comparison of the calculated mass flux (figure 2.1.5) PIPE 2 CELL 5 (measurement location RM 3003/3004) with the data curve (figure 2.5), it can be seen immediately that in this case for 0.1 seconds the outflow rate is calculated more than twice as

high. The reason for this can be found in the boiler connection. The actually occurring outflow losses from the RDB because of the restriction in the nozzles are not taken into account by this model, so that an outflow velocity which is too high and correspondingly too high an outflow rate results .

From this also results the too rapid pressure loss in the RDB (see figure 2.4) which has almost reached the pressure level of the pipe after 0.1 second.

In figures 2.1.13 to 2.1.18, the pressure profiles are plotted against the pipe axis at different points in time for better visualization. The first point at the left in the picture is the zone 5 in which VESSEL-components are connected to the blowdown pipe. The last point in the right of the picture gives the pressure in the break. All graphs show a relatively linear pressure /4
drop. In particular, the area of the connection to the RDB shows no special effects of the pressure loss resulting from the restriction. The profile plots for the mass flux can be taken from figures 2.1.16 to 2.1.18. All profile plots, even in the following chapters, are always referenced to the same point in time so that a direct comparison is possible.

2.2 HDR 2/3 automatic boiler connection

In the following sections, we shall discuss in comparison to the previous chapter, different possibilities for the boiler connection and their effects on the outflow rate as well as the pressure curves. In this model (see figure 2.2.1), the calculation of the pressure loss resulting from the restriction and eddy formation in the exit opening is shifted to the pipe. This results from the fact that the boiler connection area within the first two zones is reduced to the cross-sectional area of the blowdown pipe. The TRAC program then determines for an appropriate input (minus sign in front of the NFF value in the TRAC input) the associated

ζ -value, whereby the flow direction determines whether we are dealing with a restriction or an expansion.

In the enlargement of the first two areas in the blowdown pipe the volume in these zones must also increase. However, this is not necessarily required because the TRAC input for determining the geometry is redundant. For each zone length and the inlet- resp. outlet area as well as the volume are specified.

From this it can be seen that the TRAC program does not automatically determine the volume from the area and the zone length, but that it uses the specified volume in the calculation.

The cross-sectional areas are used mainly for the calculation of the already mentioned ζ -values. It is thus possible to input the volumes corresponding to the specified geometry whereby, in the interest of an incontestable calculation, one should dispense with too great a change in the successive zone data so that a minor enlargement is possible which, however, could hardly affect the calculations. The figures 2.2.2 to 2.2.11 show the results from this calculation. From figure 2.4, one can recognize a relatively good agreement between the measured and the calculated curve shapes for the pressure. /5

In the blowdown nozzle (RP 3001/RP 3002) the pressure in the stable region lies ca. 10 bar below the data curve. This is an indication of the fact that the pressure loss in this model was calculated somewhat too high. The agreement in the curve of the mass flux in figure 2.5 is equally good.

Figures 2.2.12 to 2.2.17 again contain the profile plots for the pressure and the mass flux. One can readily recognize the kink in the curves where the pressure loss is determined based on the restriction. This produces a curve shape which is not linear in contrast to the calculation without this RDB connection.

Therefore, for better comparison, these curves from the two calculations are plotted together in figures 2.2.18 to 2.2.23.

In addition to the already mentioned differences one can see that the pressure drop in the first milliseconds between the first zone in RDB and the third zone in the pipe is not as great (dashed line) as in the calculation without the expanded connection (solid line). In contrast thereto, figure 2.2.20 shows that in the stationary region the pressure losses for the expanded connection to the RDB are considerably greater. These figures clearly show that without special measures no resistance coefficient is being used for the boiler connection.

2.3 HDR 3/3 automatic boiler connection with nozzle /6

With this model (figure 2.3.1) we shall examine more closely the effect of the boundary condition on the computer results. While in all other calculations a pressure discontinuity function which drops off linearly in 2 ms from the system pressure to 1 bar, is being used, the constant transition from system condition to surroundings (BREAK) takes place here. For this reason, a nozzle with an opening angle of 30° is inserted between BREAK-boundary condition and blowdown pipe. In order to avoid that, a water plug develops in the nozzle acts as a lay element; it is filled with steam. However, this leads to the need that for program-technical reasons, an instant pressure drop curve to 1 bar must be used in the calculation. Therefore, the time pressure curve in the first milliseconds exhibits a faster decrease to saturation pressure than in the measurement, which can be clearly seen from figure 2.4. Viewed as a whole, the calculated results agree best with the test results. For one, the outflow rate resulting from the increased outflow velocity (despite higher steam formation) deviates still less from the measured value (see figure 2.5) than is the case for HDR 2/3; and for another, the pressure level in the blowdown nozzle is increased somewhat so that the pressure steadily better

approaches the data curve.

In figures 2.3.2 to 2.3.11 all results for the blowdown pipe are plotted. Furthermore, the figures 2.3.12 to 2.3.14 present some information concerning the pressure, the temperature, and the discharge for the nozzle (PIPE 999).

Additionally, the results of this calculation for the pressure and the mass flux are contained in figures 2.3.15 to 2.3.20 in the form of profile plots. For this, figures 2.3.21 to 2.3.26 show the comparison with the first calculation.

The differences are to be found more in the highly transient region of the first five milliseconds, which points to a strong oscillation in pressure and a somewhat greater outflow rate.

2.4 HDR 4/5 and HDR 5/4 /7
Boiler connection = pipe cross-sectional area with and without ξ -value

For the sake of completeness two calculations shall still be mentioned which are intended to test an additional potential for the boiler connection.

Here in both cases the RDB is differentiated in such a way that the area of the connection zone corresponds exactly to the cross-sectional area of the pipe. Additionally in the calculation HDR 4/5 the annular space is divided into two annuli in order to obtain a better local resolution in the computer results and in order to additionally input a ξ -value for the outflow loss $\xi = 0.5$ in the first zone of the blowdown pipe (see section 2.4.1). The calculation HDR 5/4 (see figure 2.5.1), in contrast thereto, is carried out without these two changes.

A comparison of the calculated results in figure 2.4 shows that the shape of the curve for the pressure in the RDB is considerably worse than in the preceding calculation. The same is true for the mass flux whereby in particular the curve for the calculation HDR 5/4 deviates very greatly from the data curve. In figures 2.3.2 to 2.4.11 and 2.5.2 to 2.5.11 we have again plotted the result of the calculation.

The equal-area transition, whether with or without ζ-value brings about no noticeable improvement in the results, neither in the pressure curve nor in the mass flux.

3. Discussion of the result /8

If one compares the results of the calculation for pressure and mass flux plotted in figures 2.4 and 2.5 with the data curve, one can see that the calculation HDR 3/3 gives the best fit with the data curve.

The deciding measure for improvement of the computer results is obtained by the enlarged connection of the pipes to the RDB.

Similarly, certain improvements of the results are obtained with the nozzle, but not to the same degree.

Without taking into account a resistance coefficient through the reduction of the flow surfaces, the TRAC program can calculate no pressure loss for the loss-affected flow out of the RDB.

4. References

[1] G. Hughes
TRAC-P1A Operational Start on the CYBER 176
KWU-Work Report R 11/2113/79

[2] TRAC-PD2
An Advanced Best Estimate Computer Program for PWR LOCA Analysis
Los Alamos Scientific Laboratory
NUREG/CR-2054

[3] HDR-Safety Program
4. Status Report Dec. 10, 1980
Nuclear Research Center Karlsruhe
PHDR-Work Report 3/5/80

[4] J. Herterich
Verification calculation for the program system TRAC-PD2 with the aid of some tests, either through measurements or analyses
Thesis
Bochum-Erlangen, April 81

HDR Test Series /:

Chapter 2.1 HDR 1/3 1. calculation/boiler variation 3 (see figure 2.1.:
area ratio $F_{KR} = \frac{\text{boiler connection area}}{\text{pipe area}} =$
$\frac{0.66954\ m^2}{0.03142\ m^2} = 21.309$
pressure- boundary condition in 2 ms to 1 bar

Chapter 2.2 HDR 2/3 2. calculation/boiler variation 3 (s. figure 2.2.1)
area ratio $F_{KR} = 1$ through enlargement of the pipe
area within two zones to boiler connection area
pressure-boundary condition in 2 ms to 1 bar

Chapter 2.3 HDR 3/3 3. calculation/boiler variation 3 (s. fig. 2.3.1)
area ratio $F_{KR} = 1$ same as HDR 2/3
with nozzle at the break opening
pressure-boundary condition instantaneous pressure
drop to 1 bar

Chapter 2.4 HDR 4/5 4. calculation/boiler variation 5 (s. fig. 2.4.1)
area ratio $F_{KR} = 1$ through proper choice of the boiler
subdivision (no enlargement of the pipe)
2 radial zones in annular space
input of a resistance coefficient for the outflow from
the boiler $\zeta = 0.5$
pressure-boundary condition in 2 ms to 1 bar

HDR 5/4 5. calculation/boiler variation 4 (s. fig. 2.5.1)
area ratio $F_{KR} = 1$ as in HDR 4/5 but only 1 radial
zone in annular space
pressure-boundary condition in 2 ms to 1 bar

Table 2.1

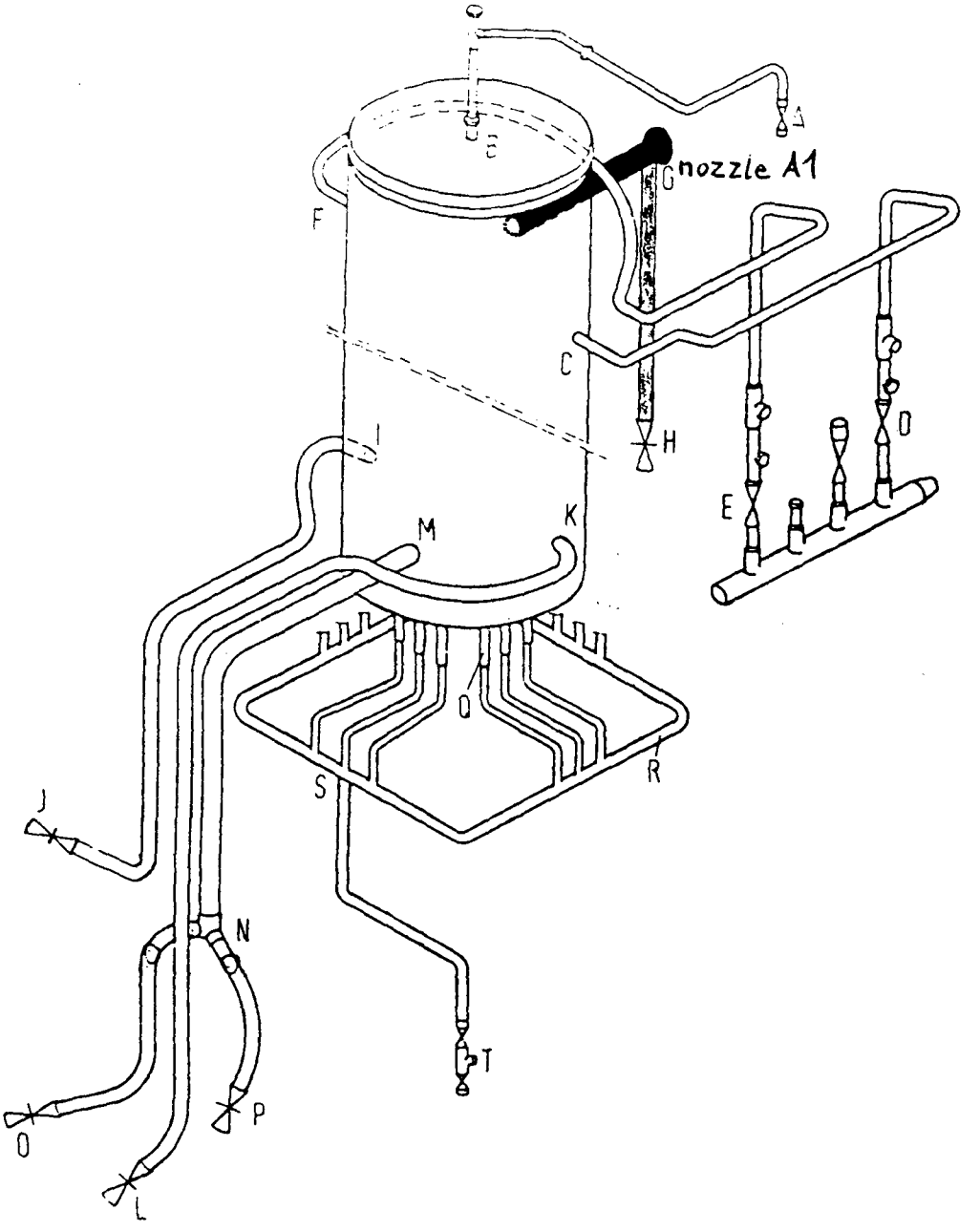

Schematic Isometry of Lines and Loops Participating During Blowdown

Fig. 2.1

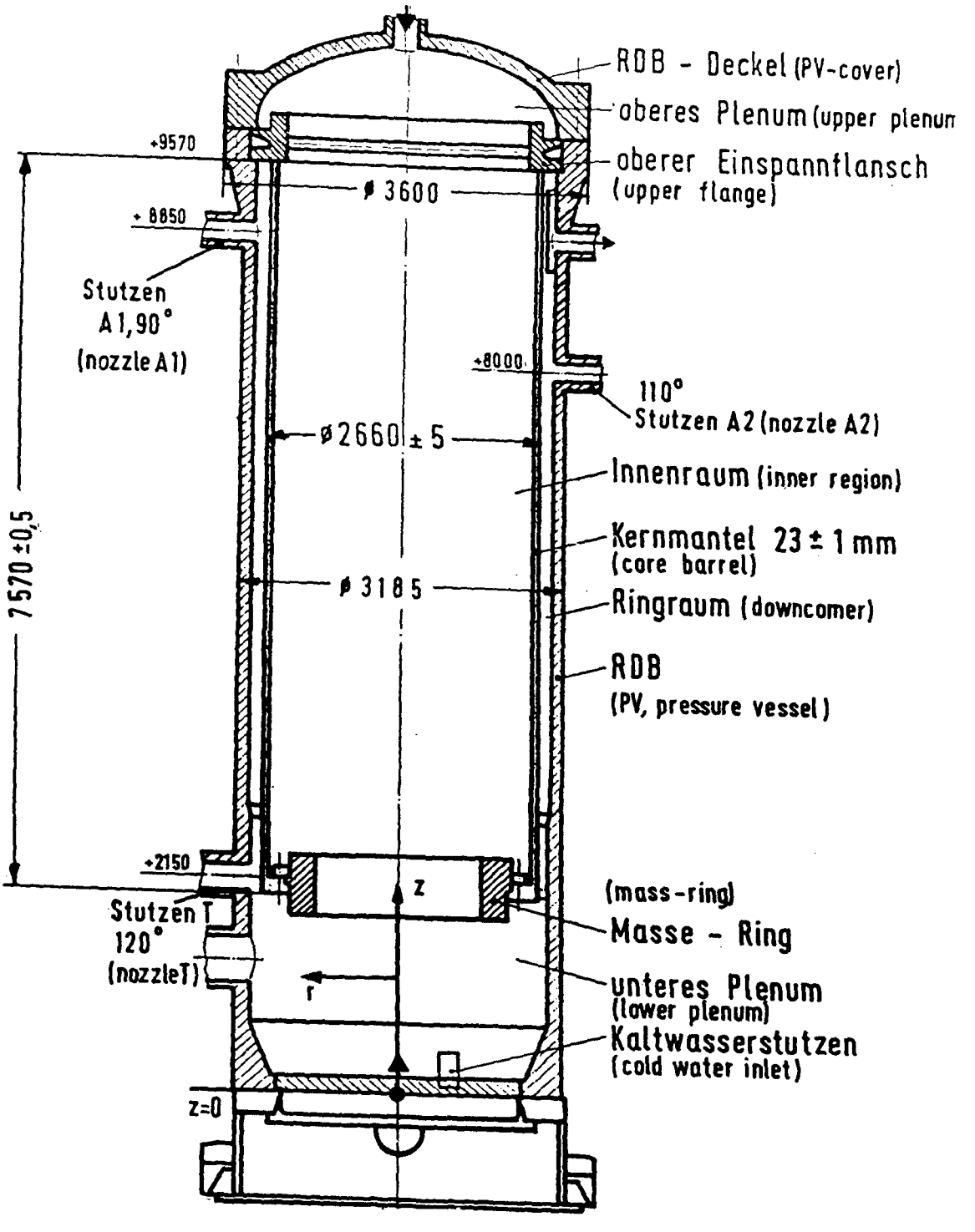

RPV AND SHROUDGEOMETRY FOR THE BLOWDOWN EXPERIMENT

Fig. 2.2

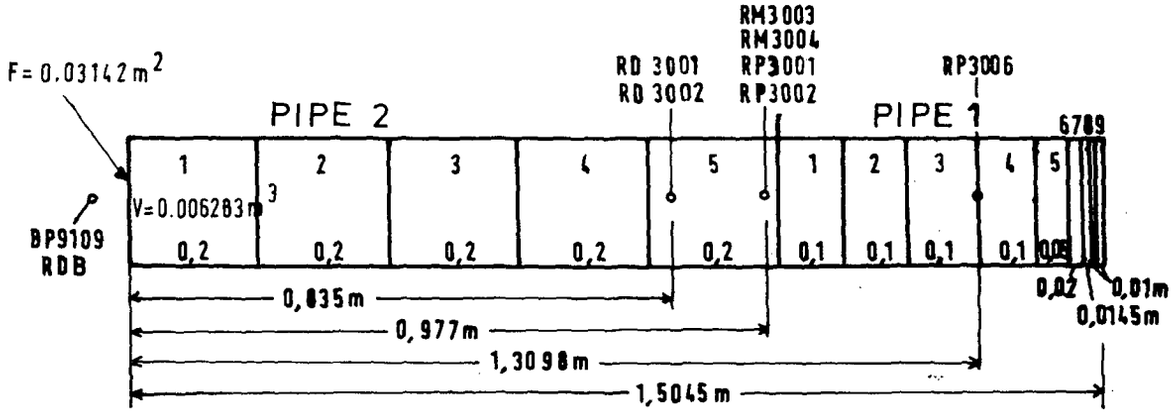

BREAK NOZZLE FOR THE MODELS HDR 1/3 4/5 5/4

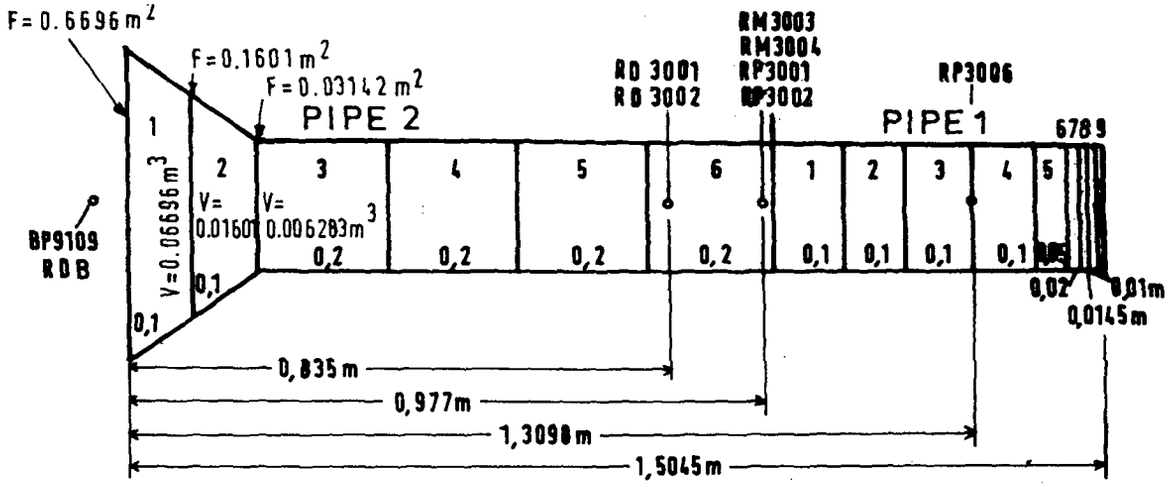

BREAK NOZZLE FOR THE MODELS HDR 2/3 3/3

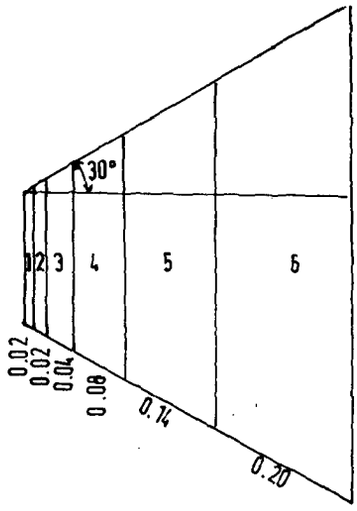

BREAK ORIFICE FOR THE MODEL HDR 3/3

Fig. 2.3

KWU TRAC - PD2

THE EFFECT OF DIFFERENT PARAMETERS

RECALCULATION OF THE HDR-TESTS WITH THE VESSEL COMPONENT

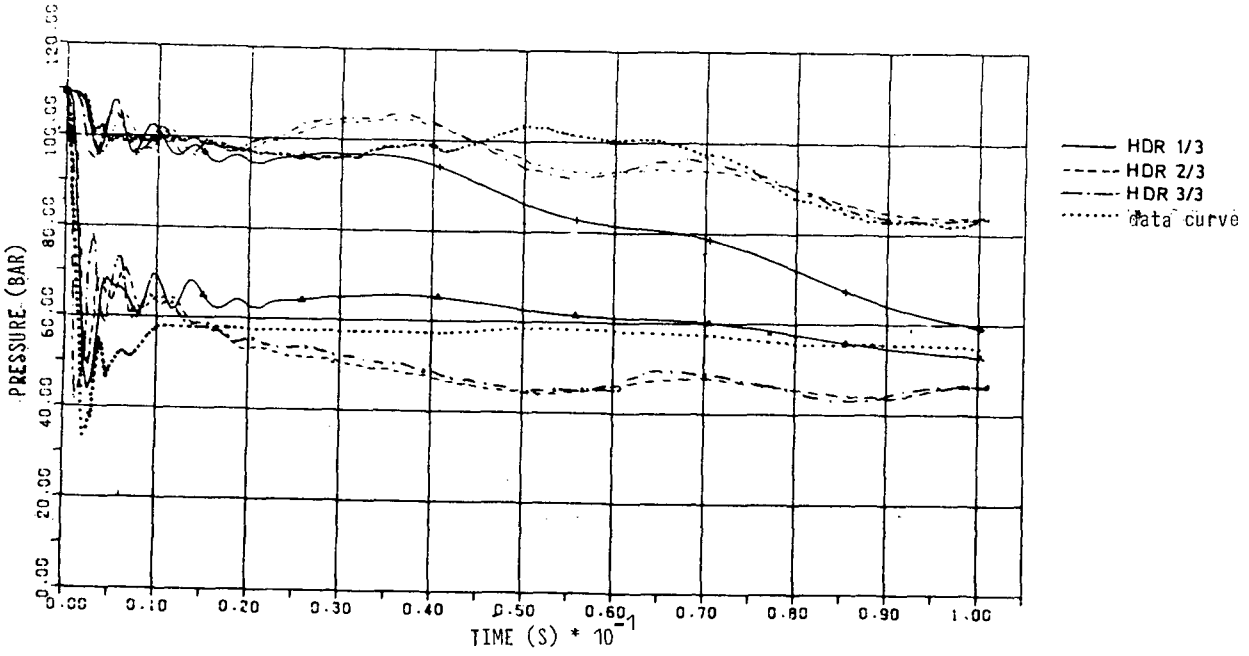

PRESSURE

KWU TRAC - PD2

THE EFFECT OF DIFFERENT PARAMETERS

RECALCULATION OF THE HDR-TESTS WITH THE VESSEL COMPONENT

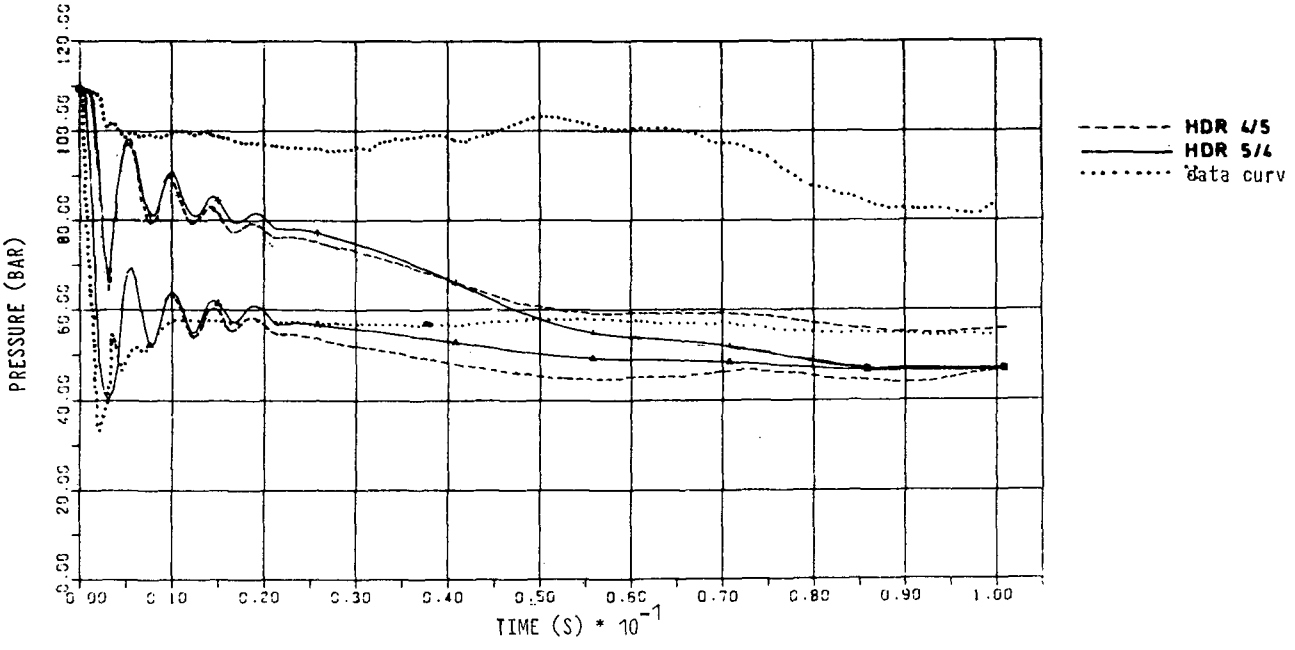

PRESSURE

Fig. 2.4

KWU TRAC - PD2

THE EFFECT OF DIFFERENT PARAMETERS

RECALCULATION OF THE HDR-TESTS WITH THE VESSEL COMPONENT

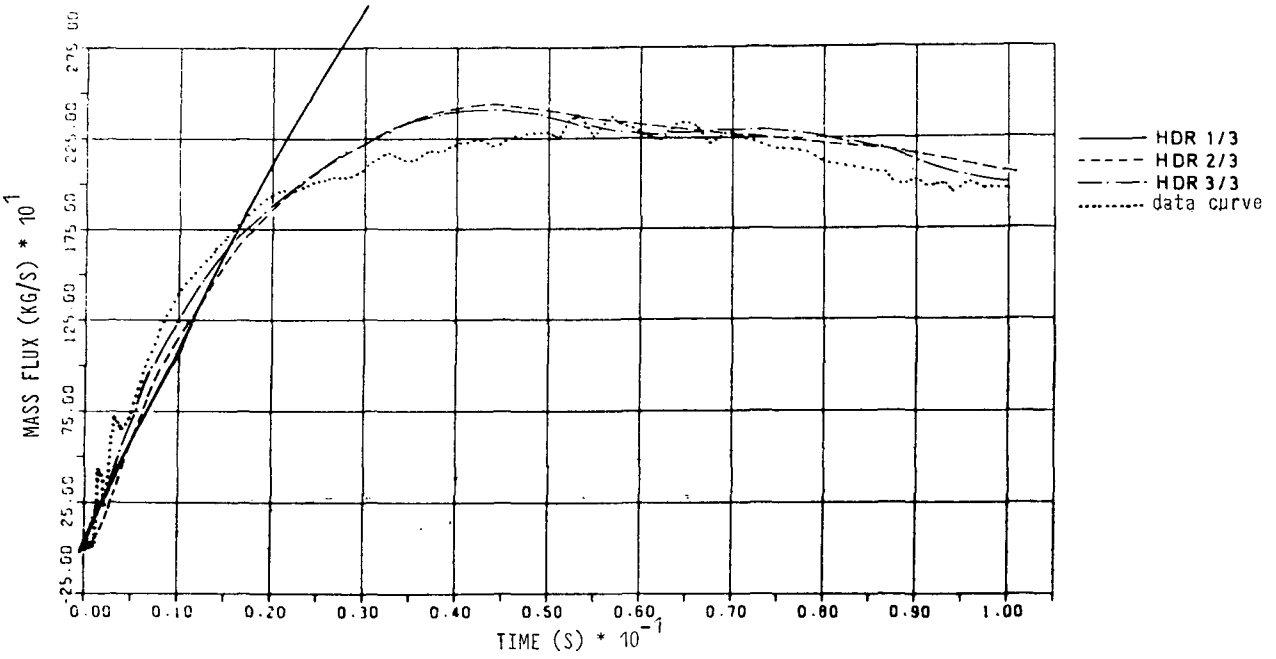

MASS FLUX

KWU TRAC - PD2

THE EFFECT OF DIFFERENT PARAMETERS

RECALCULATION OF THE HDR-TESTS WITH THE VESSEL COMPONENT

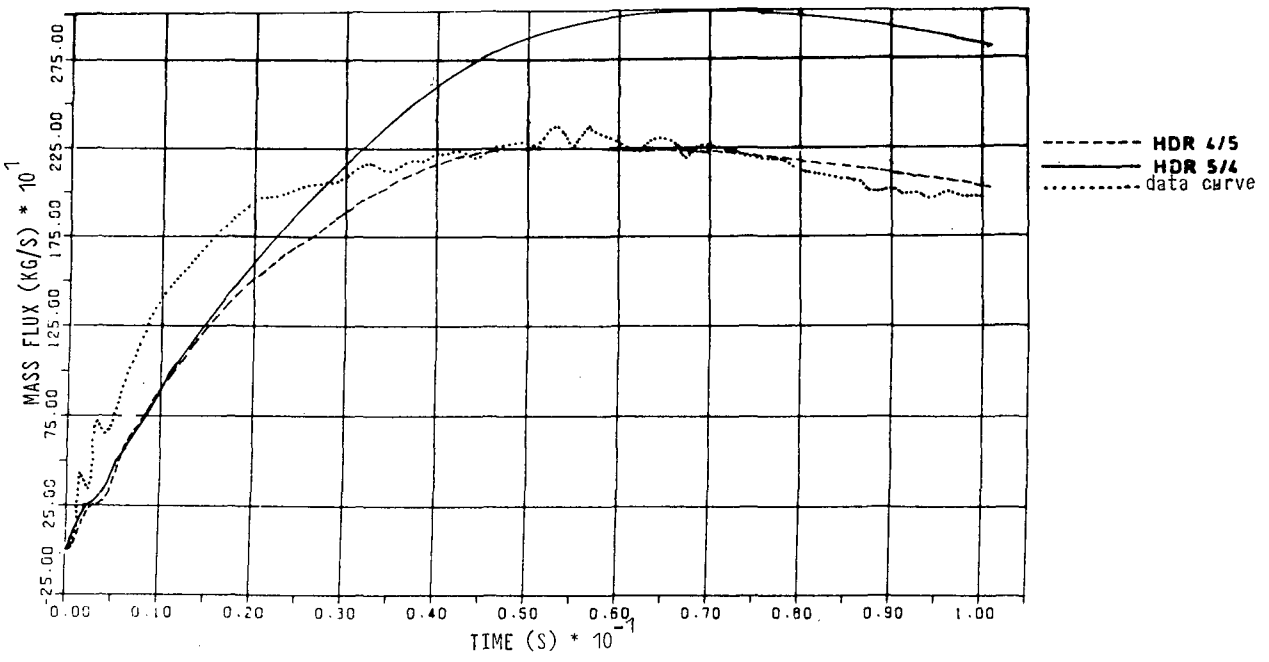

MASS FLUX

Fig. 2.5

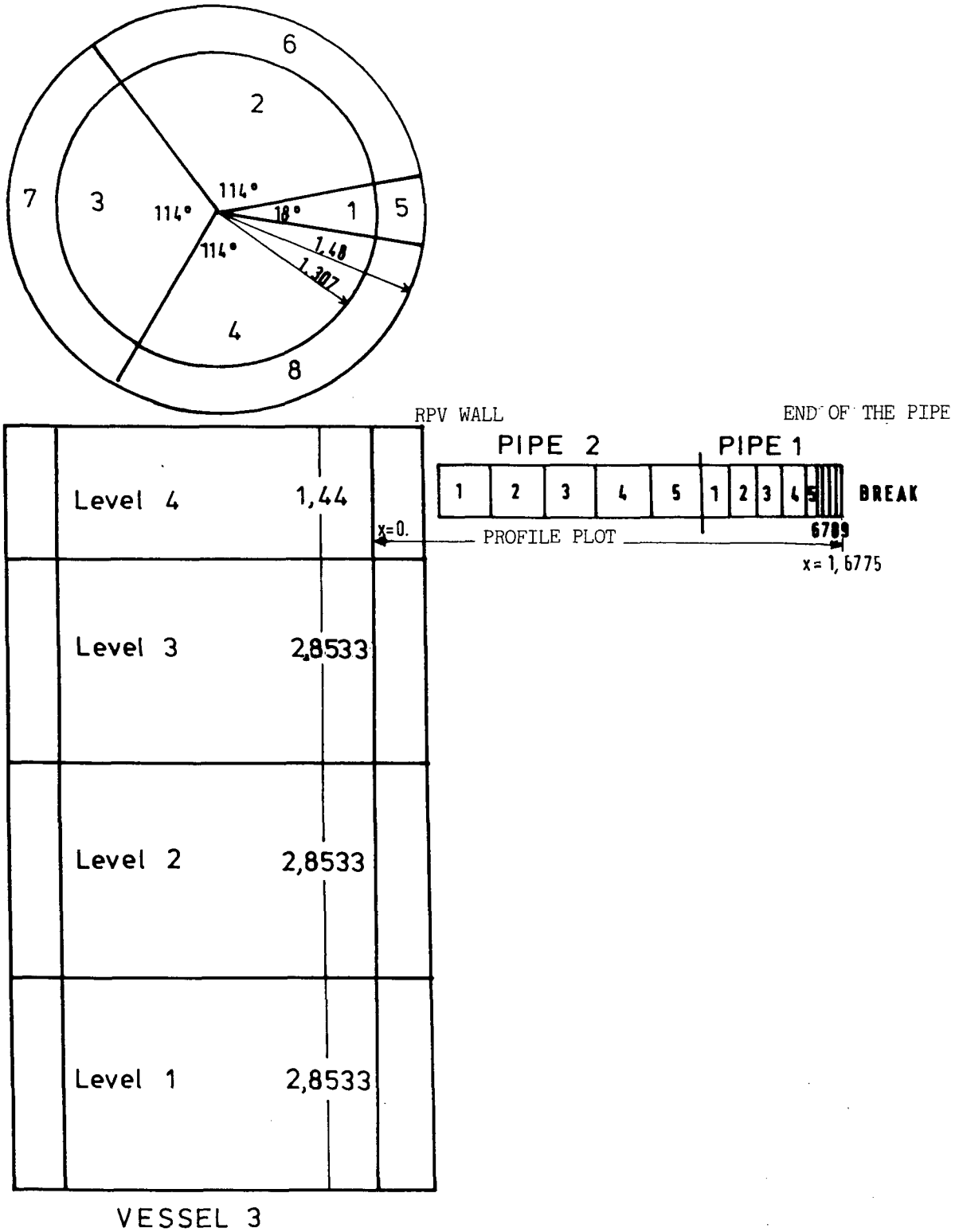

HDR 1/3

Fig. 2.1.1

KWU TRAC - PD2

THE EFFECT OF DIFFERENT PARAMETERS ON THE OUTFLOW RATE

RECALCULATION OF THE HDR-TESTS WITH THE VESSEL COMPONENT

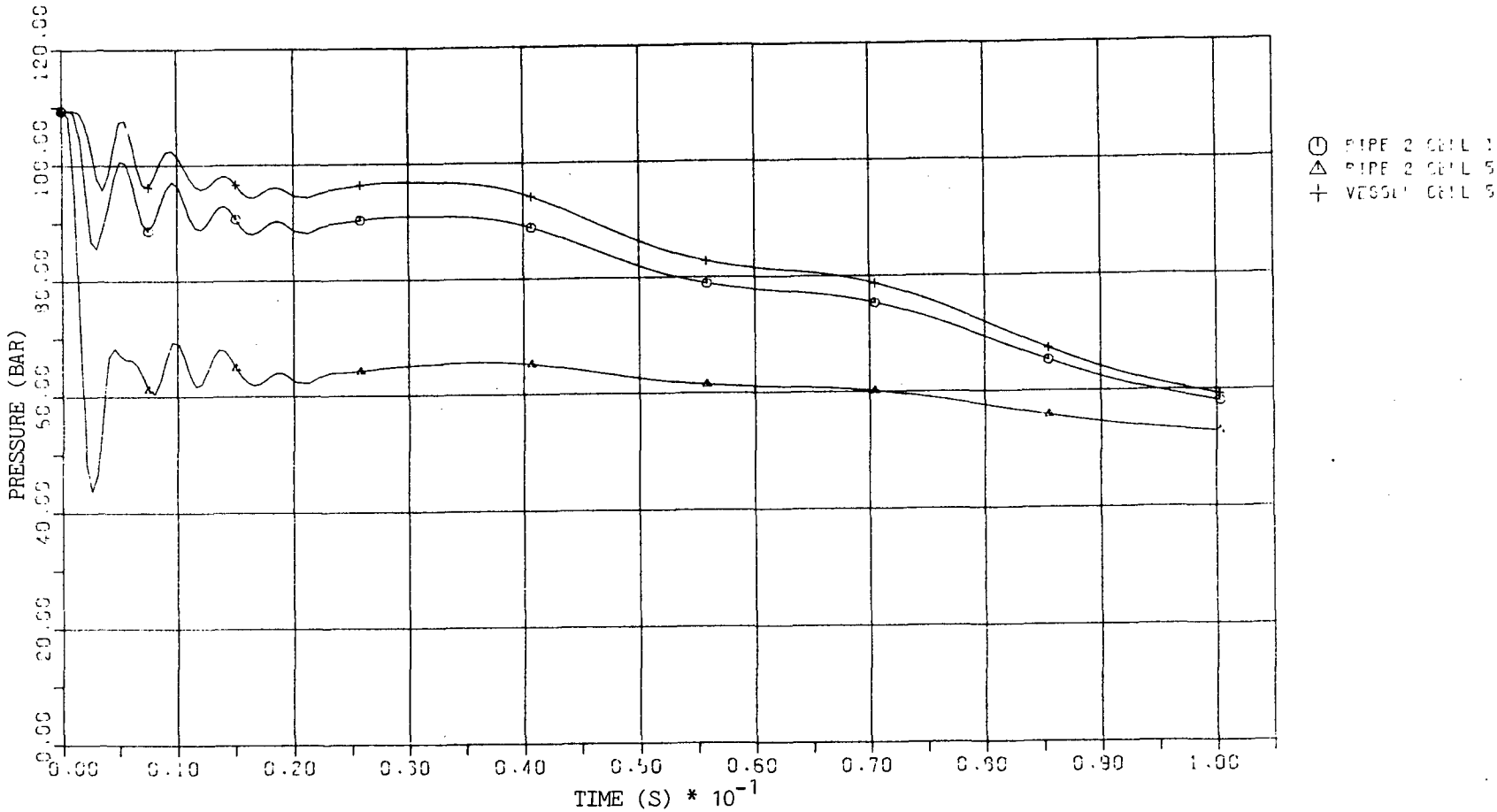

PIPE 2 / VESSEL TYPE 3

PRESSURE

Fig. 2.1.2

KWU TRAC - PD2

THE EFFECT OF DIFFERENT PARAMETERS ON THE OUTFLOW RATE

RECALCULATION OF THE HDR-TESTS WITH THE VESSEL COMPONENT

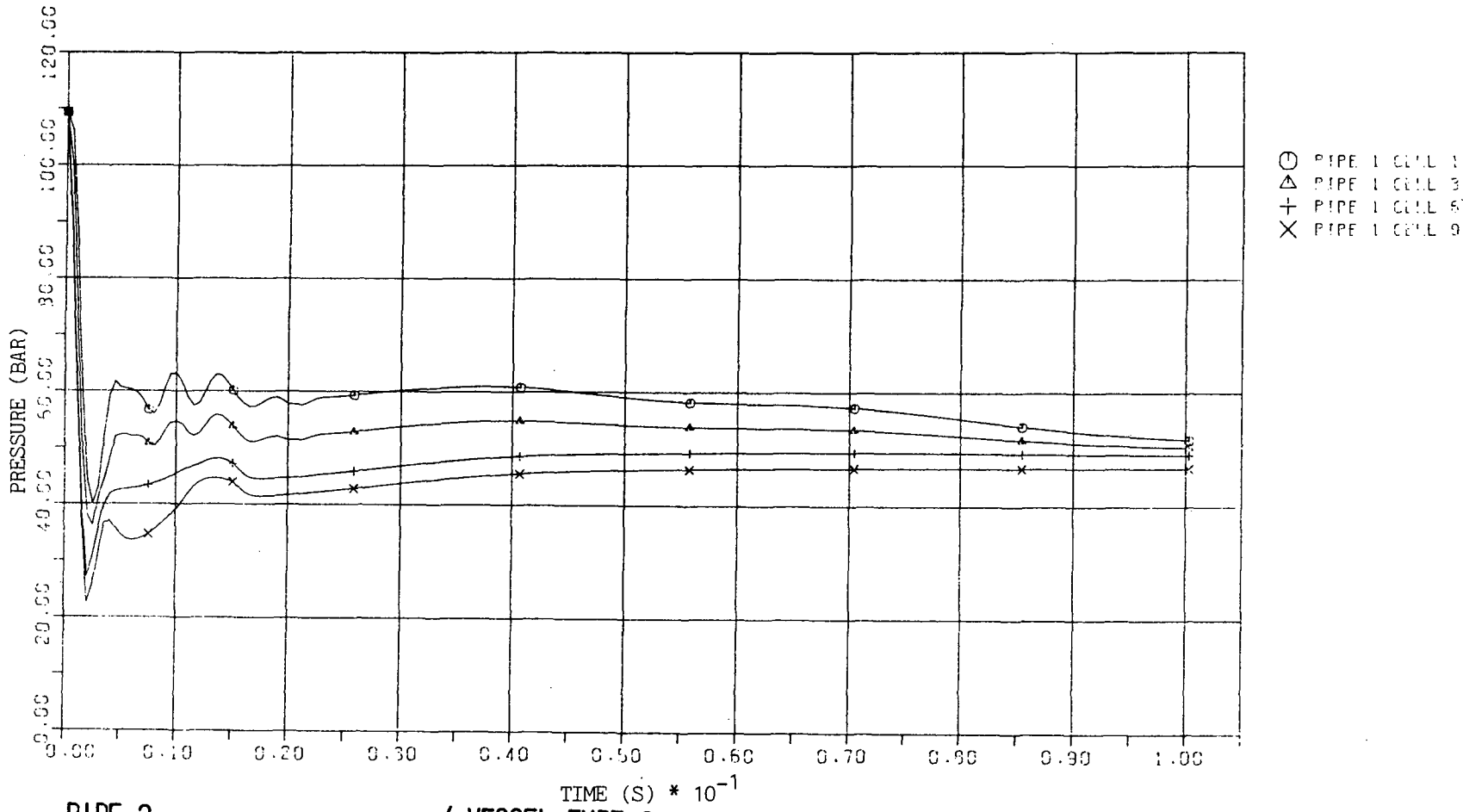

PIPE 2 / VESSEL TYPE 3

PRESSURE

Fig. 2.1.3

KWU TRAC -PD2

THE EFFECT OF DIFFERENT PARAMETERS ON THE OUTFLOW RATE

RECALCULATION OF THE HDR-TESTS WITH THE VESSEL COMPONENT

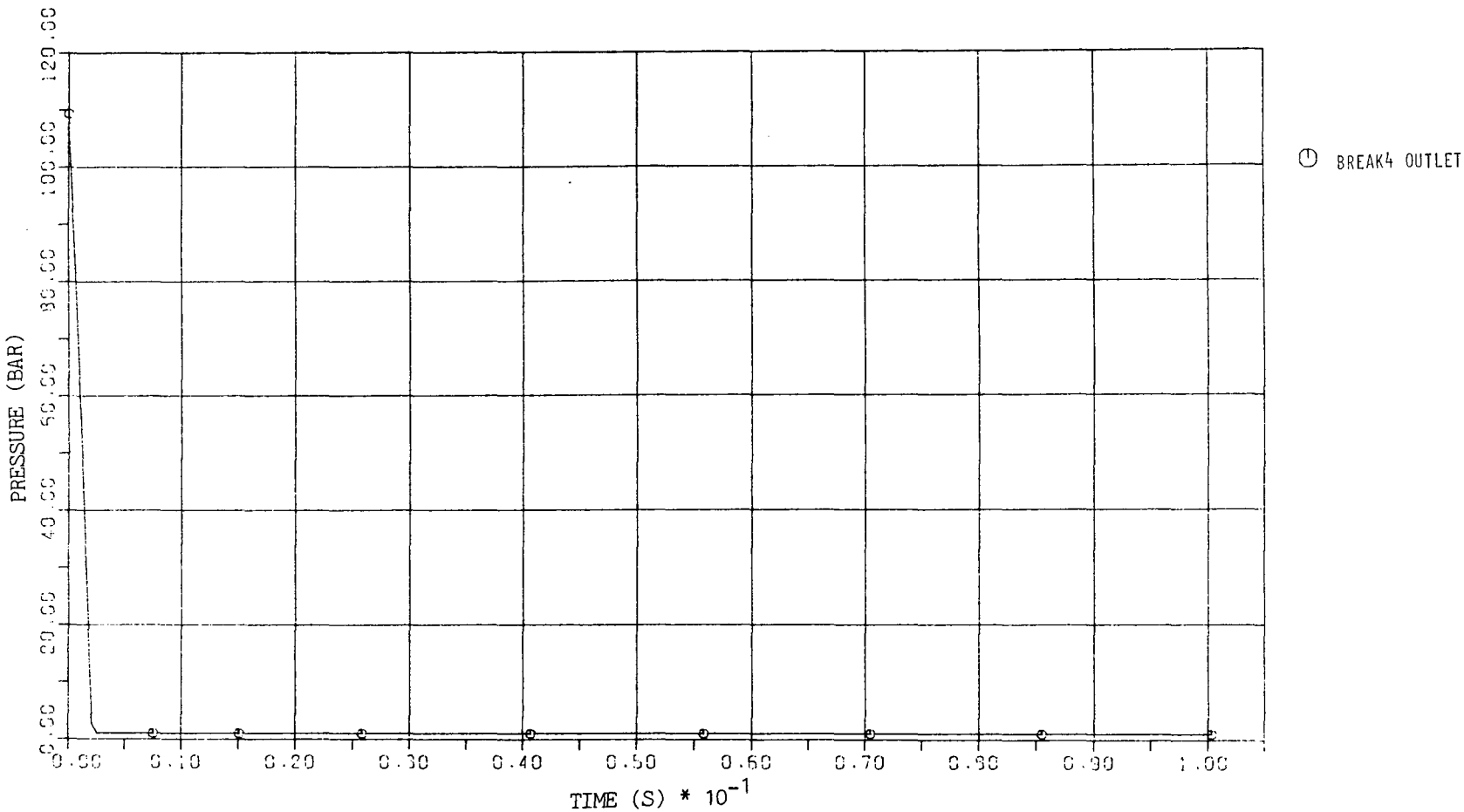

PIPE 2 / VESSEL TYPE 3

PRESSURE

Fig. 2.1.4

KWU TRAC - PD2

THE EFFECT OF DIFFERENT PARAMETERS ON THE OUTFLOW RATE

RECALCULATION OF THE HDR-TESTS WITH THE VESSEL COMPONENT

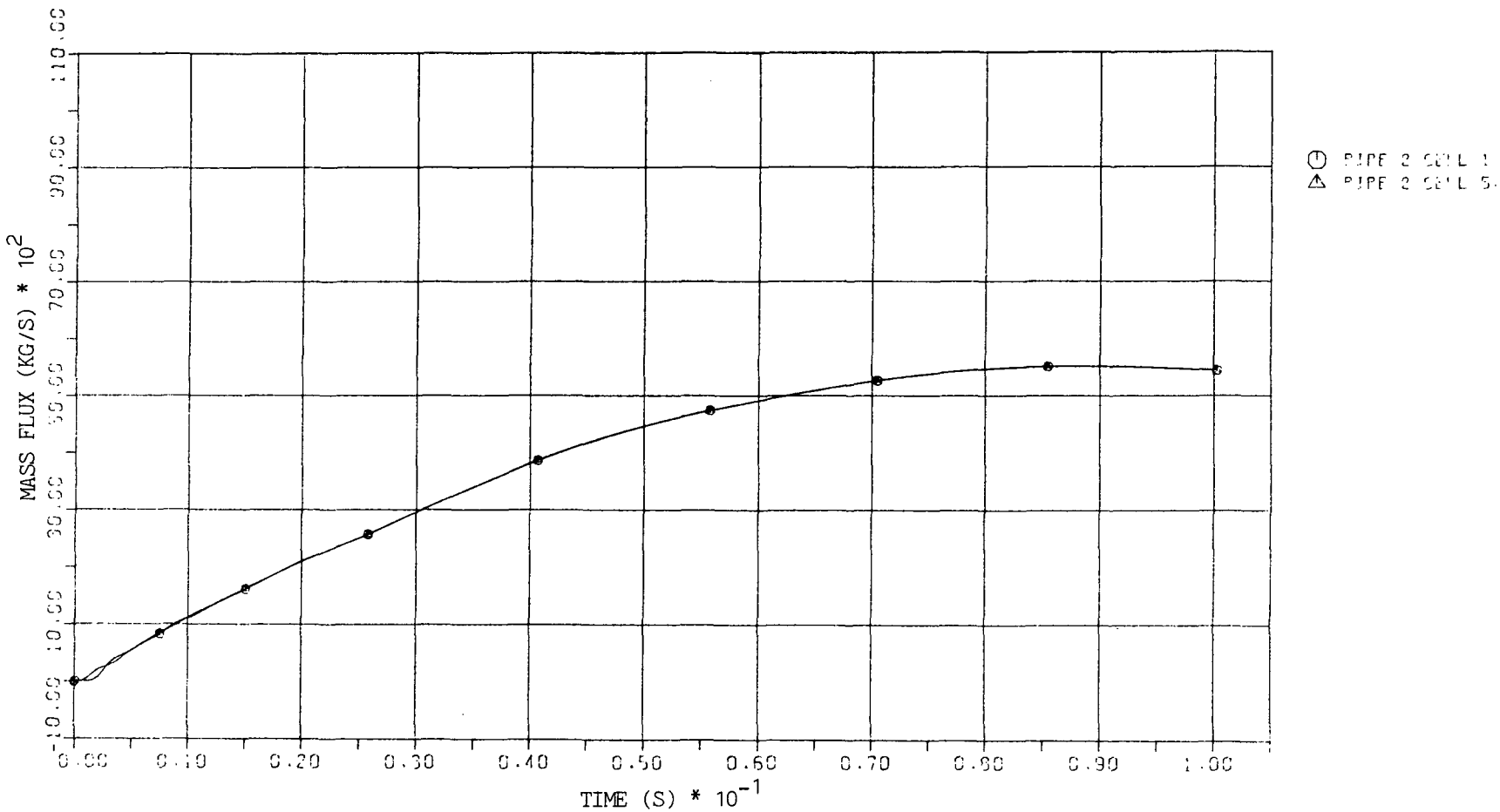

PIPE 2 / VESSEL TYPE 3

MASS FLUX

Fig. 2.1.5

KWU TRAC - PD2

THE EFFECT OF DIFFERENT PARAMETERS ON THE OUTFLOW RATE

RECALCULATION OF THE HDR-TESTS WITH THE VESSEL COMPONENT

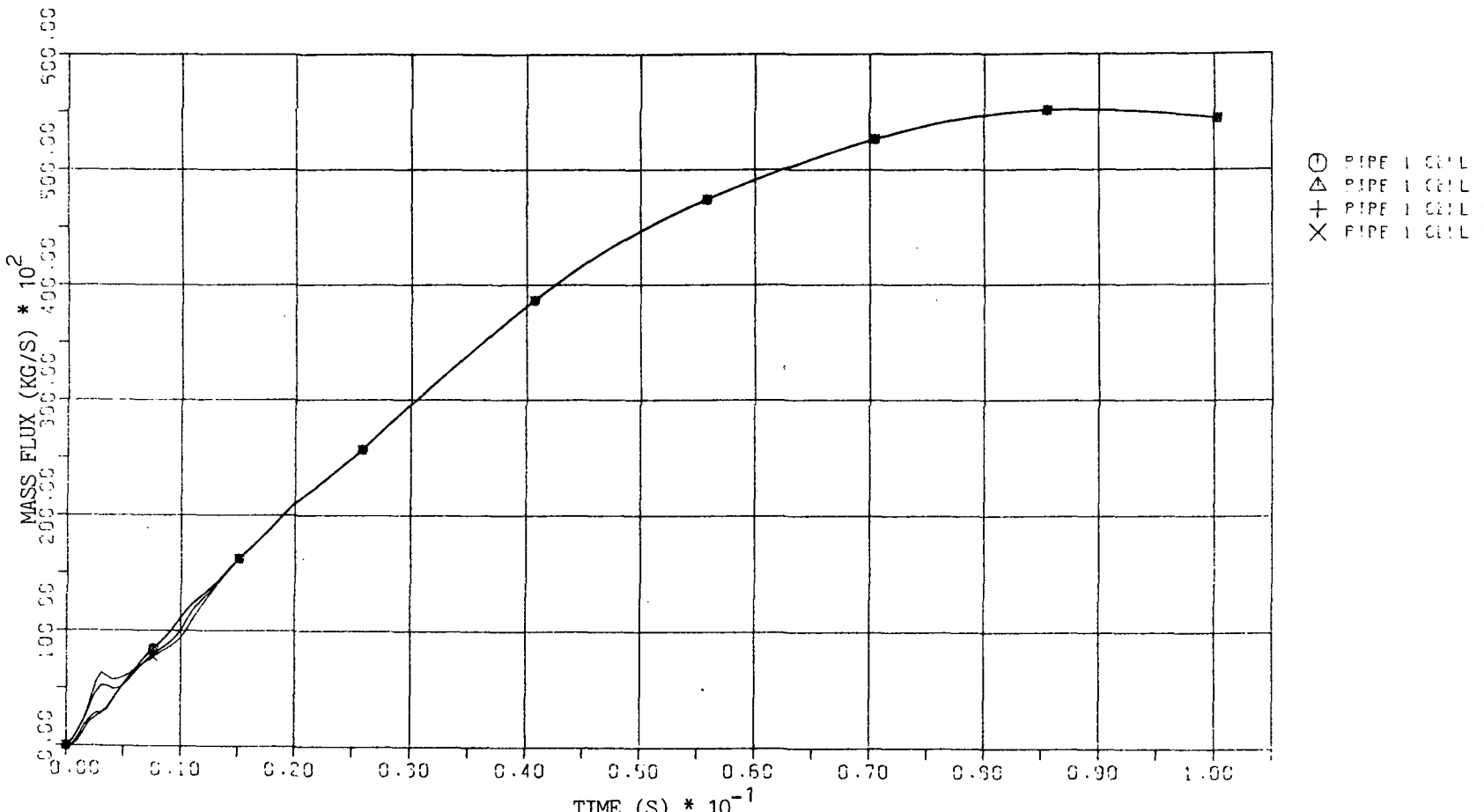

PIPE 2 / VESSEL TYPE 3

MASS FLUX

Fig. 2.1.6

KWU TRAC - PD2

THE EFFECT OF DIFFERENT PARAMETERS ON THE OUTFLOW RATE

RECALCULATION OF THE HDR-TESTS WITH THE VESSEL COMPONENT

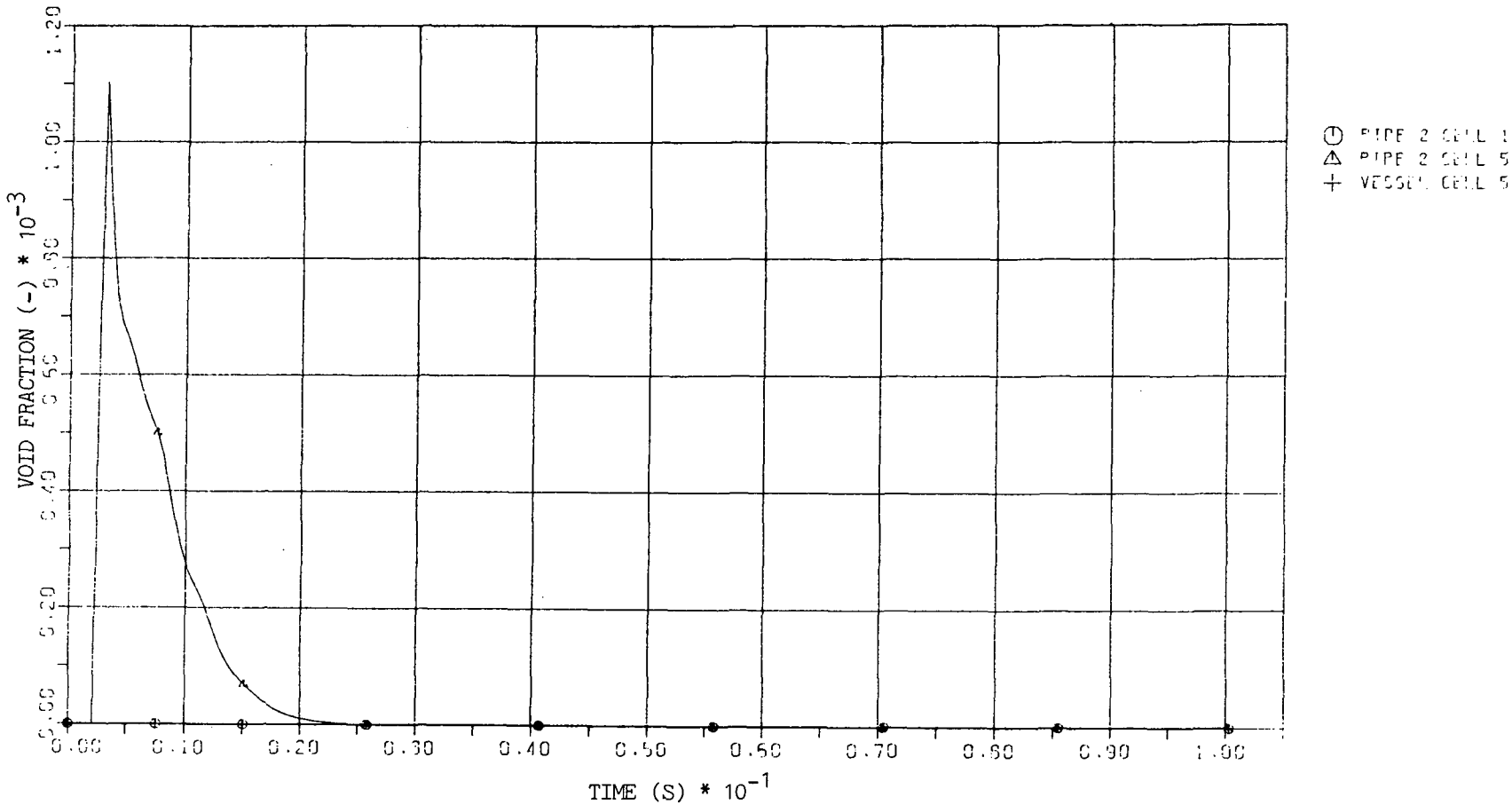

PIPE 2 / VESSEL TYPE 3

VOID FRACTION

Fig. 2.1.7

KWU TRAC - PD2

THE EFFECT OF DIFFERENT PARAMETERS ON THE OUTFLOW RATE

RECALCULATION OF THE HDR-TESTS WITH THE VESSEL COMPONENT

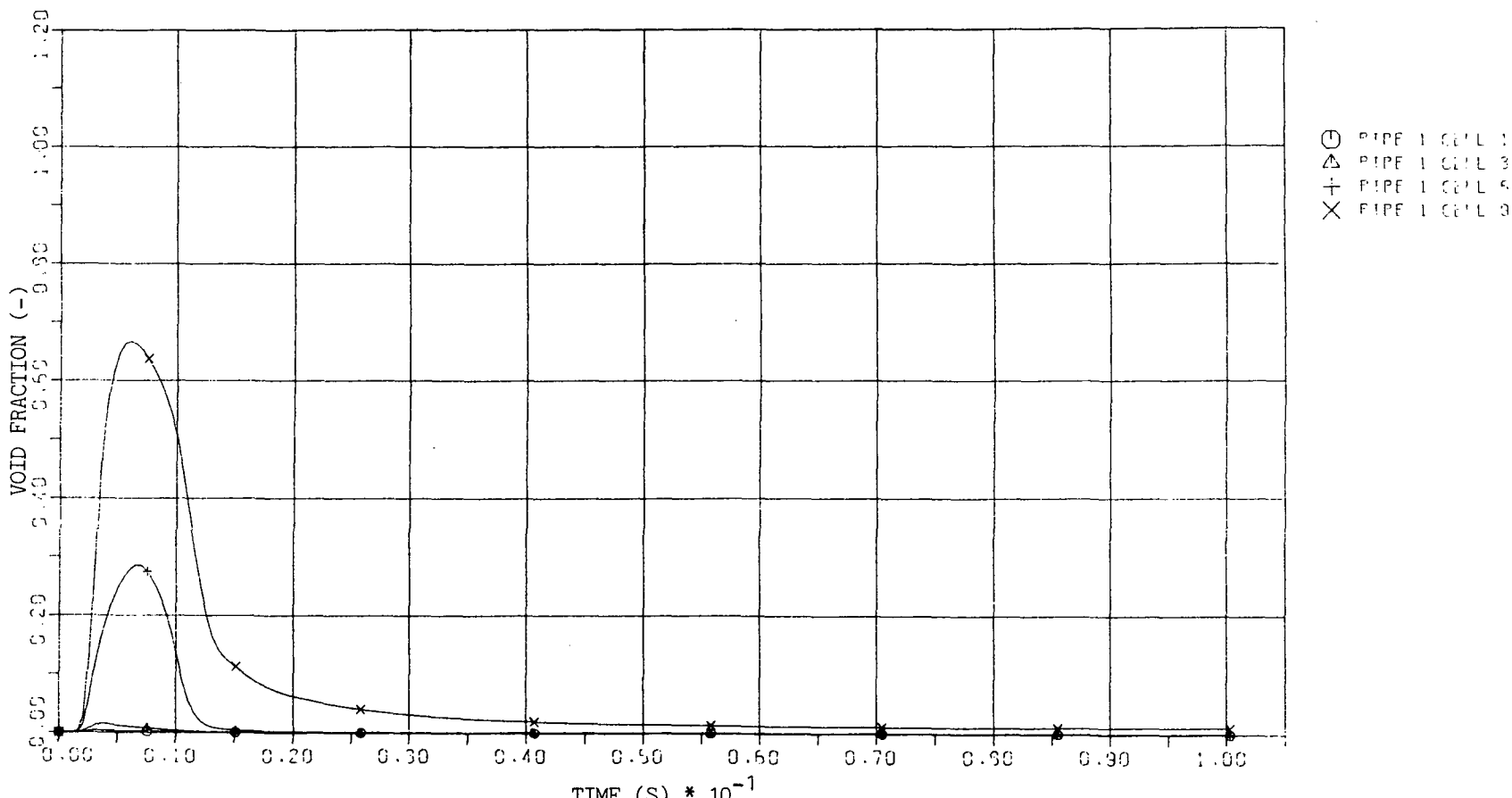

PIPE 2 / VESSEL TYPE 3

VOID FRACTION

Fig. 2.1.8

KWU TRAC -PD2

THE EFFECT OF DIFFERENT PARAMETERS ON THE OUTFLOW RATE

RECALCULATION OF THE HDR-TESTS WITH THE VESSEL COMPONENT

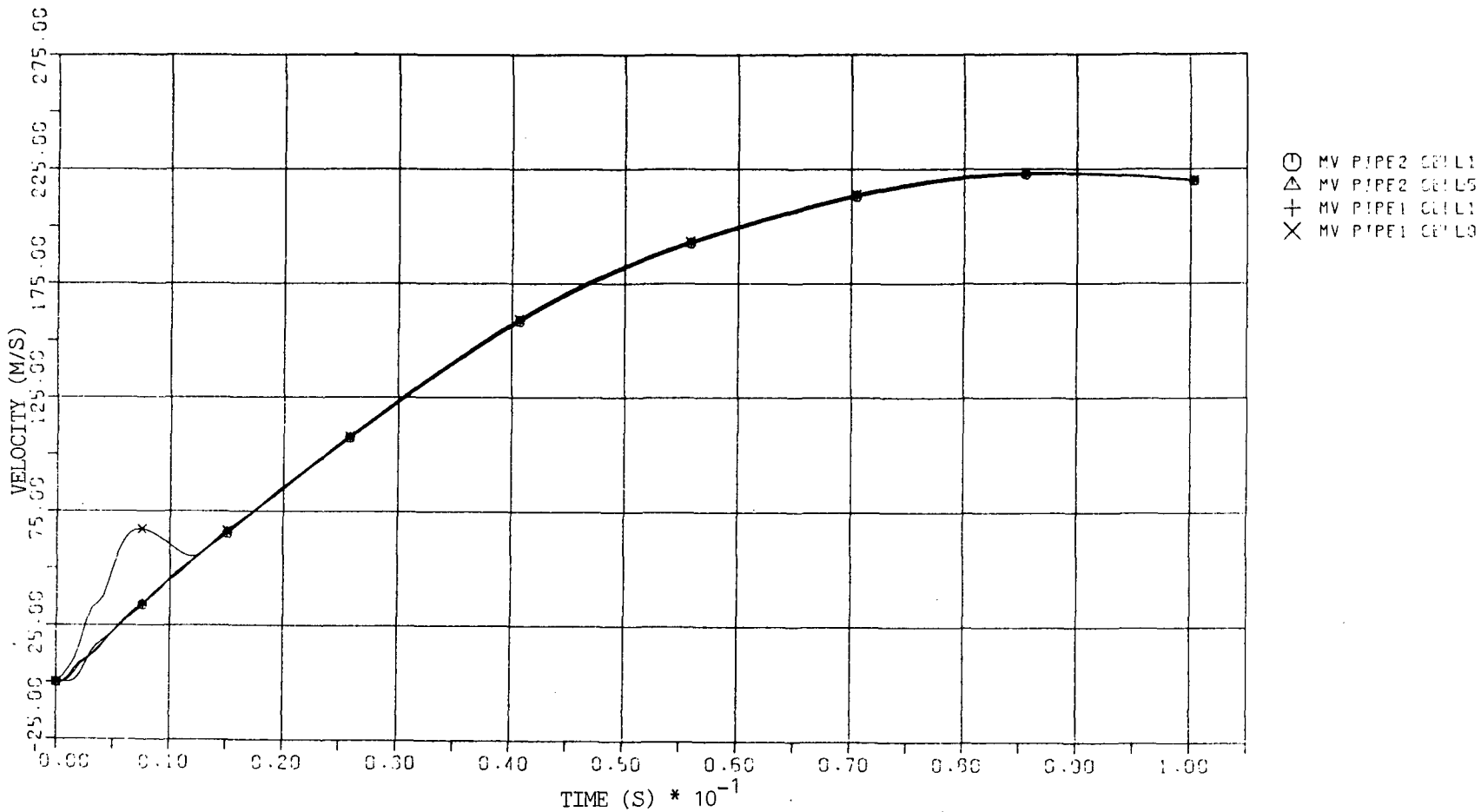

PIPE 2 / VESSEL TYPE 3

VELOCITY

Fig. 2.1.9

KWU TRAC - PD2

THE EFFECT OF DIFFERENT PARAMETERS ON THE OUTFLOW RATE

RECALCULATION OF THE HDR-TESTS WITH THE VESSEL COMPONENT

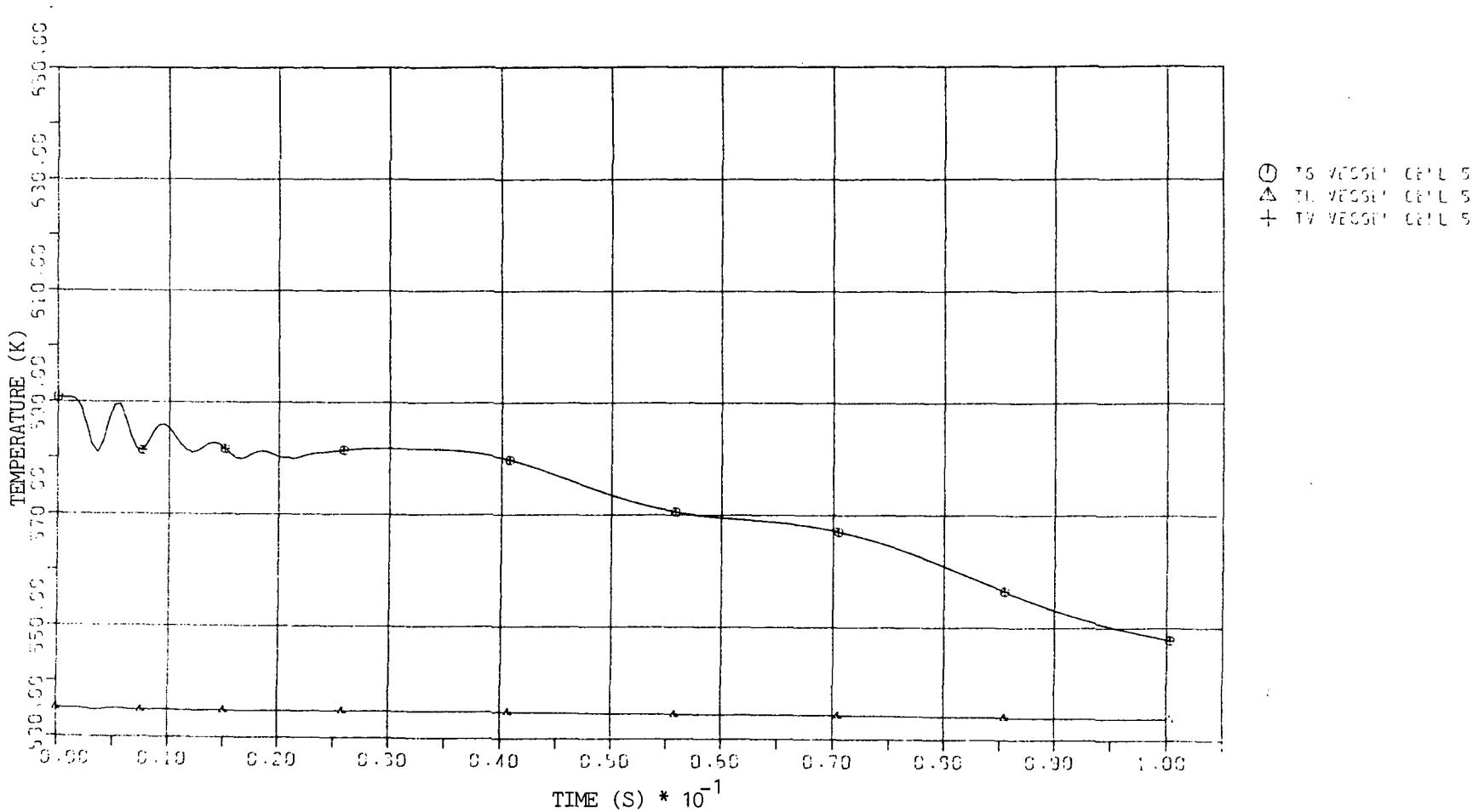

PIPE 2 / VESSEL TYPE 3

TEMPERATURE

Fig. 2.1.10

KWU TRAC - PD2

THE EFFECT OF DIFFERENT PARAMETERS ON THE OUTFLOW RATE

RECALCULATION OF THE HDR-TESTS WITH THE VESSEL COMPONENT

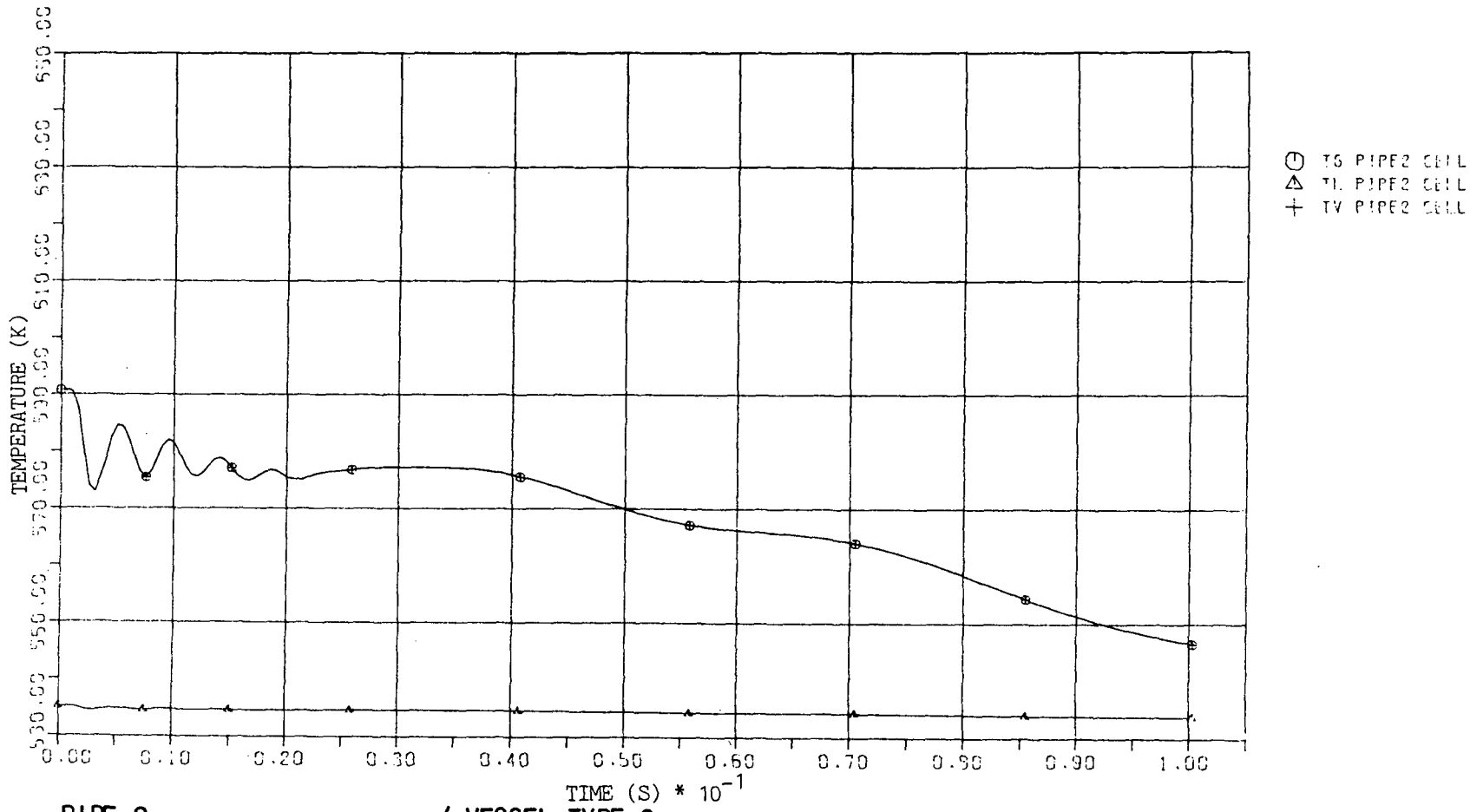

PIPE 2 / VESSEL TYPE 3

TEMPERATURE

Fig. 2.1.11

KWU TRAC - PD2

THE EFFECT OF DIFFERENT PARAMETERS ON THE OUTFLOW RATE

RECALCULATION OF THE HDR-TESTS WITH THE VESSEL COMPONENT

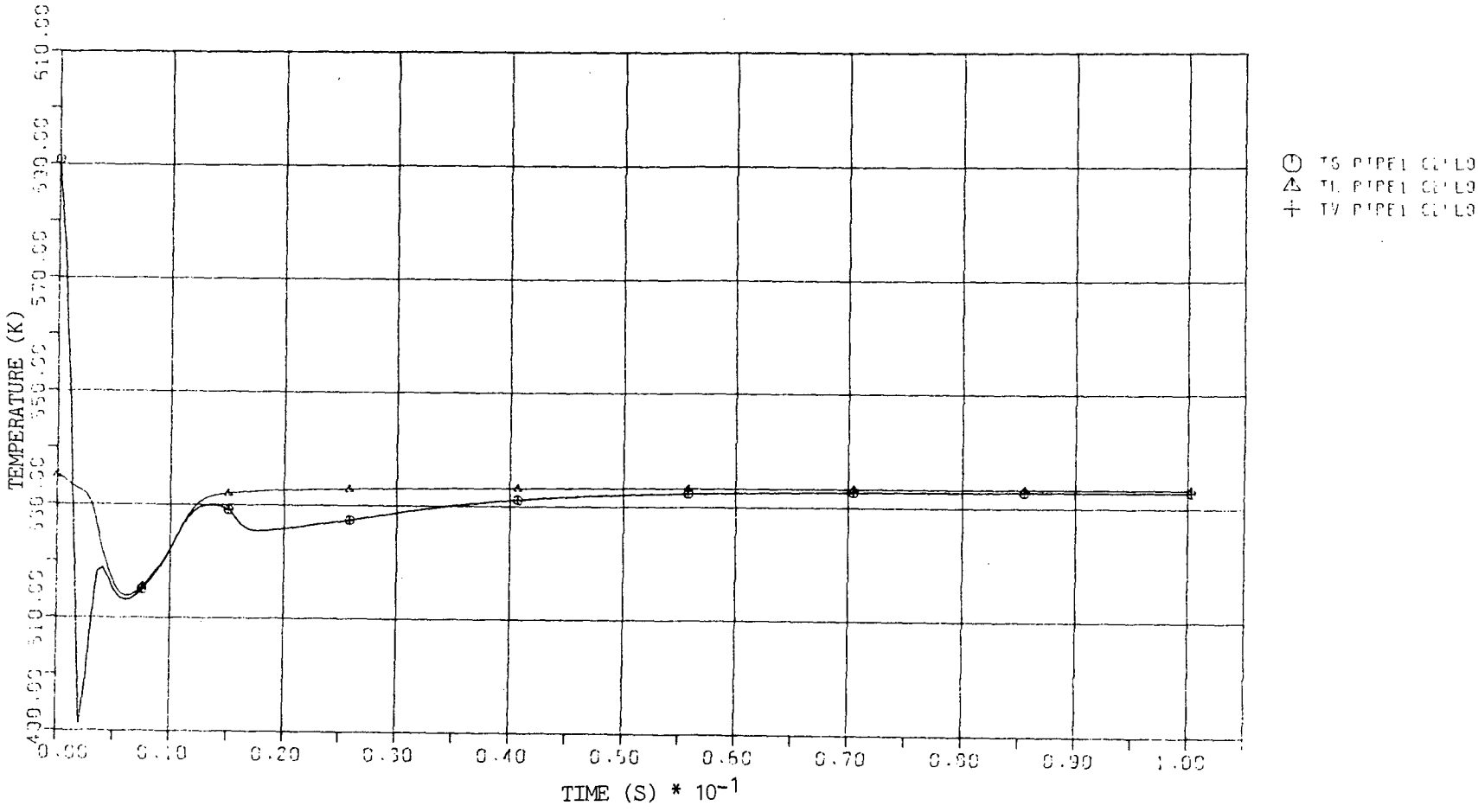

PIPE 2 / VESSEL TYPE 3

TEMPERATURE

Fig. 2.1.12

KWU PROFILE PLOT TRAC - PD2 PARAMETER STUDY

THE EFFECT OF DIFFERENT PARAMETERS ON THE PRESSURE

AND THE MASS FLUX

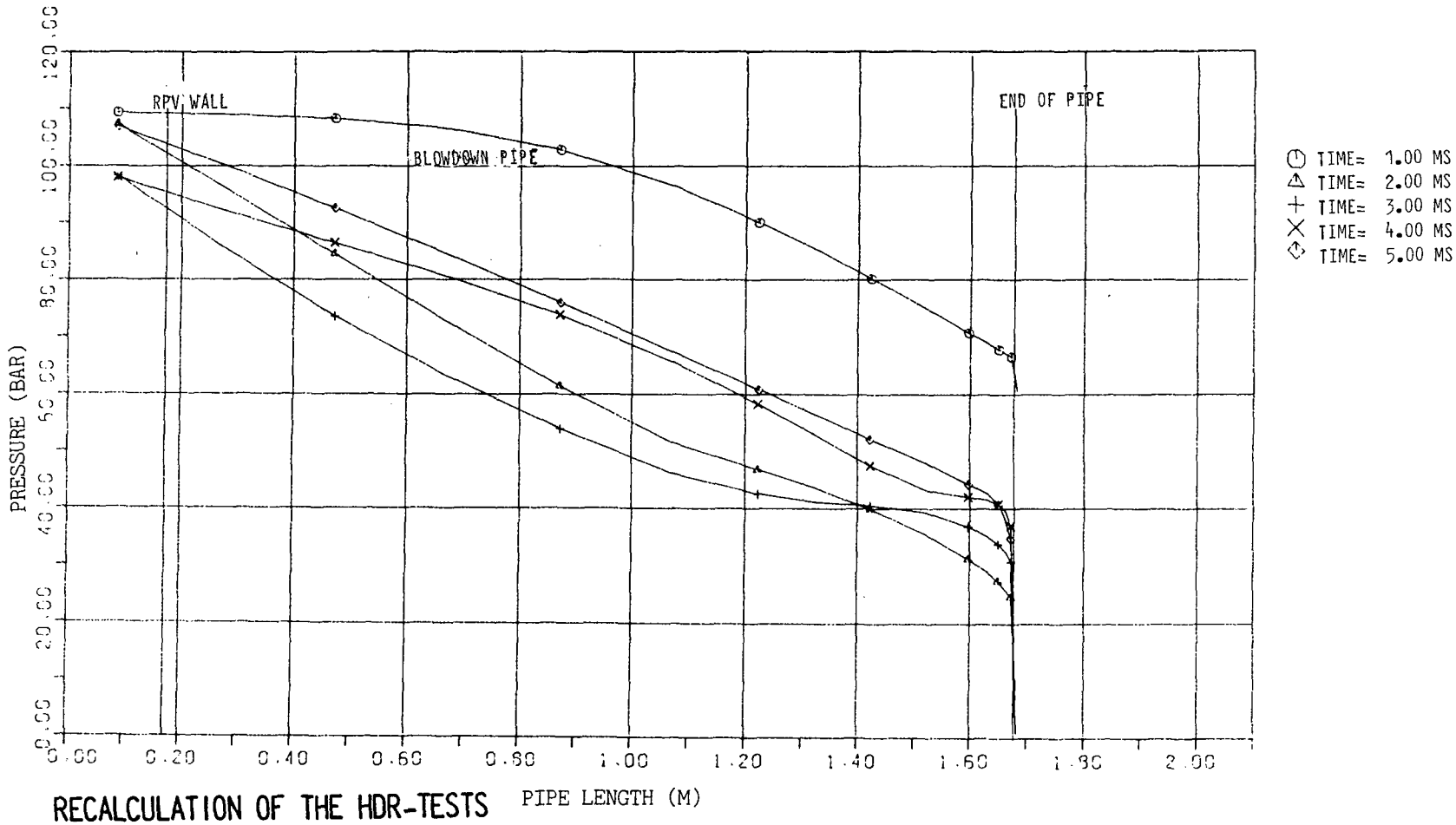

RECALCULATION OF THE HDR-TESTS

PRESSURE WITHOUT ORIFICE AND WITHOUT EXPANSION AT THE RPV

Fig. 2.1.13

KWU PROFILE PLOT TRAC - PD2 PARAMETER STUDY

THE EFFECT OF DIFFERENT PARAMETERS ON THE PRESSURE

AND THE MASS FLUX

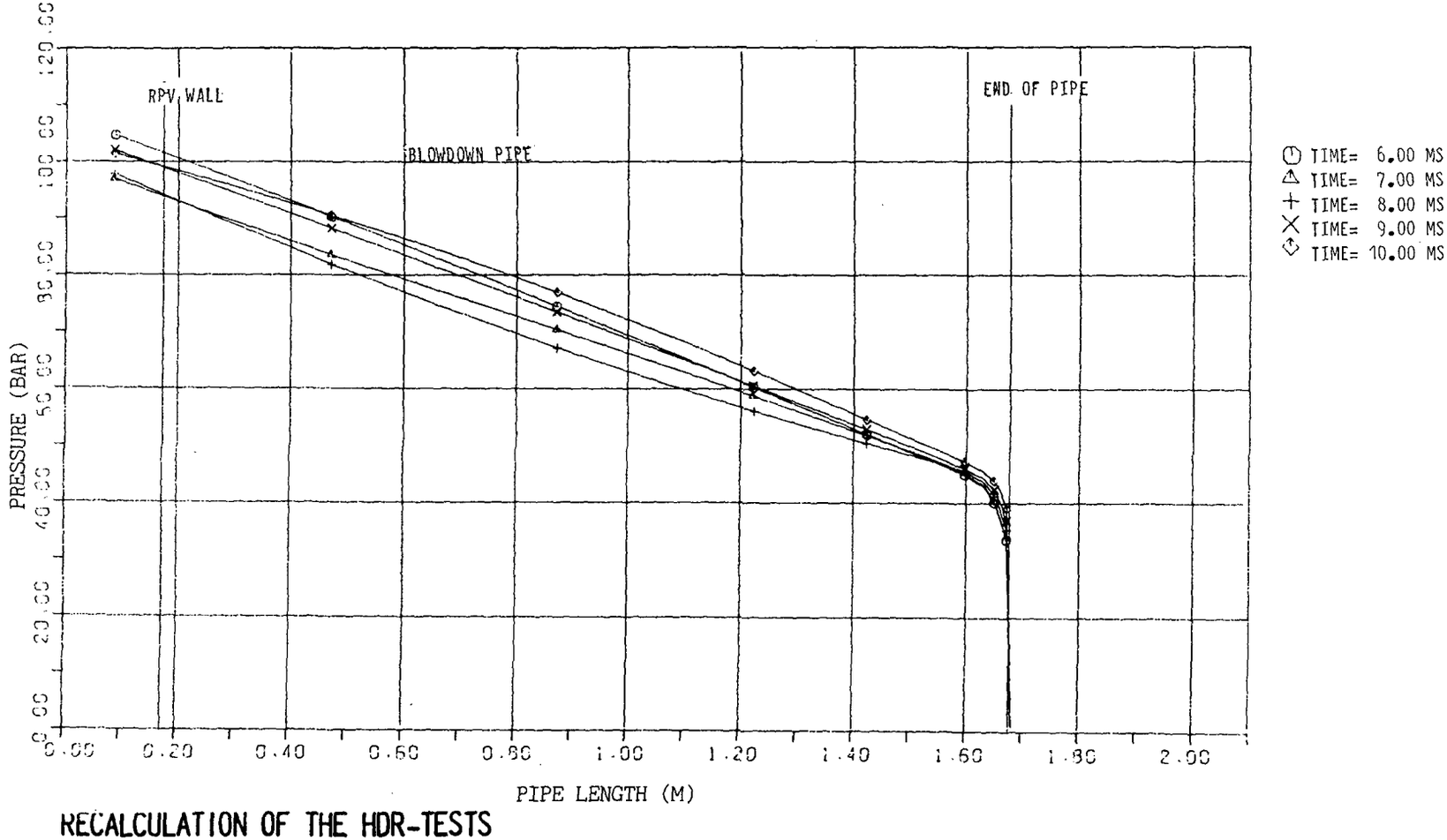

RECALCULATION OF THE HDR-TESTS

PRESSURE WITHOUT ORIFICE AND WITHOUT EXPANSION AT THE RPV

Fig. 2.1.14

KWU PROFILE PLOT TRAC - PD2 PARAMETER STUDY

THE EFFECT OF DIFFERENT PARAMETERS ON THE PRESSURE

AND THE MASS FLUX

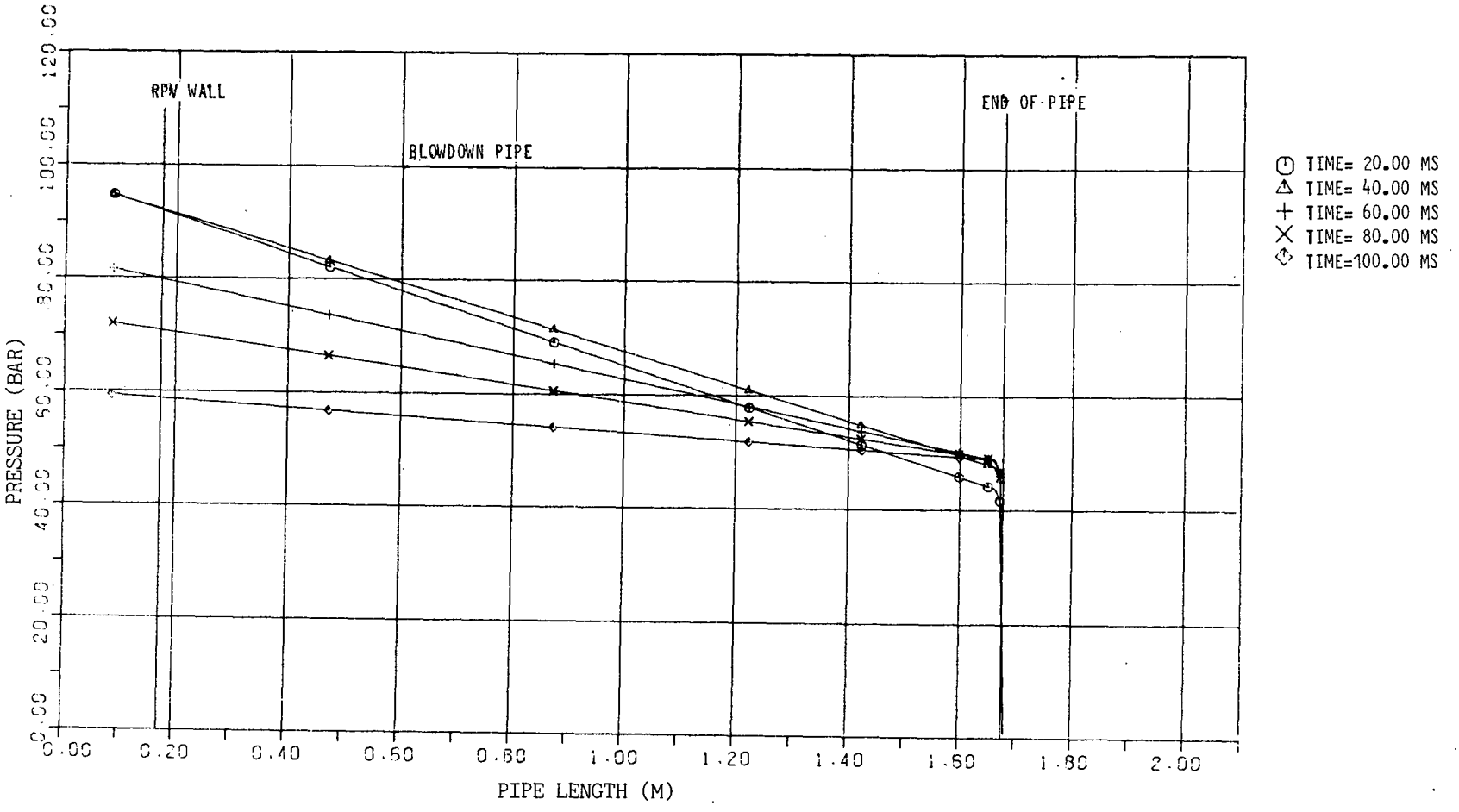

RECALCULATION OF THE HDR-TESTS

PRESSURE WITHOUT ORIFICE AND WITHOUT EXPANSION AT THE RPV

Fig. 2.1.15

KWU PROFILE PLOT TRAC - PD2 PARAMETER STUDY

THE EFFECT OF DIFFERENT PARAMETERS ON THE PRESSURE

AND THE MASS FLUX

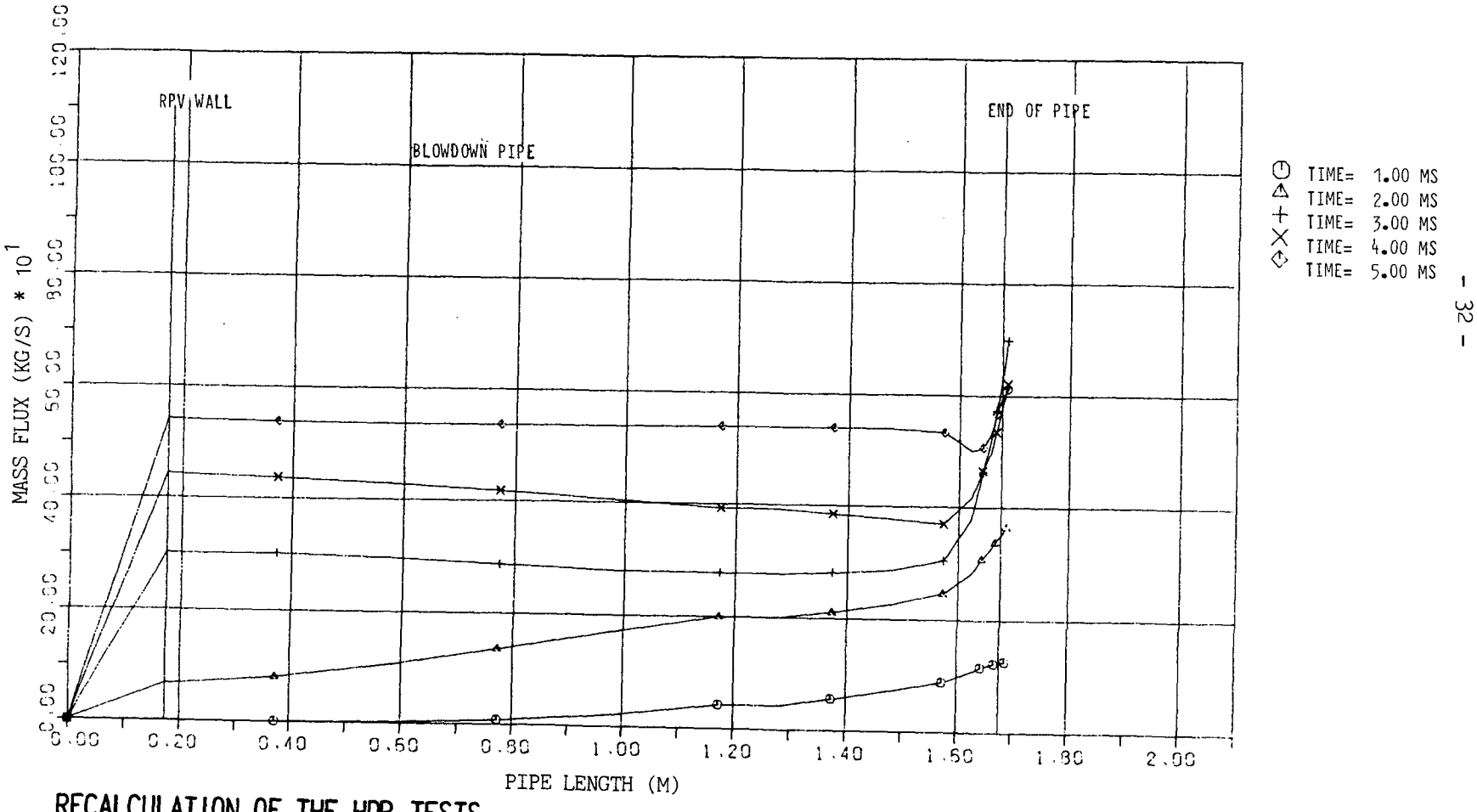

RECALCULATION OF THE HDR-TESTS

MASS FLUX WITHOUT ORIFICE AND WITHOUT EXPANSION AT THE RPV

Fig. 2.1.16

KWU PROFILE PLOT TRAC - PD2 PARAMETER STUDY

THE EFFECT OF DIFFERENT PARAMETERS ON THE PRESSURE

AND THE MASS FLUX

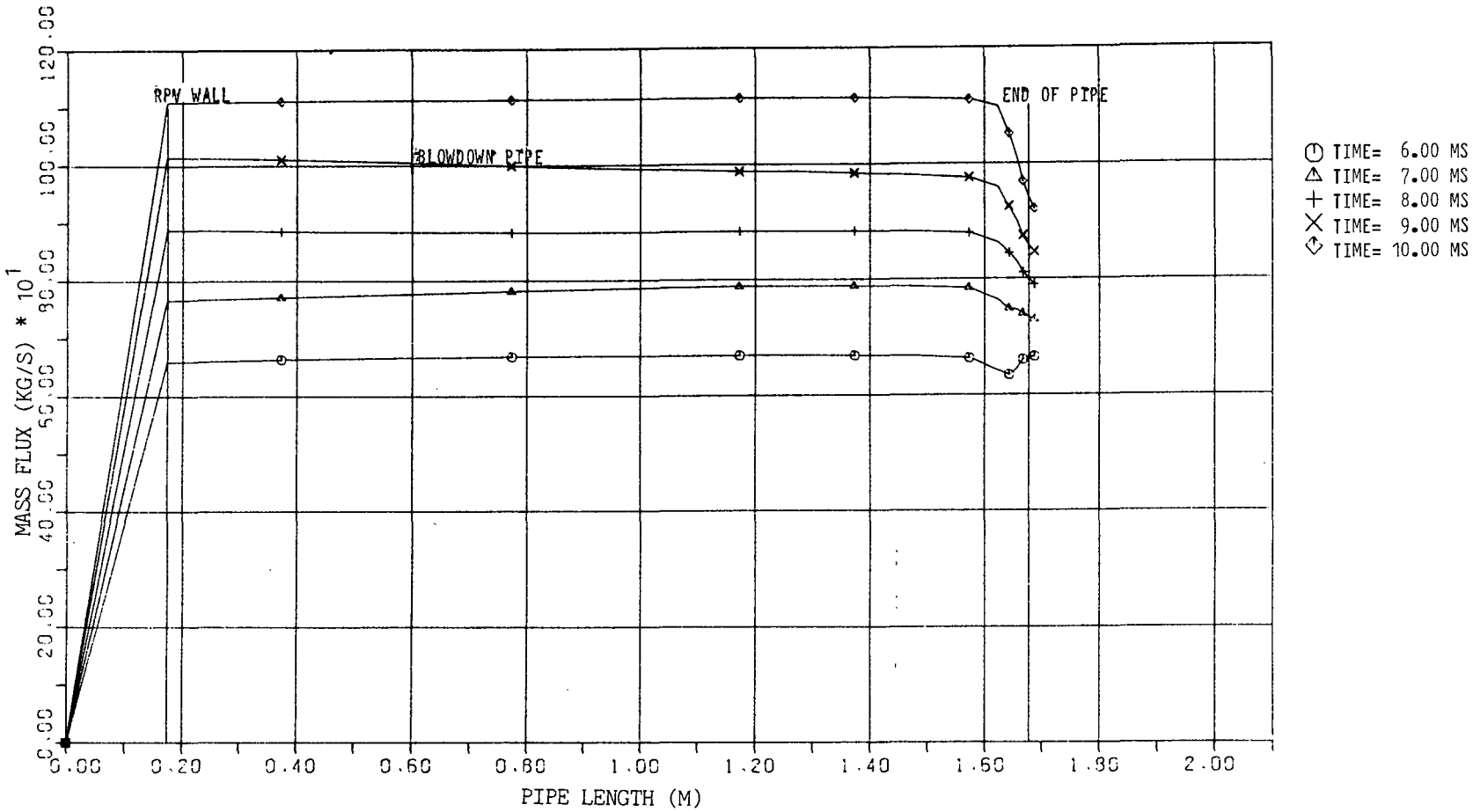

RECALCULATION OF THE HDR-TESTS

MASS FLUX WITHOUT ORIFICE AND WITHOUT EXPANSION AT THE RPV

Fig. 2.1.17

KWU PROFILE PLOT TRAC - PD2 PARAMETER STUDY

THE EFFECT OF DIFFERENT PARAMETERS ON THE PRESSURE

AND THE MASS FLUX

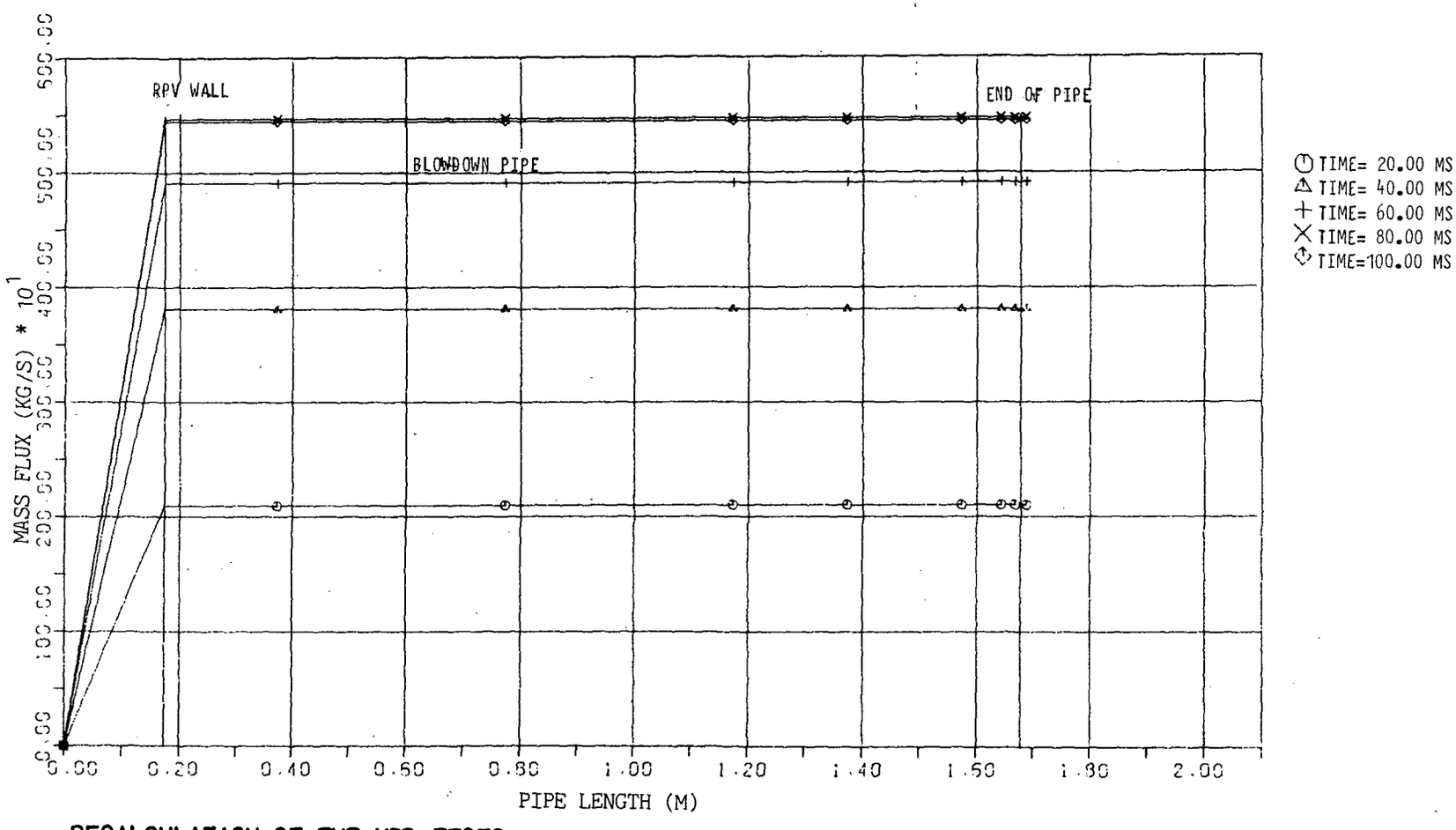

RECALCULATION OF THE HDR-TESTS

MASS FLUX WITHOUT ORIFICE AND WITHOUT EXPANSION AT THE RPV

Fig. 2.1.18

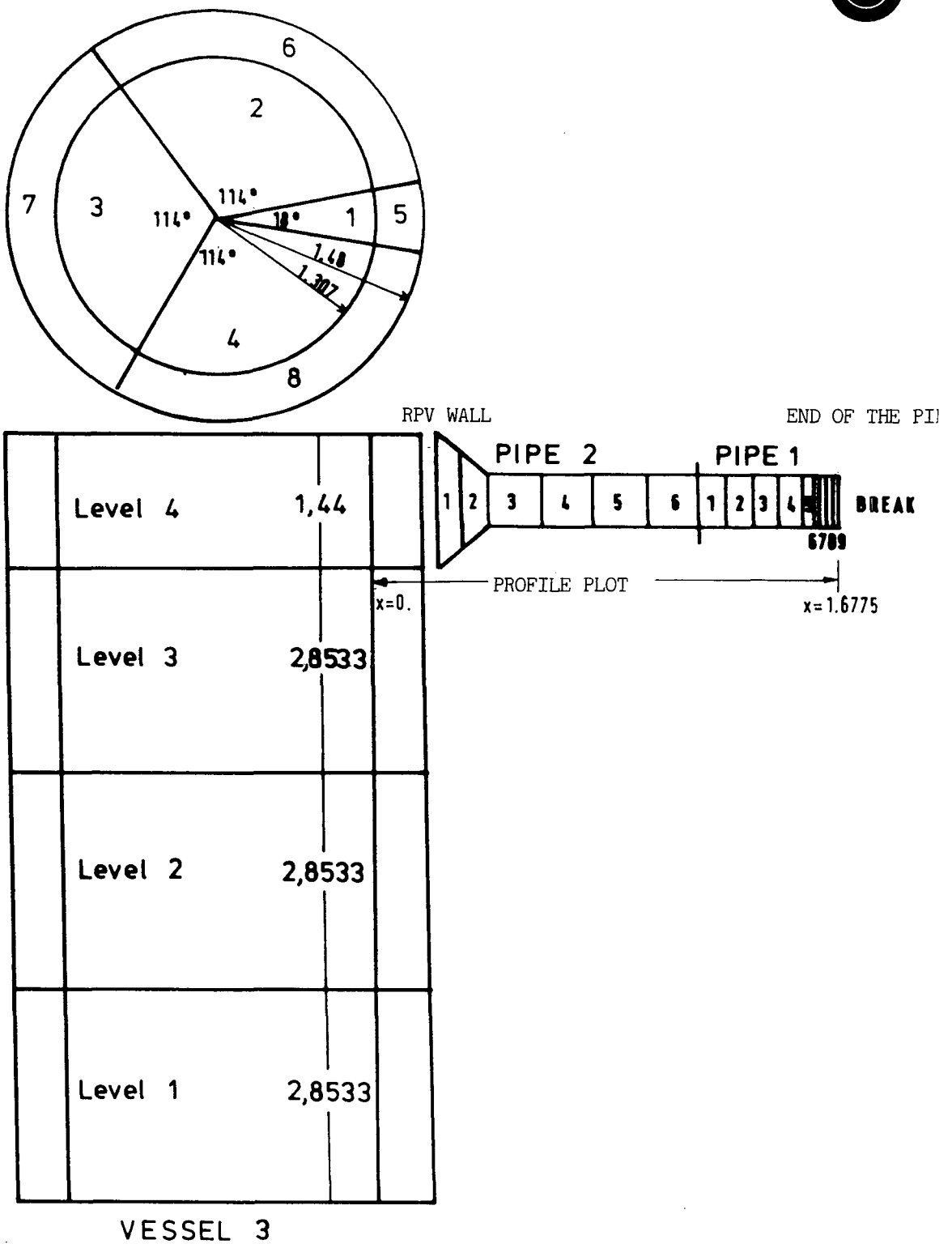

HDR 2/3

Fig. 2.2.1

KWU TRAC - PD2

THE EFFECT OF DIFFERENT PARAMETERS ON THE OUTFLOW RATE

RECALCULATION OF THE HDR-TESTS WITH THE VESSEL COMPONENT

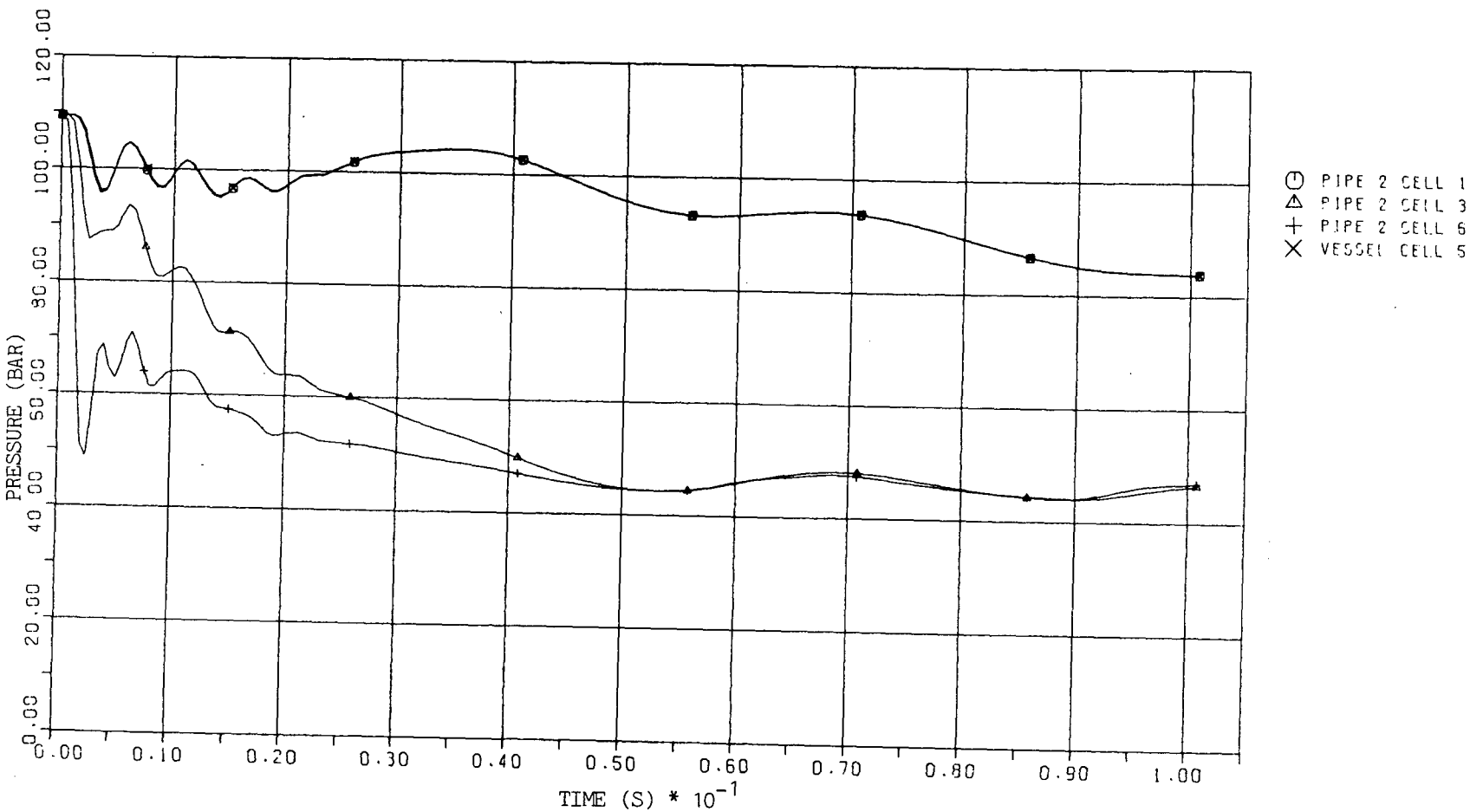

PIPE 2 / VESSEL TYPE 3 / AUTOMATIC BOILER CONNECTION

PRESSURE

Fig. 2.2.2

KWU TRAC -PD2

THE EFFECT OF DIFFERENT PARAMETERS ON THE OUTFLOW RATE

RECALCULATION OF THE HDR-TESTS WITH THE VESSEL COMPONENT

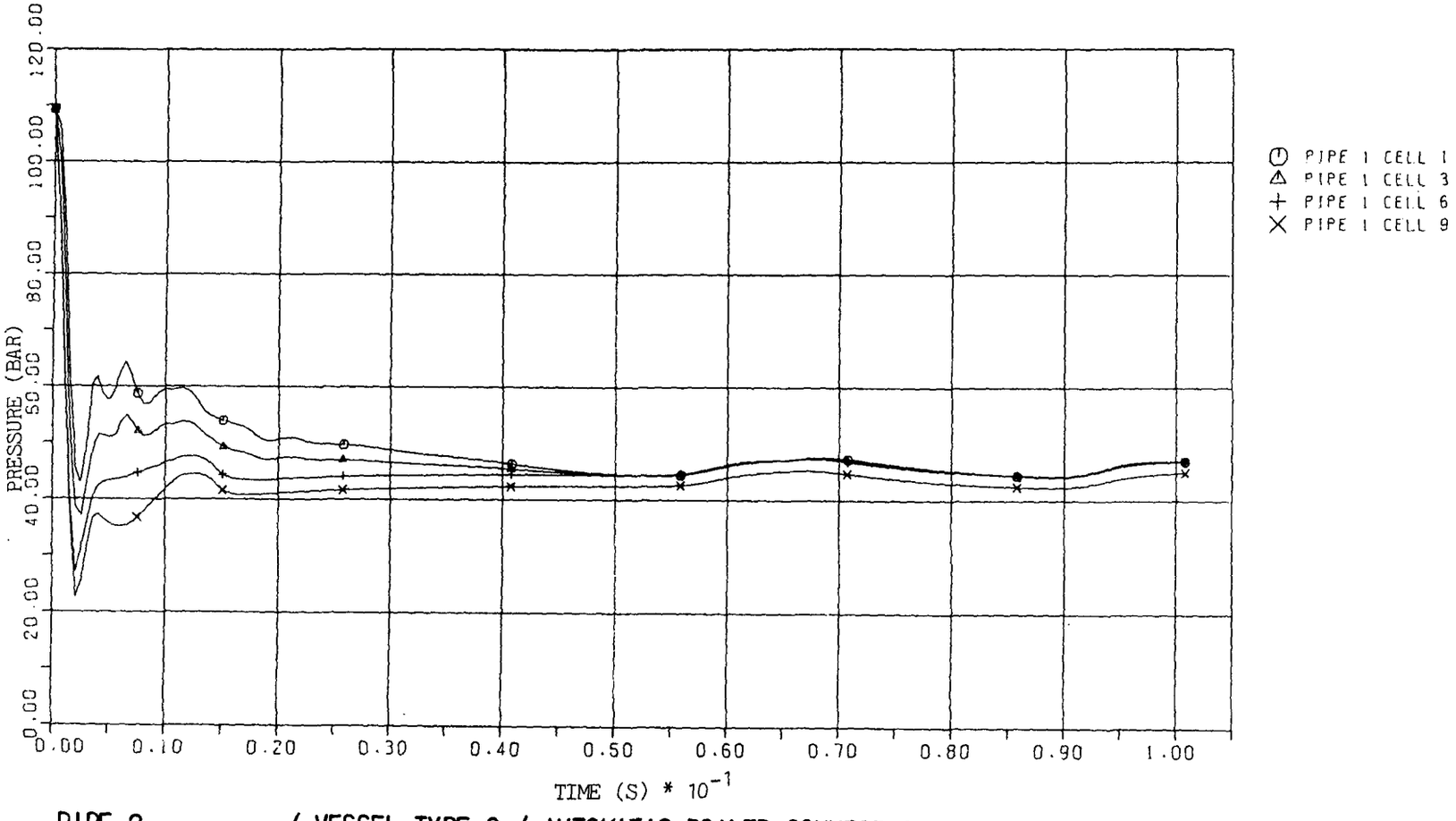

PIPE 2 / VESSEL TYPE 3 / AUTOMATIC BOILER CONNECTION

PRESSURE

Fig. 2.2.3

KWU TRAC - PD2

THE EFFECT OF DIFFERENT PARAMETERS ON THE OUTFLOW RATE

RECALCULATION OF THE HDR-TESTS WITH THE VESSEL COMPONENT

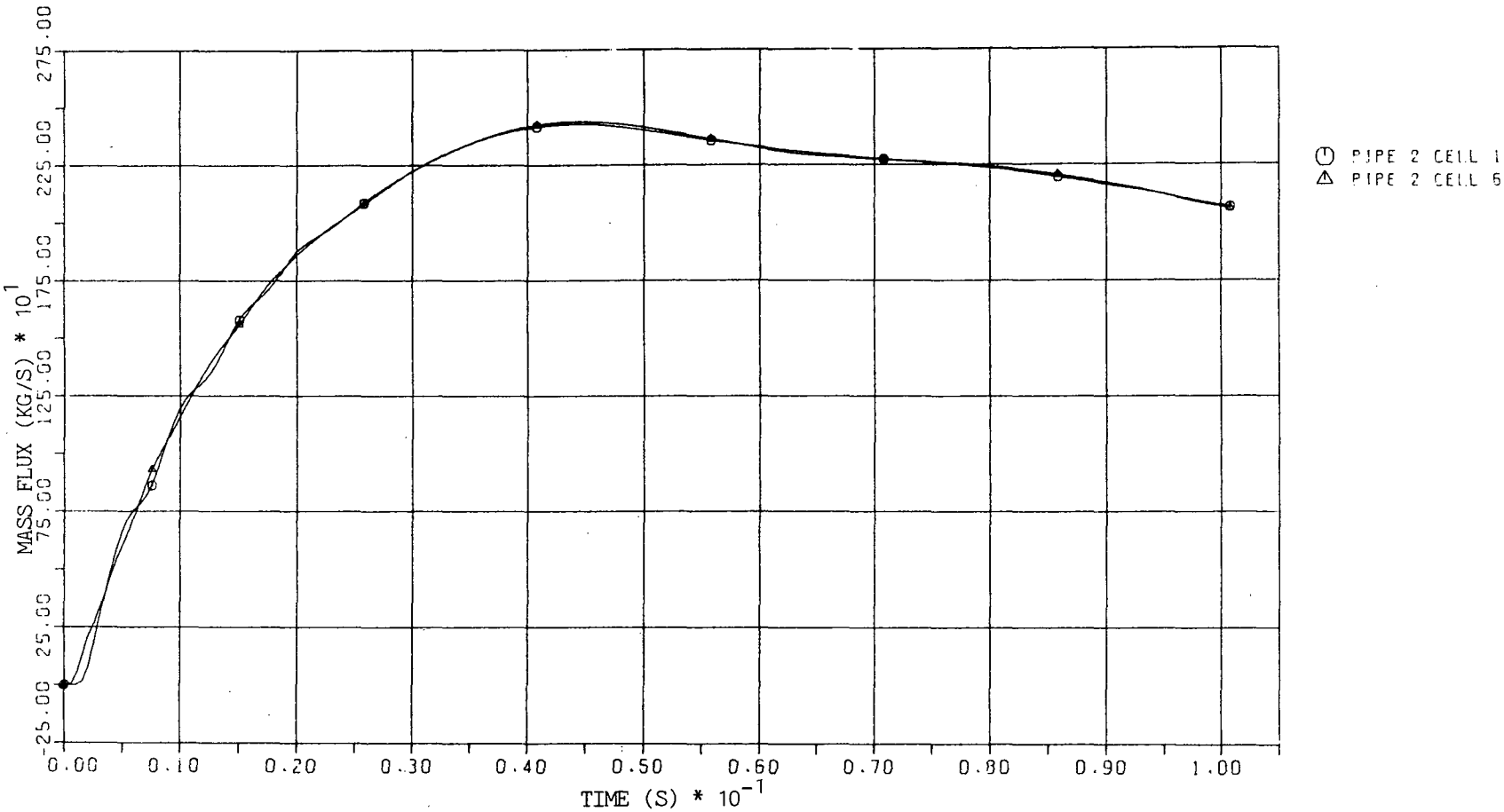

PIPE 2 / VESSEL TYPE 3 / AUTOMATIC BOILER CONNECTION

MASS FLUX

Fig. 2.2.4

KWU TRAC - PD2

THE EFFECT OF DIFFERENT PARAMETERS ON THE OUTFLOW RATE

RECALCULATION OF THE HDR-TESTS WITH THE VESSEL COMPONENT

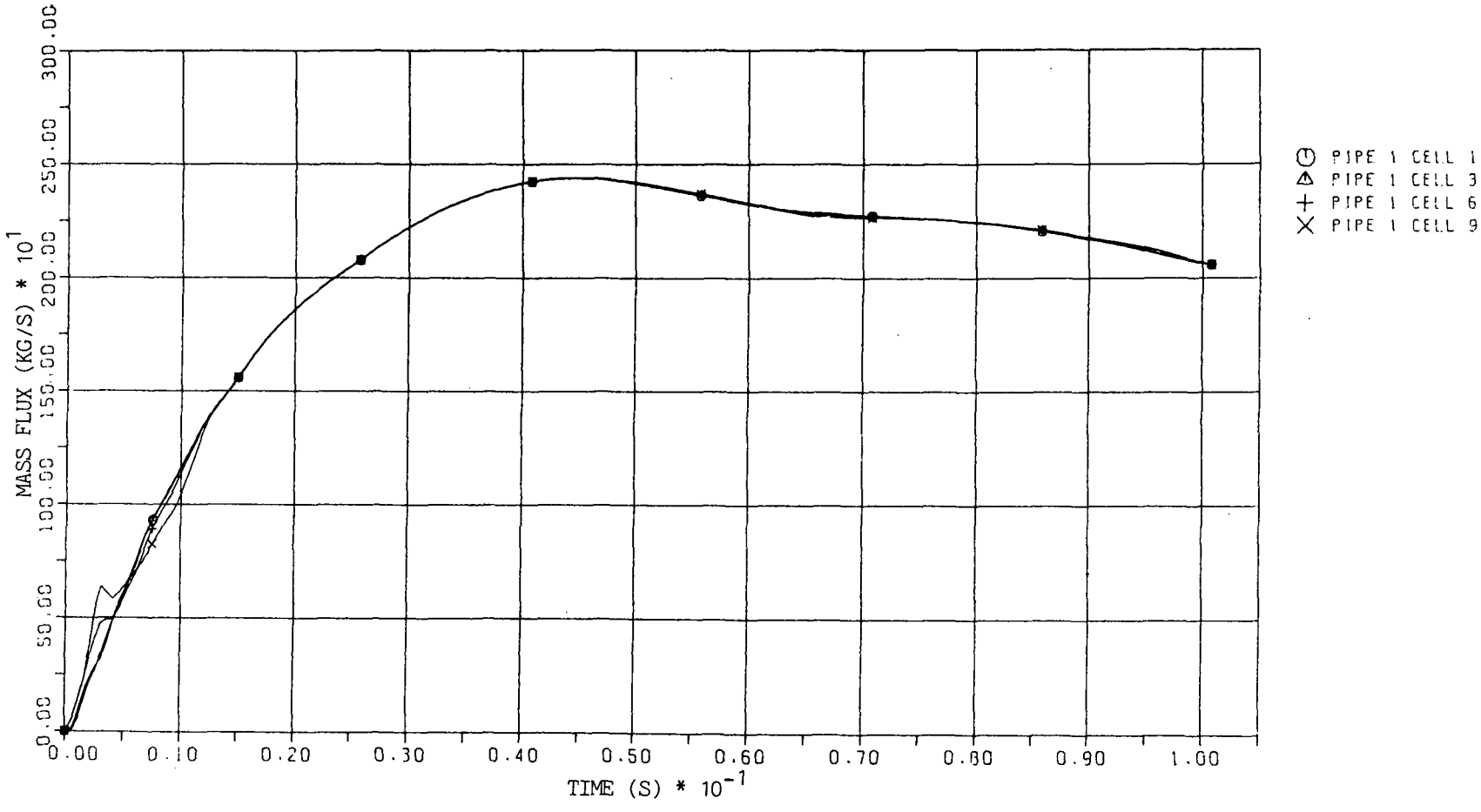

PIPE 2 / VESSEL TYPE 3 / AUTOMATIC BOILER CONNECTION

MASS FLUX

Fig. 2.2.5

KWU TRAC - PD2

THE EFFECT OF DIFFERENT PARAMETERS ON THE OUTFLOW RATE

RECALCULATION OF THE HDR-TESTS WITH THE VESSEL COMPONENT

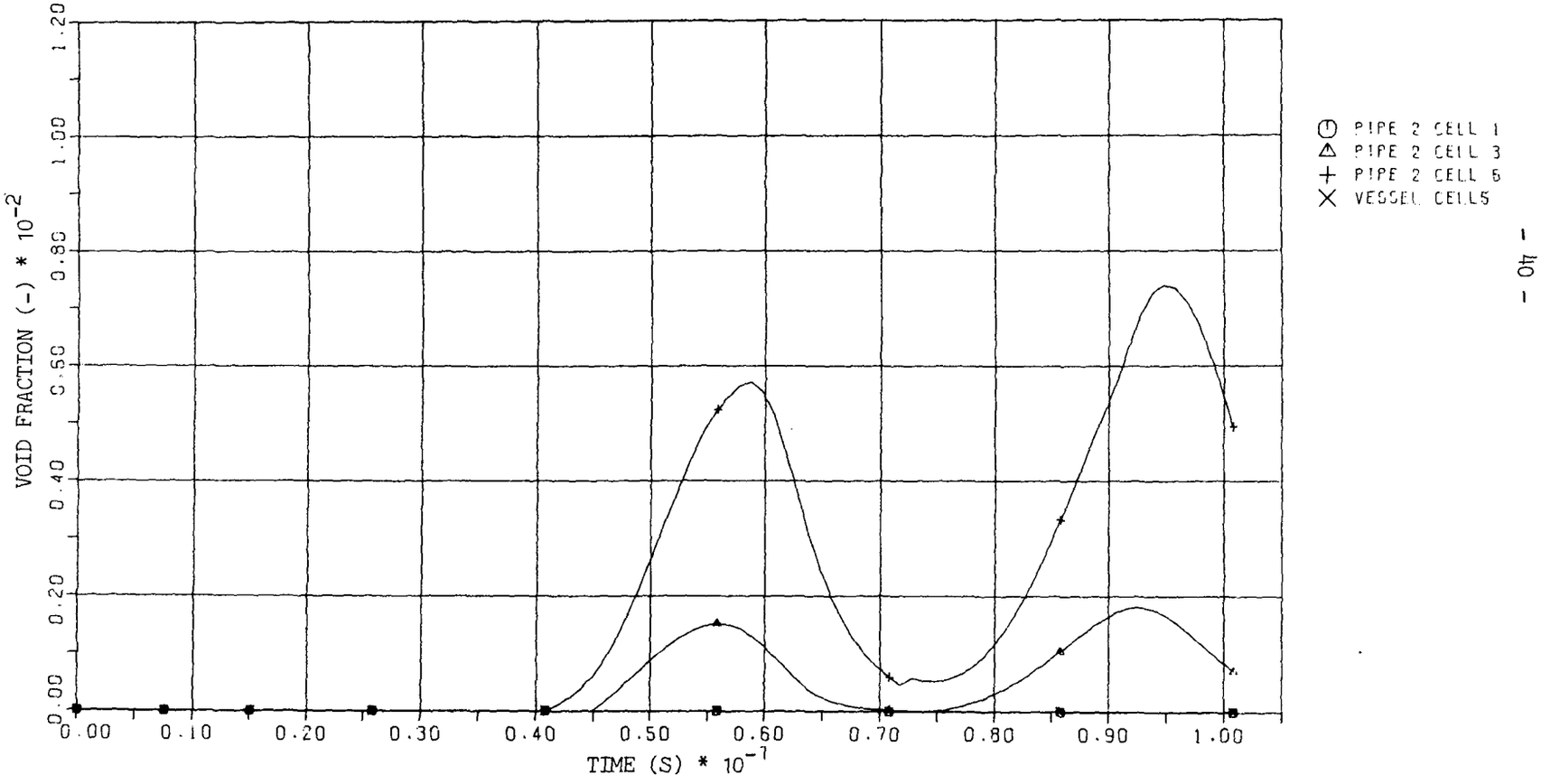

PIPE 2 / VESSEL TYPE 3 / AUTOMATIC BOILER CONNECTION

VOID FRACTION

Fig. 2.2.6

KWU TRAC - PD2

THE EFFECT OF DIFFERENT PARAMETERS ON THE OUTFLOW RATE

RECALCULATION OF THE HDR-TESTS WITH THE VESSEL COMPONENT

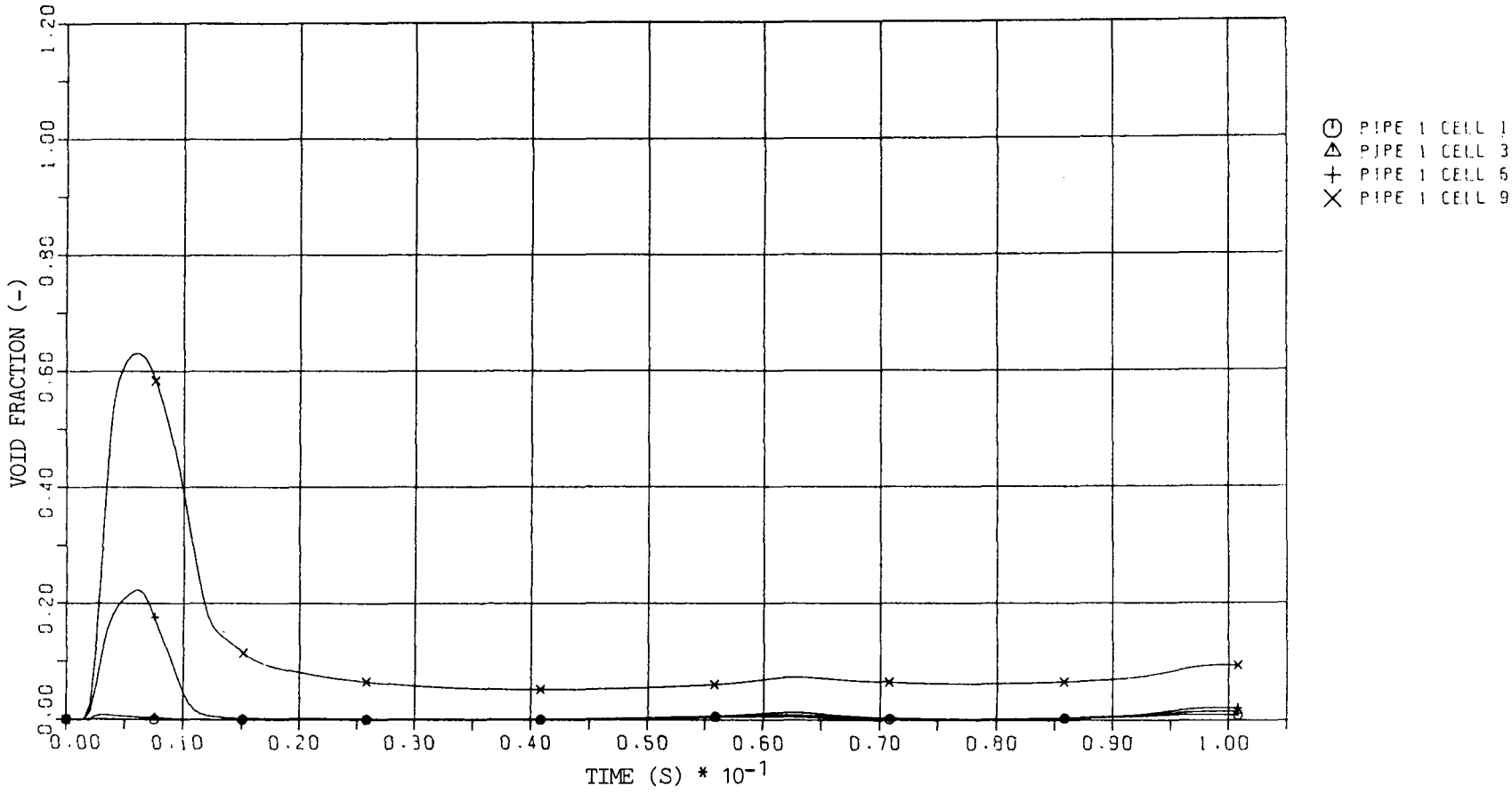

PIPE 2 / VESSEL TYPE 3 / AUTOMATIC BOILER CONNECTION

VOID FRACTION

Fig. 2.2.7

KWU TRAC -PD2

THE EFFECT OF DIFFERENT PARAMETERS ON THE OUTFLOW RATE

RECALCULATION OF THE HDR-TESTS WITH THE VESSEL COMPONENT

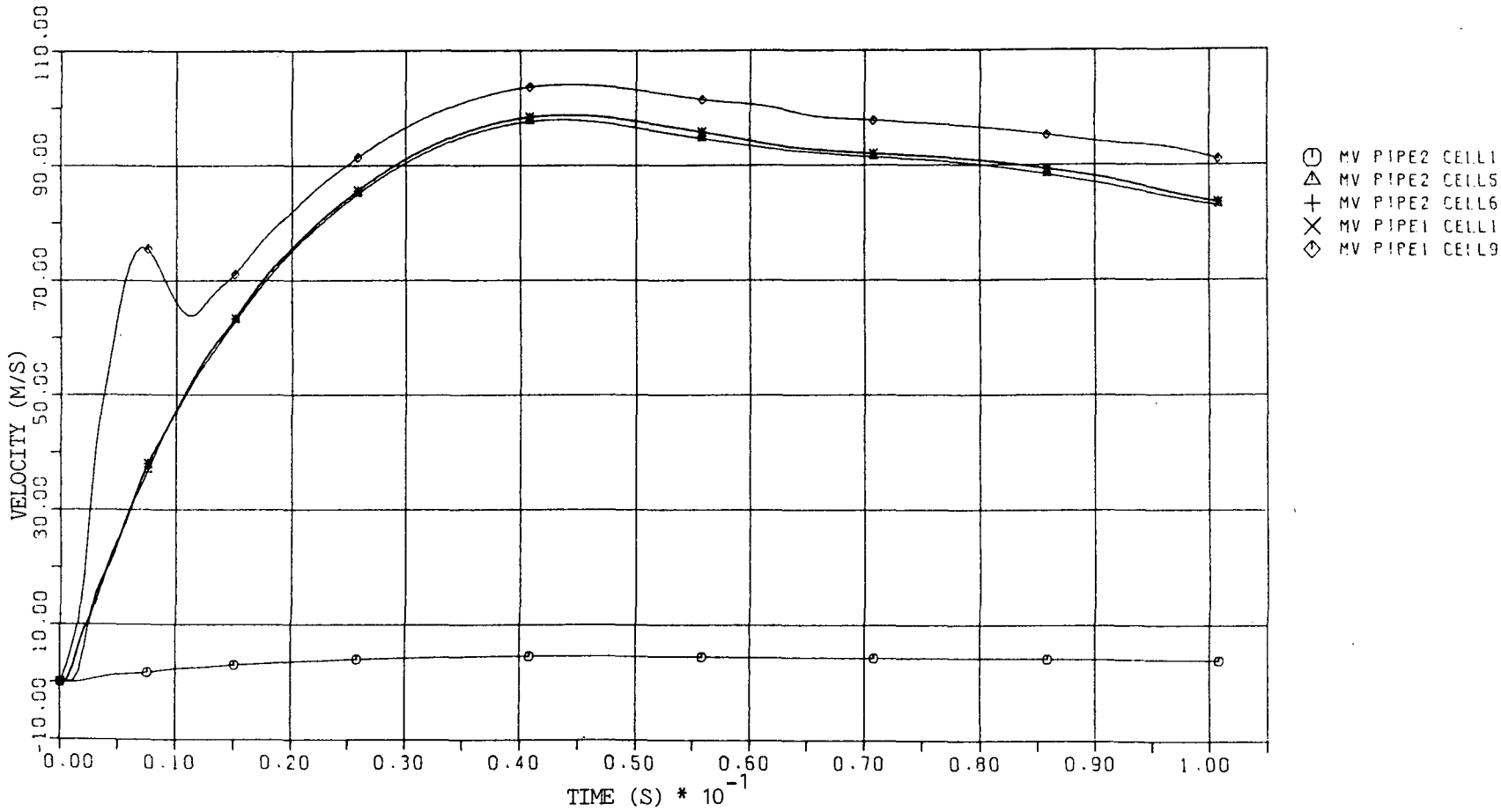

PIPE 2 / VESSEL TYPE 3 / AUTOMATIC BOILER CONNECTION

VELOCITY

Fig. 2.2.8

KWU TRAC - PD2

THE EFFECT OF DIFFERENT PARAMETERS ON THE OUTFLOW RATE

RECALCULATION OF THE HDR-TESTS WITH THE VESSEL COMPONENT

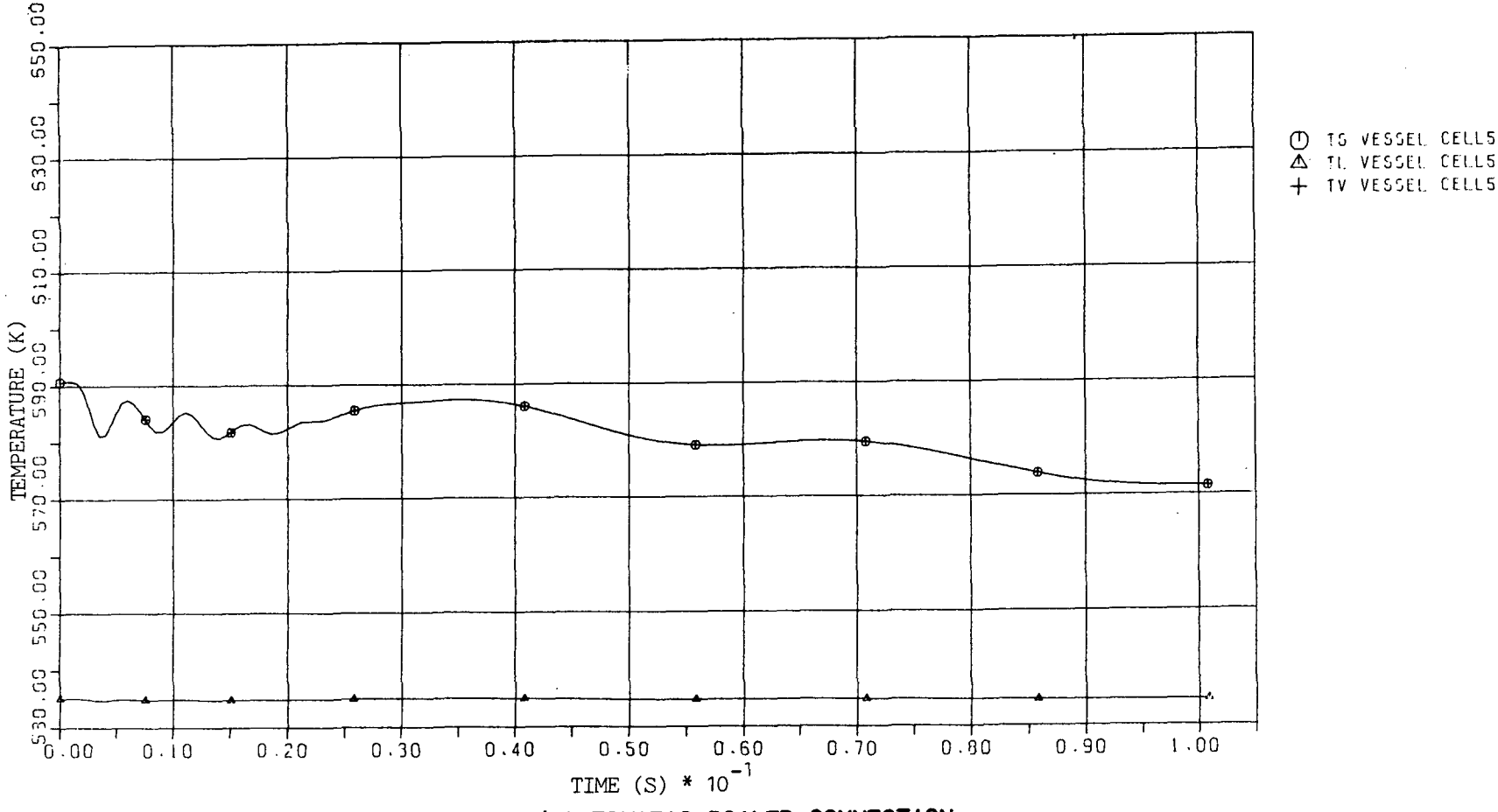

PIPE 2 / VESSEL TYPE 3 / AUTOMATIC BOILER CONNECTION

TEMPERATURE

Fig. 2.2.9

KWU TRAC -PD2

THE EFFECT OF DIFFERENT PARAMETERS ON THE OUTFLOW RATE

RECALCULATION OF THE HDR-TESTS WITH THE VESSEL COMPONENT

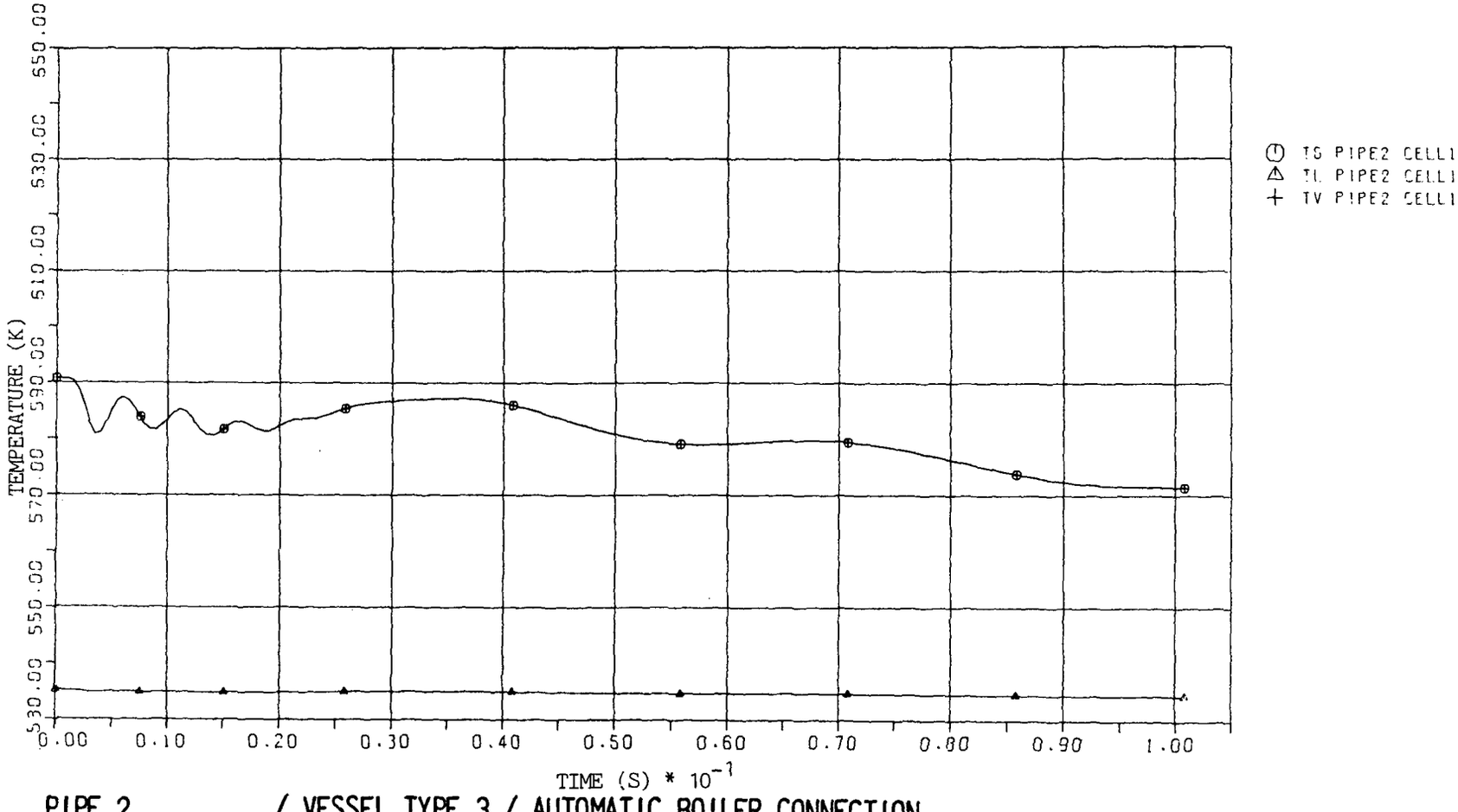

PIPE 2 / VESSEL TYPE 3 / AUTOMATIC BOILER CONNECTION

TEMPERATURE

Fig. 2.2.10

KWU TRAC - PD2

THE EFFECT OF DIFFERENT PARAMETERS ON THE OUTFLOW RATE

RECALCULATION OF THE HDR-TESTS WITH THE VESSEL COMPONENT

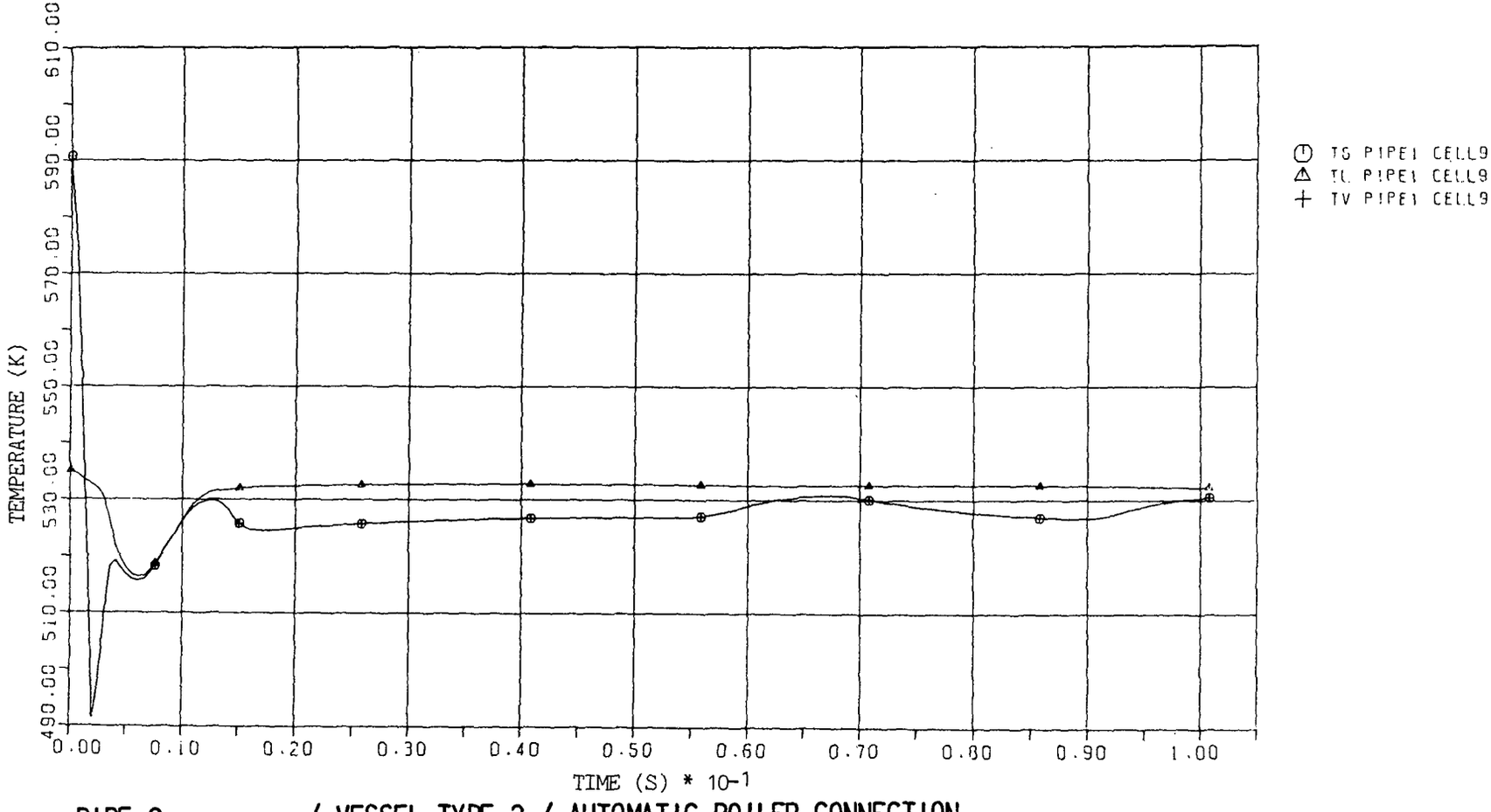

PIPE 2 / VESSEL TYPE 3 / AUTOMATIC BOILER CONNECTION

TEMPERATURE

Fig. 2.2.11

KWU PROFILE PLOT TRAC - PD2 PARAMETER STUDY

THE EFFECT OF DIFFERENT PARAMETERS ON THE PRESSURE

AND THE MASS FLUX

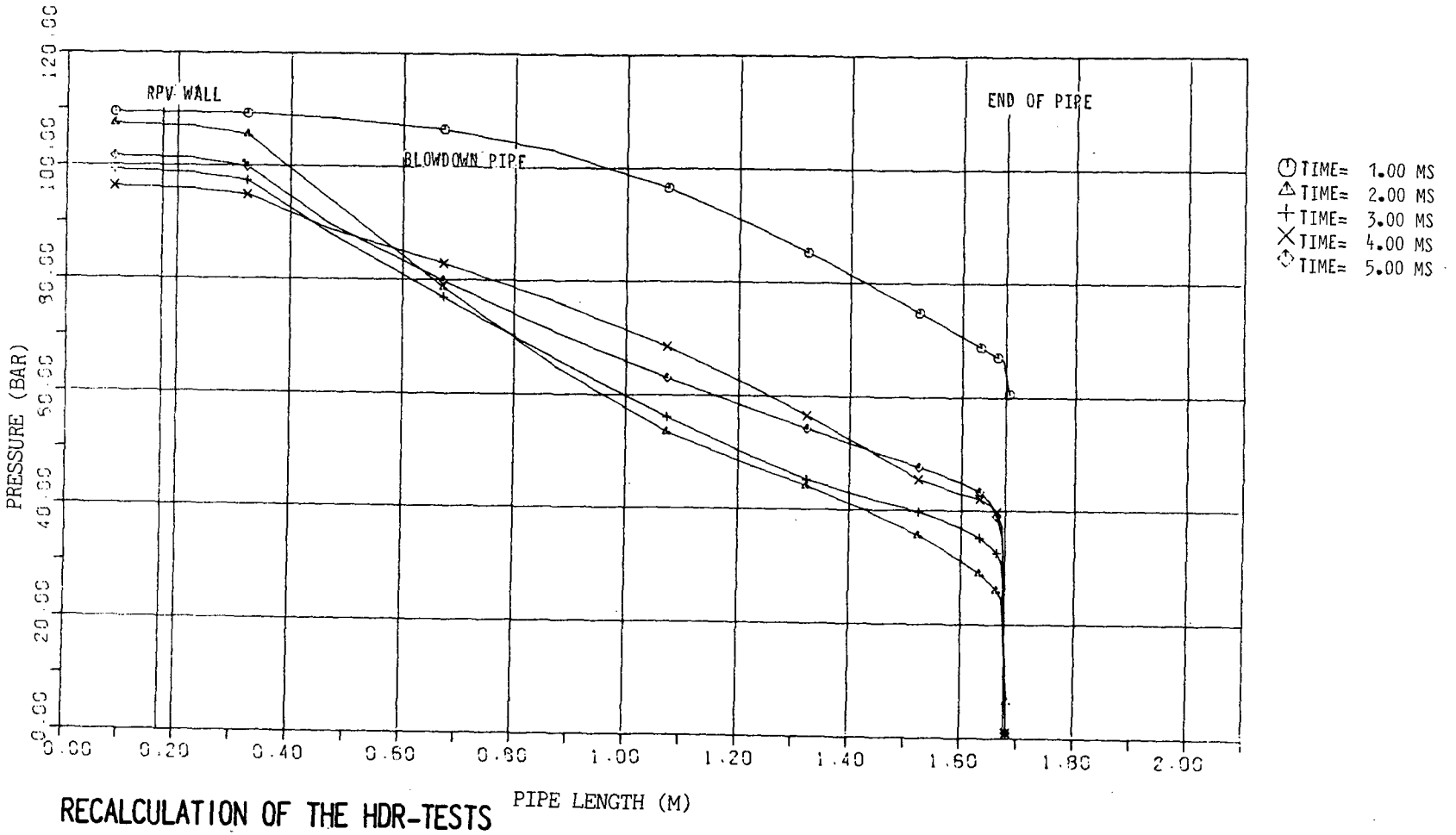

RECALCULATION OF THE HDR-TESTS

PRESSURE WITHOUT ORIFICE AND WITH EXPANSION AT THE RPV

Fig. 2.2.12

KWU PROFILE PLOT TRAC - PD2 PARAMETER STUDY

THE EFFECT OF DIFFERENT PARAMETERS ON THE PRESSURE

AND THE MASS FLUX

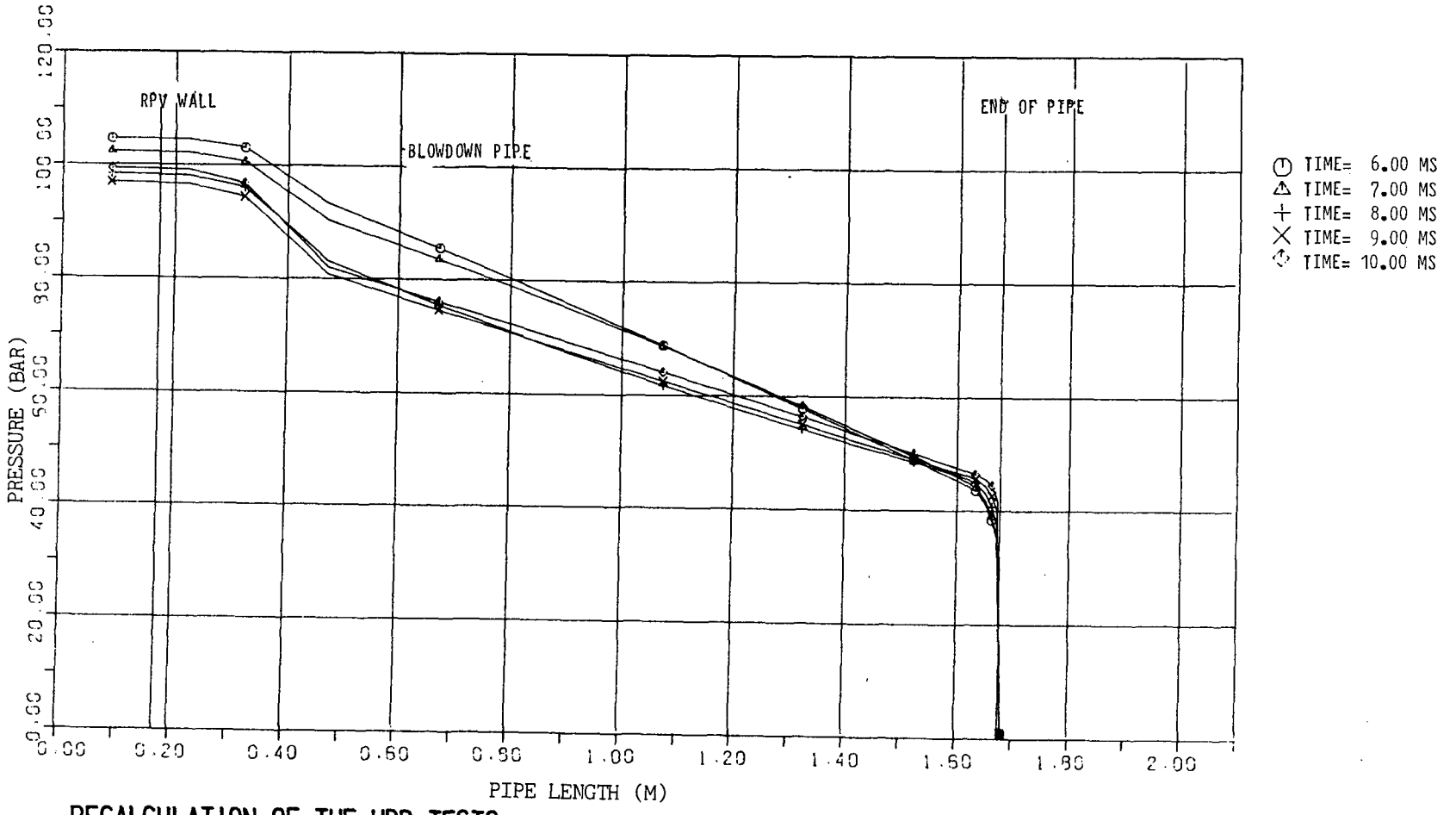

RECALCULATION OF THE HDR-TESTS

PRESSURE WITHOUT ORIFICE AND WITH EXPANSION AT THE RPV

Fig. 2.2.13

KWU PROFILE PLOT TRAC - PD2 PARAMETER STUDY

THE EFFECT OF DIFFERENT PARAMETERS ON THE PRESSURE

AND THE MASS FLUX

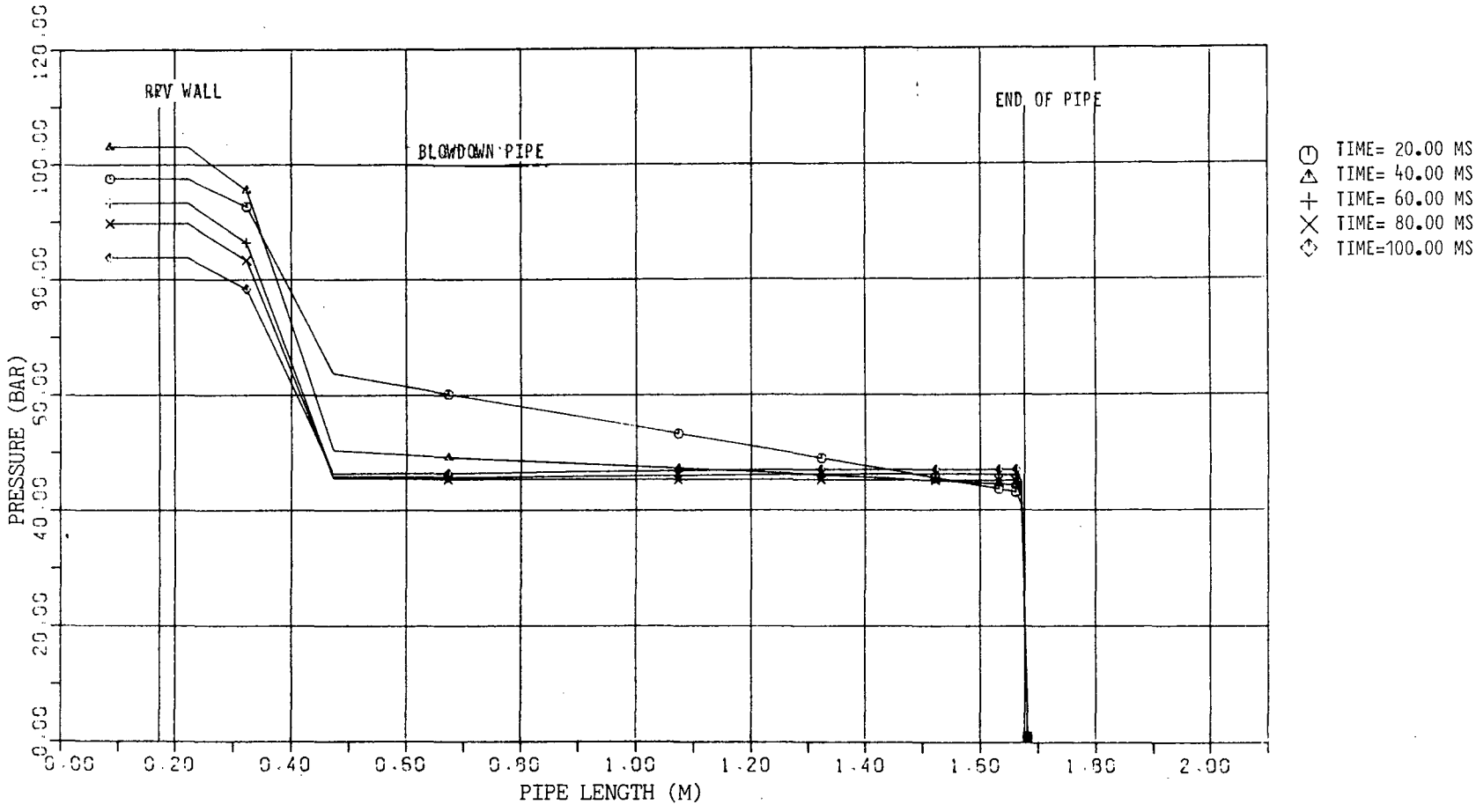

RECALCULATION OF THE HDR-TESTS

PRESSURE WITHOUT ORIFICE AND WITH EXPANSION AT THE RPV

Fig. 2.2.14

KWU PROFILE PLOT TRAC - PD2 PARAMETER STUDY

THE EFFECT OF DIFFERENT PARAMETERS ON THE PRESSURE

AND THE MASS FLUX

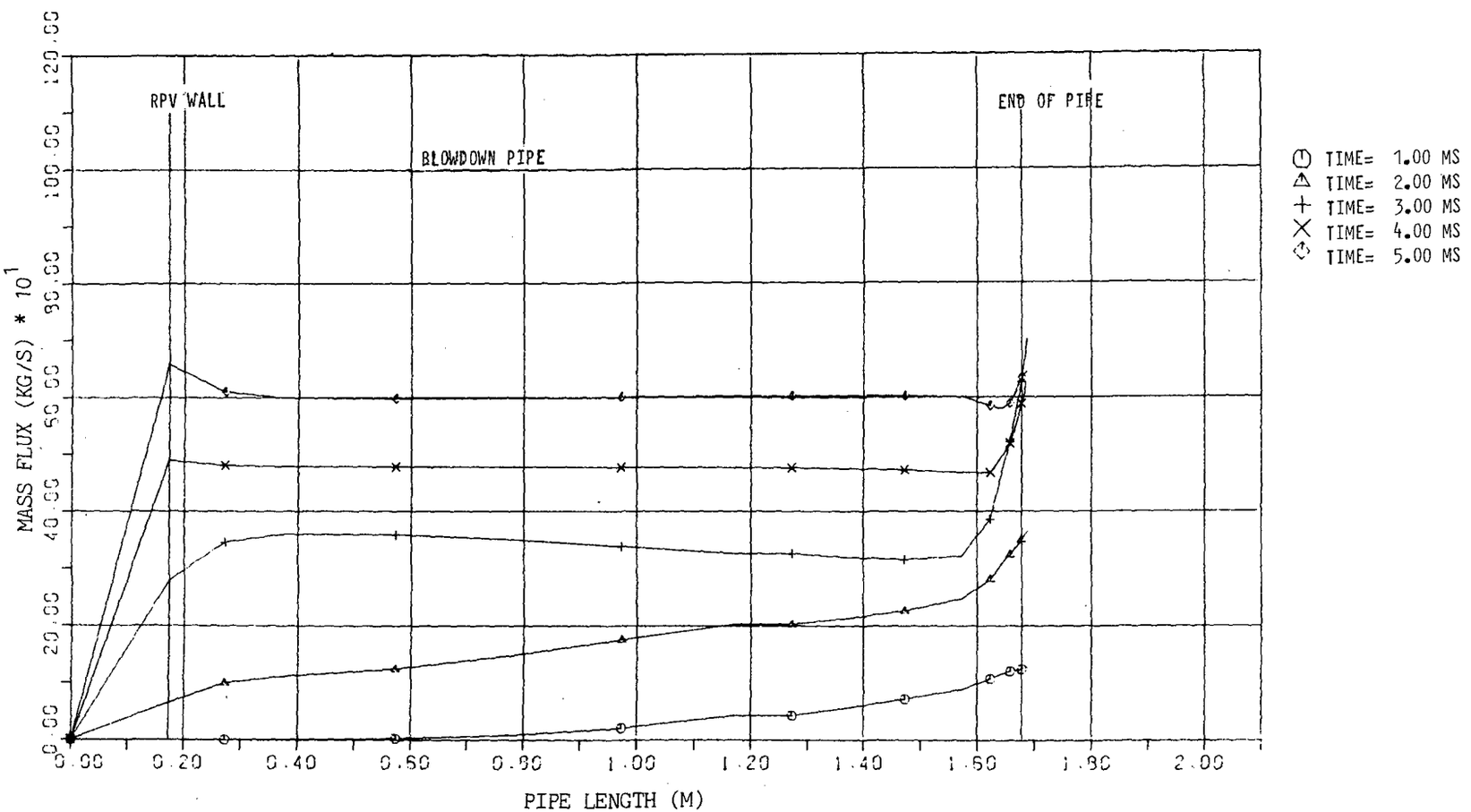

RECALCULATION OF THE HDR-TESTS

MASS FLUX WITHOUT ORIFICE AND WITH EXPANSION AT THE RPV

Fig. 2.2.15

KWU PROFILE PLOT TRAC - PD2 PARAMETER STUDY

THE EFFECT OF DIFFERENT PARAMETERS ON THE PRESSURE

AND THE MASS FLUX

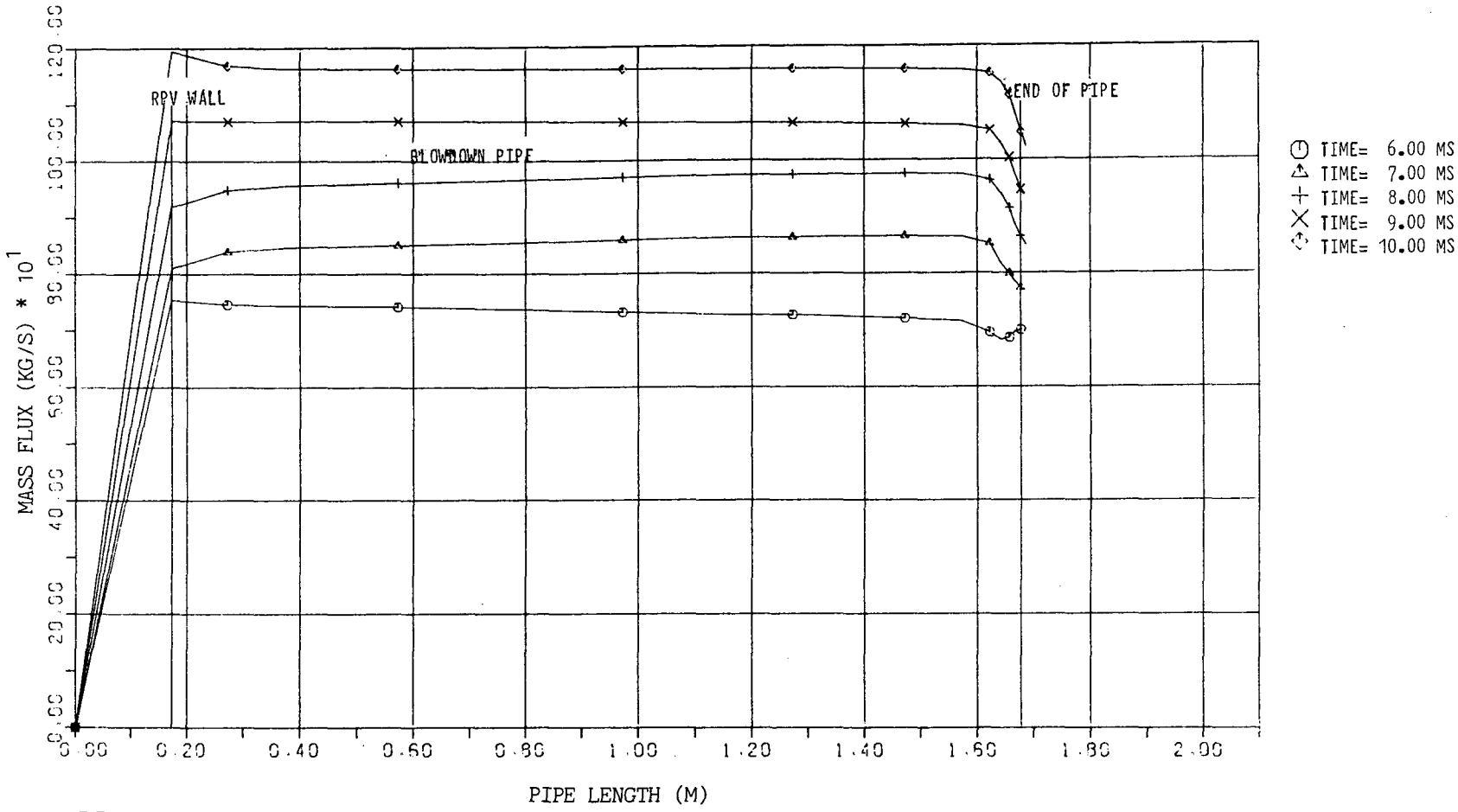

RECALCULATION OF THE HDR-TESTS

MASS FLUX WITHOUT ORIFICE AND WITH EXPANSION AT THE RPV

Fig. 2.2.16

KWU PROFILE PLOT TRAC - PD2 PARAMETER STUDY

THE EFFECT OF DIFFERENT PARAMETERS ON THE PRESSURE

AND THE MASS FLUX

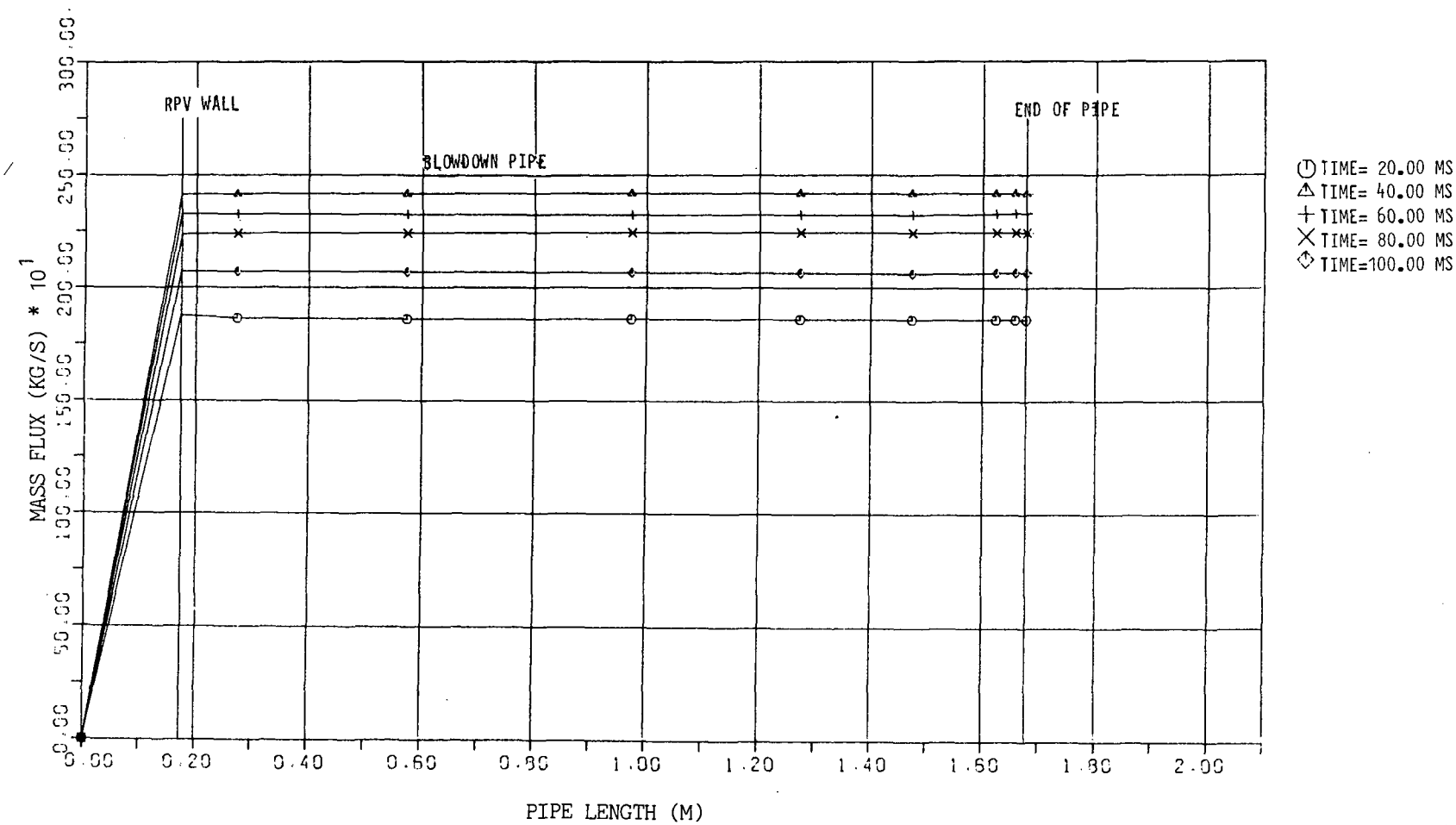

RECALCULATION OF THE HDR-TESTS

MASS FLUX WITHOUT ORIFICE AND WITH EXPANSION AT THF RPV

Fig. 2.2.17

KWU PROFILE PLOT TRAC - PD2 PARAMETER STUDY

THE EFFECT OF DIFFERENT PARAMETERS ON THE PRESSURE

AND THE MASS FLUX

T2/HDR1-3/WITHOUT ORIFICE/WITHOUT EXPANSION

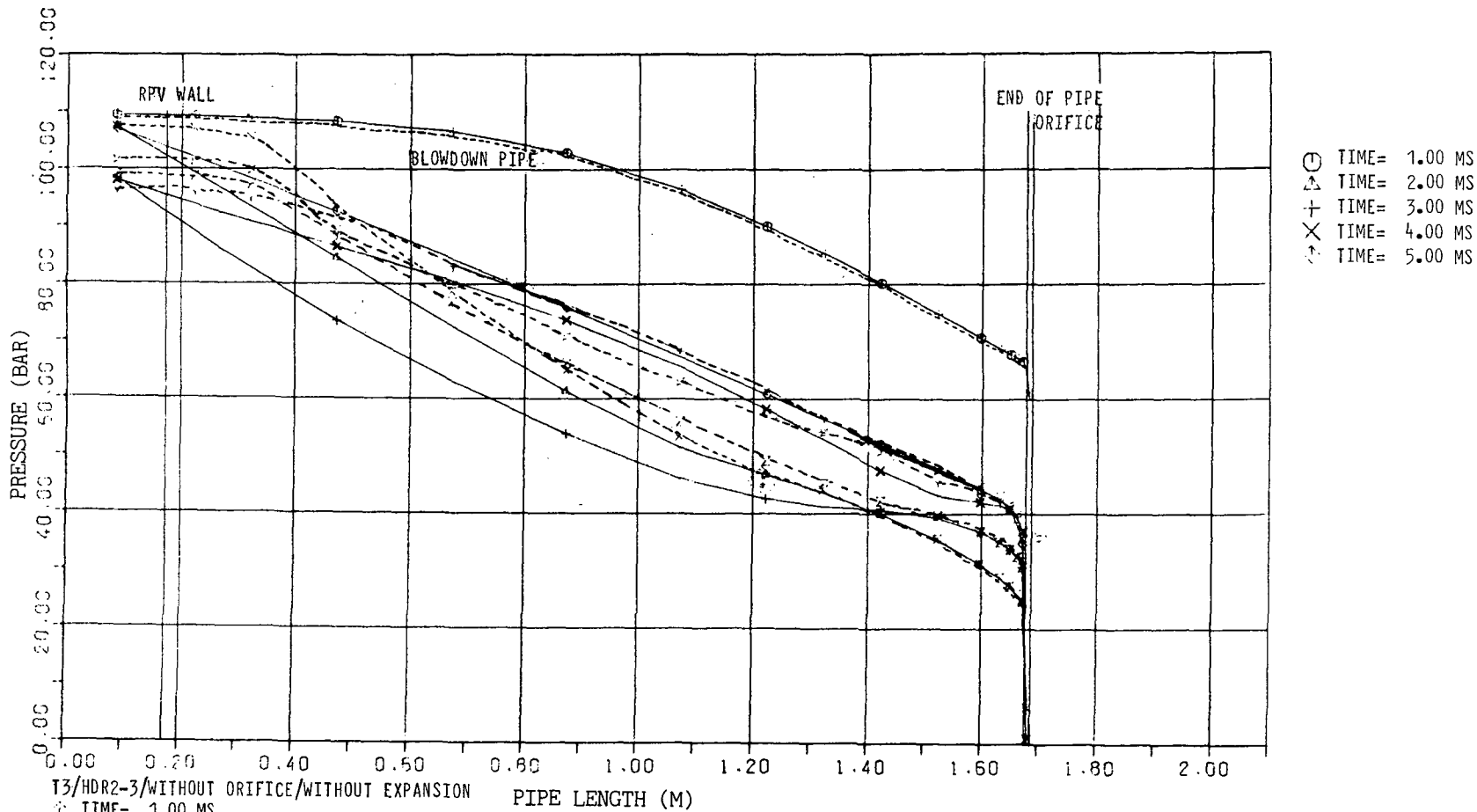

T3/HDR2-3/WITHOUT ORIFICE/WITHOUT EXPANSION

TIME= 1.00 MS
TIME= 2.00 MS
TIME= 3.00 MS
TIME= 4.00 MS
TIME= 5.00 MS

RECALCULATION OF THE HDR-TESTS

PRESSURE

Fig. 2.2.18

KWU PROFILE PLOT TRAC - PD2 PARAMETER STUDY

THE EFFECT OF DIFFERENT PARAMETERS ON THE PRESSURE AND THE MASS FLUX

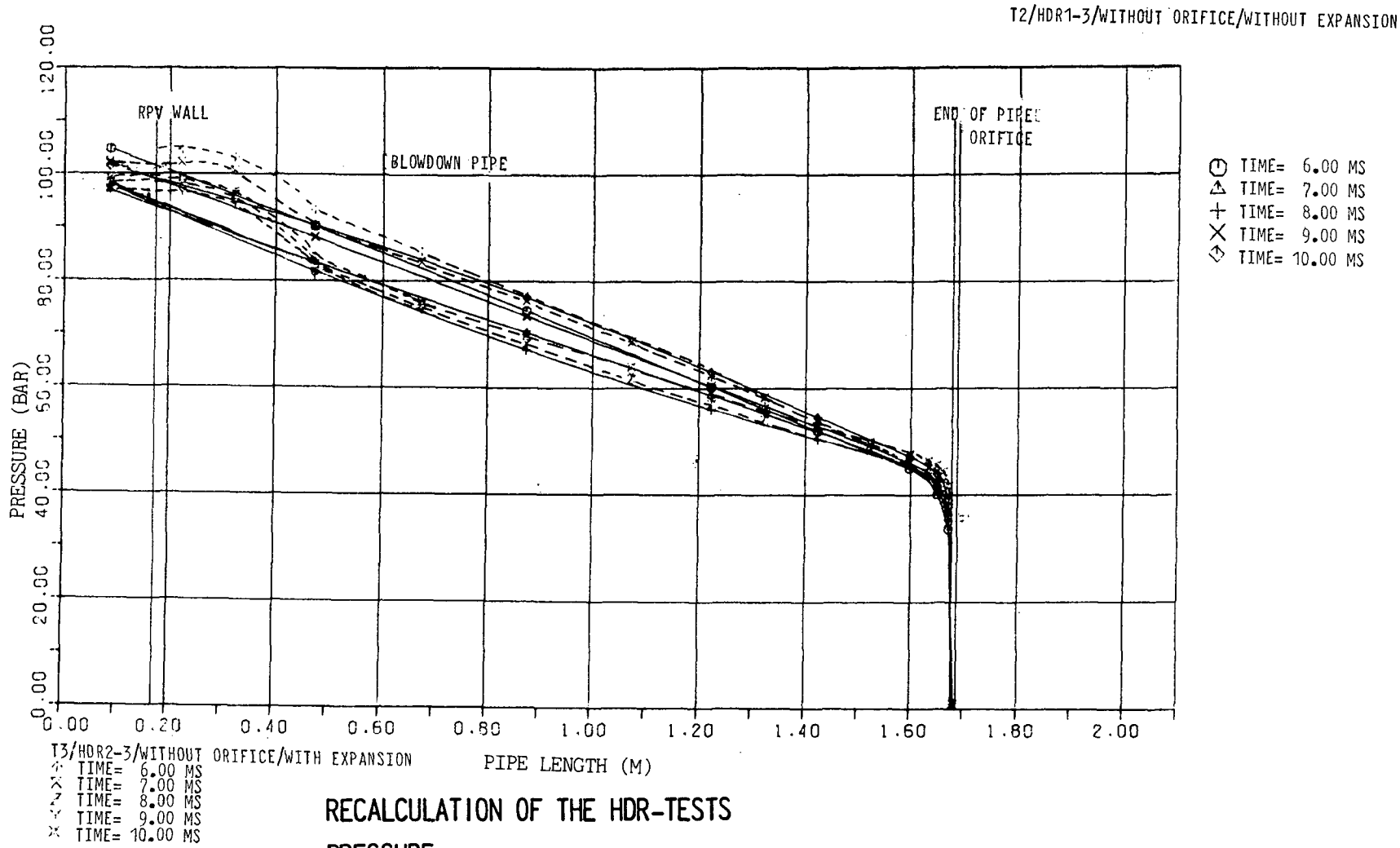

RECALCULATION OF THE HDR-TESTS

PRESSURE

Fig. 2.2.19

KWU PROFILE PLOT TRAC - PD2 PARAMETER STUDY

THE EFFECT OF DIFFERENT PARAMETERS ON THE PRESSURE

AND THE MASS FLUX

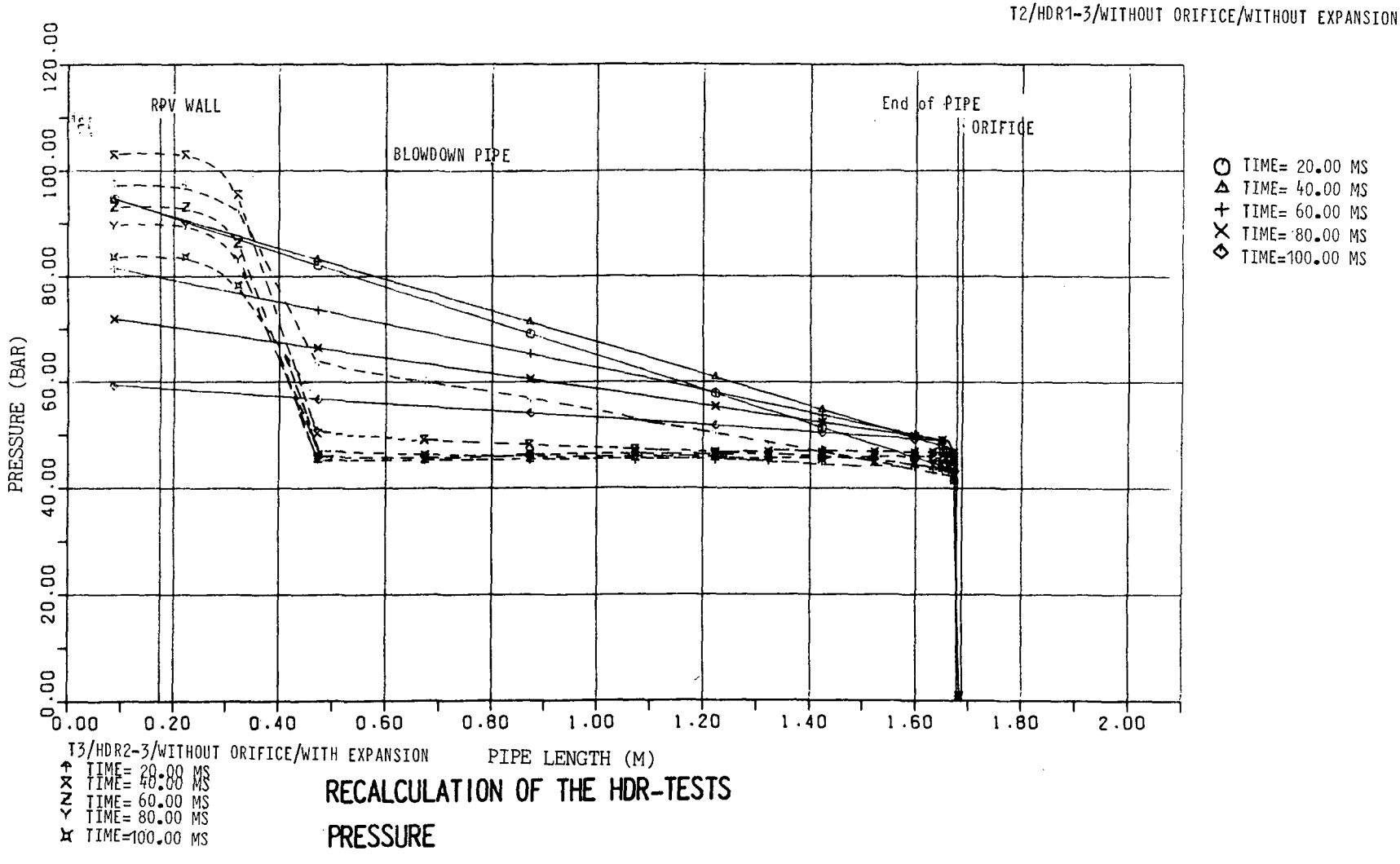

RECALCULATION OF THE HDR-TESTS

PRESSURE

Fig. 2.2.20

KWU PROFILE PLOT TRAC - PD2 PARAMETER STUDY

THE EFFECT OF DIFFERENT PARAMETERS ON THE PRESSURE AND THE MASS FLUX

T2/HDR1-3/WITHOUT ORIFICE/WITHOUT EXPANSION

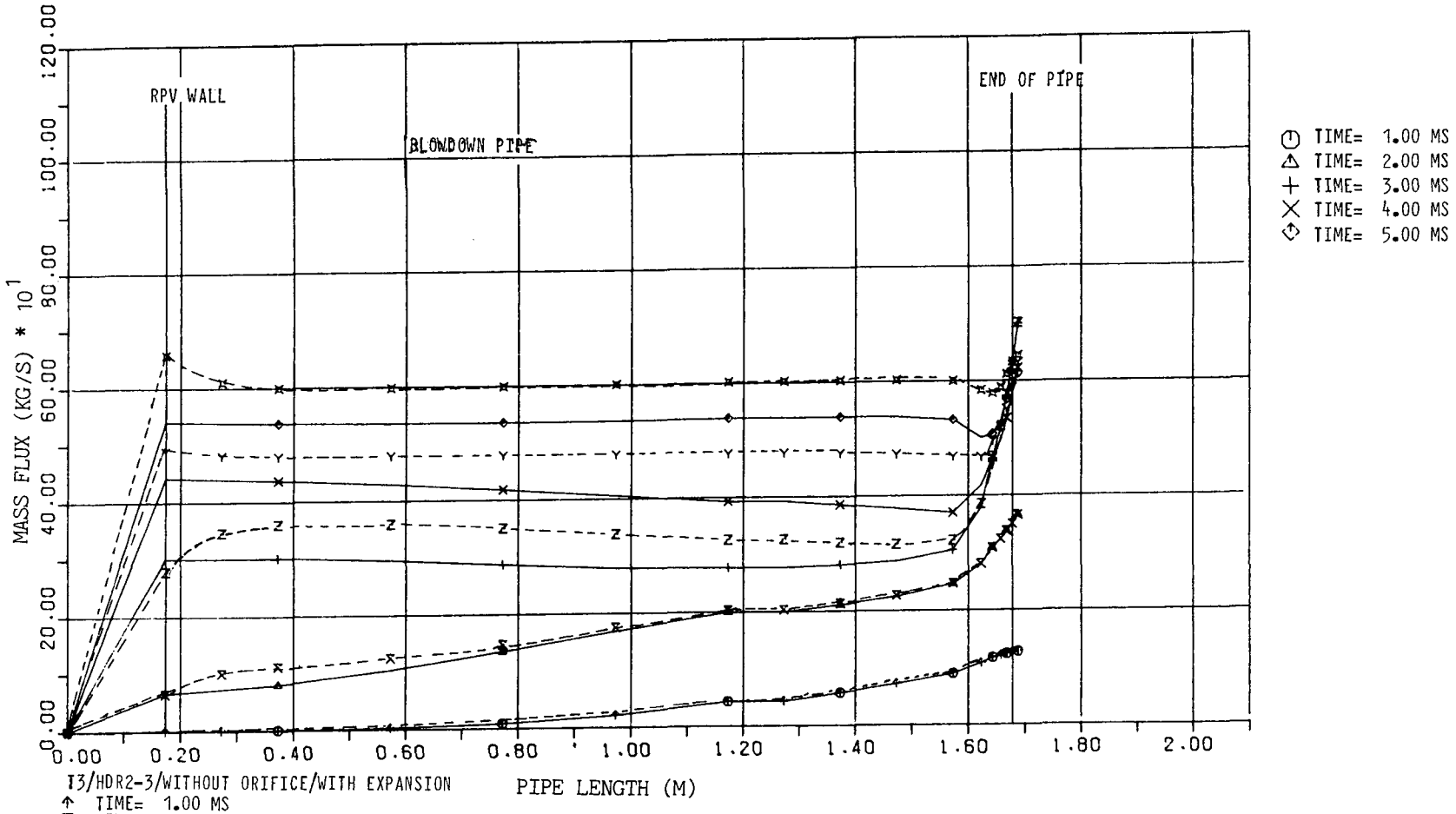

T3/HDR2-3/WITHOUT ORIFICE/WITH EXPANSION

TIME= 1.00 MS
TIME= 2.00 MS
TIME= 3.00 MS
TIME= 4.00 MS
TIME= 5.00 MS

RECALCULATION OF THE HDR-TESTS

MASS FLUX

Fig. 2.2.21

KWU PROFILE PLOT TRAC - PD2 PARAMETER STUDY

THE EFFECT OF DIFFERENT PARAMETERS ON THE PRESSURE

AND THE MASS FLUX

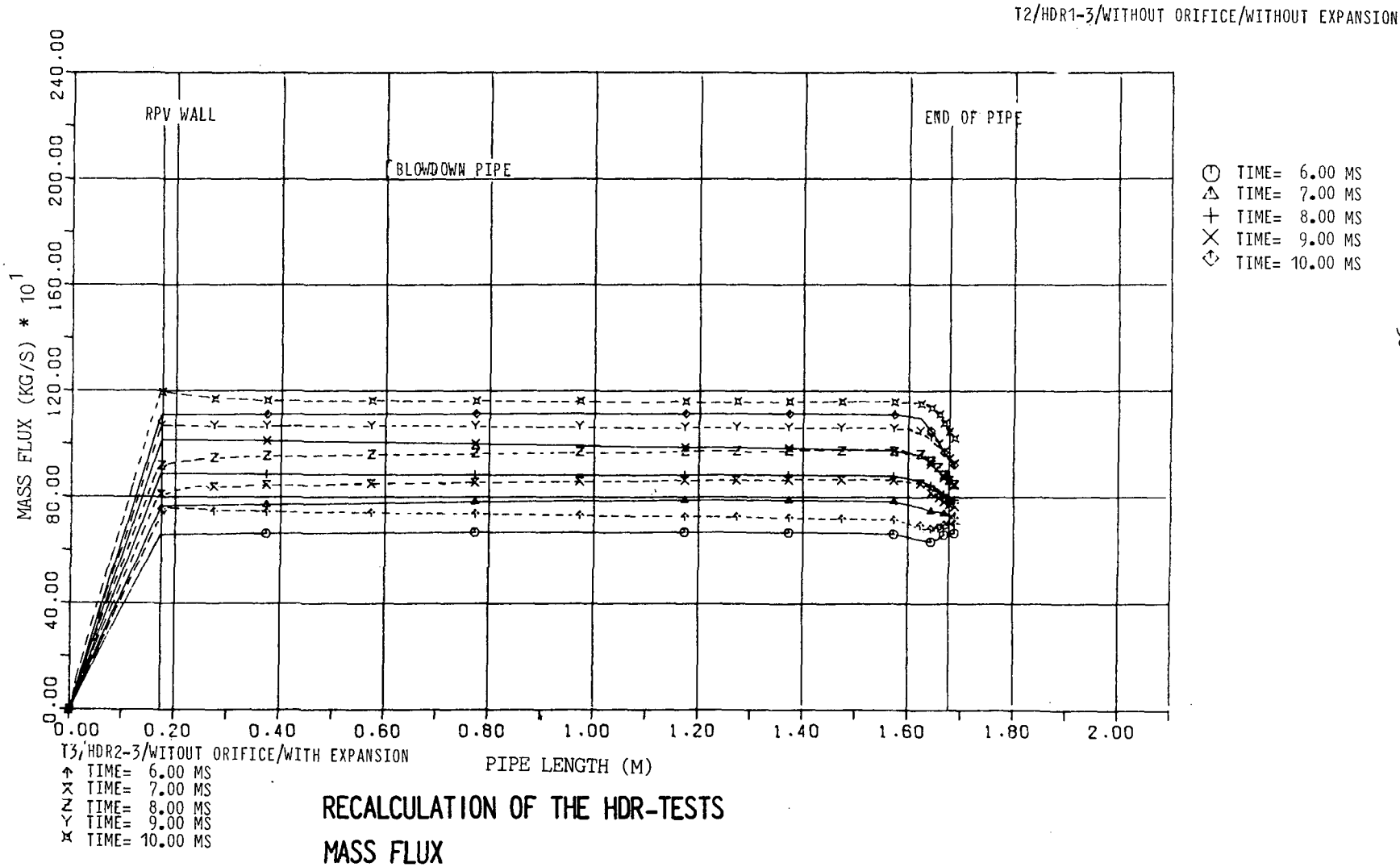

RECALCULATION OF THE HDR-TESTS

MASS FLUX

Fig. 2.2.22

KWU PROFILE PLOT TRAC - PD2 PARAMETER STUDY

THE EFFECT OF DIFFERENT PARAMETERS ON THE PRESSURE AND THE MASS FLUX

T2/HDR1-3/WITHOUT ORIFICE/WITHOUT EXPANSION

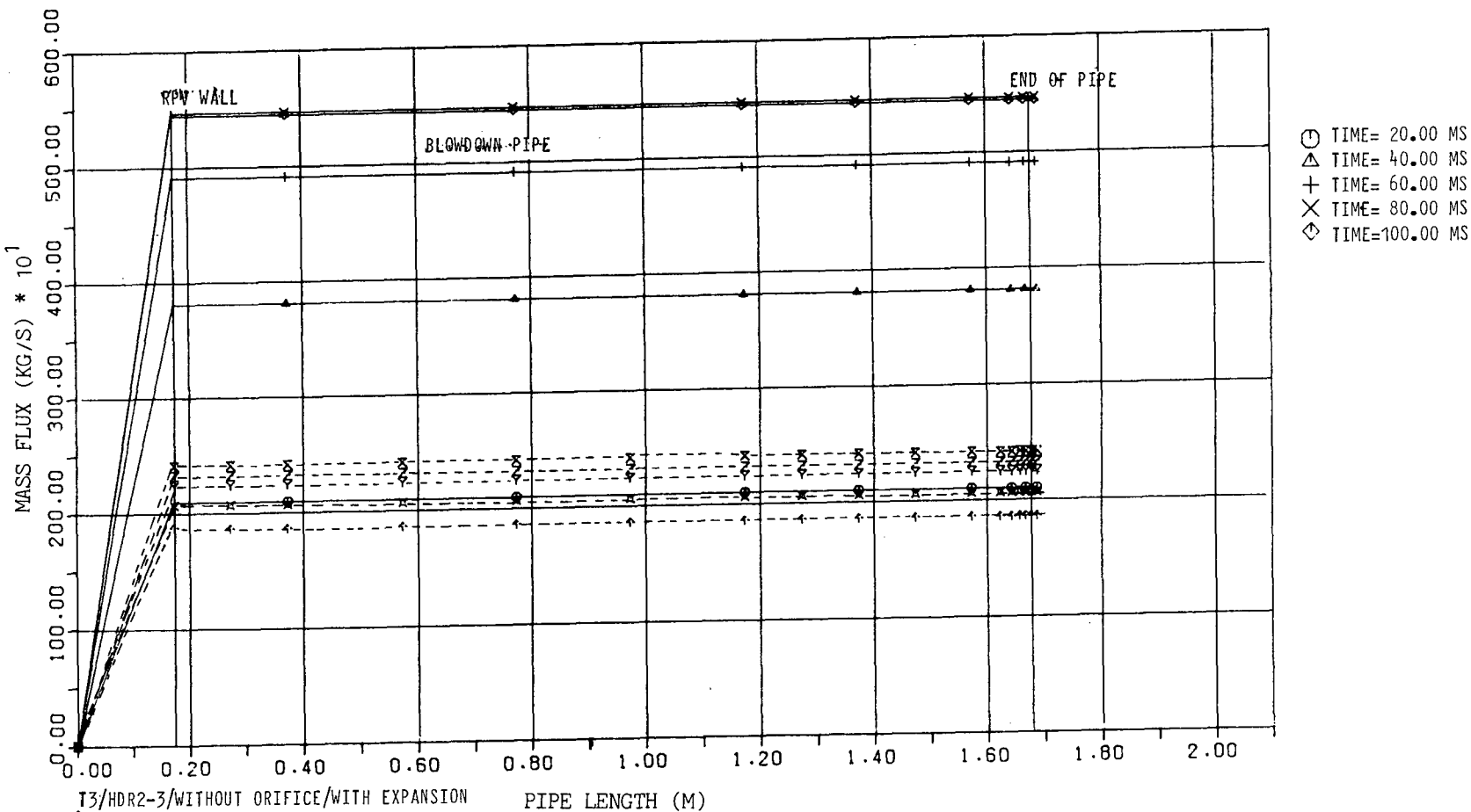

RECALCULATION OF THE HDR-TESTS

MASS FLUX

Fig. 2.2.23

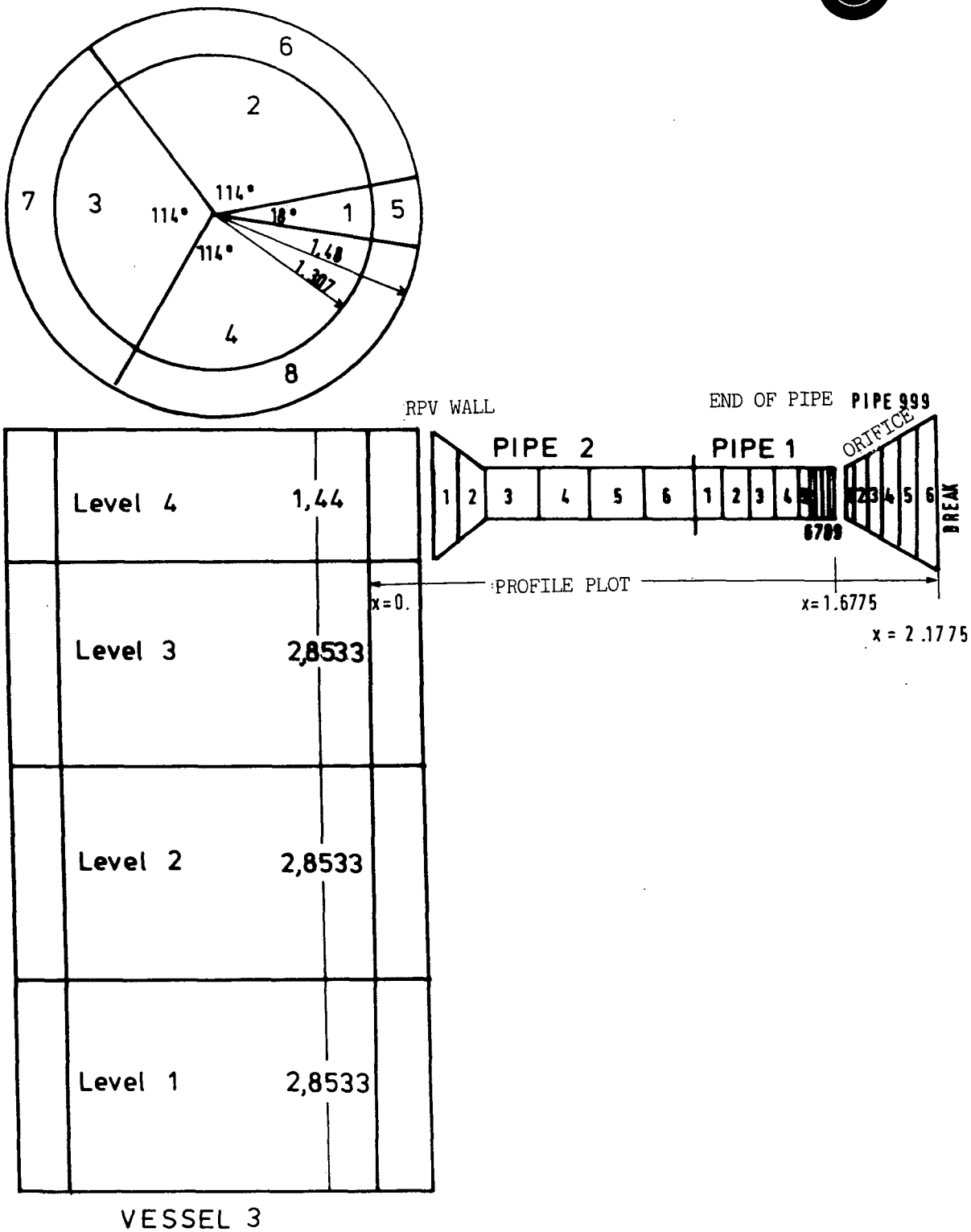

HDR 3/3

Fig. 2.3.1

KWU TRAC - PD2

THE EFFECT OF DIFFERENT PARAMETERS ON THE OUTFLOW RATE

RECALCULATION OF THE HDR-TESTS WITH THE VESSEL COMPONENT

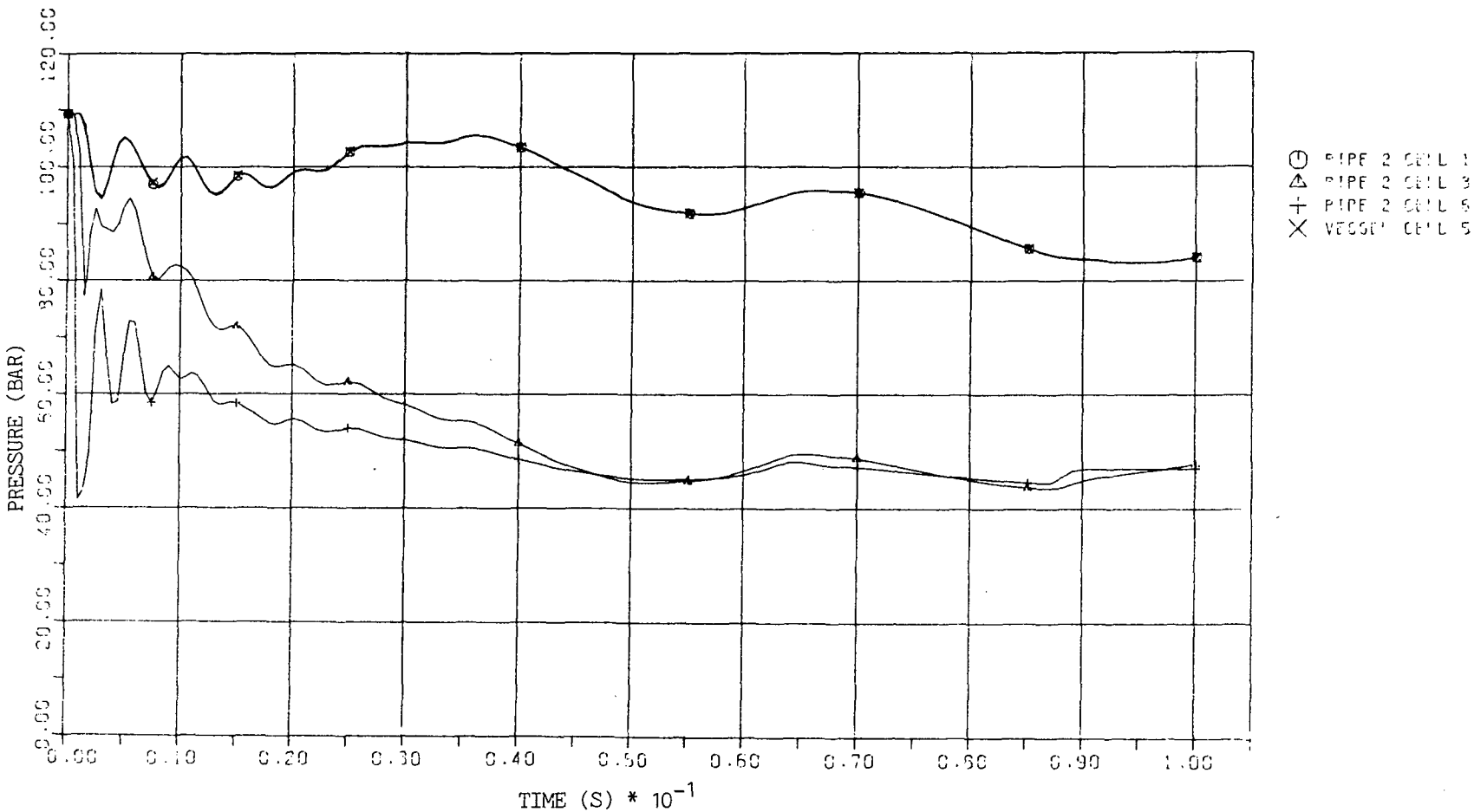

PIPE 2 / VESSEL TYPE 3 / AUTOMATIC BOILER CONNECTION WITH ORIFICE

PRESSURE

Fig. 2.3.2

KWU TRAC - PD2

THE EFFECT OF DIFFERENT PARAMETERS ON THE OUTFLOW RATE

RECALCULATION OF THE HDR-TESTS WITH THE VESSEL COMPONENT

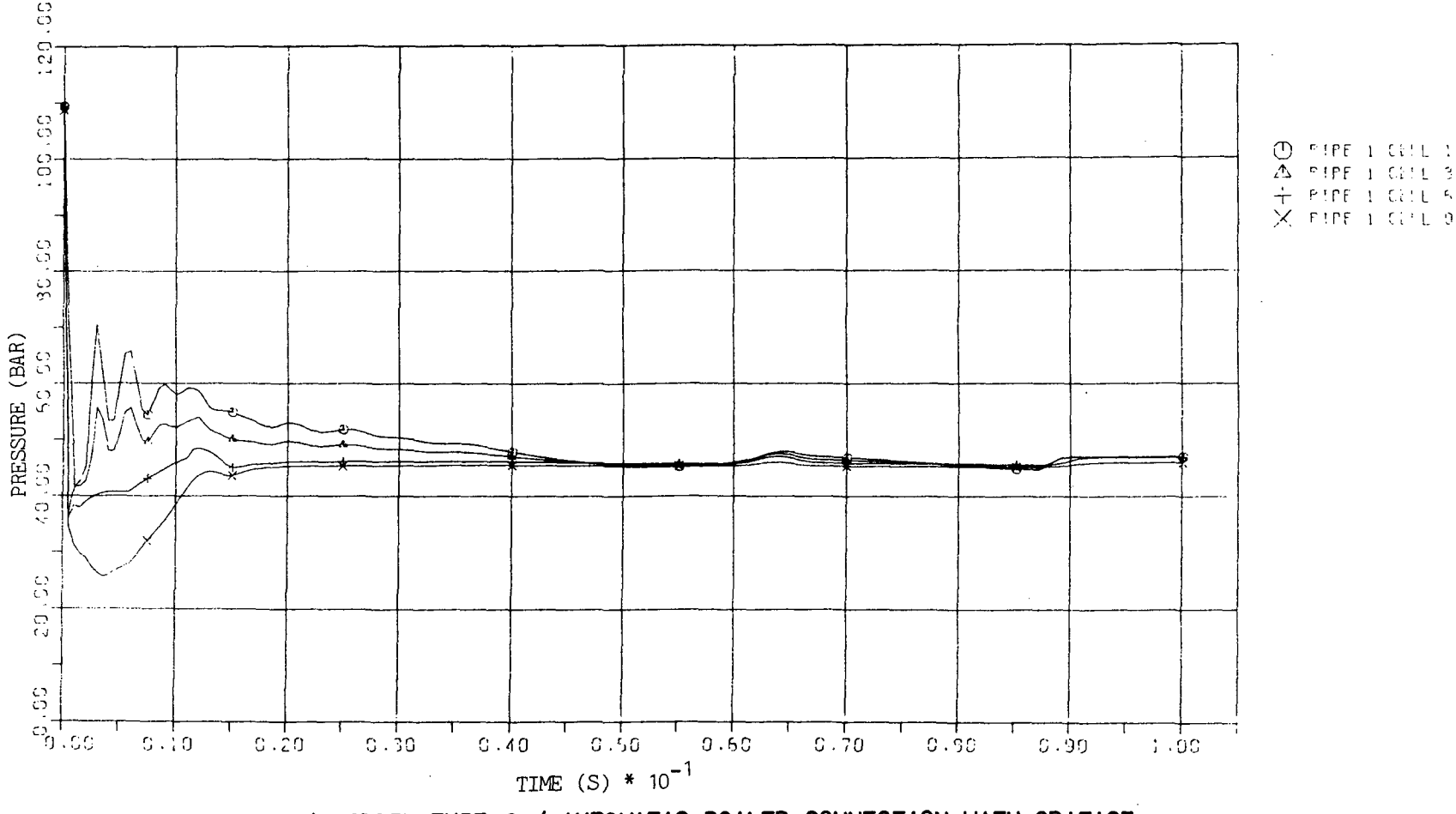

PIPE 2 / VESSEL TYPE 3 / AUTOMATIC BOILER CONNECTION WITH ORIFICE

PRESSURE

Fig.2.3.3

KWU TRAC -PD2

THE EFFECT OF DIFFERENT PARAMETERS ON THE OUTFLOW RATE

RECALCULATION OF THE HDR-TESTS WITH THE VESSEL COMPONENT

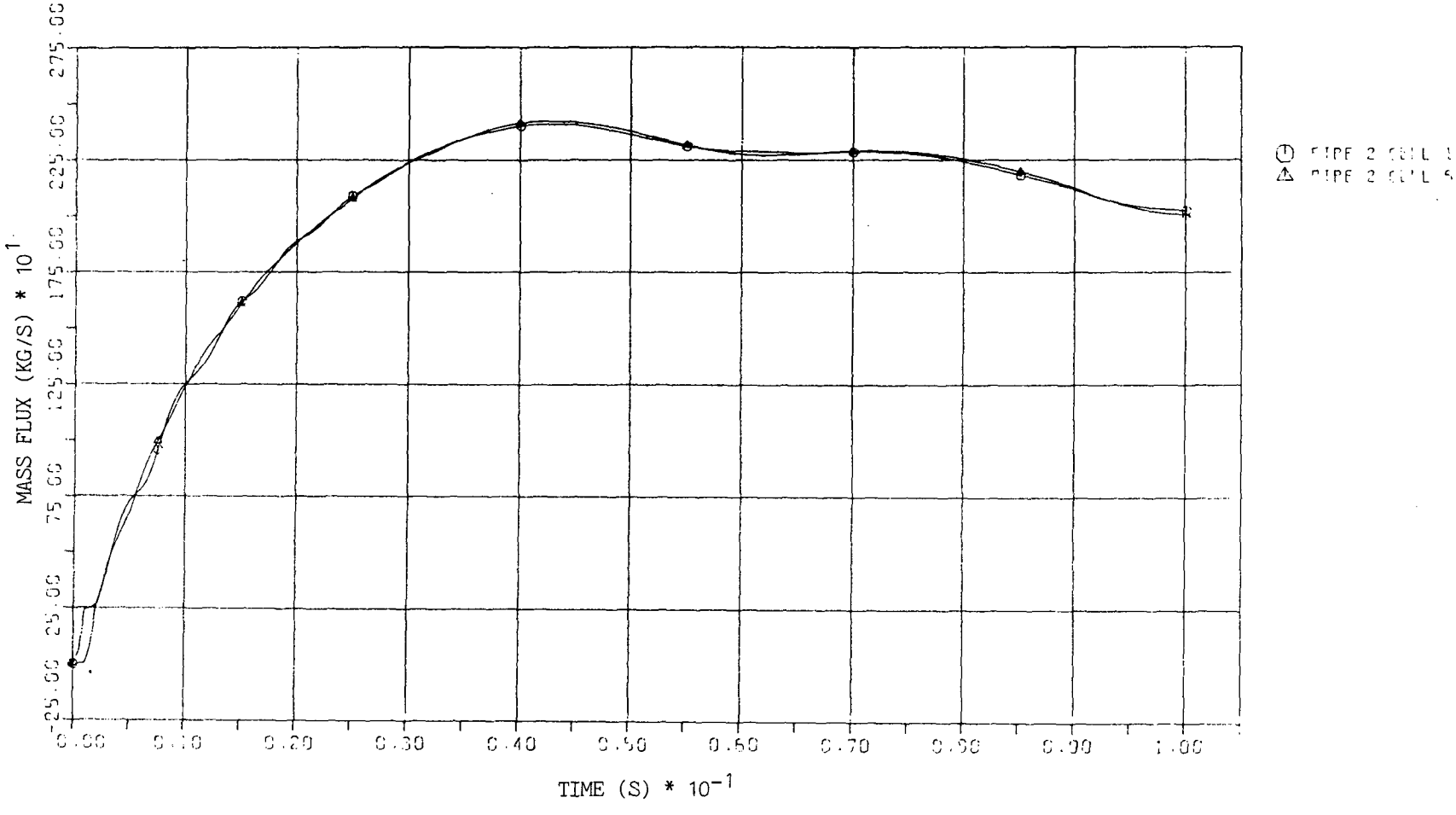

PIPE 2 / VESSEL TYPE 3 / AUTOMATIC BOILER CONNECTION WITH ORIFICE

MASS FLUX

Fig. 2.3.4

KWU TRAC - PD2

THE EFFECT OF DIFFERENT PARAMETERS ON THE OUTFLOW RATE

RECALCULATION OF THE HDR-TESTS WITH THE VESSEL COMPONENT

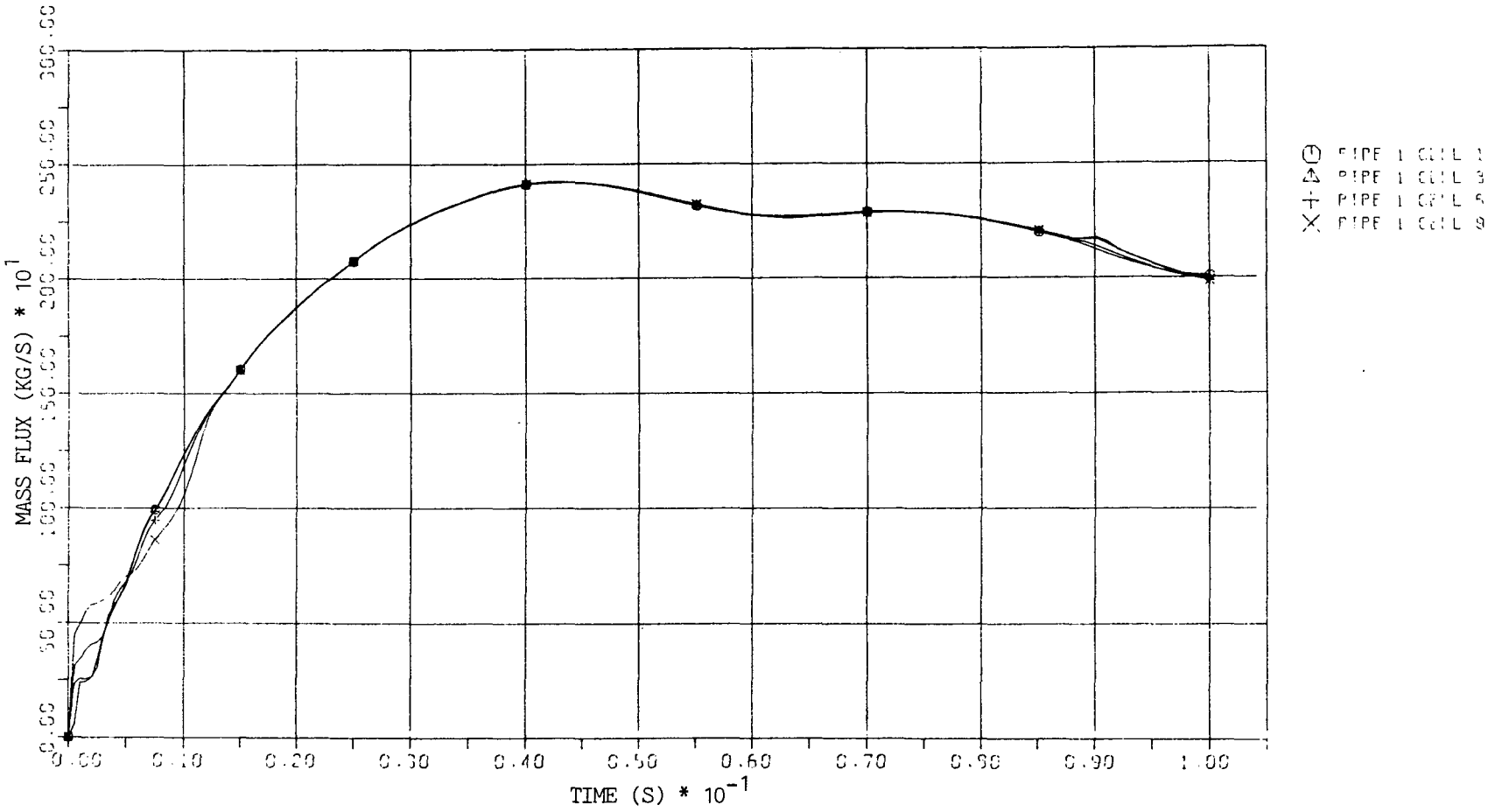

PIPE 2 / VESSEL TYPE 3 / AUTOMATIC BOILER CONNECTION WITH ORIFICE

MASS FLUX

Fig. 2.3.5

KWU TRAC - PD2

THE EFFECT OF DIFFERENT PARAMETERS ON THE OUTFLOW RATE

RECALCULATION OF THE HDR-TESTS WITH THE VESSEL COMPONENT

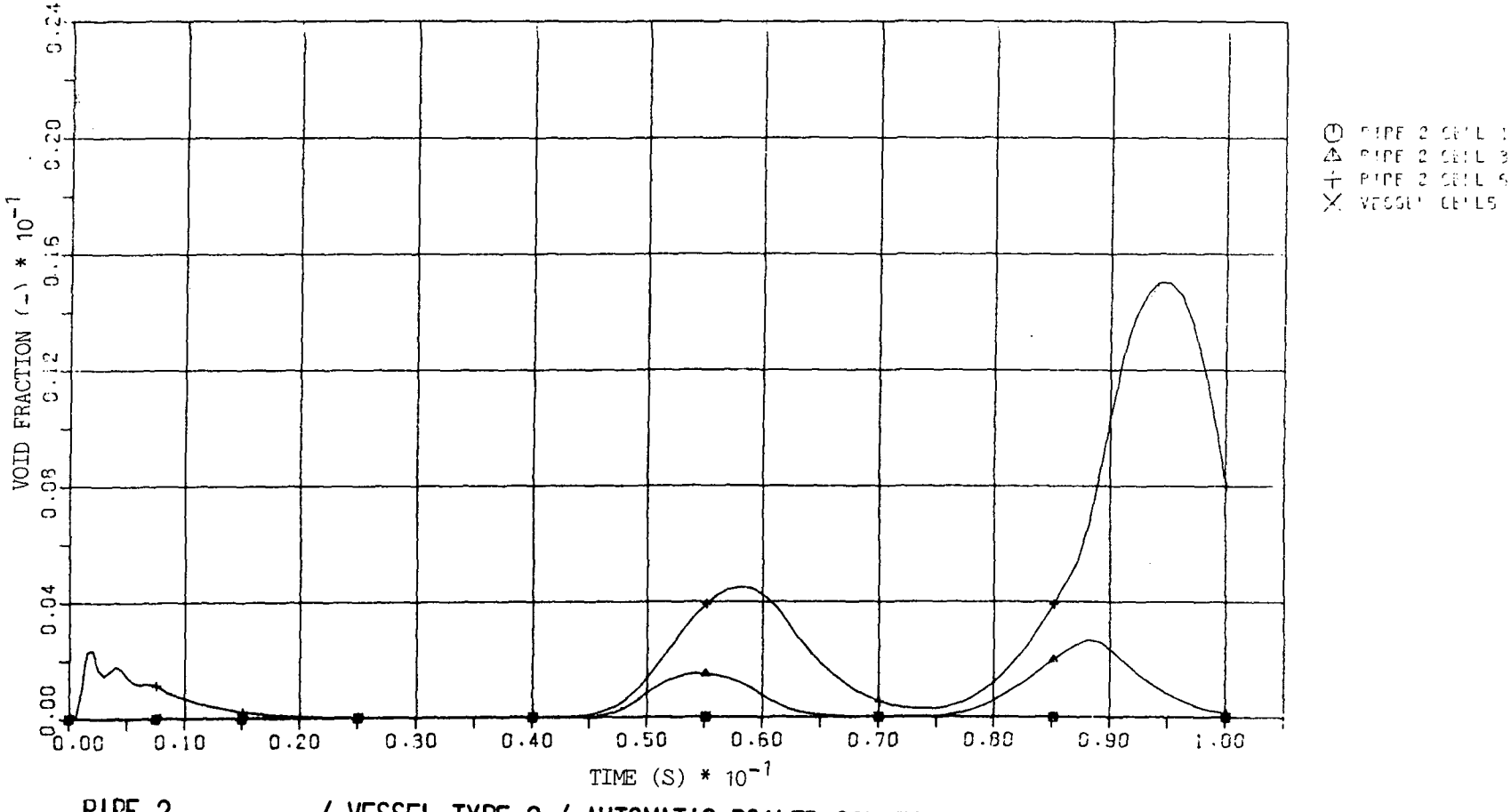

PIPE 2 / VESSEL TYPE 3 / AUTOMATIC BOILER CONNECTION WITH ORIFICE

VOID FRACTION

Fig. 2.3.6

KWU TRAC - PD2

THE EFFECT OF DIFFERENT PARAMETERS ON THE OUTFLOW RATE

RECALCULATION OF THE HDR-TESTS WITH THE VESSEL COMPONENT

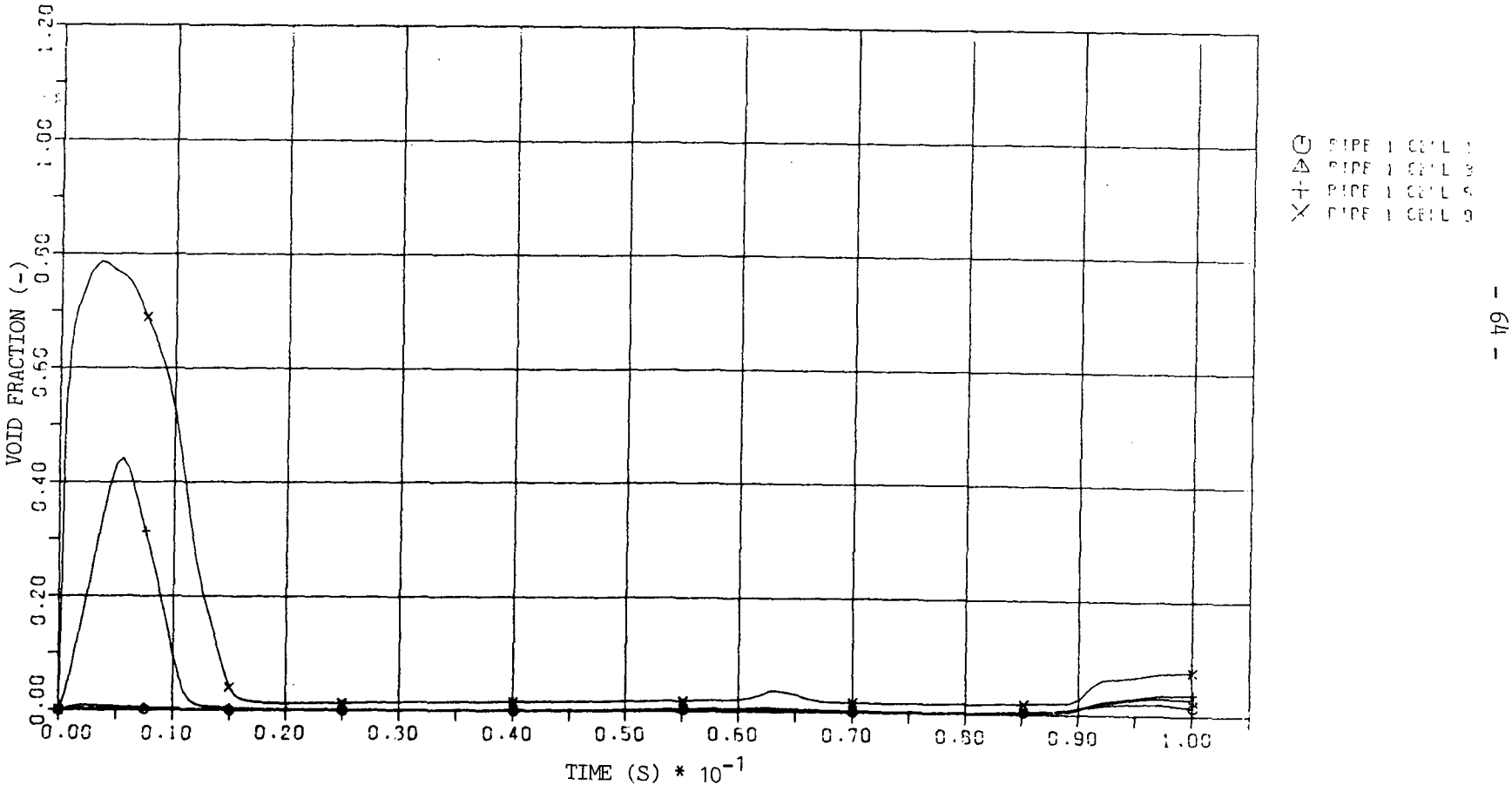

PIPE 2 / VESSEL TYPE 3 / AUTOMATIC BOILER CONNECTION WITH ORIFICE

VOID FRACTION

Fig. 2.3.7

KWU TRAC - PD2

THE EFFECT OF DIFFERENT PARAMETERS ON THE OUTFLOW RATE

RECALCULATION OF THE HDR-TESTS WITH THE VESSEL COMPONENT

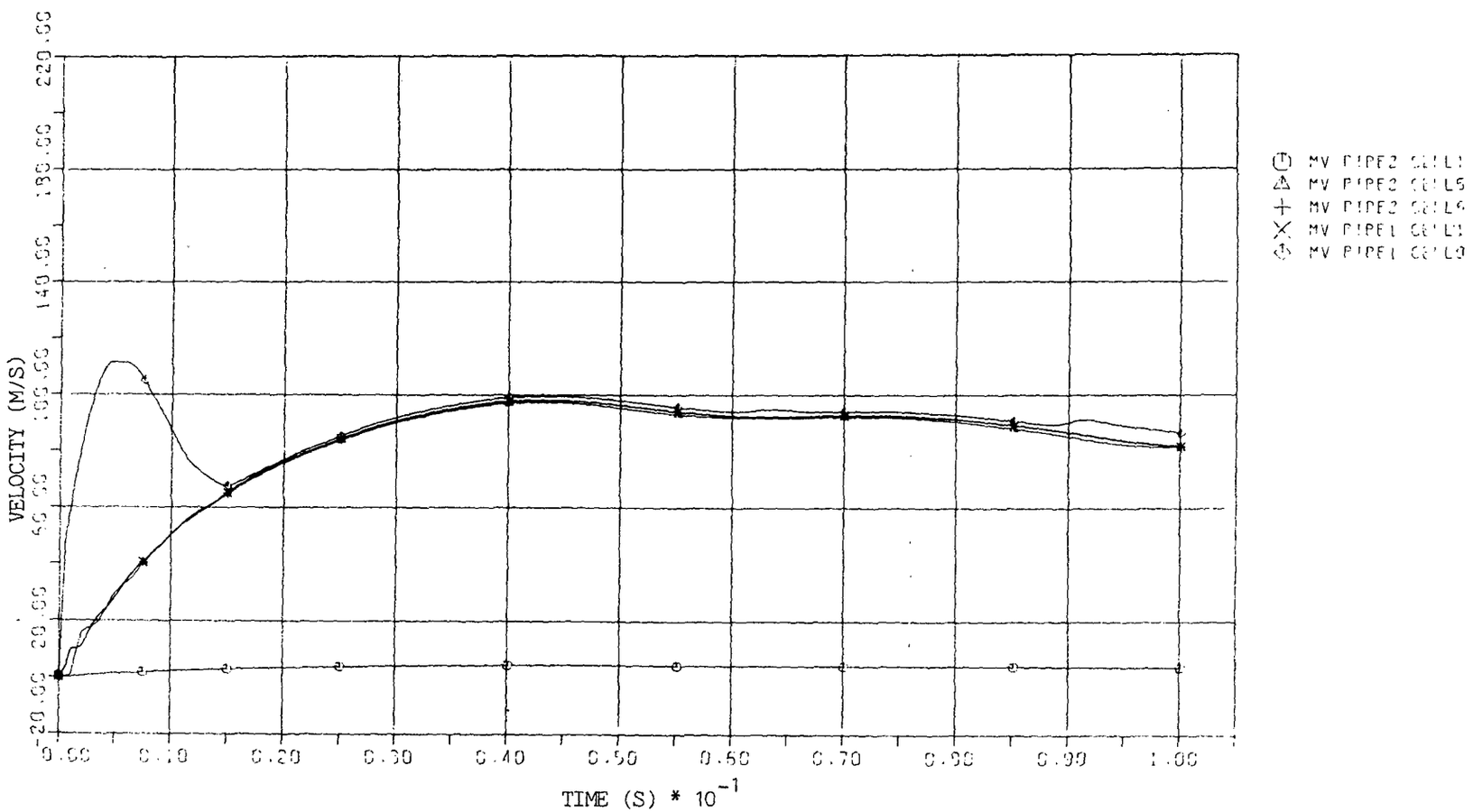

PIPE 2 / VESSEL TYPE 3 / AUTOMATIC BOILER CONNECTION WITH ORIFICE

VELOCITY

Fig. 2.3.8

KWU TRAC - PD2

THE EFFECT OF DIFFERENT PARAMETERS ON THE OUTFLOW RATE

RECALCULATION OF THE HDR-TESTS WITH THE VESSEL COMPONENT

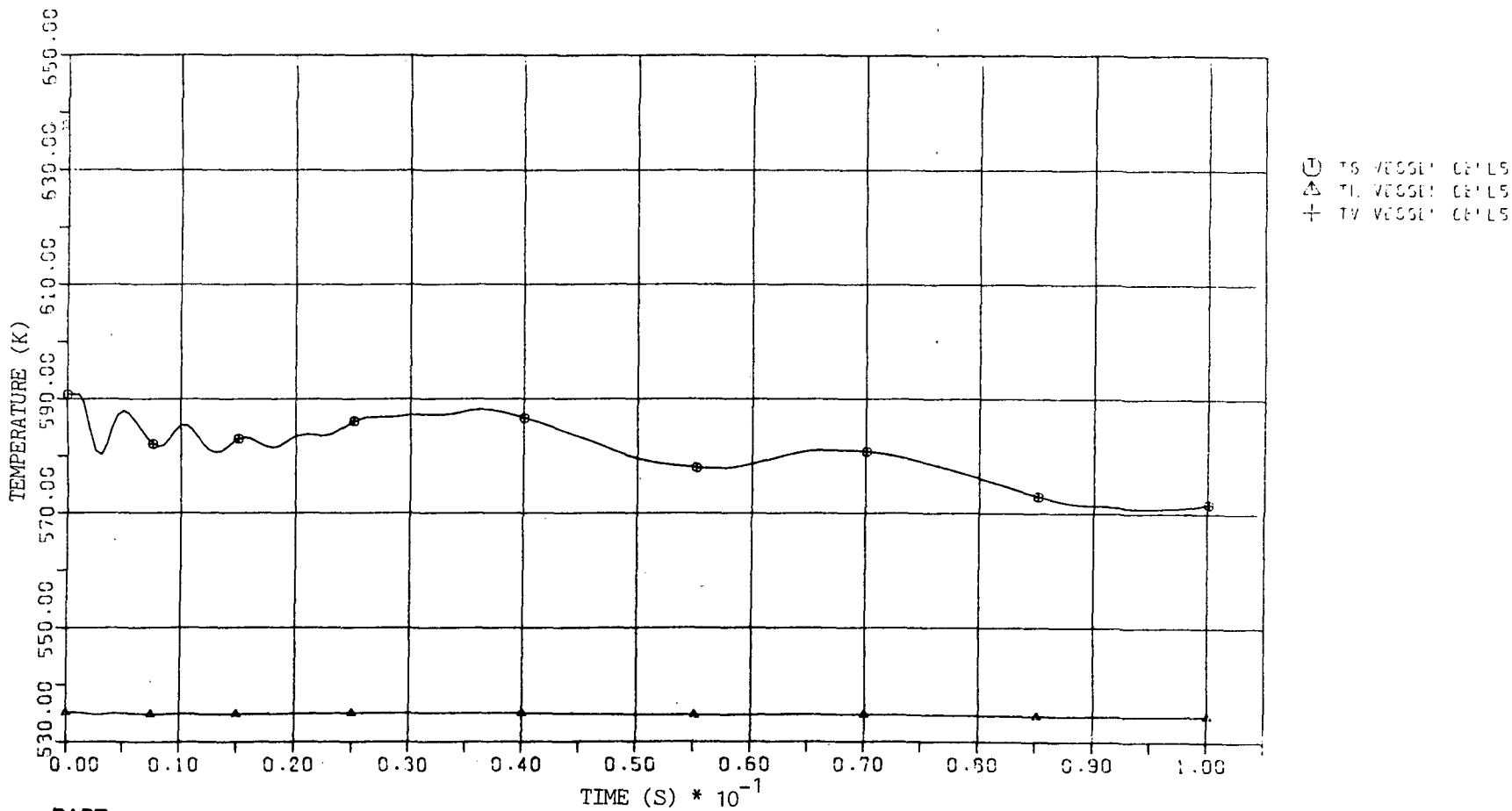

PIPE 2 / VESSEL TYPE 3 / AUTOMATIC BOILER CONNECTION WITH ORIFICE

TEMPERATURE

Fig. 2.3.9

KWU TRAC - PD2

THE EFFECT OF DIFFERENT PARAMETERS ON THE OUTFLOW RATE

RECALCULATION OF THE HDR-TESTS WITH THE VESSEL COMPONENT

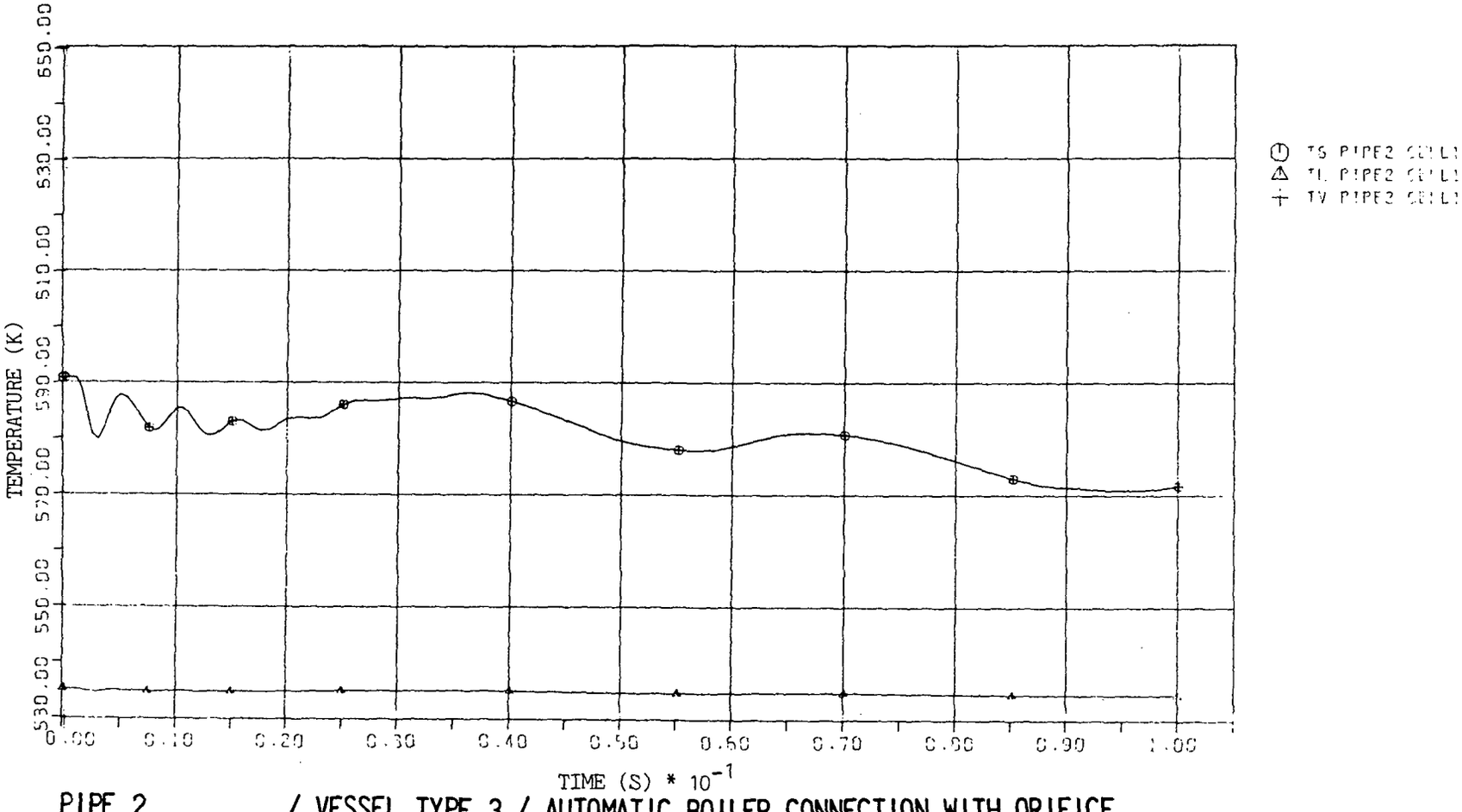

PIPE 2 / VESSEL TYPE 3 / AUTOMATIC BOILER CONNECTION WITH ORIFICE

TEMPERATURE

Fig. 2.3.10

KWU TRAC -PD2

THE EFFECT OF DIFFERENT PARAMETERS ON THE OUTFLOW RATE

RECALCULATION OF THE HDR-TESTS WITH THE VESSEL COMPONENT

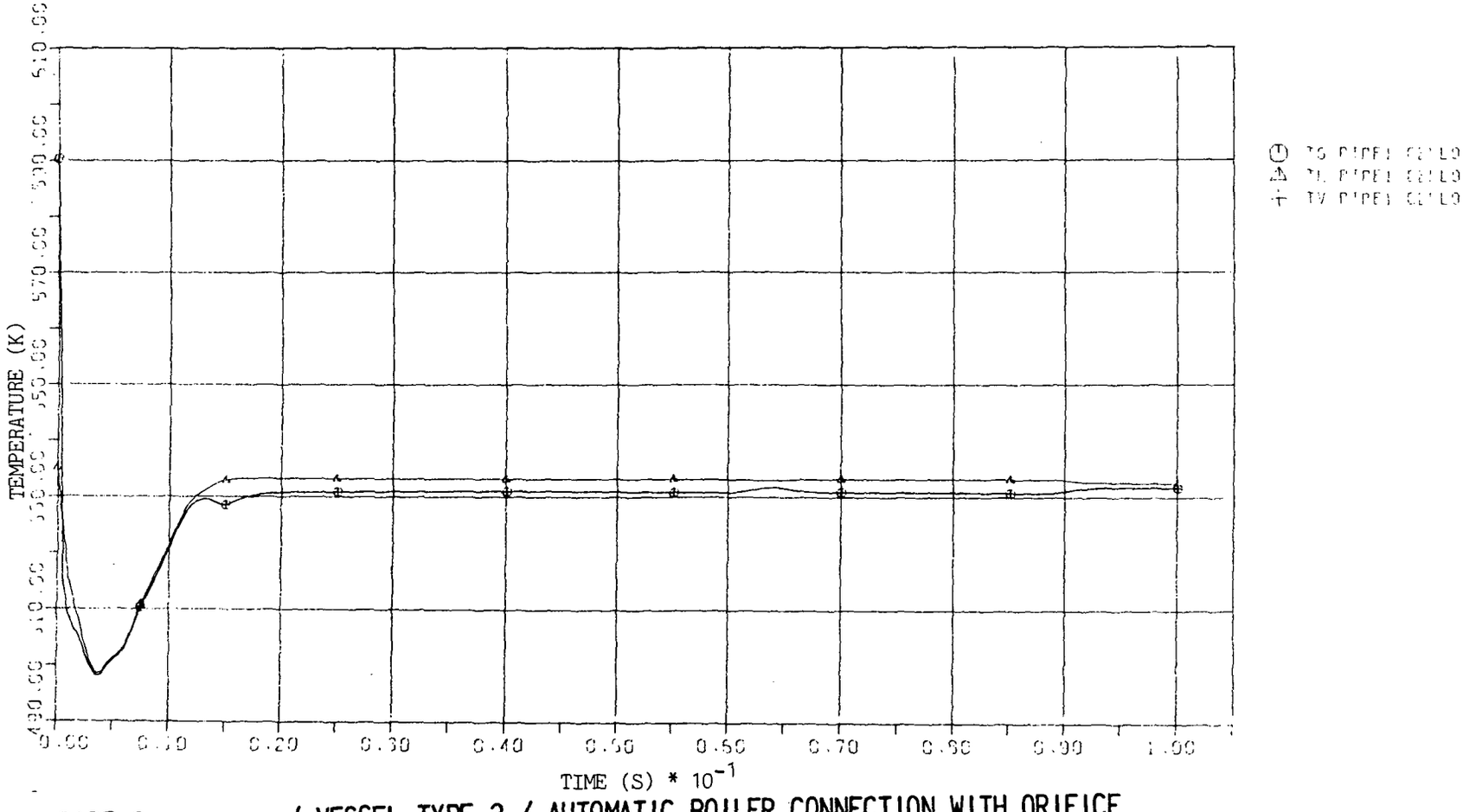

PIPE 2 / VESSEL TYPE 3 / AUTOMATIC BOILER CONNECTION WITH ORIFICE

TEMPERATURE

Fig. 2.3.11

KWU TRAC - PD2

THE EFFECT OF DIFFERENT PARAMETERS ON THE OUTFLOW RATE

RECALCULATION OF THE HDR-TESTS WITH THE VESSEL COMPONENT

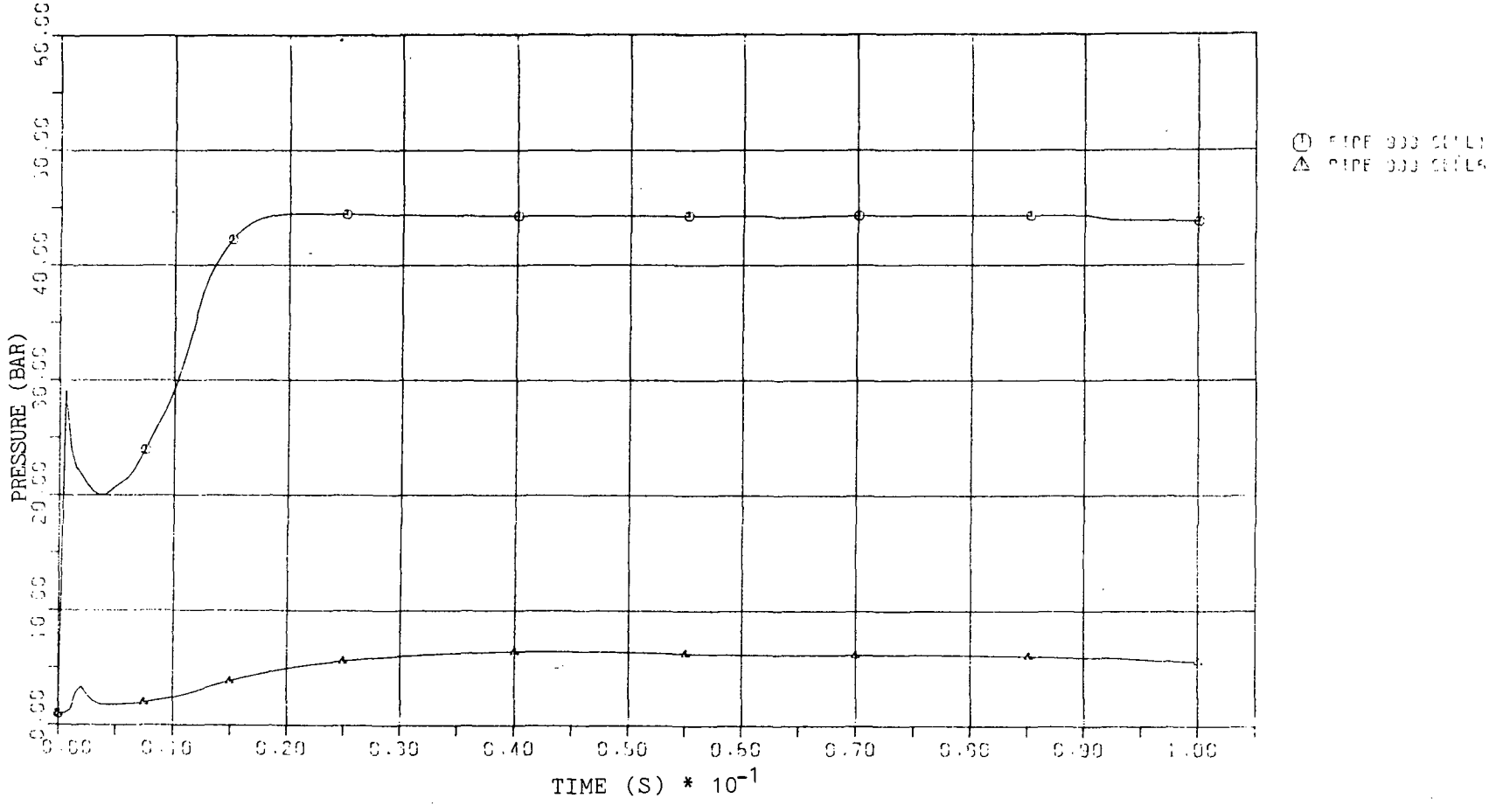

PIPE 2 / VESSEL TYPE 3 / AUTOMATIC BOILER CONNECTION WITH ORIFICE

PRESSURE

Fig. 2.3.12

KWU TRAC - PD2

THE EFFECT OF DIFFERENT PARAMETERS ON THE OUTFLOW RATE

RECALCULATION OF THE HDR-TESTS WITH THE VESSEL COMPONENT

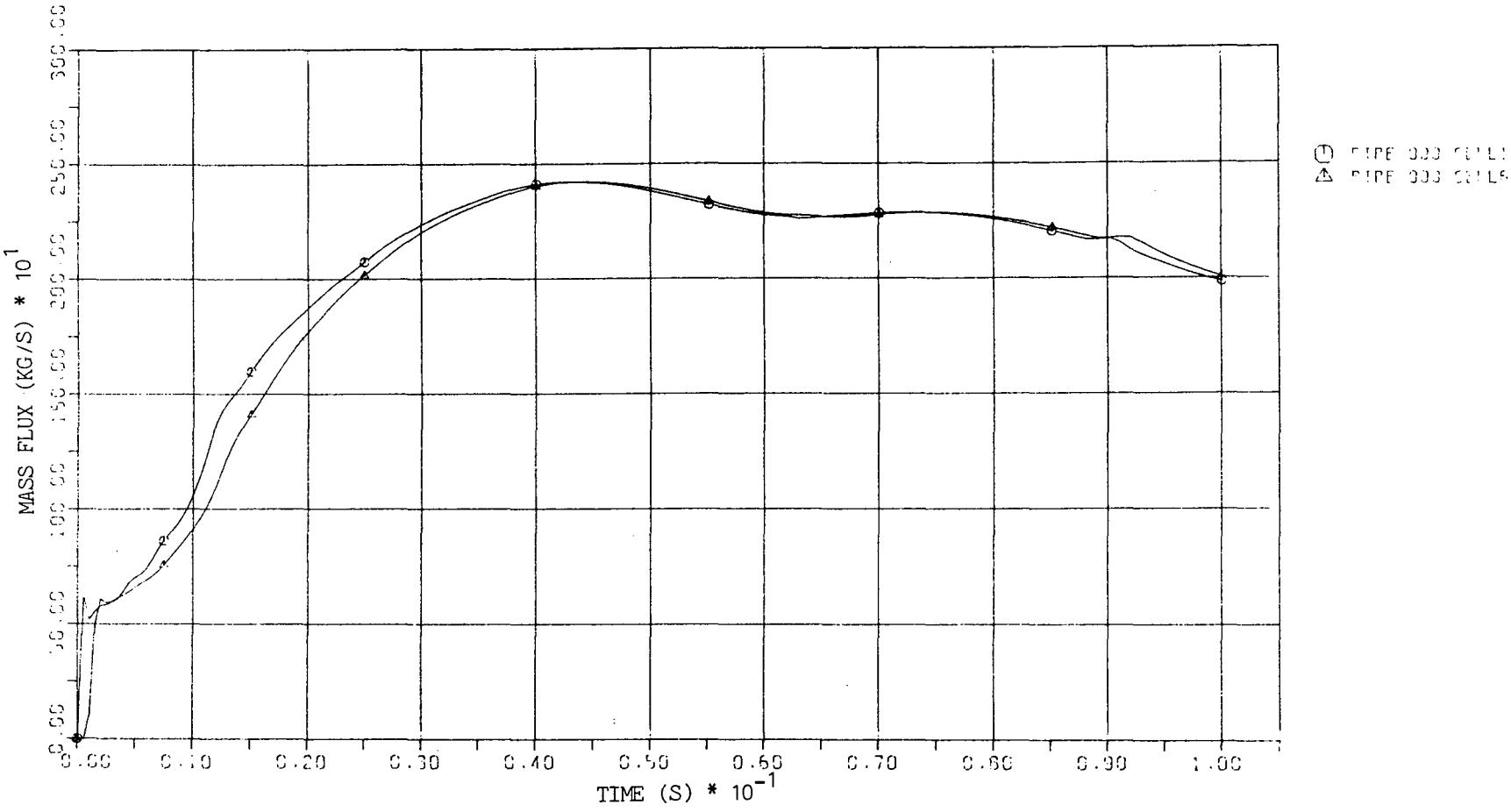

PIPE 2 / VESSEL TYPE 3 / AUTOMATIC BOILER CONNECTION WITH ORIFICE

Fig. 2.3.13

KWU TRAC - PD2

THE EFFECT OF DIFFERENT PARAMETERS ON THE OUTFLOW RATE

RECALCULATION OF THE HDR-TESTS WITH THE VESSEL COMPONENT

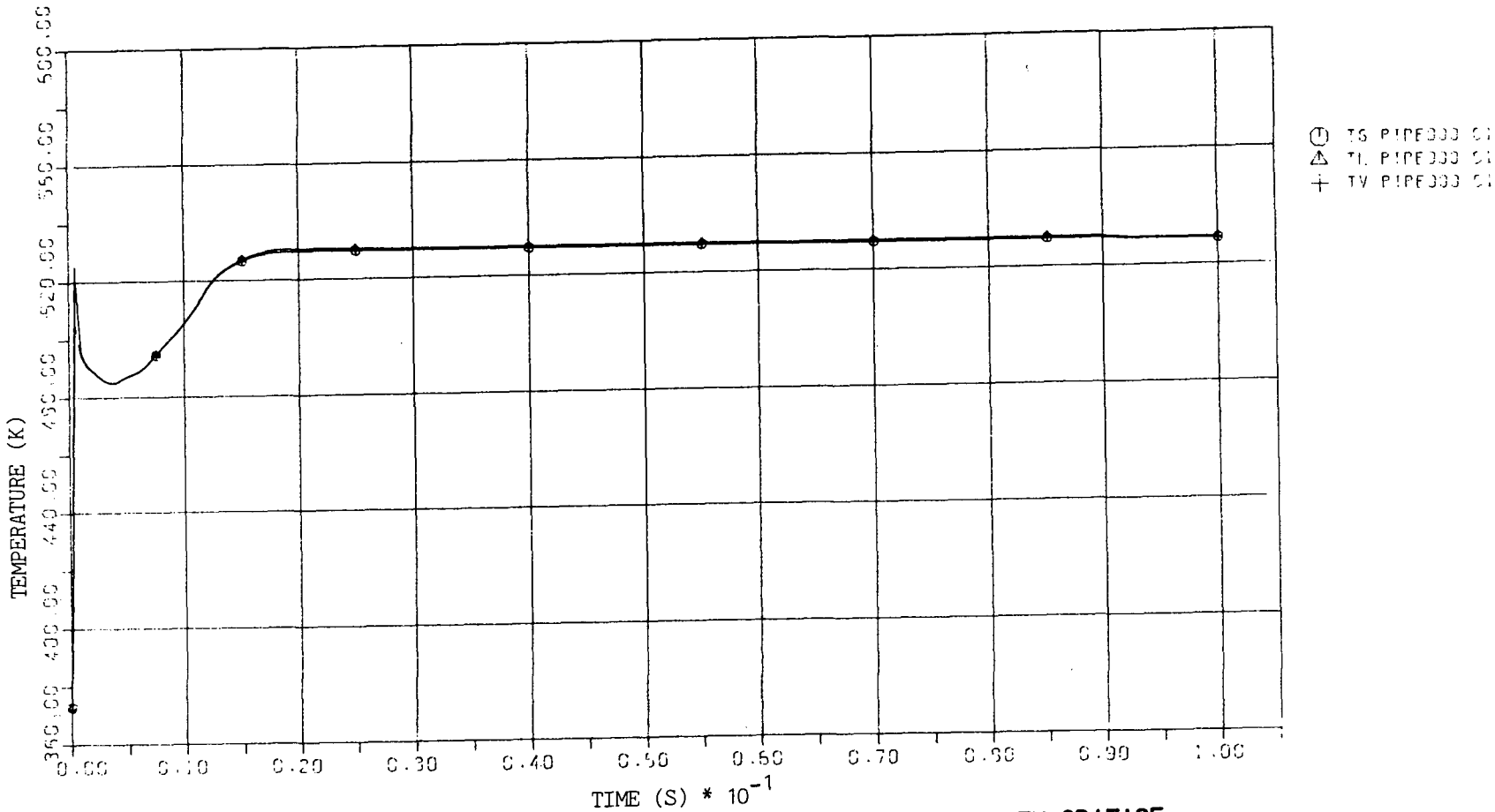

PIPE 2 / VESSEL TYPE 3 / AUTOMATIC BOILER CONNECTION WITH ORIFICE

TEMPERATURE

Fig. 2.3.14

KWU PROFILE PLOT TRAC - PD2 PARAMETER STUDY

THE EFFECT OF DIFFERENT PARAMETERS ON THE PRESSURE

AND THE MASS FLUX

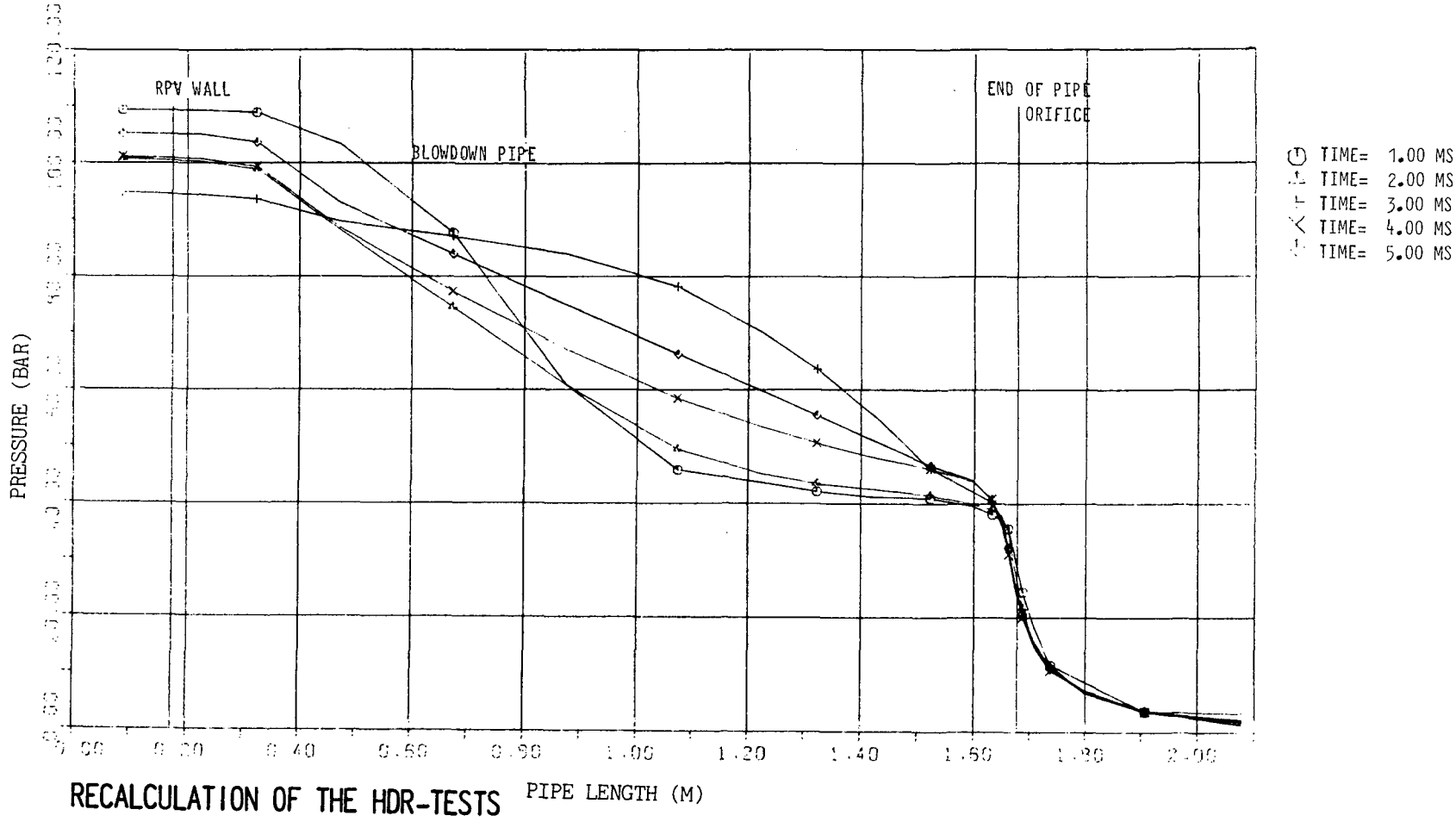

RECALCULATION OF THE HDR-TESTS

PRESSURE WITH ORIFICE AND WITH EXPANSION AT THE RPV

Fig. 2.3.15

KWU PROFILE PLOT TRAC - PD2 PARAMETER STUDY

THE EFFECT OF DIFFERENT PARAMETERS ON THE PRESSURE

AND THE MASS FLUX

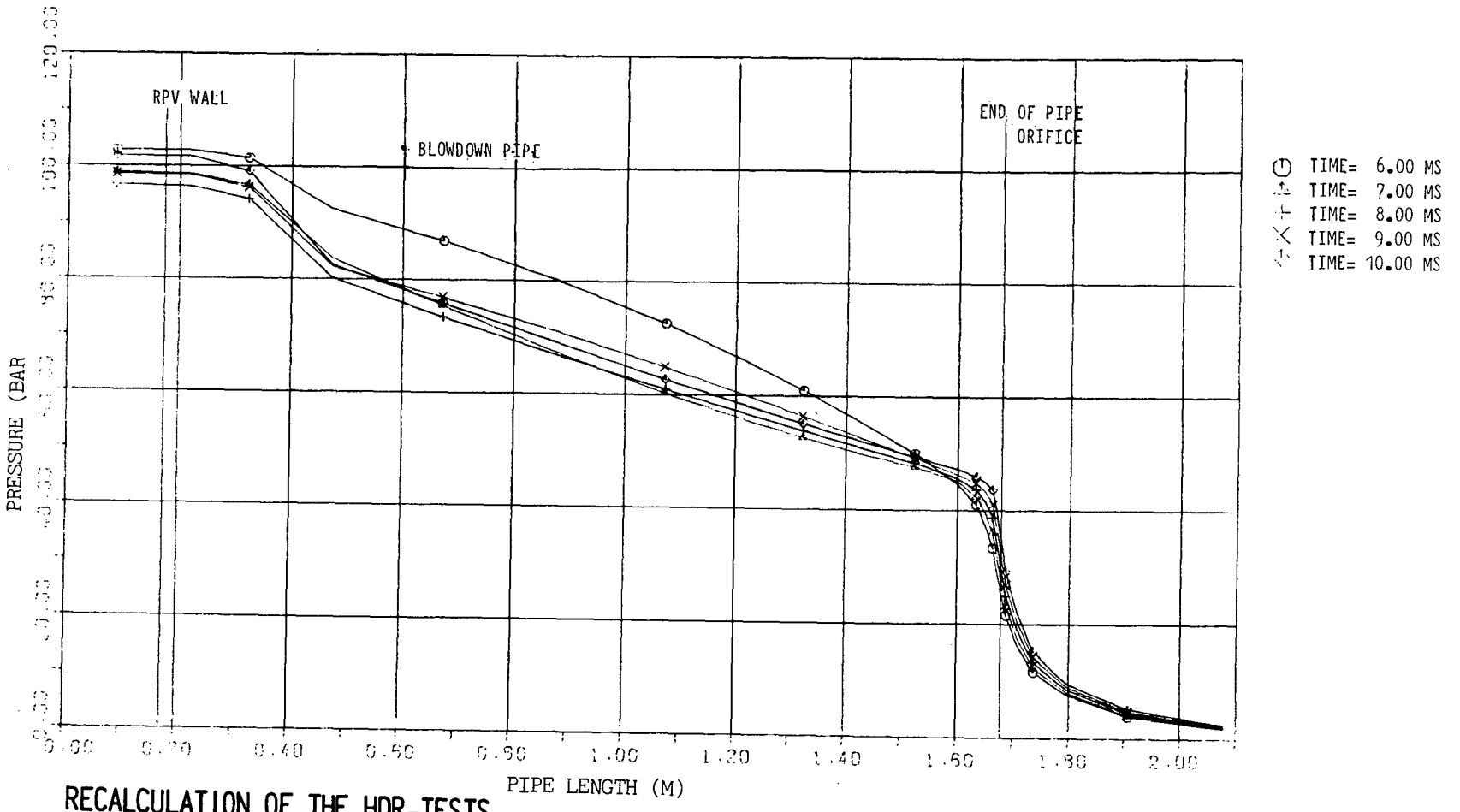

RECALCULATION OF THE HDR-TESTS

PRESSURE WITH ORIFICE AND WITH EXPANSION AT THE RPV

Fig. 2.3.16

KWU PROFILE PLOT TRAC - PD2 PARAMETER STUDY

THE EFFECT OF DIFFERENT PARAMETERS ON THE PRESSURE

AND THE MASS FLUX

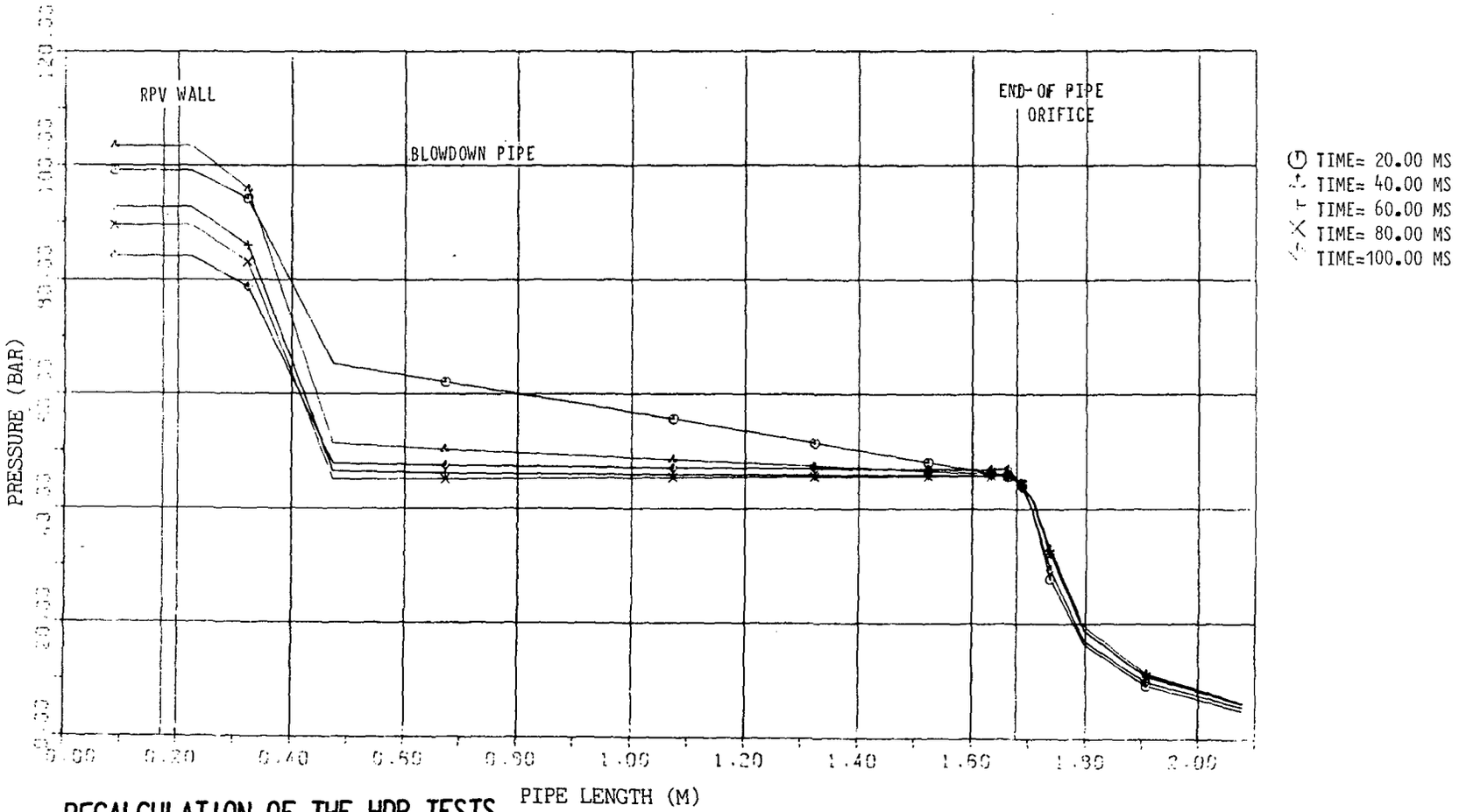

RECALCULATION OF THE HDR-TESTS

PRESSURE WITH ORIFICE AND WITH EXPANSION AT THE RPV

Fig. 2.3.17

KWU PROFILE PLOT TRAC - PD2 PARAMETER STUDY

THE EFFECT OF DIFFERENT PARAMETERS ON THE PRESSURE

AND THE MASS FLUX

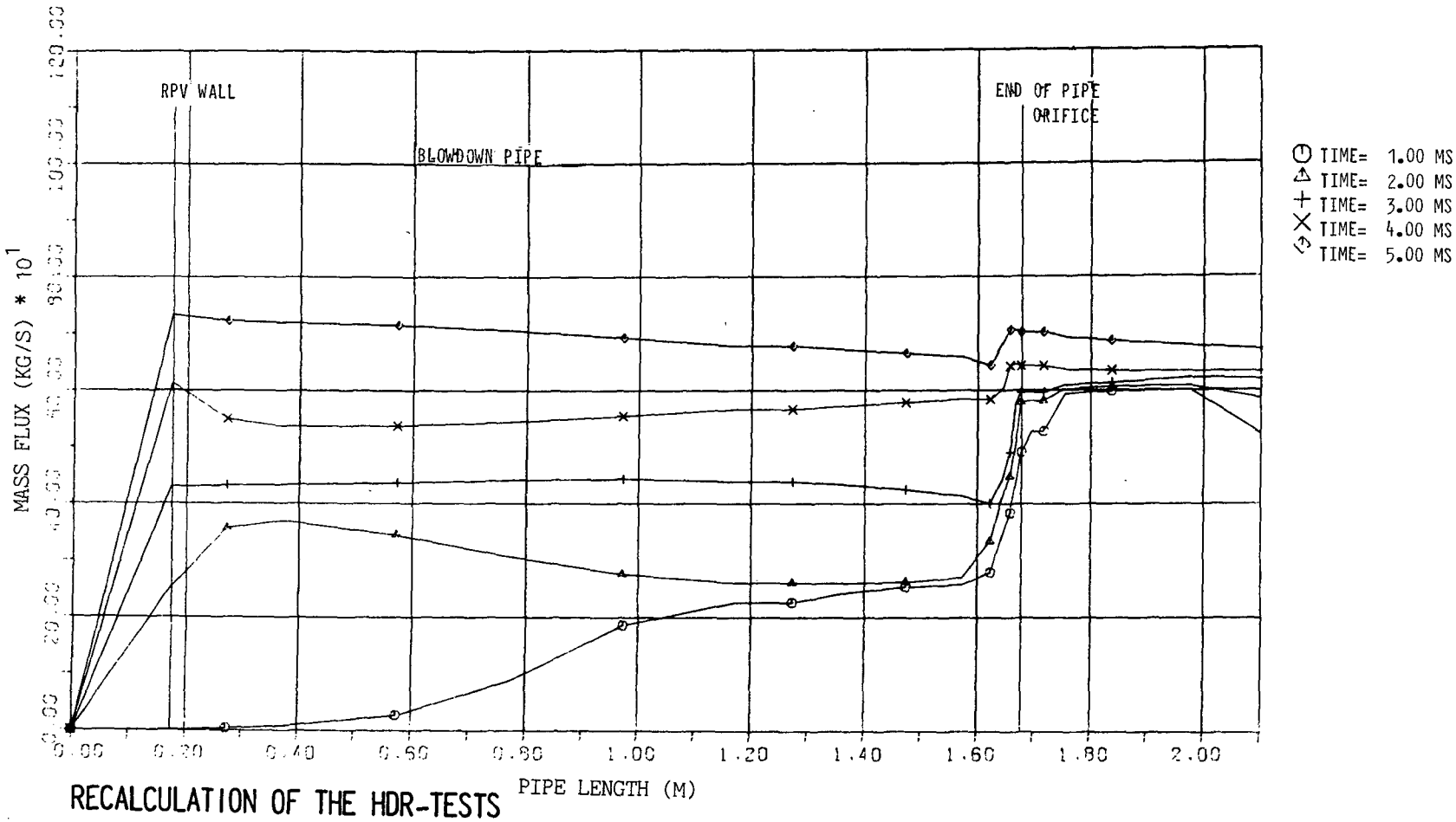

RECALCULATION OF THE HDR-TESTS

MASS FLUX WITH ORIFICE AND WITH EXPANSION AT THF RPV

Fig. 2.3.18

KWU PROFILE PLOT TRAC - PD2 PARAMETER STUDY

THE EFFECT OF DIFFERENT PARAMETERS ON THE PRESSURE

AND THE MASS FLUX

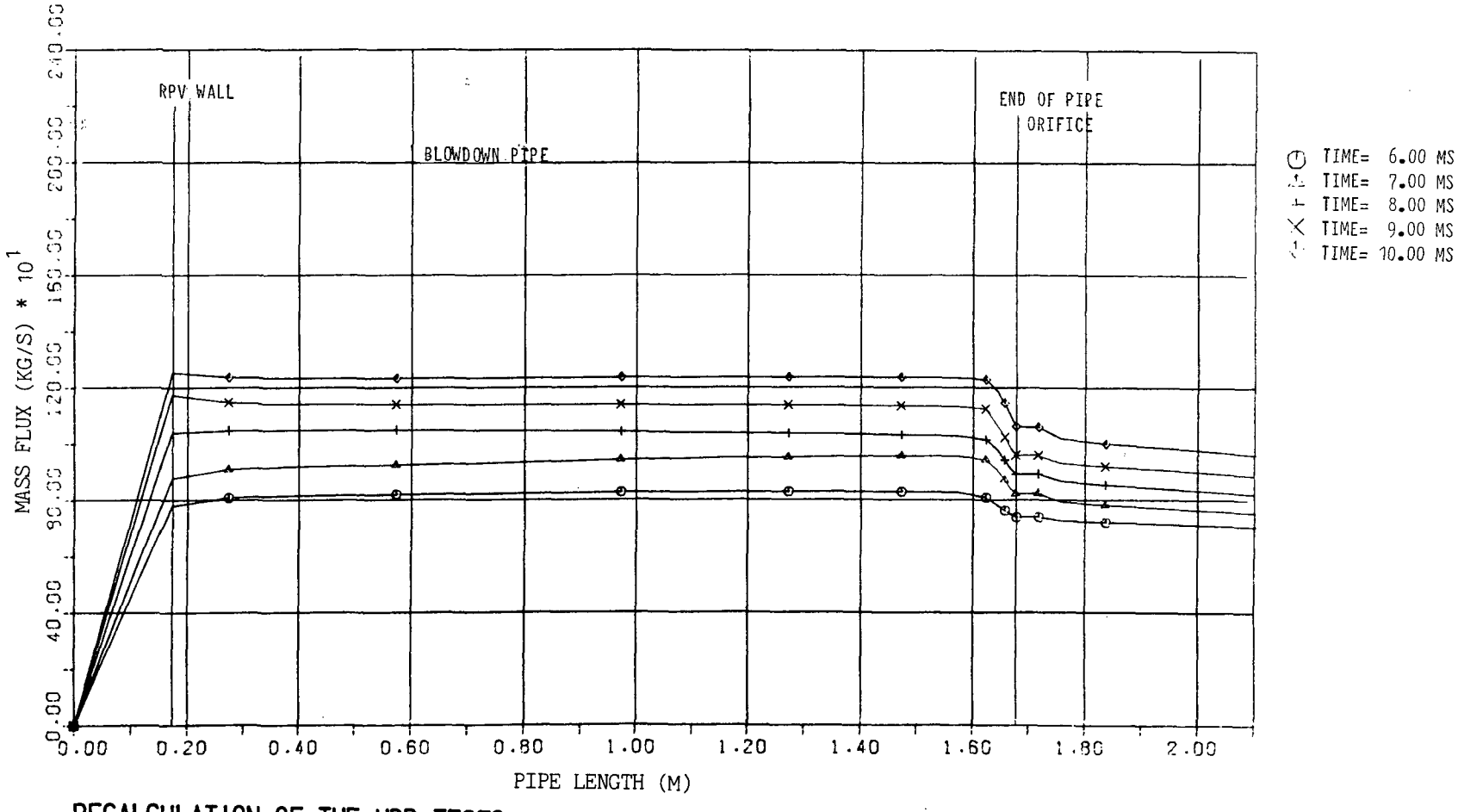

RECALCULATION OF THE HDR-TESTS

MASS FLUX WITH ORIFICE AND WITH EXPANSION AT THE RPV

Fig. 2.3.19

KWU PROFILE PLOT TRAC - PD2 PARAMETER STUDY

THE EFFECT OF DIFFERENT PARAMETERS ON THE PRESSURE

AND THE MASS FLUX

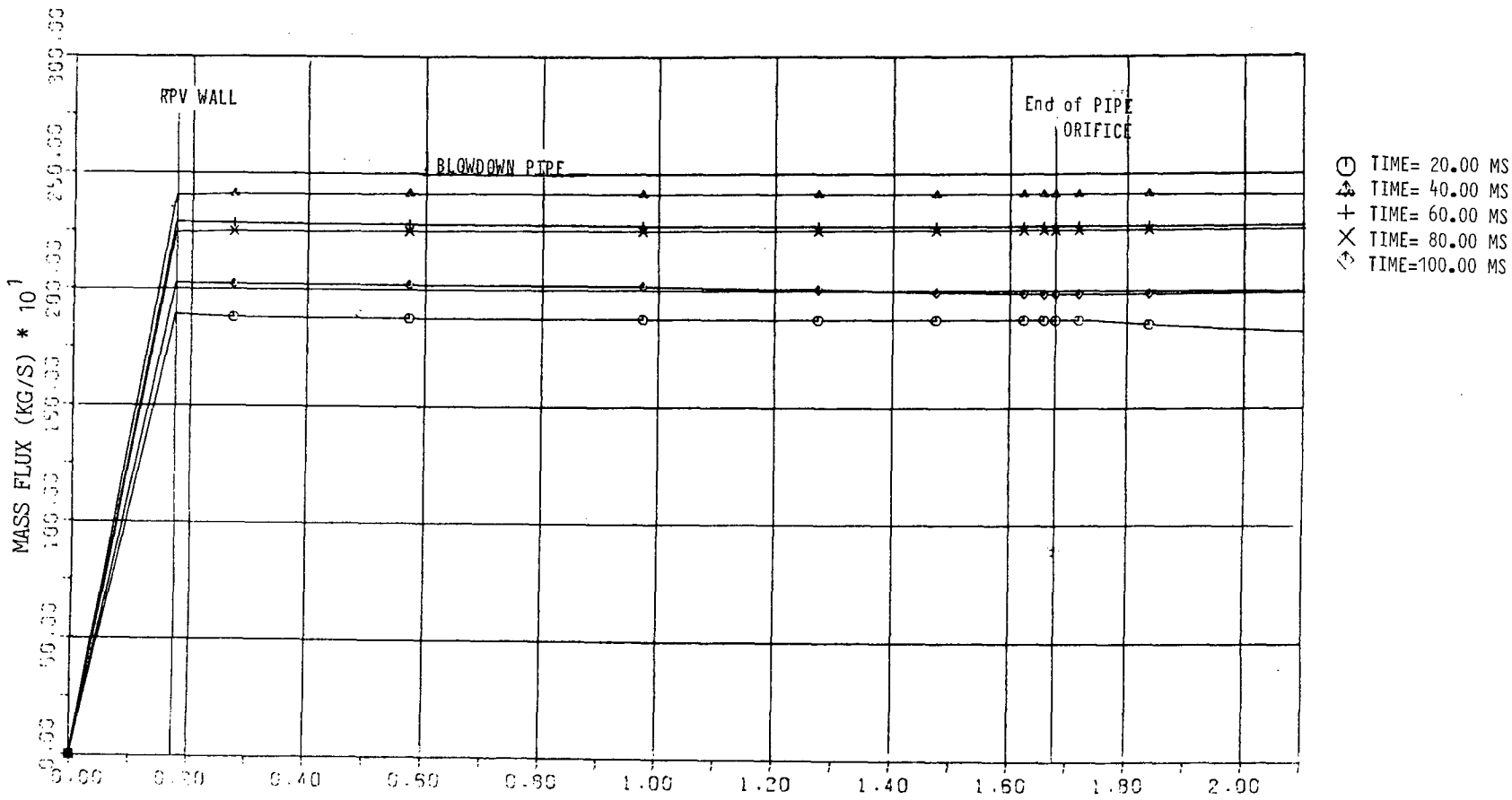

RECALCULATION OF THE HDR-TESTS

MASS FLUX WITH ORIFICE AND WITH EXPANSION AT THE RPV

Fig. 2.3.20

KWU PROFILE PLOT TRAC - PD2 PARAMETER STUDY

THE EFFECT OF DIFFERENT PARAMETERS ON THE PRESSURE

AND THE MASS FLUX

T2/HDR1-3/WITHOUT ORIFICE/WITHOUT EXPANSION

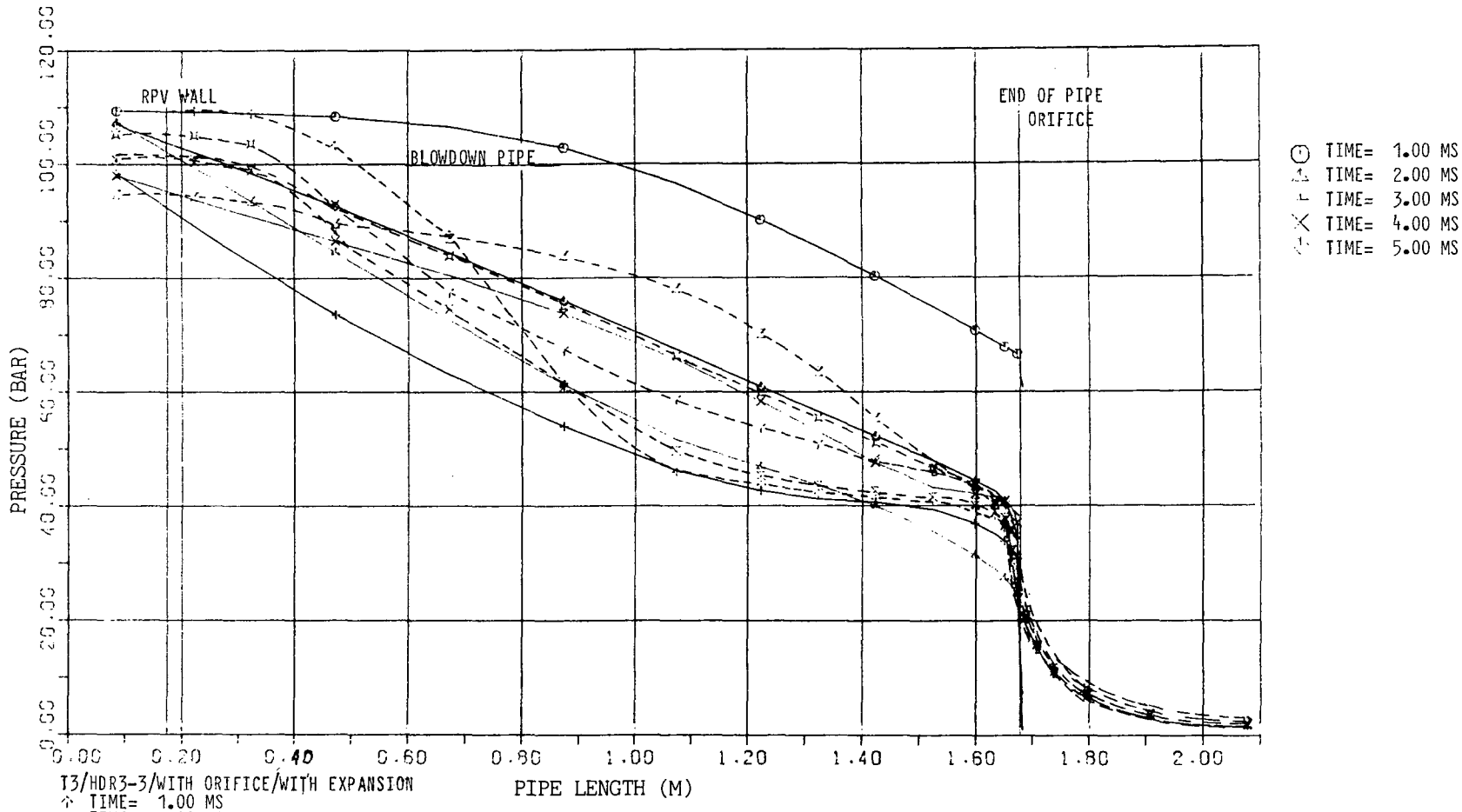

T3/HDR3-3/WITH ORIFICE/WITH EXPANSION
TIME= 1.00 MS
TIME= 2.00 MS
TIME= 3.00 MS
TIME= 4.00 MS
TIME= 5.00 MS

RECALCULATION OF THE HDR-TESTS

PRESSURE

Fig. 2.3.21

KWU PROFILE PLOT TRAC - PD2 PARAMETER STUDY

THE EFFECT OF DIFFERENT PARAMETERS ON THE PRESSURE

AND THE MASS FLUX

T2/HDR1-3/WITHOUT ORIFICE/WITHOUT EXPANSION

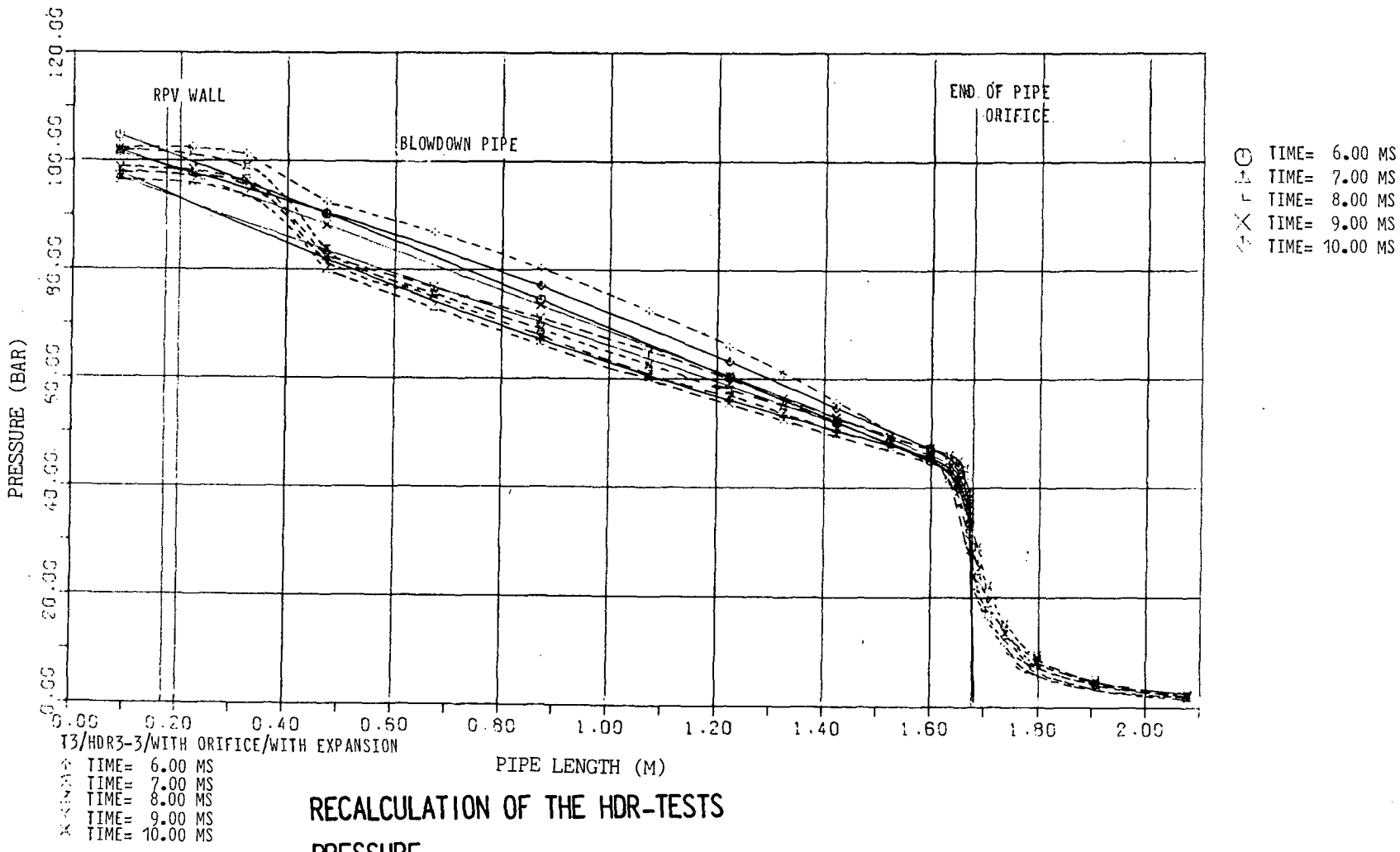

RECALCULATION OF THE HDR-TESTS

PRESSURE

Fig. 2.3.22

KWU PROFILE PLOT TRAC - PD2 PARAMETER STUDY

THE EFFECT OF DIFFERENT PARAMETERS ON THE PRESSURE

AND THE MASS FLUX

T2/HDR1-3/WITHOUT ORIFICE/WITHOUT EXPANSION

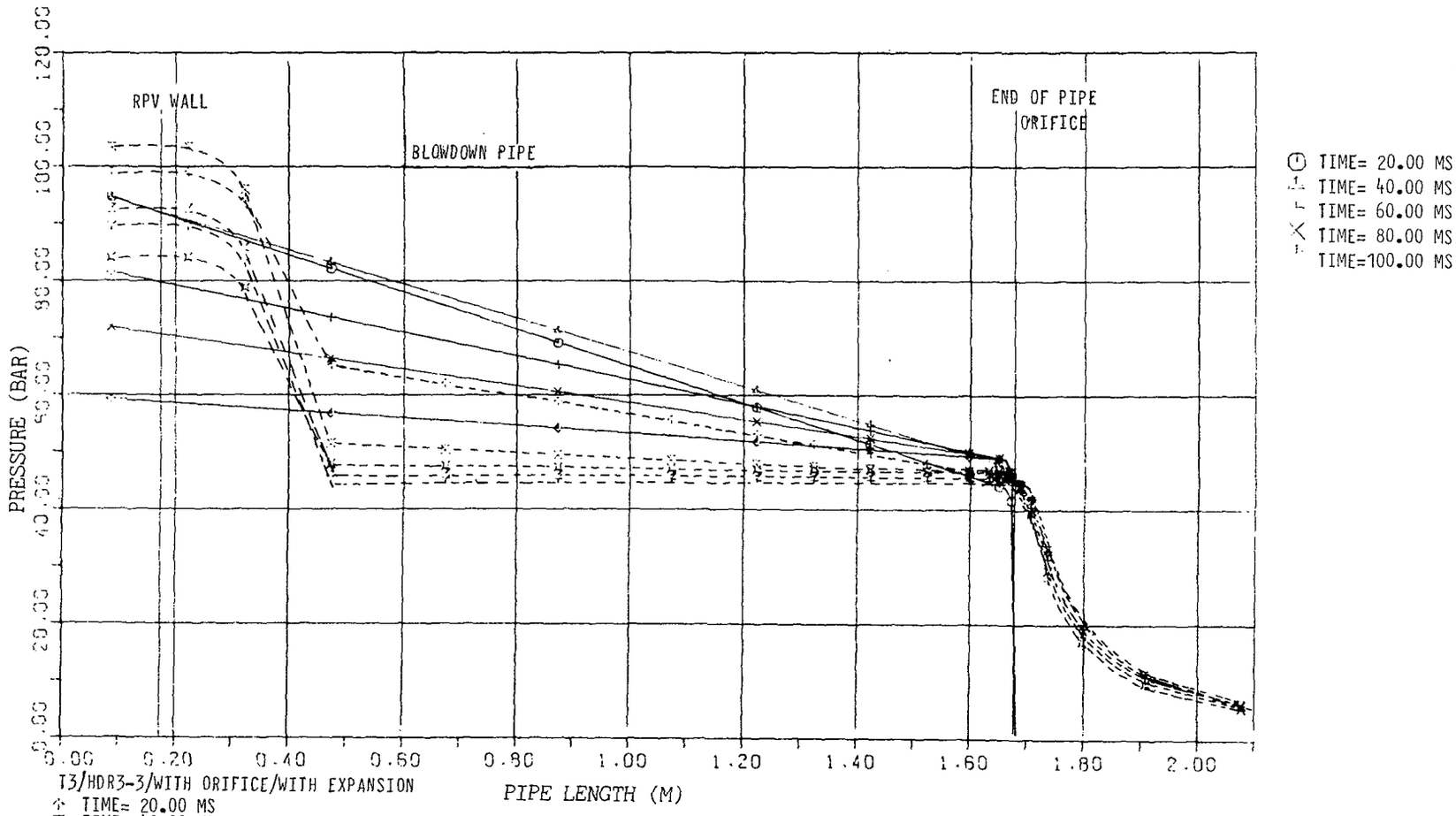

T3/HDR3-3/WITH ORIFICE/WITH EXPANSION

TIME= 20.00 MS
TIME= 40.00 MS
TIME= 60.00 MS
TIME= 80.00 MS
TIME=100.00 MS

RECALCULATION OF THE HDR-TESTS

PRESSURE

Fig. 2.3.23

KWU PROFILE PLOT TRAC - PD2 PARAMETER STUDY

THE EFFECT OF DIFFERENT PARAMETERS ON THE PRESSURE

AND THE MASS FLUX

T2/HDR1-3/WITHOUT ORIFICE/WITHOUT EXPANSION

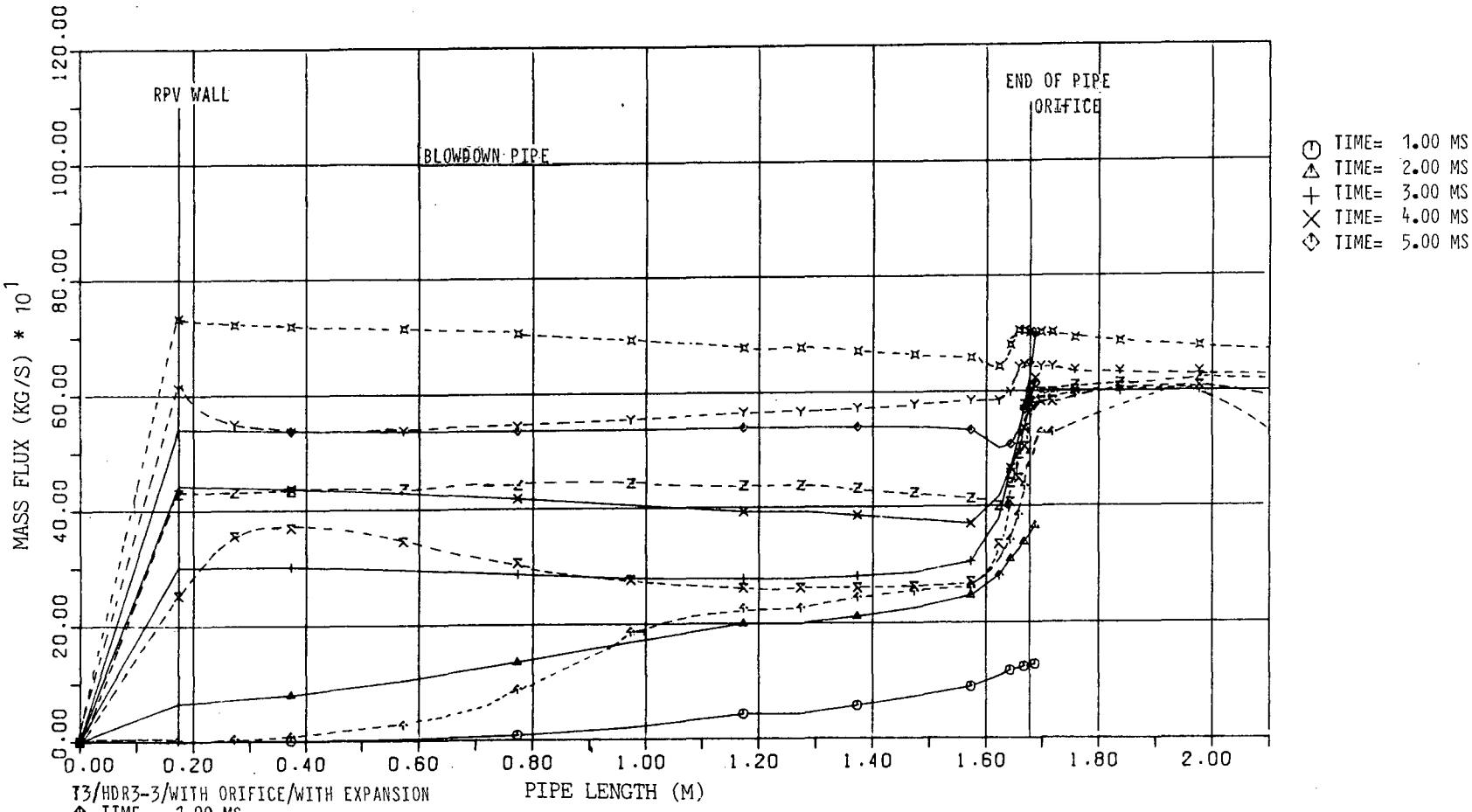

T3/HDR3-3/WITH ORIFICE/WITH EXPANSION
TIME= 1.00 MS
TIME= 2.00 MS
TIME= 3.00 MS
TIME= 4.00 MS
TIME= 5.00 MS

RECALCULATION OF THE HDR-TESTS

MASS FLUX

Fig. 2.3.24

KWU PROFILE PLOT TRAC - PD2 PARAMETER STUDY

THE EFFECT OF DIFFERENT PARAMETERS ON THE PRESSURE

AND THE MASS FLUX

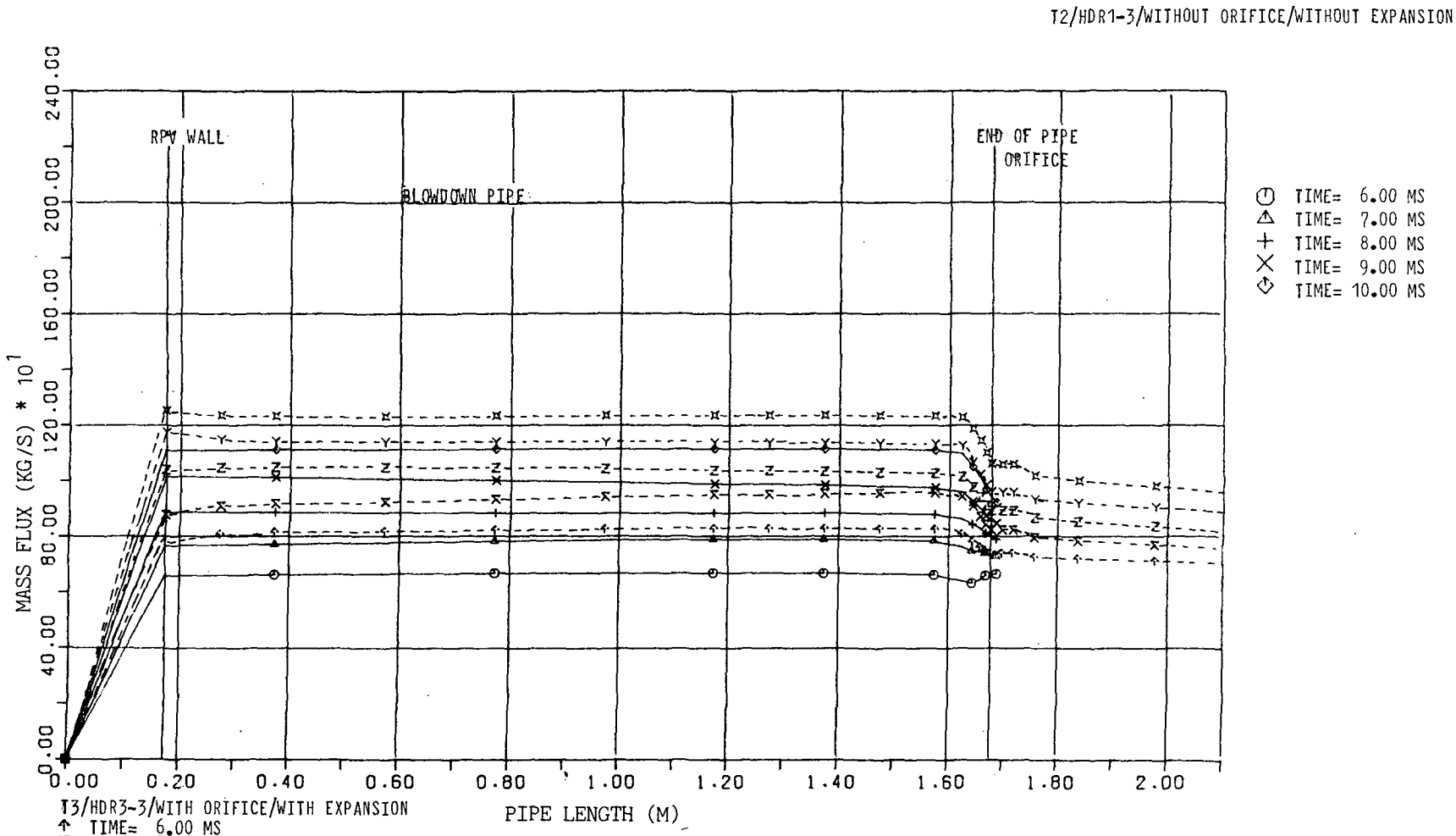

RECALCULATION OF THE HDR-TESTS

MASS FLUX

Fig. 2.3.25

KWU PROFILE PLOT TRAC - PD2 PARAMETER STUDY

THE EFFECT OF DIFFERENT PARAMETERS ON THE PRESSURE

AND THE MASS FLUX

T2/HDR1-3/WITHOUT ORIFICE/WITHOUT EXPANSION

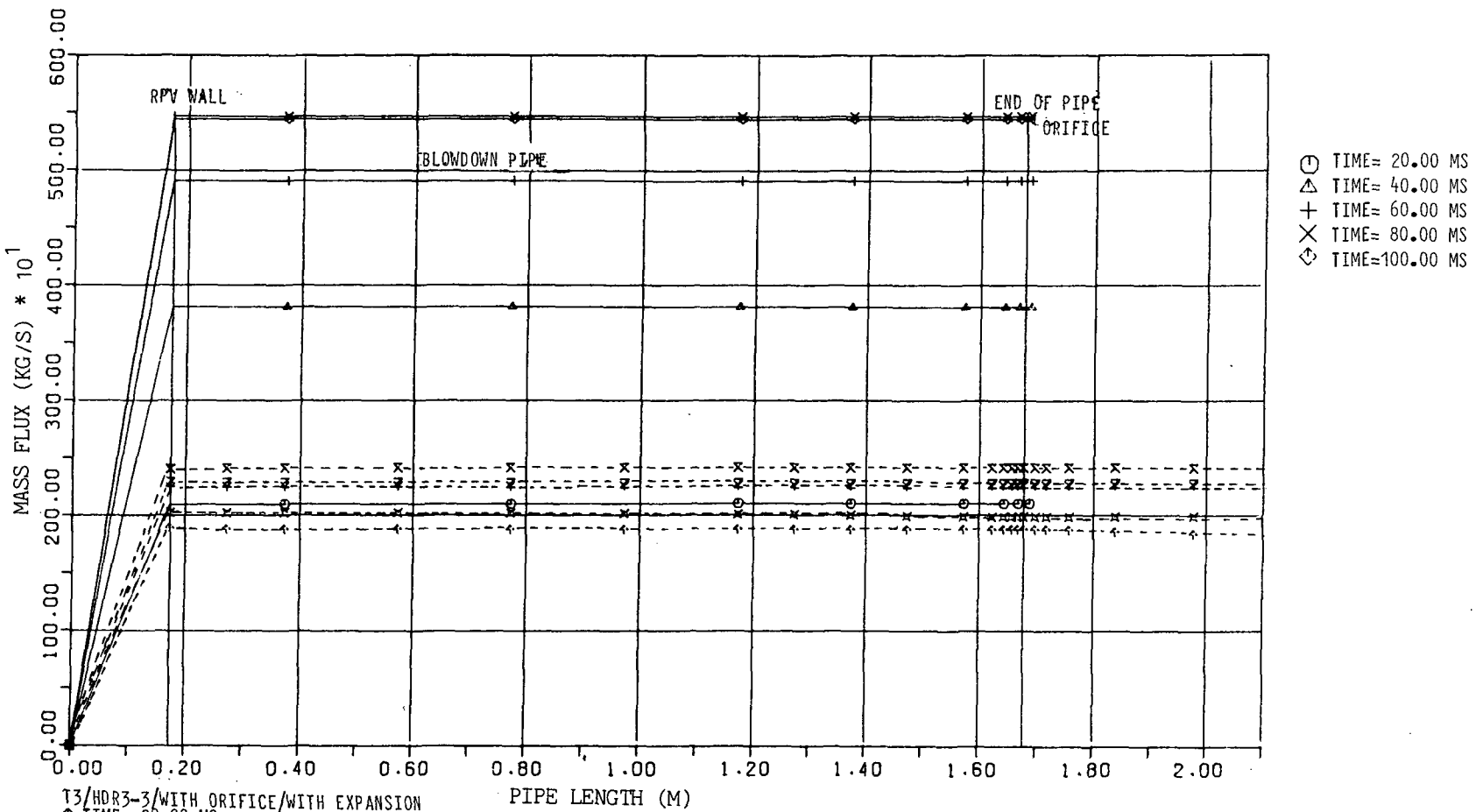

T3/HDR3-3/WITH ORIFICE/WITH EXPANSION
TIME= 20.00 MS
TIME= 40.00 MS
TIME= 60.00 MS
TIME= 80.00 MS
TIME=100.00 MS

RECALCULATION OF THE HDR-TESTS

MASS FLUX

Fig. 2.3.26

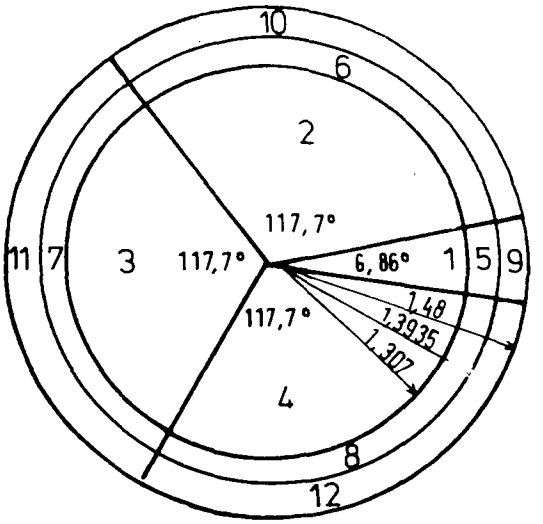

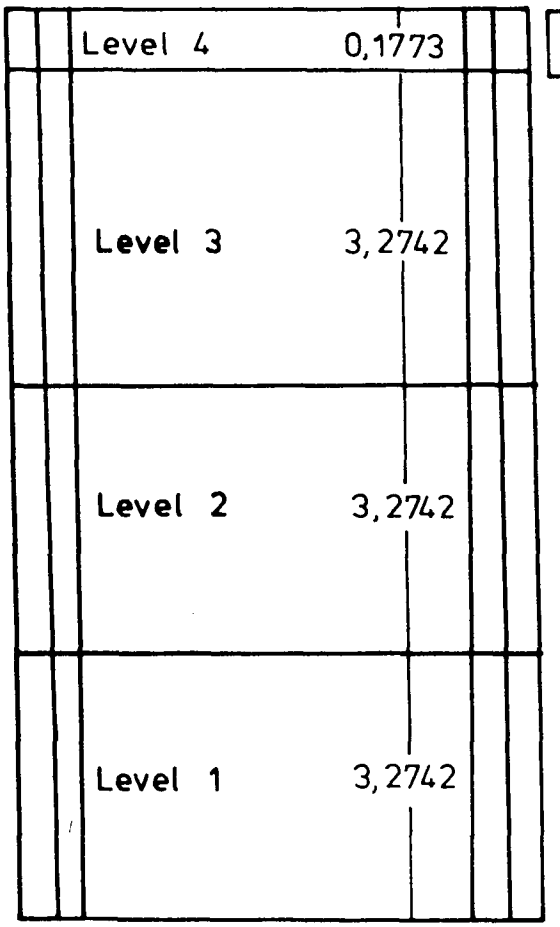

VESSEL 3

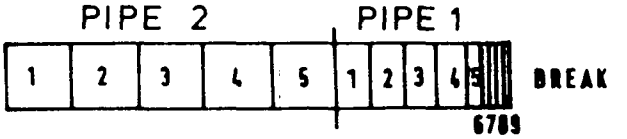

HDR 4/5

Fig. 2.4.1

KWU TRAC - PD2

THE EFFECT OF DIFFERENT PARAMETERS ON THE OUTFLOW RATE

RECALCULATION OF THE HDR-TESTS WITH THE VESSEL COMPONENT

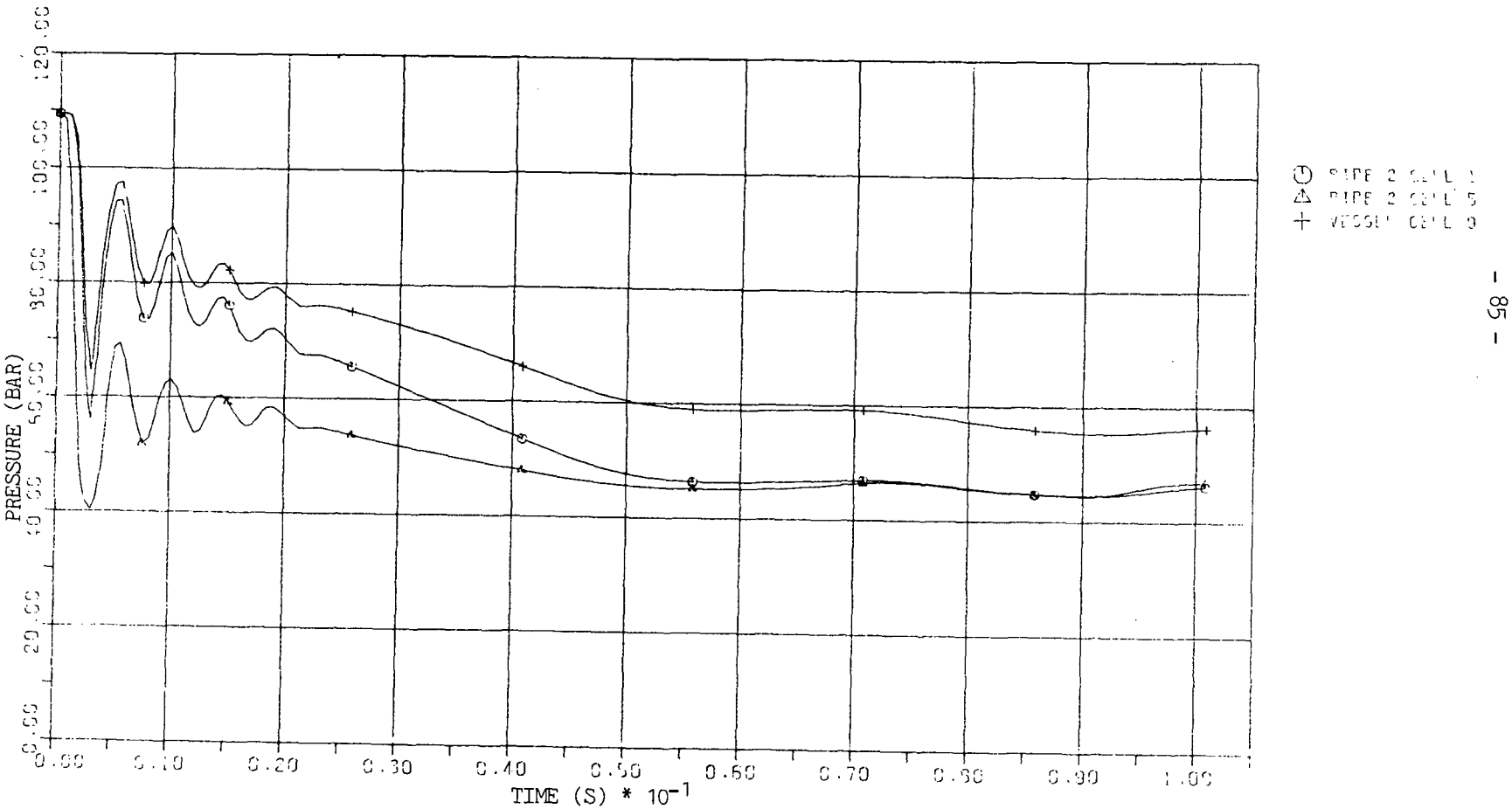

PIPE 2 / VESSEL TYPE 5 / FRICTION FACTOR (BOILER EXIT) = 0.5

PRESSURE

Fig. 2.4.2

KWU TRAC - PD2

THE EFFECT OF DIFFERENT PARAMETERS ON THE OUTFLOW RATE

RECALCULATION OF THE HDR-TESTS WITH THE VESSEL COMPONENT

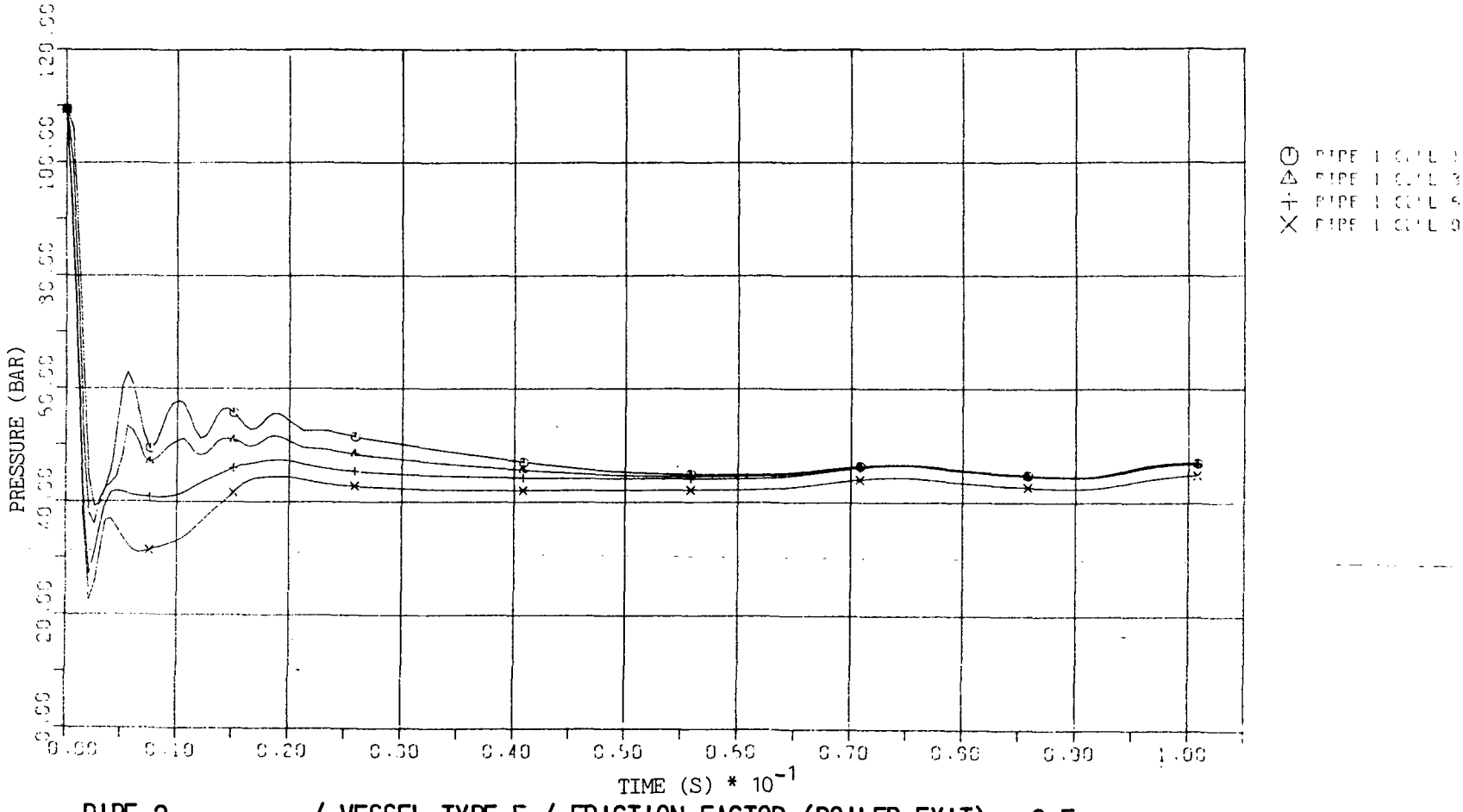

PIPE 2 / VESSEL TYPE 5 / FRICTION FACTOR (BOILER EXIT) = 0.5

PRESSURE

Fig. 2.4.3

KWU TRAC - PD2

THE EFFECT OF DIFFERENT PARAMETERS ON THE OUTFLOW RATE

RECALCULATION OF THE HDR-TESTS WITH THE VESSEL COMPONENT

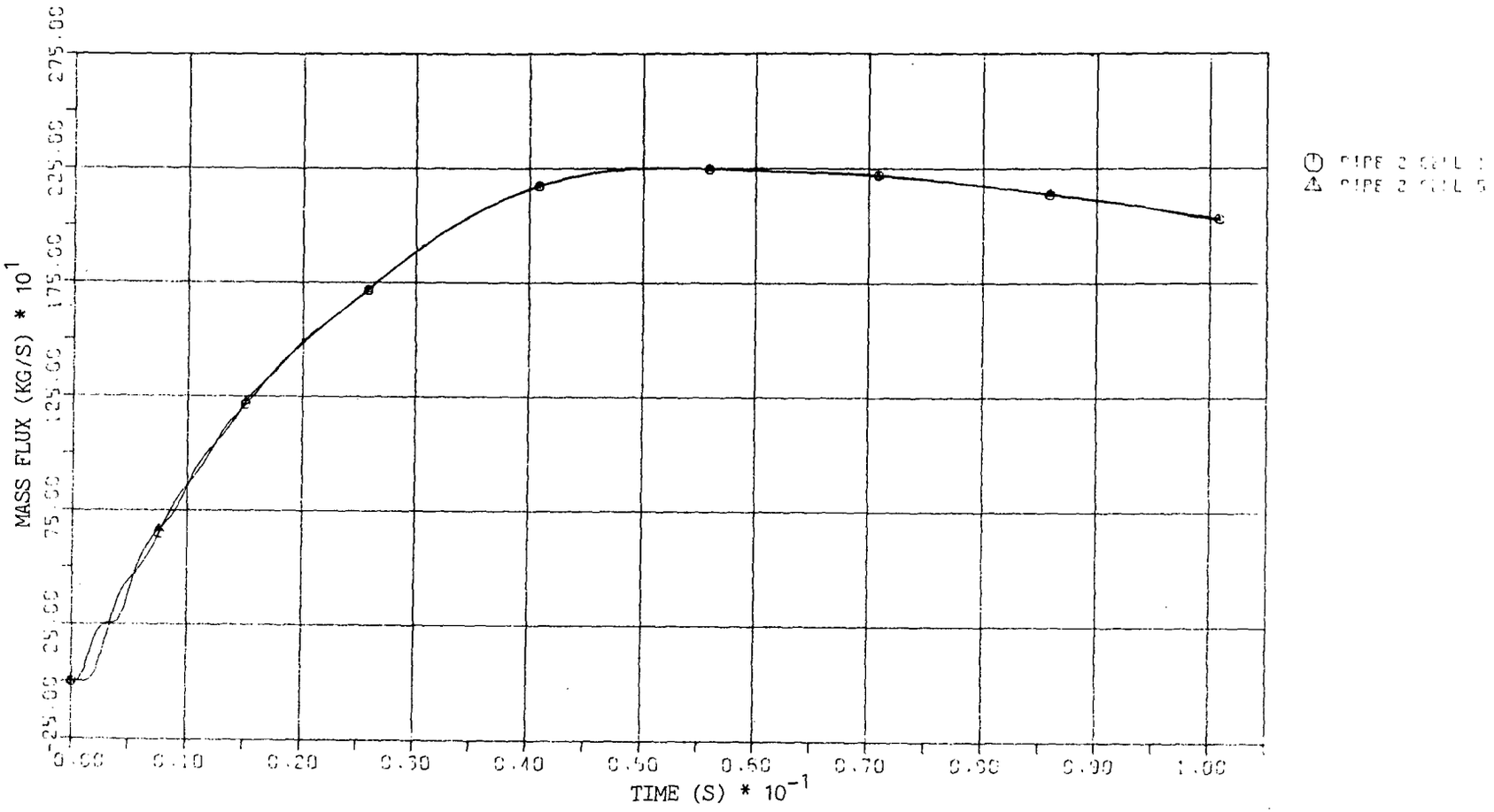

PIPE 2 / VESSEL TYPE 5 / FRICTION FACTOR (BOILER EXIT) = 0.5

MASS FLUX

Fig. 2.4.4

KWU TRAC -PD2

THE EFFECT OF DIFFERENT PARAMETERS ON THE OUTFLOW RATE

RECALCULATION OF THE HDR-TESTS WITH THE VESSEL COMPONENT

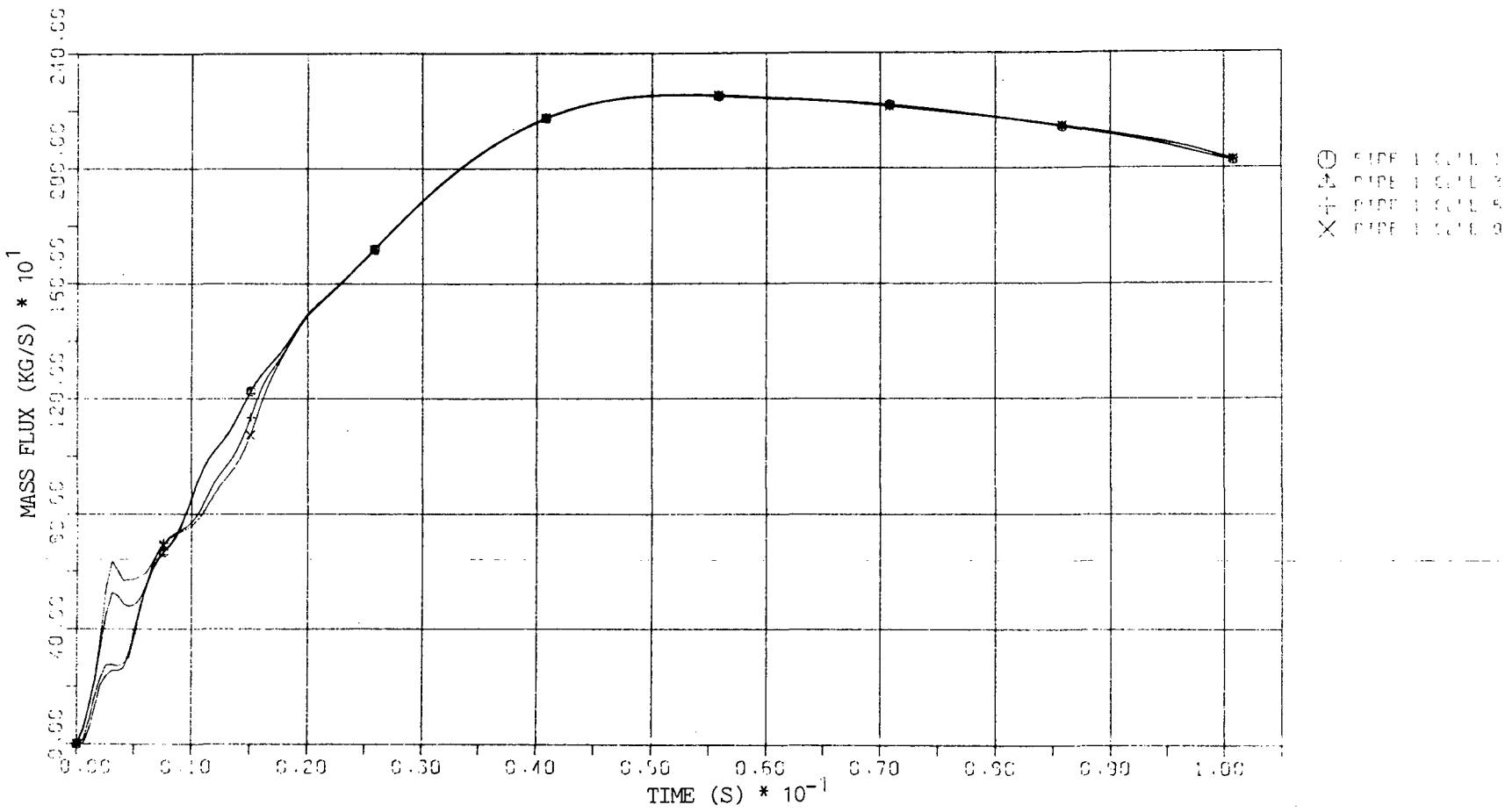

PIPE 2 / VESSEL TYPE 5 / FRICTION FACTOR (BOILER EXIT) = 0.5

MASS FLUX

Fig. 2.4.5

KWU TRAC - PD2

THE EFFECT OF DIFFERENT PARAMETERS ON THE OUTFLOW RATE

RECALCULATION OF THE HDR-TESTS WITH THE VESSEL COMPONENT

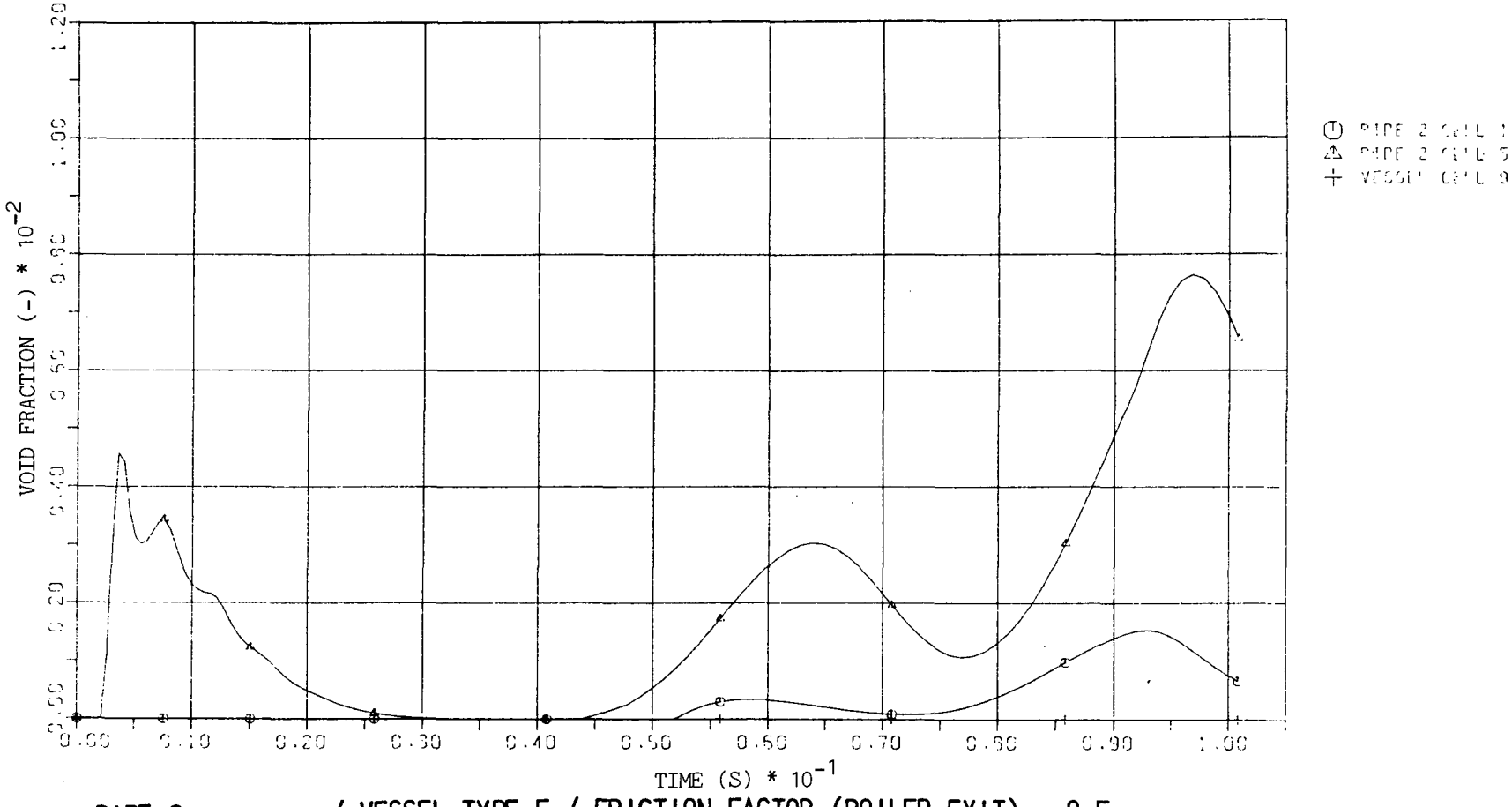

PIPE 2 / VESSEL TYPE 5 / FRICTION FACTOR (BOILER EXIT) = 0.5

VOID FRACTION

Fig. 2.4.6

KWU TRAC -PD2

THE EFFECT OF DIFFERENT PARAMETERS ON THE OUTFLOW RATE

RECALCULATION OF THE HDR-TESTS WITH THE VESSEL COMPONENT

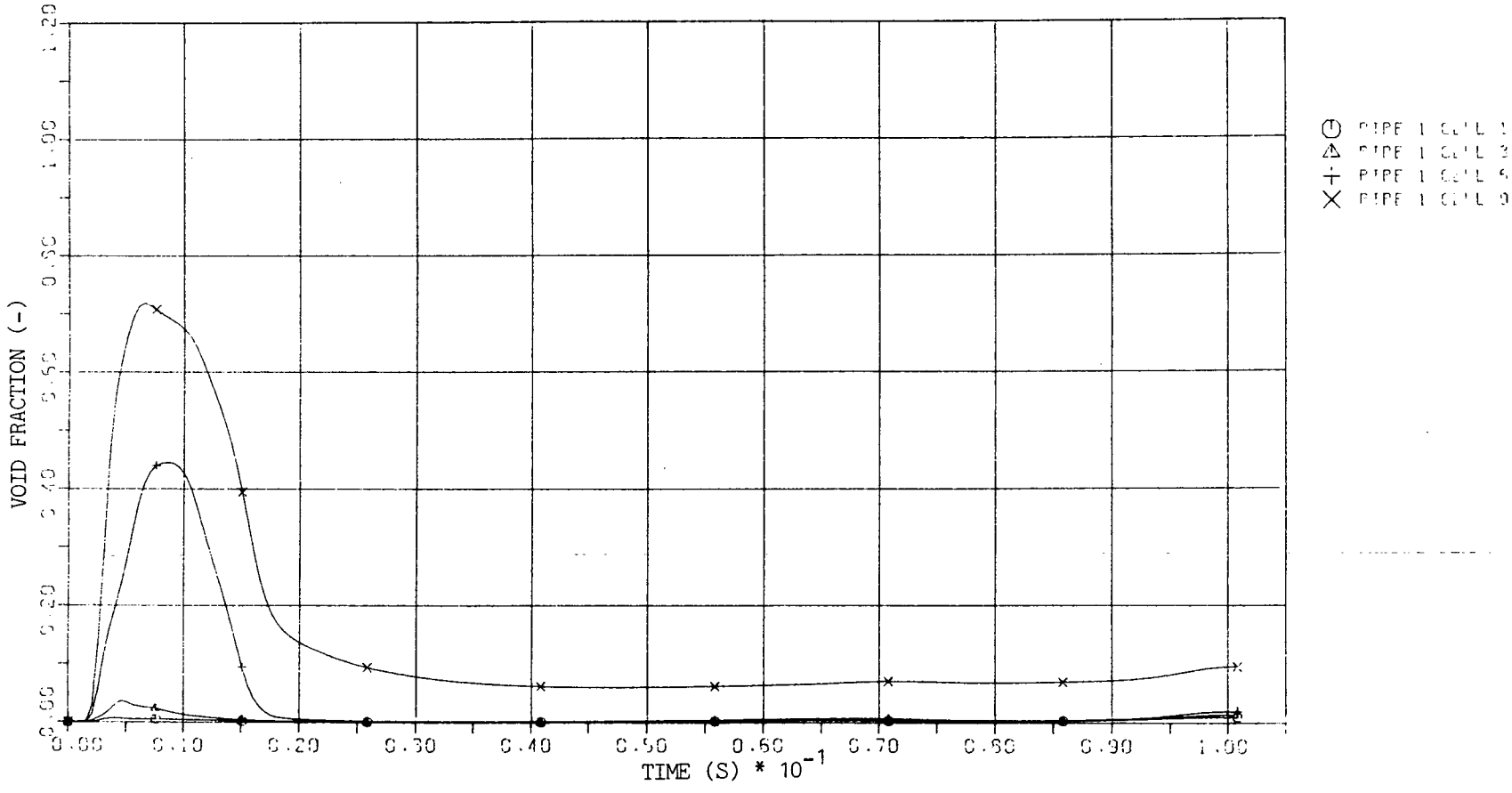

PIPE 2 / VESSEL TYPE 5 / FRICTION FACTOR (BOILER EXIT) = 0.5

VOID FRACTION

Fig. 2.4.7

KWU TRAC - PD2

THE EFFECT OF DIFFERENT PARAMETERS ON THE OUTFLOW RATE

RECALCULATION OF THE HDR-TESTS WITH THE VESSEL COMPONENT

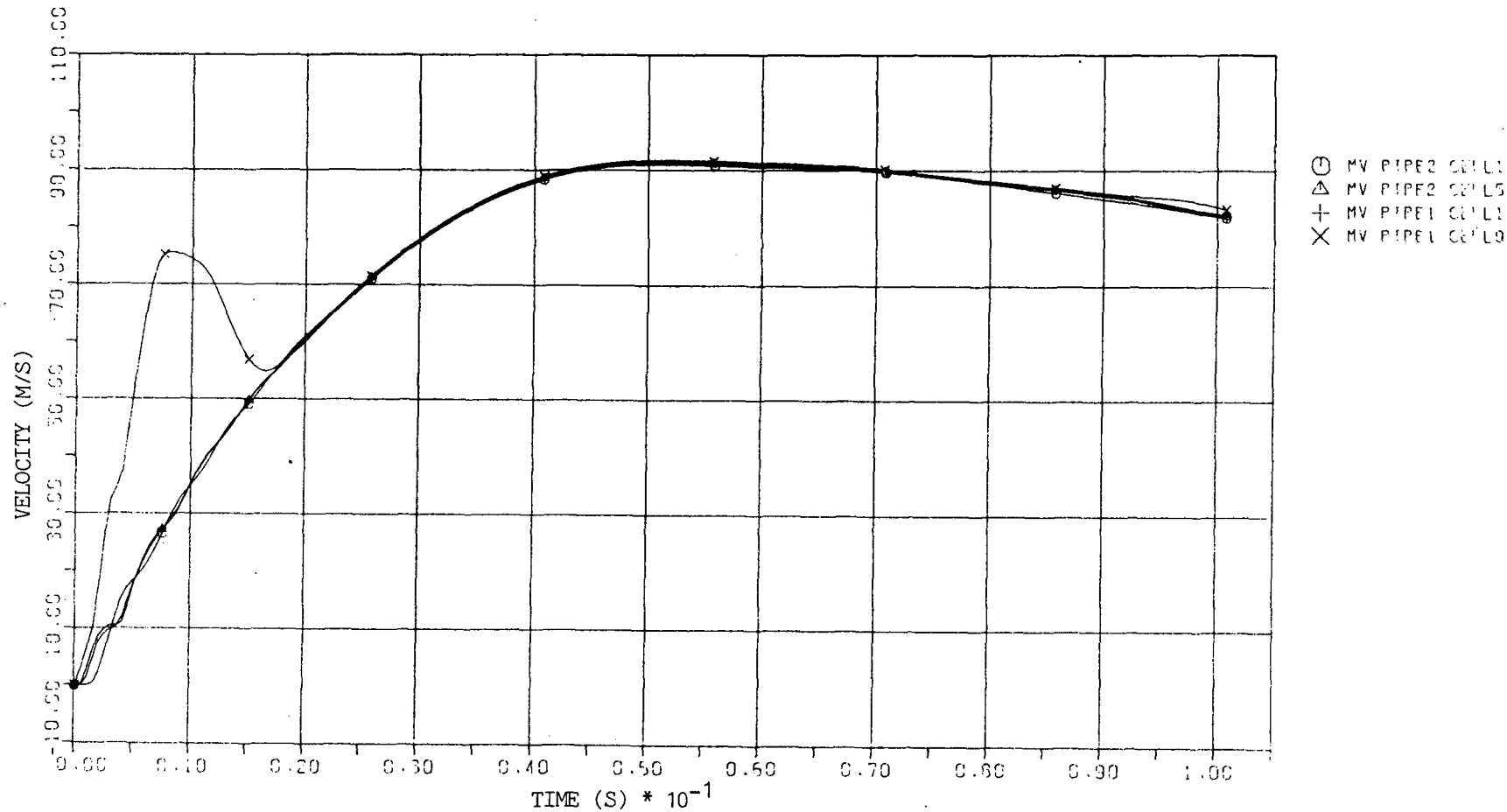

PIPE 2 / VESSEL TYPE 5 / FRICTION FACTOR (BOILER EXIT) = 0.5

VELOCITY

Fig. 2.4.8

KWU TRAC - PD2

THE EFFECT OF DIFFERENT PARAMETERS ON THE OUTFLOW RATE

RECALCULATION OF THE HDR-TESTS WITH THE VESSEL COMPONENT

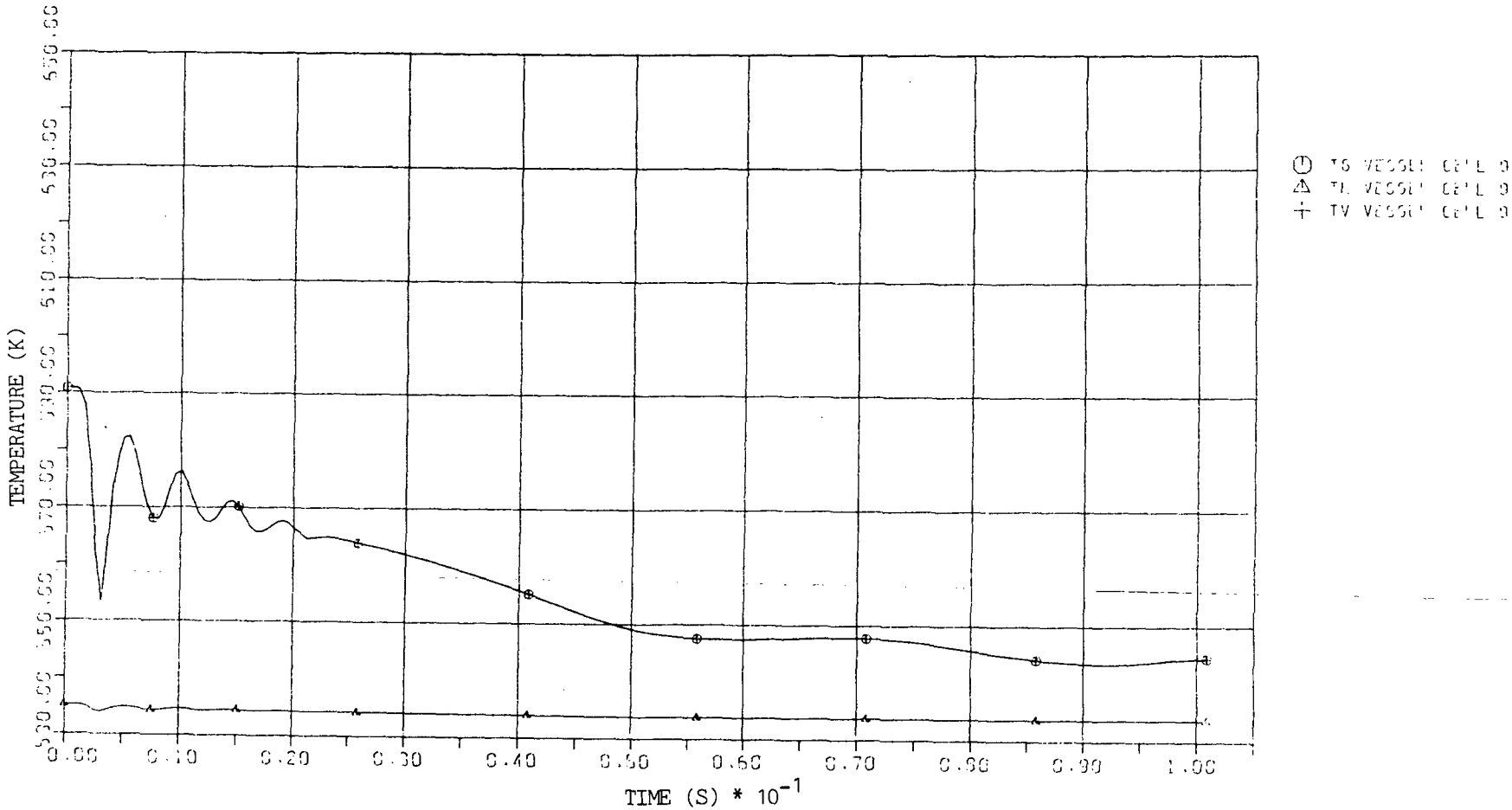

PIPE 2 / VESSEL TYPE 5 / FRICTION FACTOR (BOILER EXIT) = 0.5

TEMPERATURE

Fig. 2.4.9

KWU TRAC - PD2

THE EFFECT OF DIFFERENT PARAMETERS ON THE OUTFLOW RATE

RECALCULATION OF THE HDR-TESTS WITH THE VESSEL COMPONENT

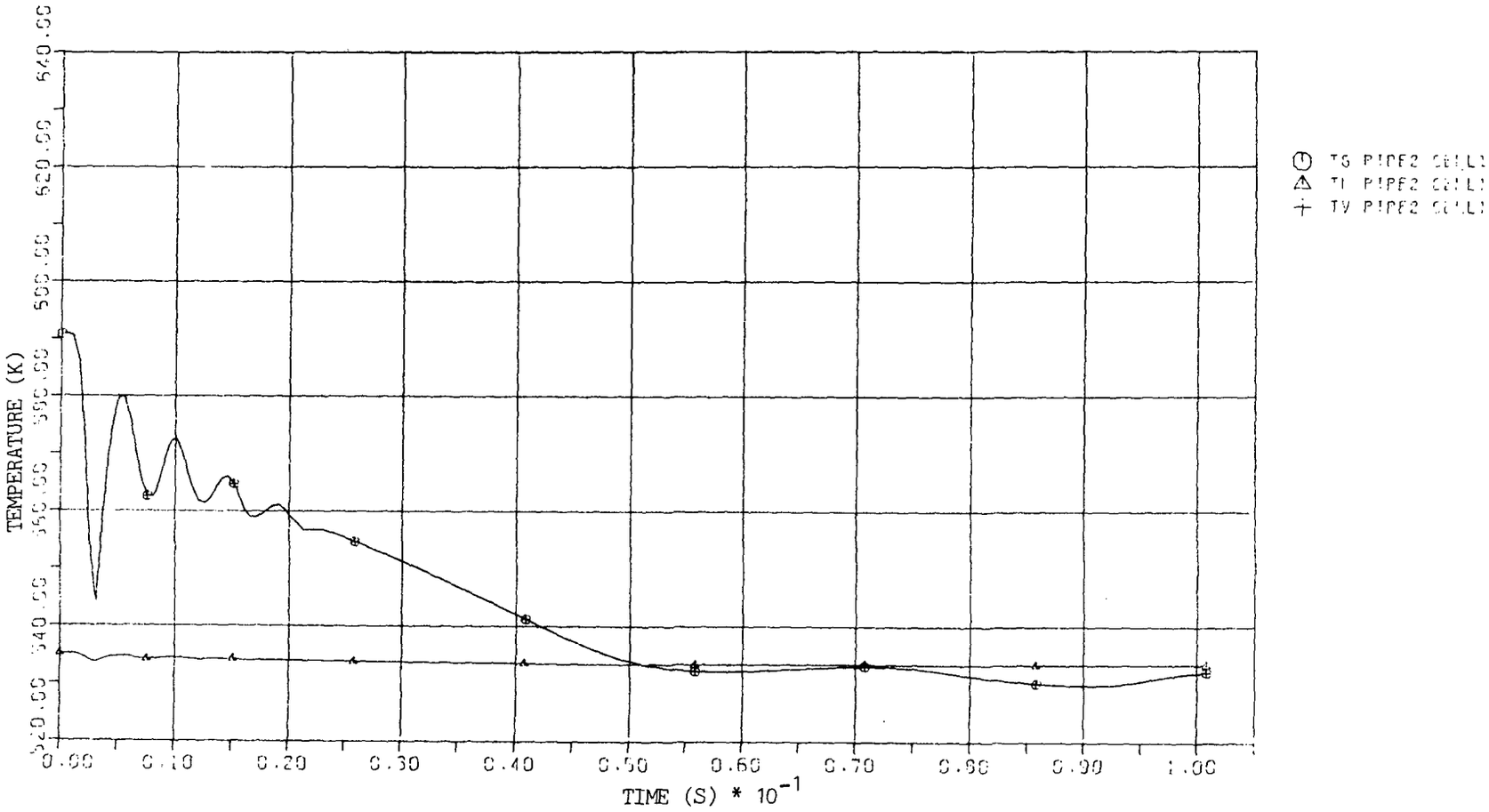

PIPE 2 / VESSEL TYPE 5 / FRICTION FACTOR (BOILER EXIT) = 0.5

TEMPERATURE

Fig. 2.4.10

KWU TRAC -PD2

THE EFFECT OF DIFFERENT PARAMETERS ON THE OUTFLOW RATE

RECALCULATION OF THE HDR-TESTS WITH THE VESSEL COMPONENT

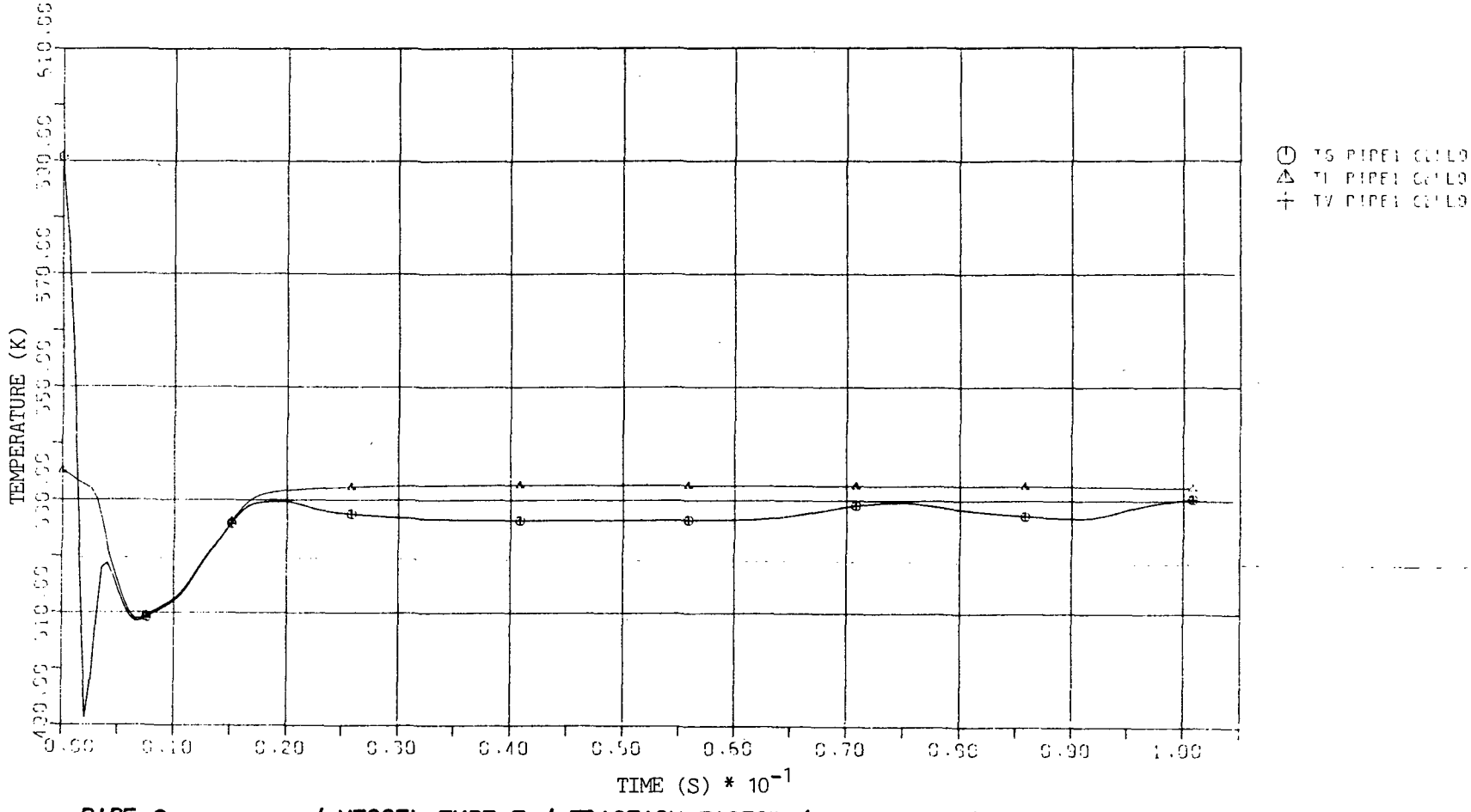

PIPE 2 / VESSEL TYPE 5 / FRICTION FACTOR (BOILER EXIT) = 0.5

TEMPERATURE

Fig. 2.4.11

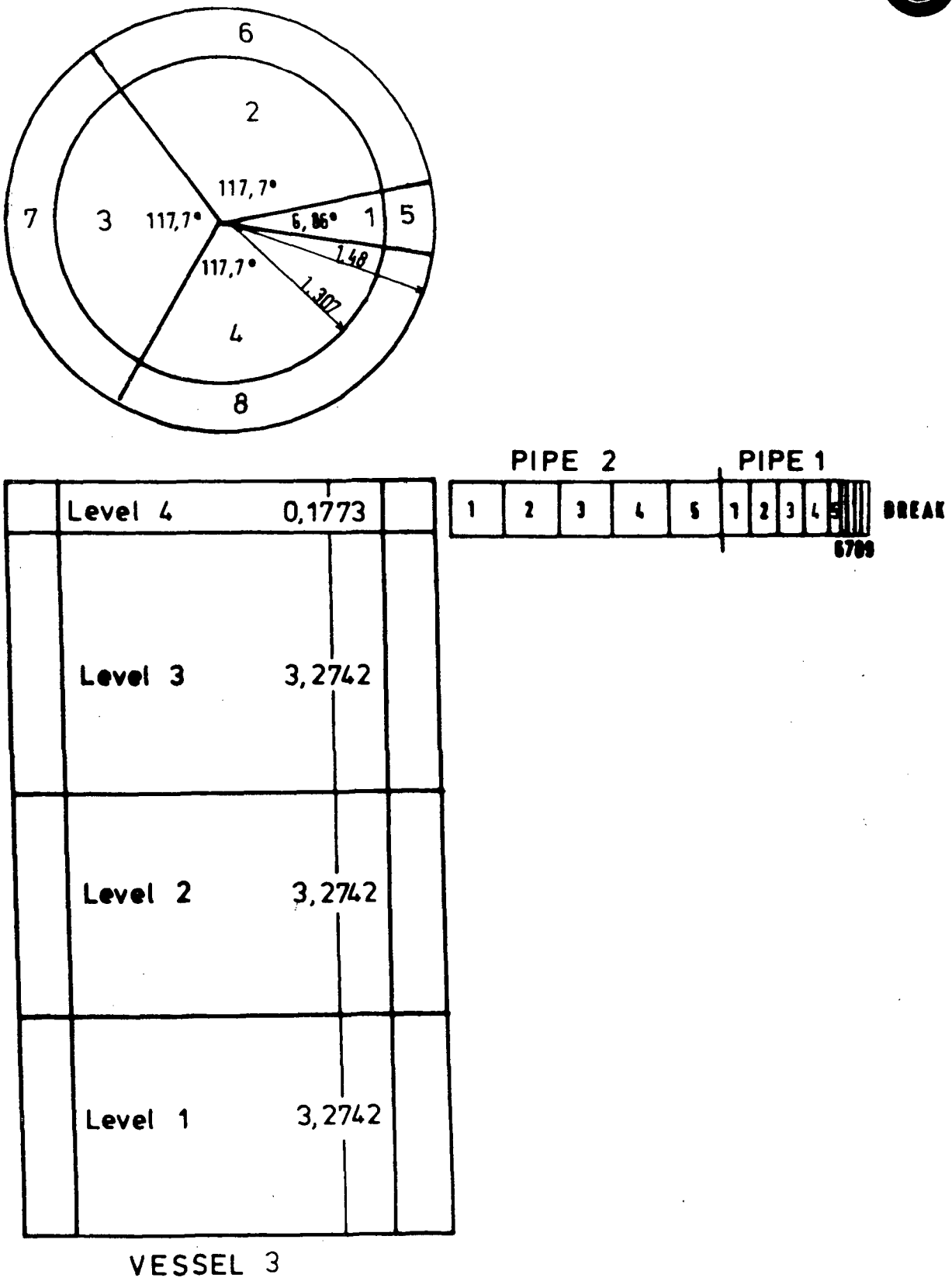

HDR 5/4

Fig. 2.5.1

KWU TRAC - PD2

THE EFFECT OF DIFFERENT PARAMETERS ON THE OUTFLOW RATE

RECALCULATION OF THE HDR-TESTS WITH THE VESSEL COMPONENT

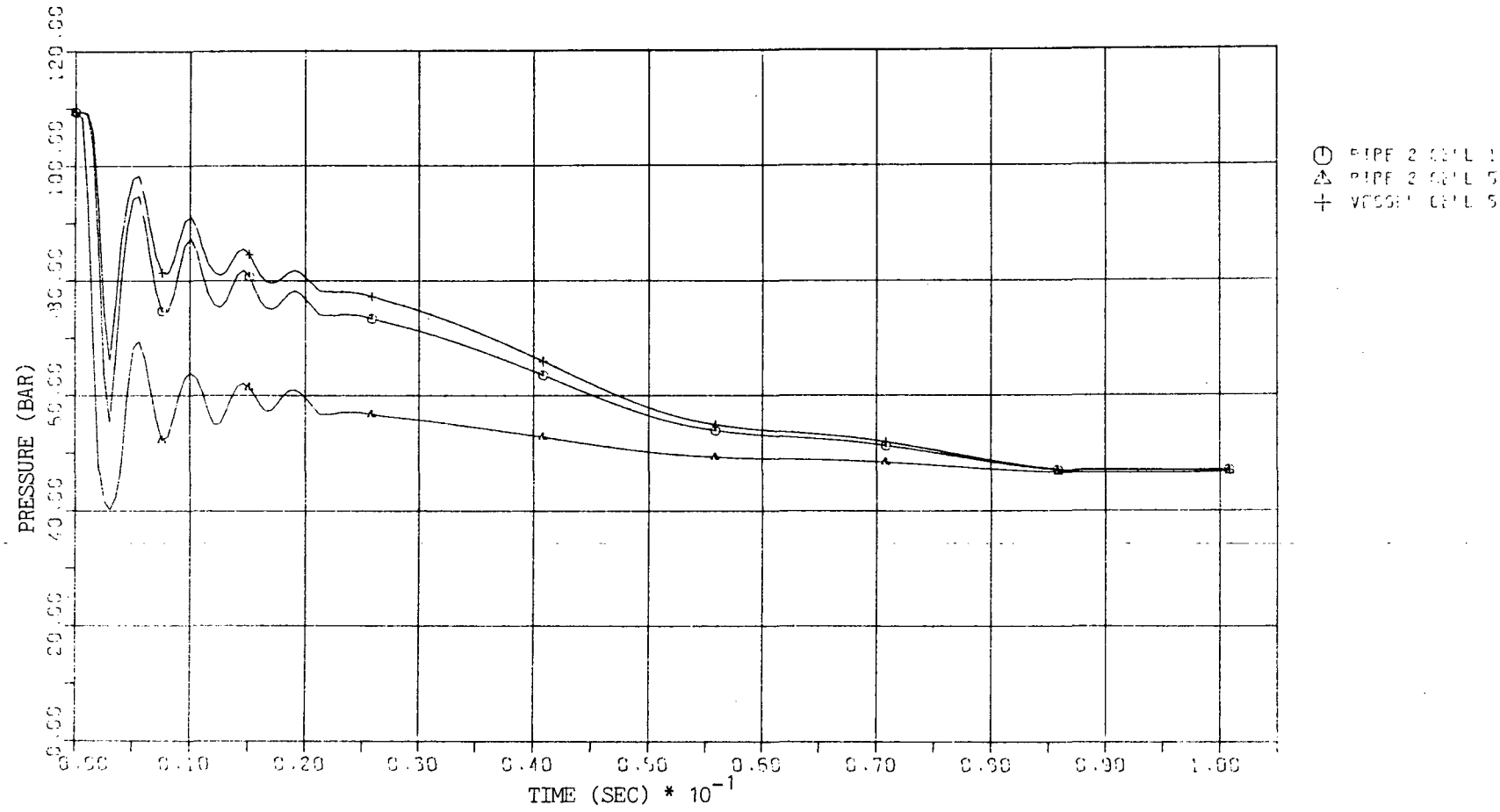

PIPE 2 / VESSEL TYPE 4

PRESSURE

Fig. 2.5.2

KWU TRAC - PD2

THE EFFECT OF DIFFERENT PARAMETERS ON THE OUTFLOW RATE

RECALCULATION OF THE HDR-TESTS WITH THE VESSEL COMPONENT

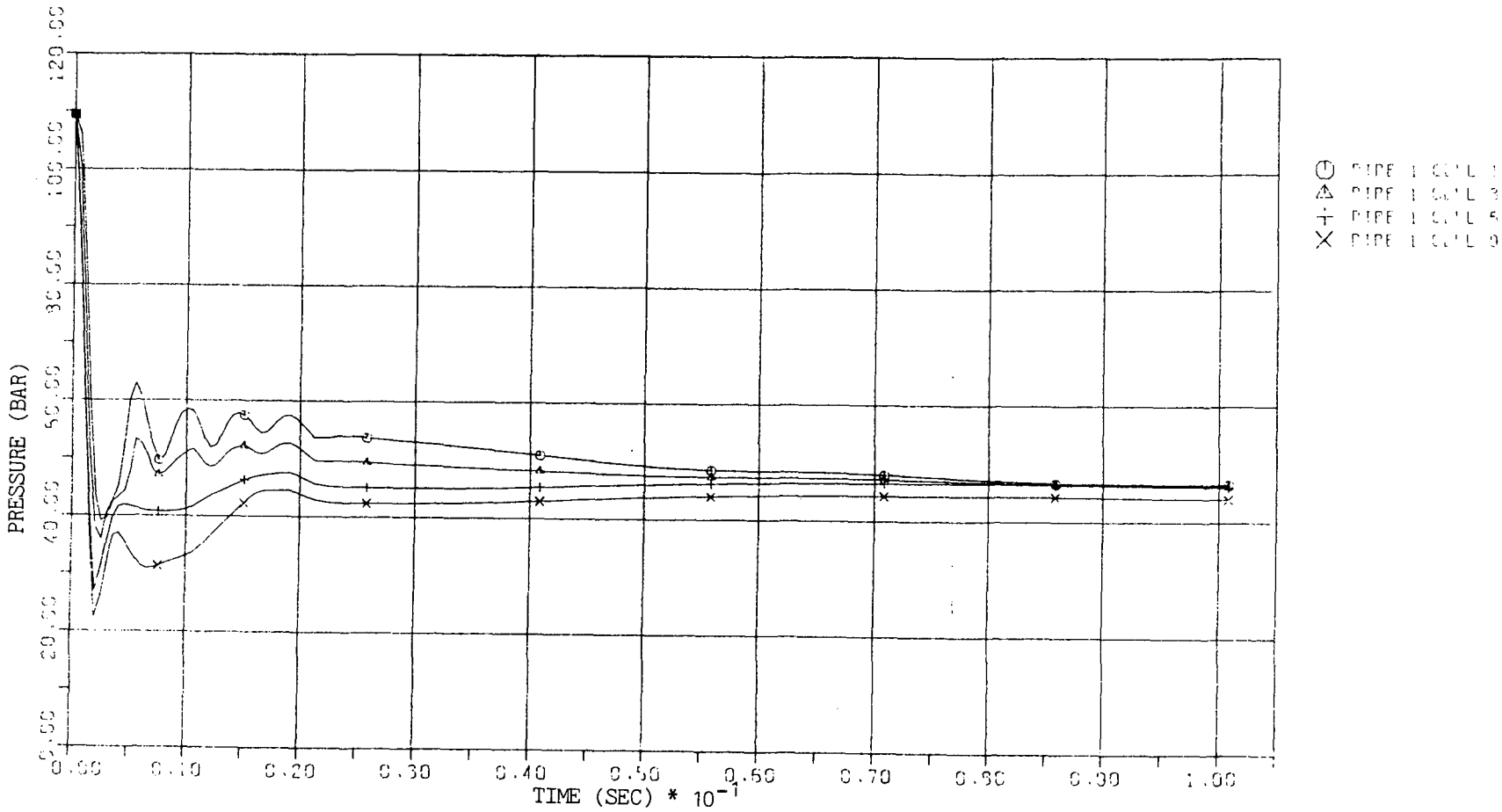

PIPE 2 / VESSEL TYPE 4

PRESSURE

Fig. 2.5.3

KWU TRAC -PD2

THE EFFECT OF DIFFERENT PARAMETERS ON THE OUTFLOW RATE

RECALCULATION OF THE HDR-TESTS WITH THE VESSEL COMPONENT

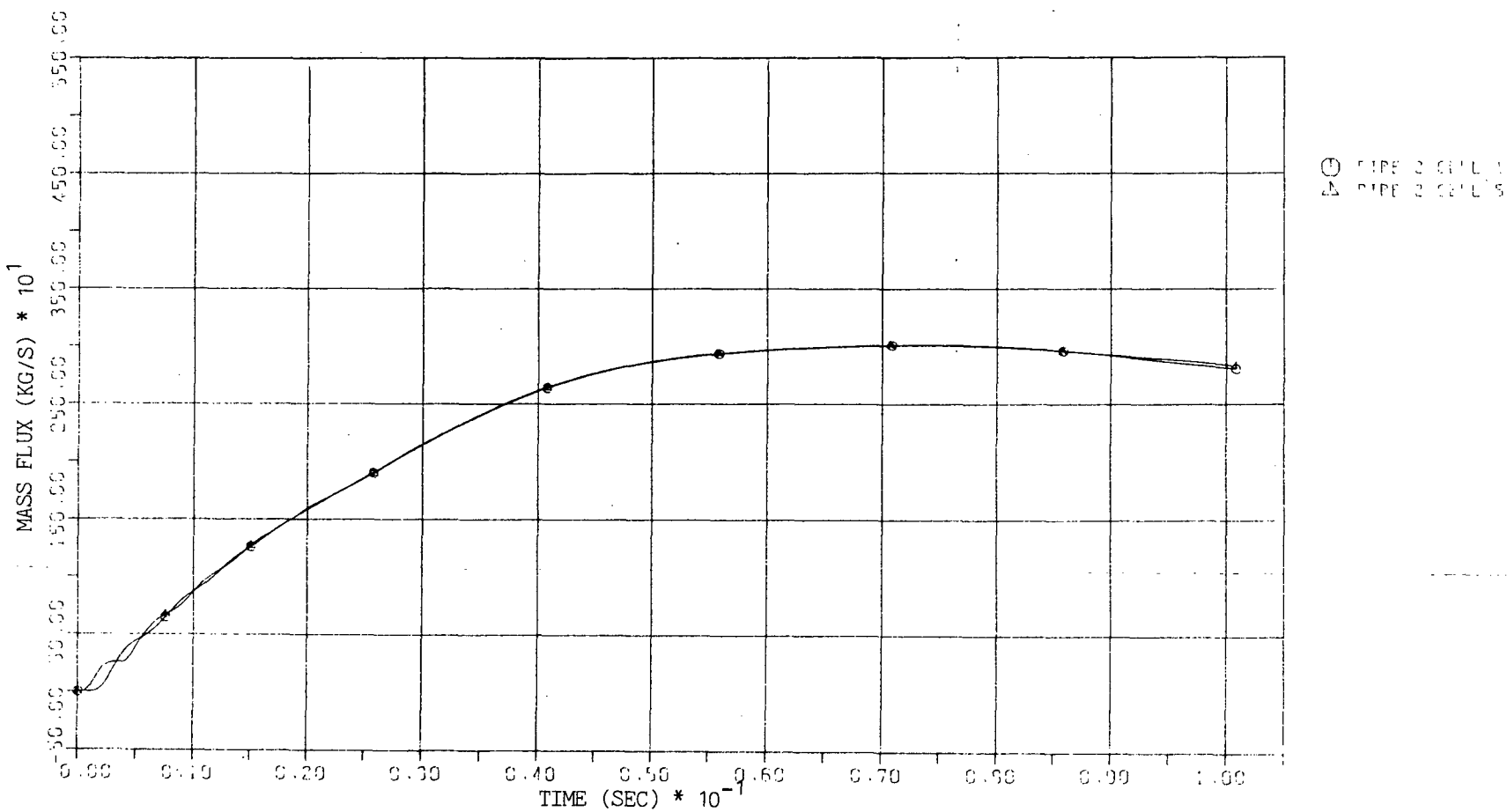

PIPE 2 / VESSEL TYPE 4

MASS FLUX

Fig. 2.5.4

KWU TRAC - PD2

THE EFFECT OF DIFFERENT PARAMETERS ON THE OUTFLOW RATE

RECALCULATION OF THE HDR-TESTS WITH THE VESSEL COMPONENT

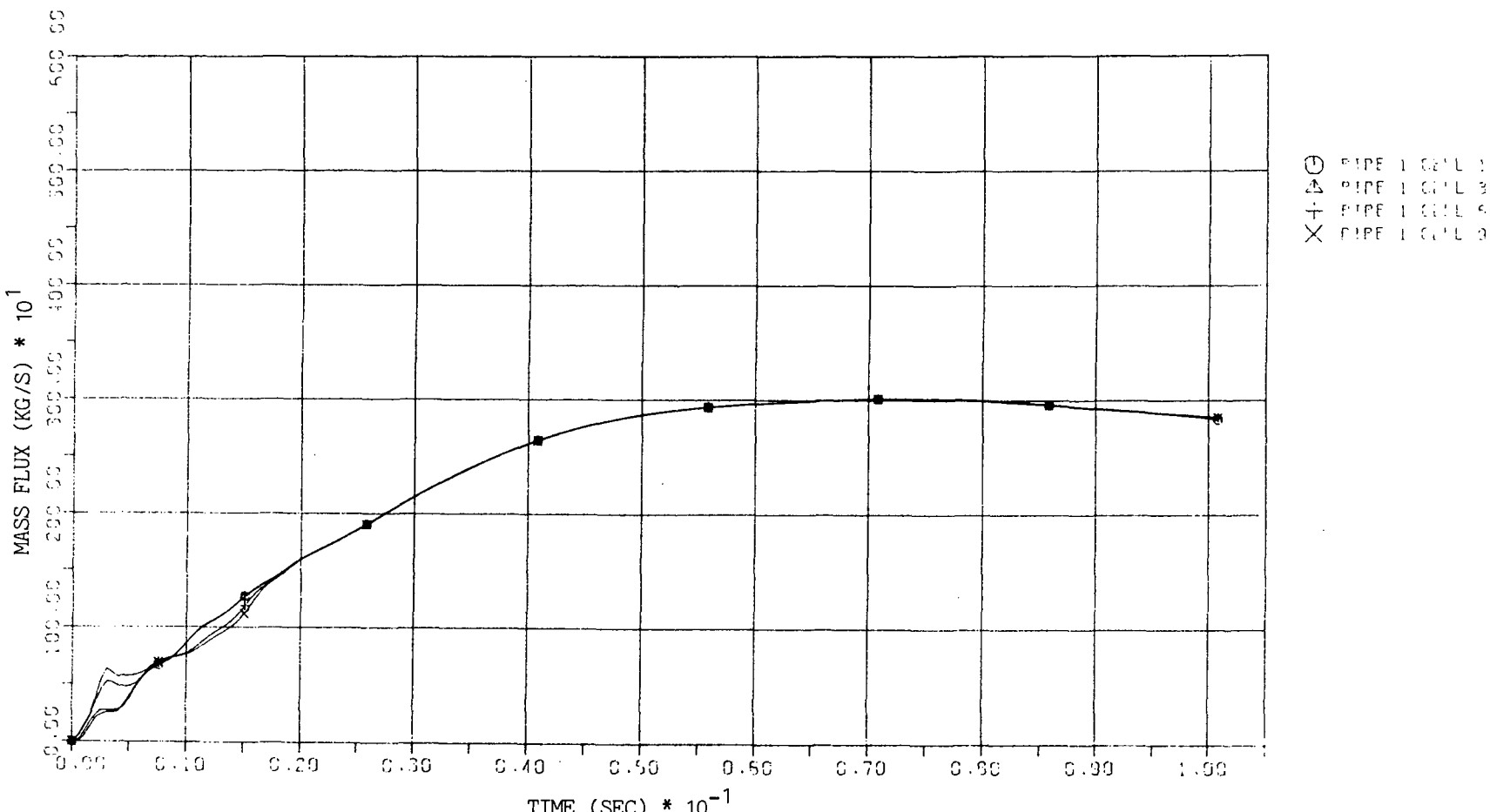

PIPE 2 / VESSEL TYPE 4

MASS FLUX

Fig. 2.5.5

KWU TRAC - PD2

THE EFFECT OF DIFFERENT PARAMETERS ON THE OUTFLOW RATE

RECALCULATION OF THE HDR-TESTS WITH THE VESSEL COMPONENT

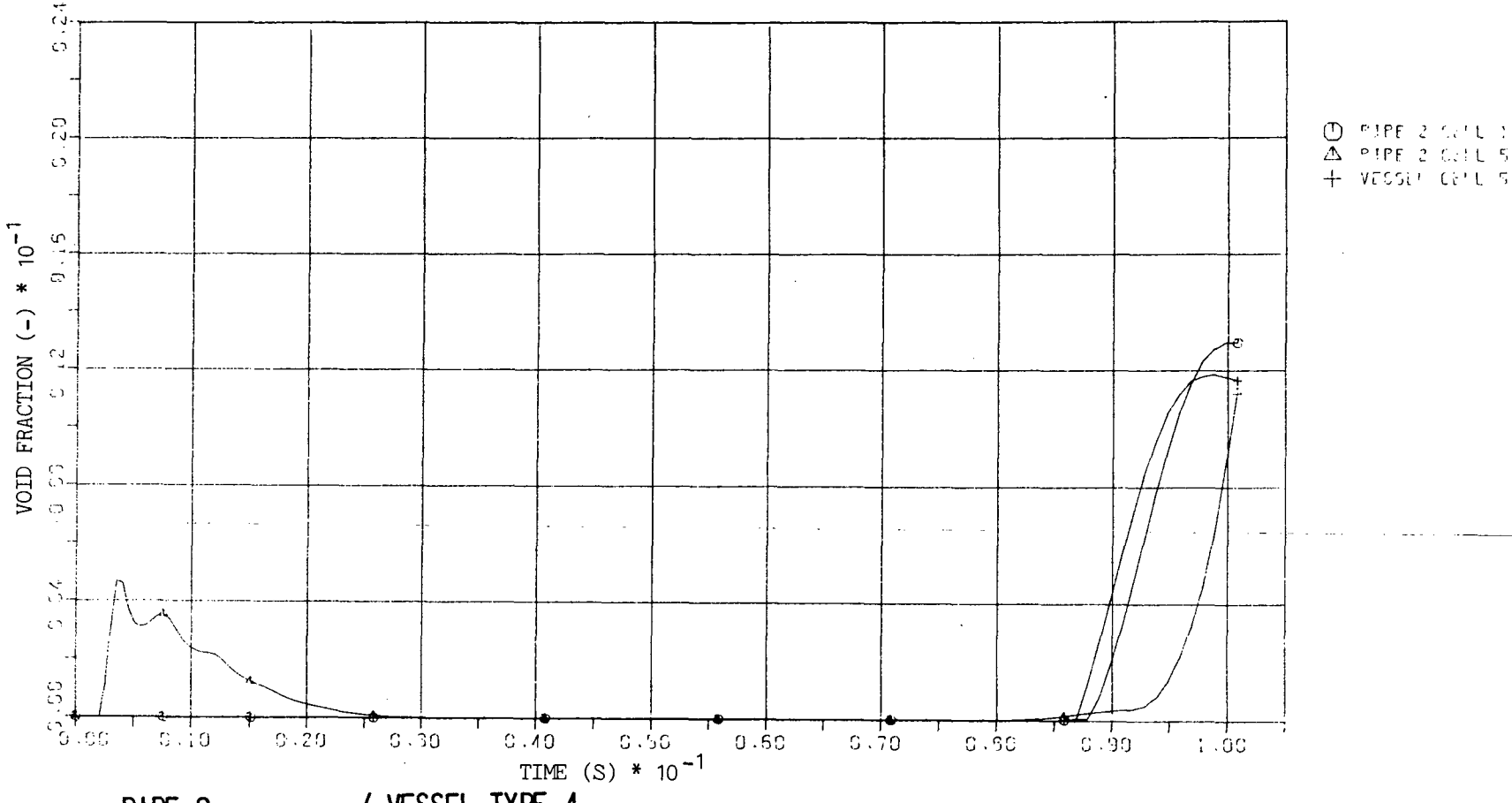

PIPE 2 / VESSEL TYPE 4

VOID FRACTION

Fig. 2.5.6

KWU TRAC - PD2

THE EFFECT OF DIFFERENT PARAMETERS ON THE OUTFLOW RATE

RECALCULATION OF THE HDR-TESTS WITH THE VESSEL COMPONENT

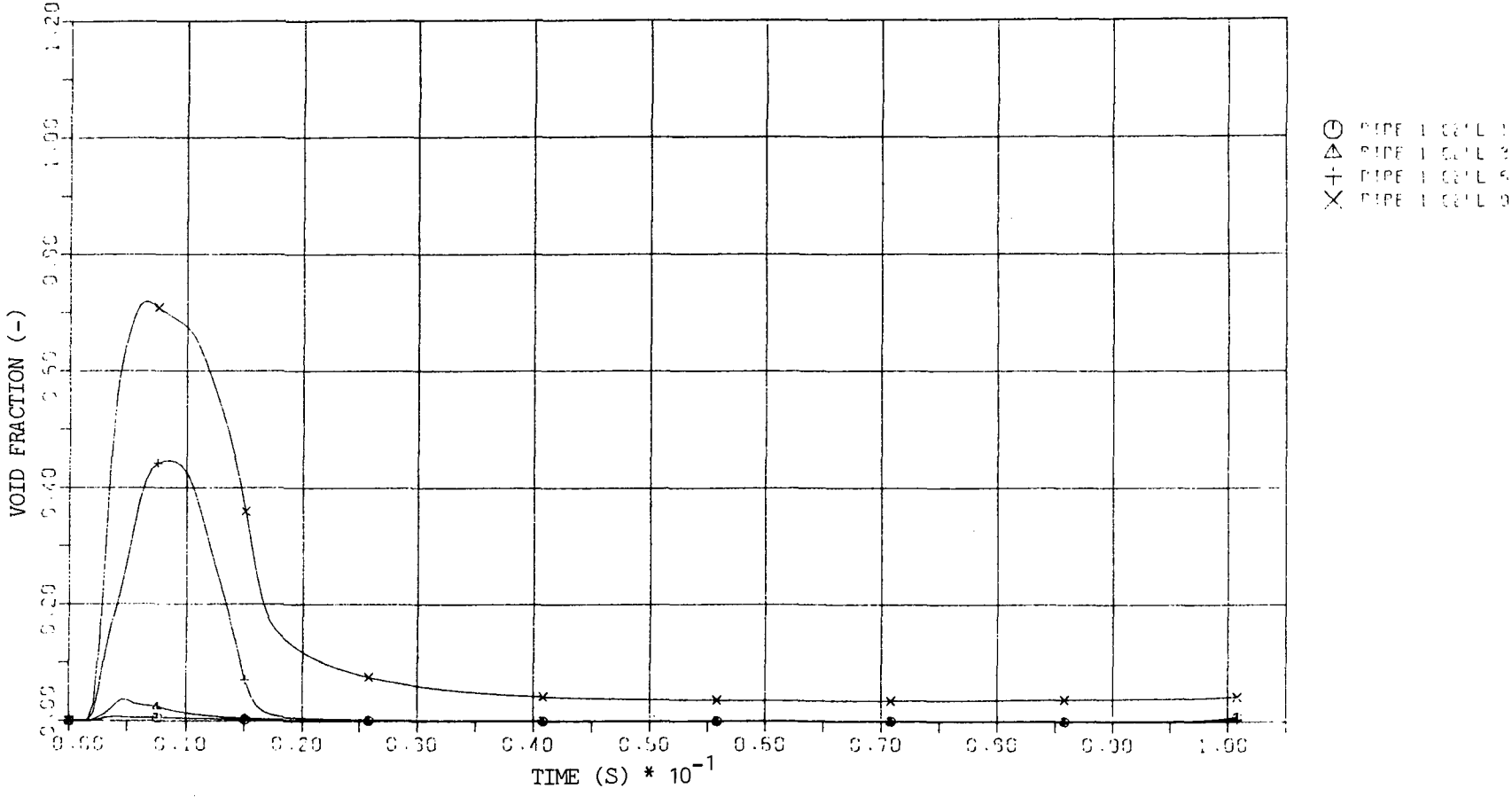

PIPE 2 / VESSEL TYPE 4

VOID FRACTION

Fig. 2.5.7

KWU TRAC - PD2

THE EFFECT OF DIFFERENT PARAMETERS ON THE OUTFLOW RATE

RECALCULATION OF THE HDR-TESTS WITH THE VESSEL COMPONENT

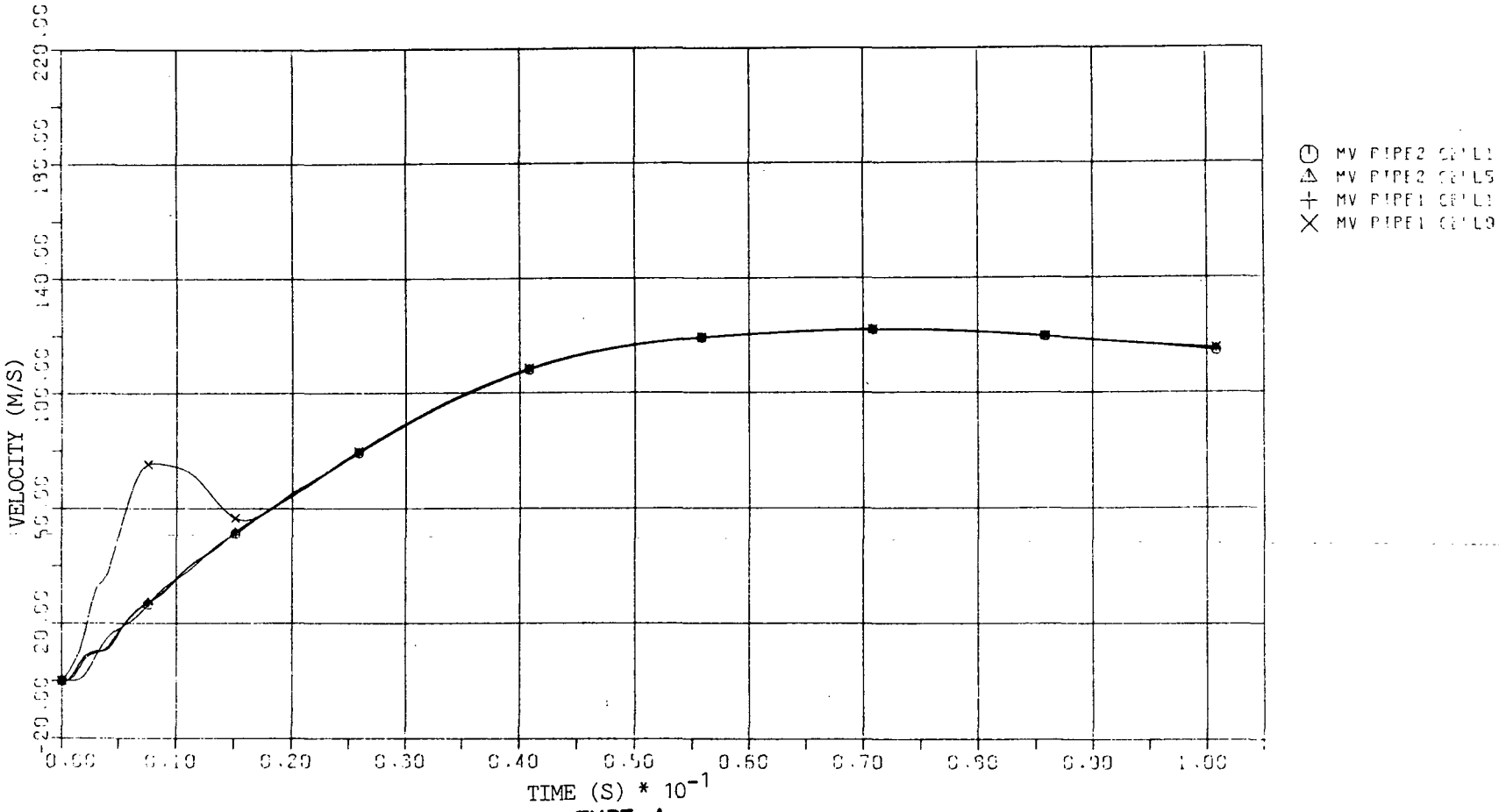

PIPE 2 / VESSEL TYPE 4

VELOCITY

Fig. 2.5.8

KWU TRAC - PD2

THE EFFECT OF DIFFERENT PARAMETERS ON THE OUTFLOW RATE

RECALCULATION OF THE HDR-TESTS WITH THE VESSEL COMPONENT

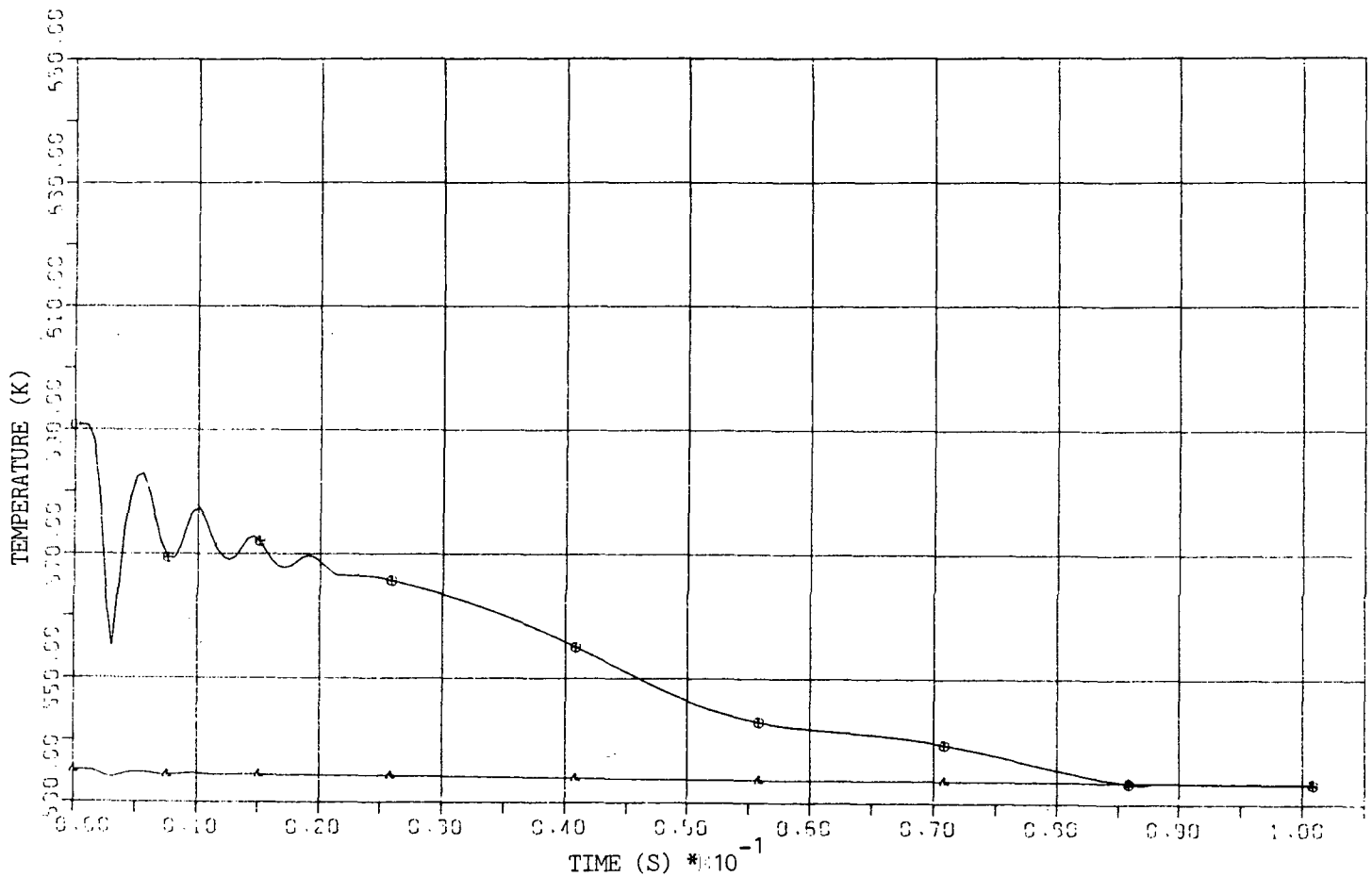

PIPE 2 / VESSEL TYPE 4

TEMPERATURE

Fig. 2.5.9

KWU TRAC -PD2

THE EFFECT OF DIFFERENT PARAMETERS ON THE OUTFLOW RATE

RECALCULATION OF THE HDR-TESTS WITH THE VESSEL COMPONENT

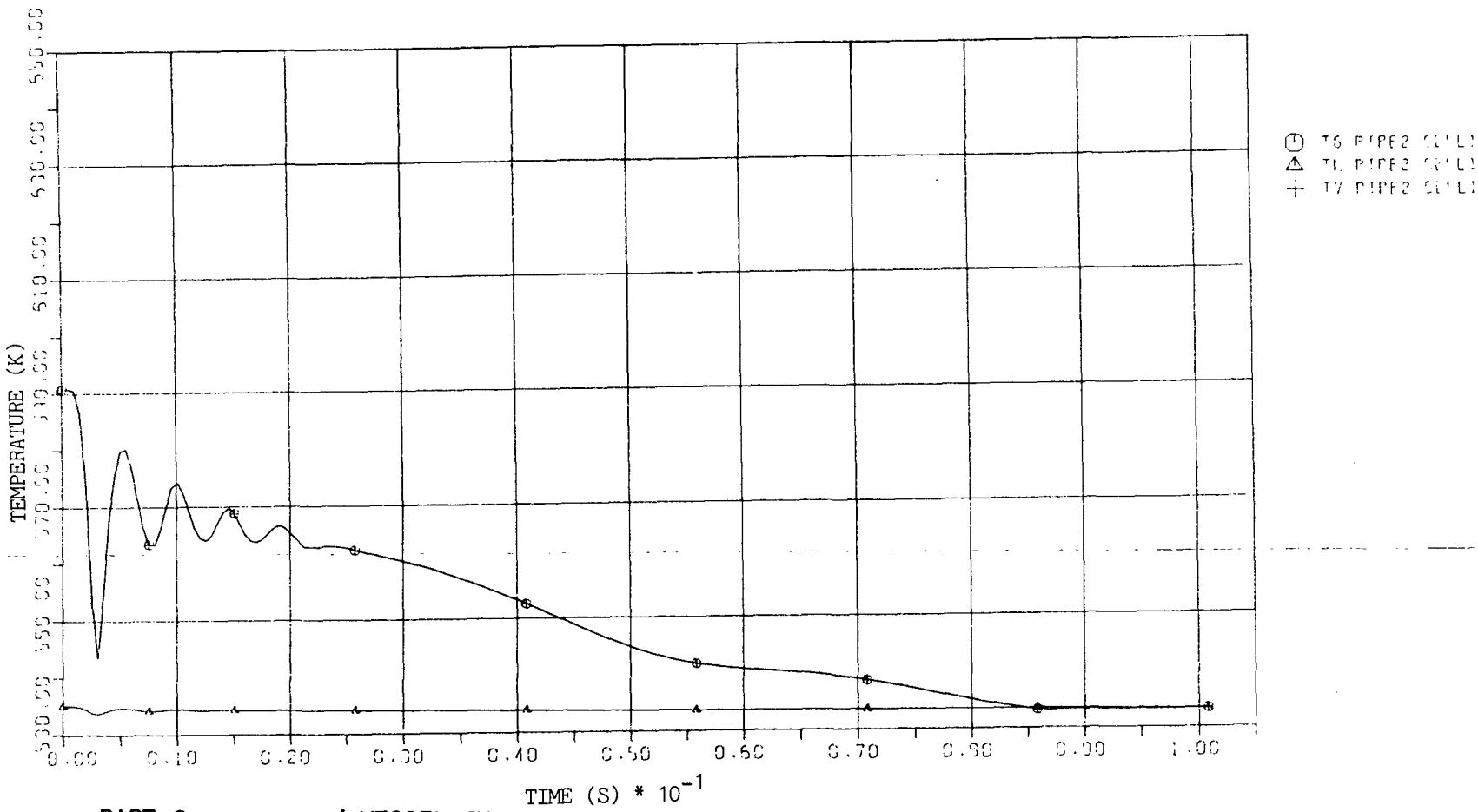

PIPE 2 / VESSEL TYPE 4

TEMPERATURE

Fig. 2.5.10

KWU TRAC - PD2

THE EFFECT OF DIFFERENT PARAMETERS ON THE OUTFLOW RATE

RECALCULATION OF THE HDR-TESTS WITH THE VESSEL COMPONENT

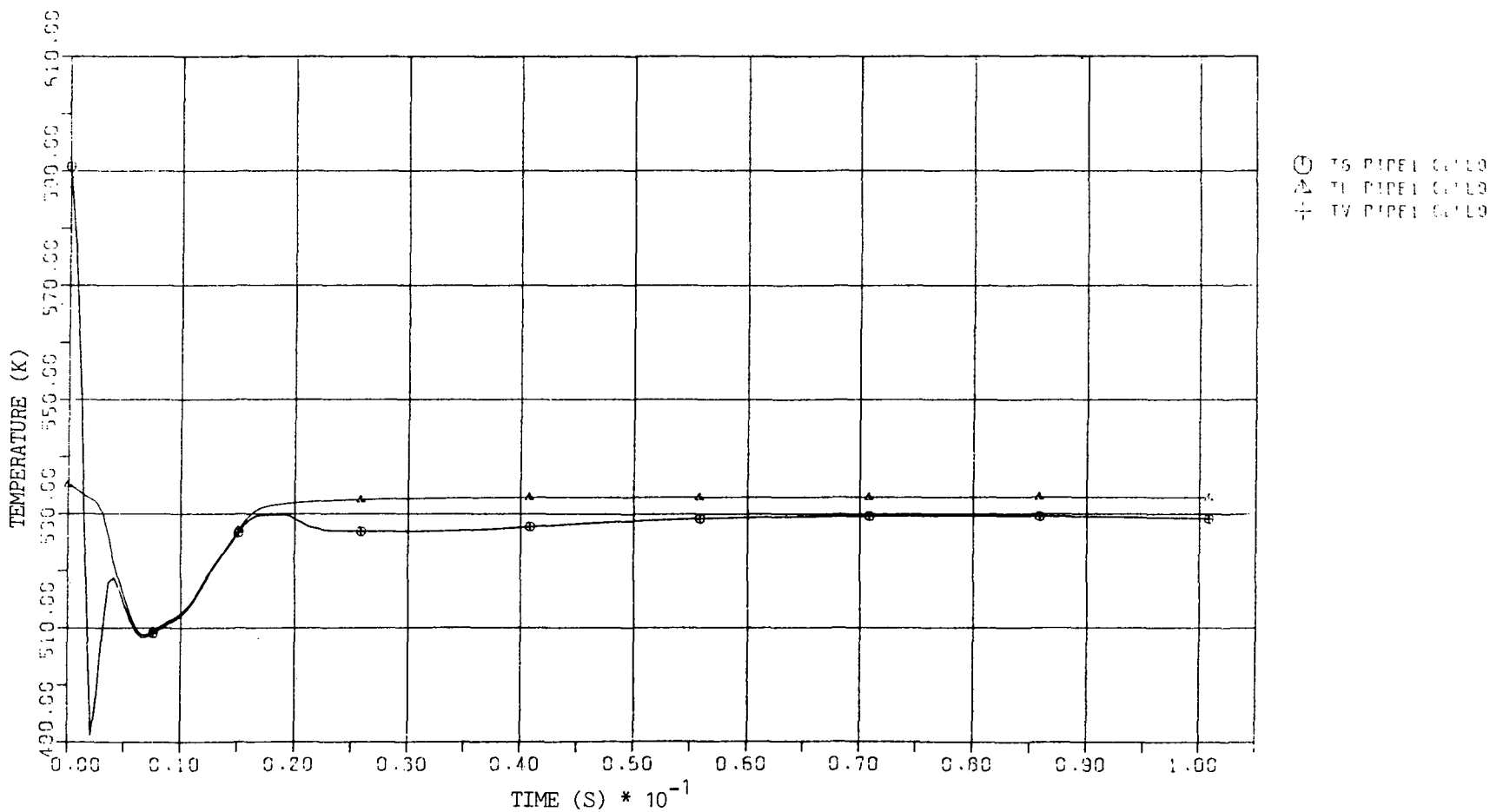

PIPE 2 / VESSEL TYPE 4

TEMPERATURE

Fig. 2.5.11

PART III: RECOMMENDATION FOR THE APPLICATION OF TRAC-PD2 TO SHORT-TERM TRANSIENTS

Part III

This page intentionally left blank.

Introduction

Since the first introduction of the TRAC-P1A computer code in March 1979 and the installation of the improved version TRAC-PD2 in the meantime in September 1980, various calculations for the Atucha II project and post-test calculations have been performed.

The knowledge gained from optimizing the computation models is explained in more detail and illustrated, if necessary, in the following chapters.

These activities were undertaken in particular in the process of verifying the new version of the TRAC-PD2 code because it becomes more and more apparent that due to its flexibility this code yields good results in particular for complex plants and thus has become indispensable for project work.

2 Automatic Calculation of Pressure Loss Coefficients for Contraction or Enlargement

From Chapter b. "Finite Difference Equations" (/1/, ref. p. 2) it can be deduced that there are two possible procedures for solving the differential equations for the one-dimensional components.

Firstly, there is the semi-implicit procedure (subroutine DF1DS) which determines the time interval by an explicit equation as shown in eqn. 2.1:

$$\Delta t = \left| \frac{\Delta x_j}{v_{m,\,j}} \right| \qquad \text{Eqn. 2.1}$$

Secondly, there is the fully implicit procedure (subroutine DF1DI) which is to be employed particularly for components where a priori high flow velocities are to be expected, e.g. the blowdown pipe. For the one-dimensional components, the user is free to choose either one of these procedures. a

In any case the RPV component (VESSEL) is calculated by the semi-implicit procedure. However, certain differences arise in the determination of the pressure loss coefficients in the pipe, depending on the solution procedure chosen. It can be seen from Chapter d.6. "Form Losses" (/1/, ref. p. 28) that the semi-implicit procedure allows for the pressure loss in the case of sudden expansion, but not in the case of contraction or outflow processes.

The fully-implicit procedure, on the other hand, calculates a Bernoulli flow, which, however, takes neither contraction nor expansion or outflow processes into account. This is due to the definition of the Bernoulli equation, which only applies to frictionless flow.

In this case, therefore, the mathematical results must be subjected to a correction as follows:

$$\Delta p = k \frac{\varrho}{2} \cdot v \cdot |v| \qquad \text{Eqn. 2.2}$$

where k follows from

$$k = (1 - \frac{A_1}{A_2})^2 \qquad \text{Eqn. 2.3}$$

for expansion, and equation 2.4

$$k = 0.5 - 0.7 \left(\frac{A_1}{A_2}\right) + 0.2 \left(\frac{A_1}{A_2}\right)^2 \qquad \text{Eqn. 2.4}$$

holds for contraction, with A_1 being the smaller and A_2 the larger flow area. These calculations are performed by a subroutine called FWALL.

In the TRAC-PD2 version, the final pressure loss is given by

$$\Delta p = \frac{(\Delta x_j + \Delta x_{j-1})}{2D_{h,\,j}} \, FRIC_j \; \varrho_m \, v_m \, |v_m| \qquad \text{Eqn. 2.5}$$

The FF value in the TRAC-OUTPUT is given by

$$FF = \frac{k_j \cdot D_{h,\,j}}{\Delta x_j + \Delta x_{j-1}} \qquad \text{Eqn. 2.6}$$

and the $FRIC_j$ values are calculated by including the appropriate ζ value in the following equation:

$$FRIC_j = \frac{\zeta_j \, D_{h,\,j}}{\Delta x_j + \Delta x_{j-1}} \qquad \text{Eqn. 2.7}$$

This way it is also possible to put in the loss coefficients by hand by calculating, say, the K value for the contraction and explicitly entering it as a FRIC value in the input of the component.

ζ values due to form losses, elbows, apertures, orifices, flow restrictors, etc. can thus also be taken into account. However, it is the purpose of the following text to determine how the semi-implicit and the fully implicit procedures cooperate with the automatic calculation of the loss coefficients.

For this purpose, the respective pressure losses upon expansion and contraction in a pipe are calculated; the surface area ratio $\frac{A_1}{A_2} = 0.25$ is the same in both cases. The actual model is represented in Fig. 2.1.

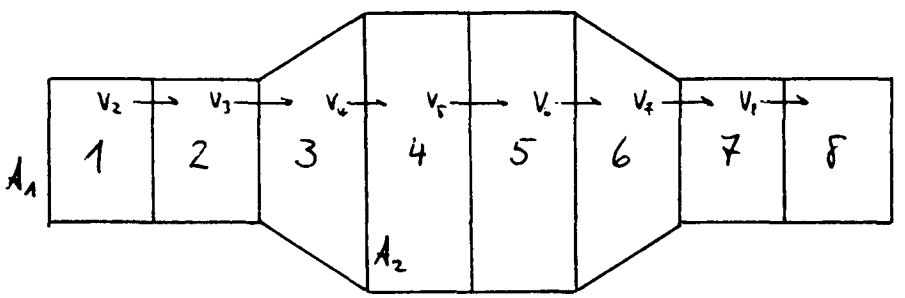

Fig. 2.1

As has already been mentioned, the semi-implicit procedure is capable of accurately calculating the pressure profile in the case of expansion without a correction. The pressure difference as determined by the TRAC and the manual calculation (Eqn. 2.8) as well as the corresponding FF values for the four possible combinations are listed in Table 2.1. This shows clearly that the statement previously made regarding the semi-implicit procedure is correct. According to Table 2.1, the fully implicit procedure only produces correct results if NFF = -1 is included in the calculation. In this case only the FF value from the TRAC output is equal to the calculated FF value. For NFF = +1 and fully implicit, the pressure regain is far too high, as in this case the frictional losses are not covered by the Bernoulli equation.

Expansion		Δp_{TRAC}^{4-2}	Δp_{CALC}^{4-2}	FF_{TRAC}	$FF_{CALC} = \frac{k\ D_{h,j}}{\Delta x_j + \Delta x_{j-1}}$
NFF - 1	FI	0.2870	0.2913	0.2267	0.2244
NFF + 1	FI	0.7228	0.2933	0.00268	0.2244
NFF - 1	SI	0.2870	0.2910	0.002684	0.2244
NFF + 1	SI	0.2880	0.2910	0.002684	0.2244

Table 2.1

$$\Delta p_{4-2} = \frac{1}{2}\rho_4 v_4^2 + \frac{1}{2}\rho_3 (k\ v_3^2 - v_3^2) \qquad \text{Eqn. 2.8}$$

$$k = (1 - \frac{A_1}{A_2})^2$$

Contraction		Δp_{TRAC}^{5-7}	Δp_{CALC}^{5-7}	FF	$FF = \frac{k\ D_{h,j}}{\Delta x_j + \Delta x_{j-1}}$
NFF - 1	FI	1.0795	1.0846	0.1370	0.1346
NFF + 1	FI	0.7987	1.0917	0.002347	0.1346
NFF - 1	SI	1.0841	1.0862	-0.08742	0.1346
NFF + 1	SI	1.2750	1.0862	0.002345	0.1346

Table 2.2

$$\Delta p_{5-7} = -\frac{1}{2}\rho v_6^2 + \frac{1}{2}\rho_7 (v_7^2 + k\ v_7^2) \qquad \text{Eqn. 2.9}$$

$$k = 0.5 - 0.7\frac{A_1}{A_2} + 0.2\ (\frac{A_1}{A_2})^2$$

In contrast to this, none of the procedures a priori cover correctly the pressure loss upon contraction, as can be seen from Table 2.2, so that for the semi implicite as well as for the fully implicit procedures the automatic calculation has to be employed.

With the option NFF = -1 and semi-implicit, the dubious case occurs that a negative loss coefficient is used in the program. This is due to the fact that the pressure loss is overestimated; the pressure is therefore boosted by means of a negative ζ value in order to obtain the correct value.

Generally it can be stated that a full agreement between TRAC and calculation by hand can only be achieved by the fully implicit procedure combined with a negative NFF value in the pressure loss as well as in the FF value. This combination should, therefore, generally be used so as to avoid all uncertainties from the start.

3 Parameter Study on HDR Tests

It is imperative to check tests in order to verify a computational program. For this reason, the PHDR/V31 tests were checked by means of the program version TRAC-PD2, so that the calculated pressures and outflow rates from the TRAC calculations could be compared with the test results. There was some uncertainty regarding the handling of the TRAC-PD2 input; a parameter study (Table 3.1) was implemented in order to clarify these problems in principle. For this purpose, the results of the model modifications elucidated in the following chapters were related to an initial calculation so as to enable the effect of the individual changes to be determined. This initial calculation is based on a model of the HDR experiment(Fig.3.1) in which the RPV(Fig.3.2) was simplified to a great extent, since it was only required as a pressure boundary condition for the basic examinations of the pressure curves and outflow rates in the blowdown nozzle. For this reason, the results are to be deemed to be of qualitative rather than of quantitative relevance; a direct comparison with the HDR measurements is only possible to a limited extent. The exact post-test calculations were performed with a more detailed model by H. Herterich /4/.

Series of HDR tests

HDR1/3	Junction of the blowdown nozzle without any special changes Ratio pipe surface: vessel junction surface = 1 : 21 PIPE2 SI/PIPE1 FI/pressure boundary condition in 2 ms to 1 bar
HDR2/3	Automatic junction of the pipe to the vessel Expansion of pipe surface to vessel junction surface PIPE FI/PIPE1 FI/pressure boundary condition in 2 ms to 1 bar
HDR3/3	Automatic junction of the pipe to the vessel with nozzle All pipes FI and NFF = -1/pressure boundary condition instantaneous
HDR4/5	New nodalisation of vessel with 2 radial zones in the downcomer Vessel junction surface = pipe surface ζ = 0.5 for the outflow from the vessel
HDR5/4	Only 1 radial zone in the downcomer Vessel junction surface = pipe surface
HDR6/5	Vessel division as for HDR4/5 Vessel function surface = pipe surface Nodelling bypass model in the blowdown nozzle

SI ≙ semi-implicit
FI ≙ fully implicit

Table 3.1

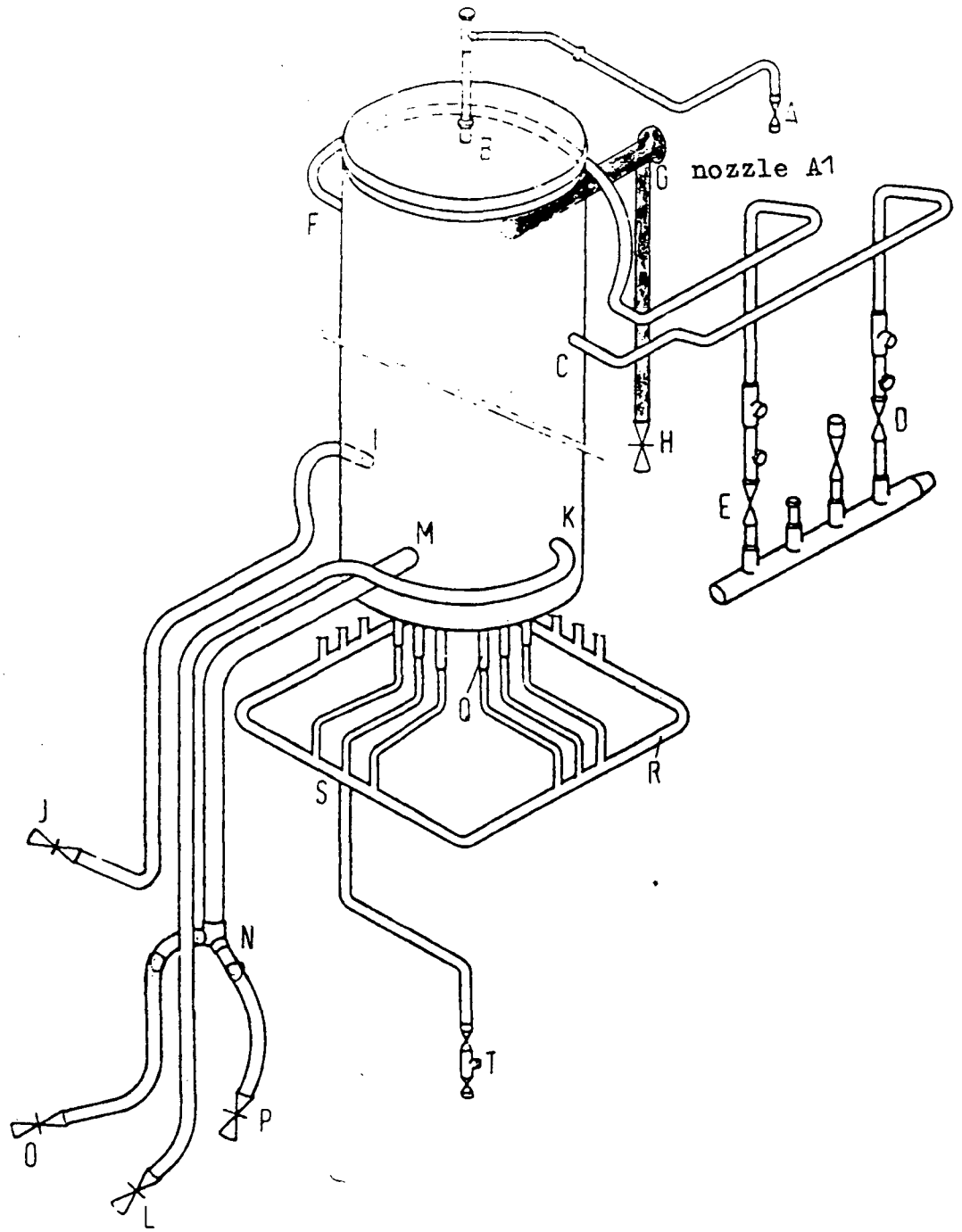

Schematic Isometry of Lines and Loops
Participating During Blowdown

Fig. 3.1

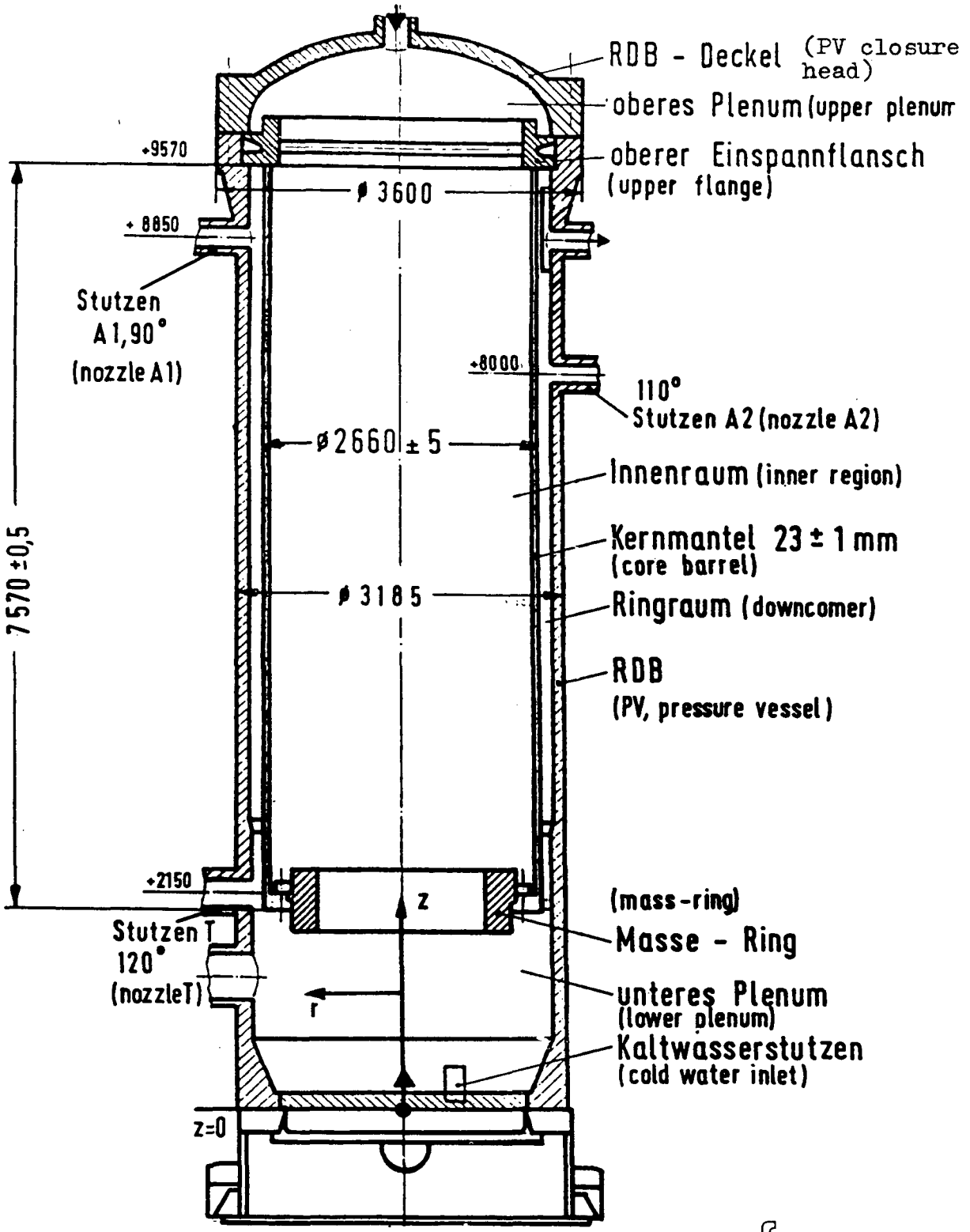

RDB und Kernmantelgeometrie für Blowdown Exp.

(RPV and Core Barrel Geometries for Blowdown Experiments)

Fig. 3.2

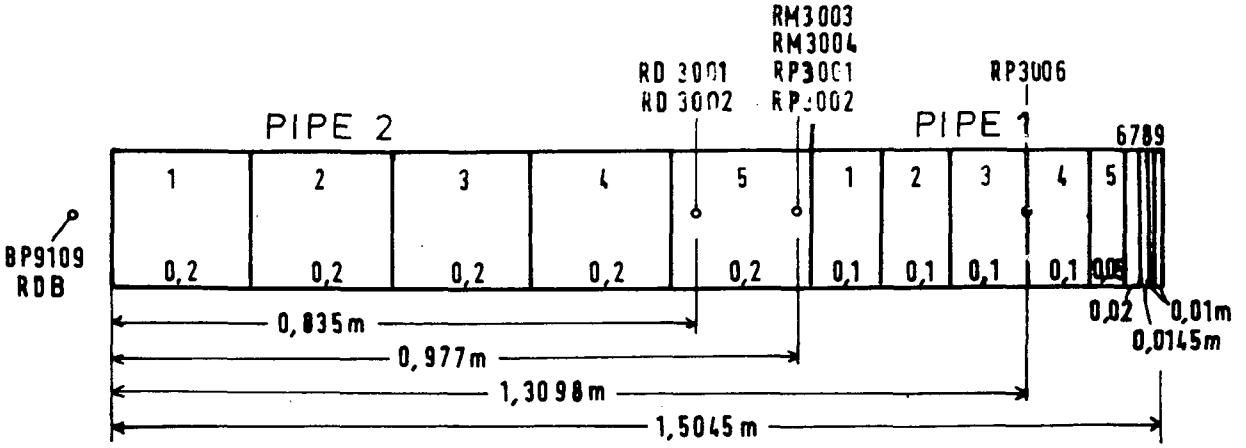

Blowdown nozzle for the HDR 1/3 4/5 5/4 models

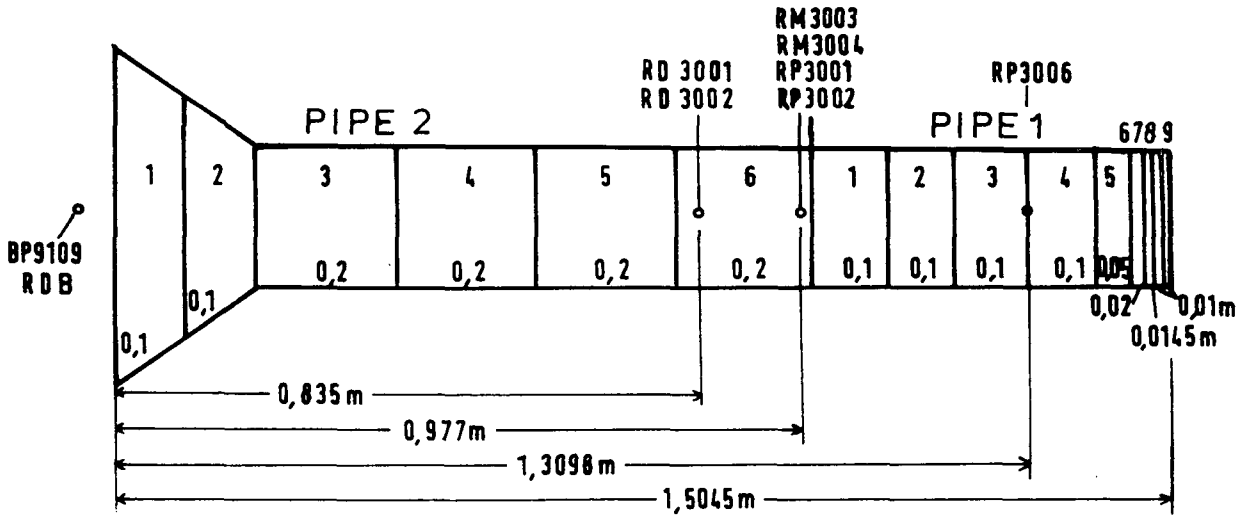

Blowdown nozzle for the HDR 2/3 3/3 models

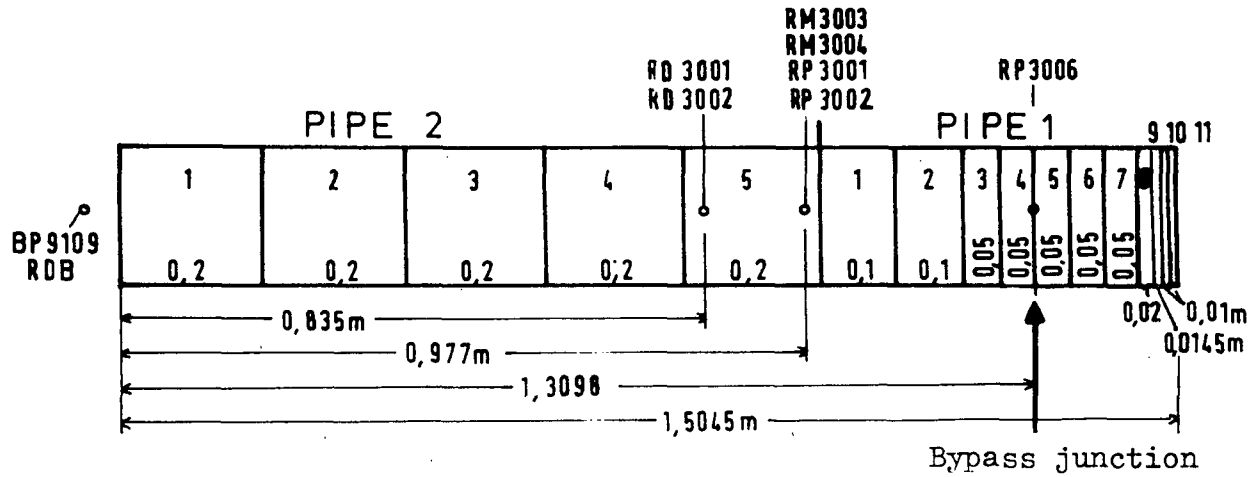

Blowdown nozzle for the HDR 6/5 model

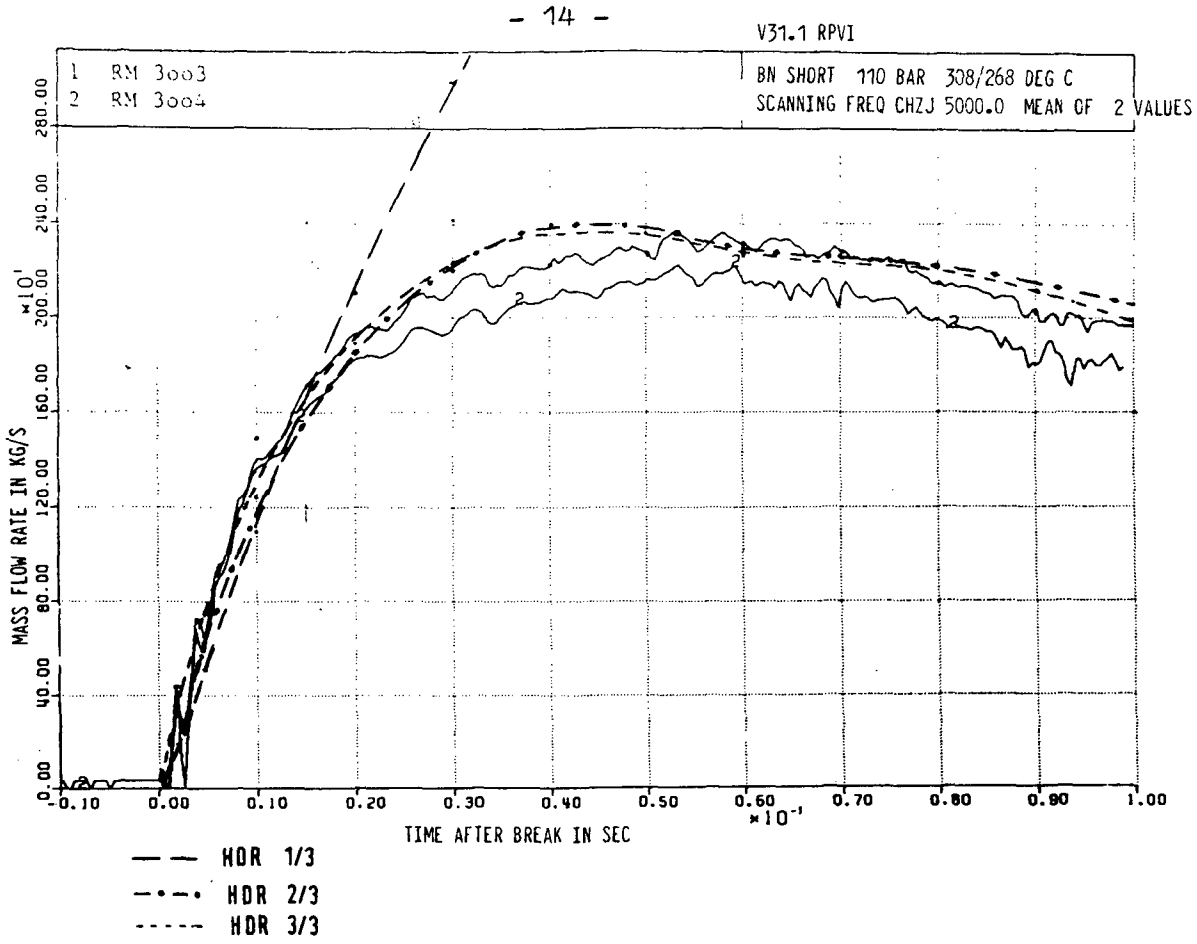
V31.1 RPVI
1 RM 3003
2 RM 3004
BN SHORT 110 BAR 308/268 DEG C
SCANNING FREQ CHZJ 5000.0 MEAN OF 2 VALUES
MASS FLOW RATE IN KG/S
×10¹
0.00
40.00
80.00
120.00
160.00
200.00
240.00
280.00
-0.10
0.00
0.10
0.20
0.30
0.40
0.50
0.60
0.70
0.80
0.90
1.00
×10⁻¹
TIME AFTER BREAK IN SEC
HDR 1/3
HDR 2/3
HDR 3/3

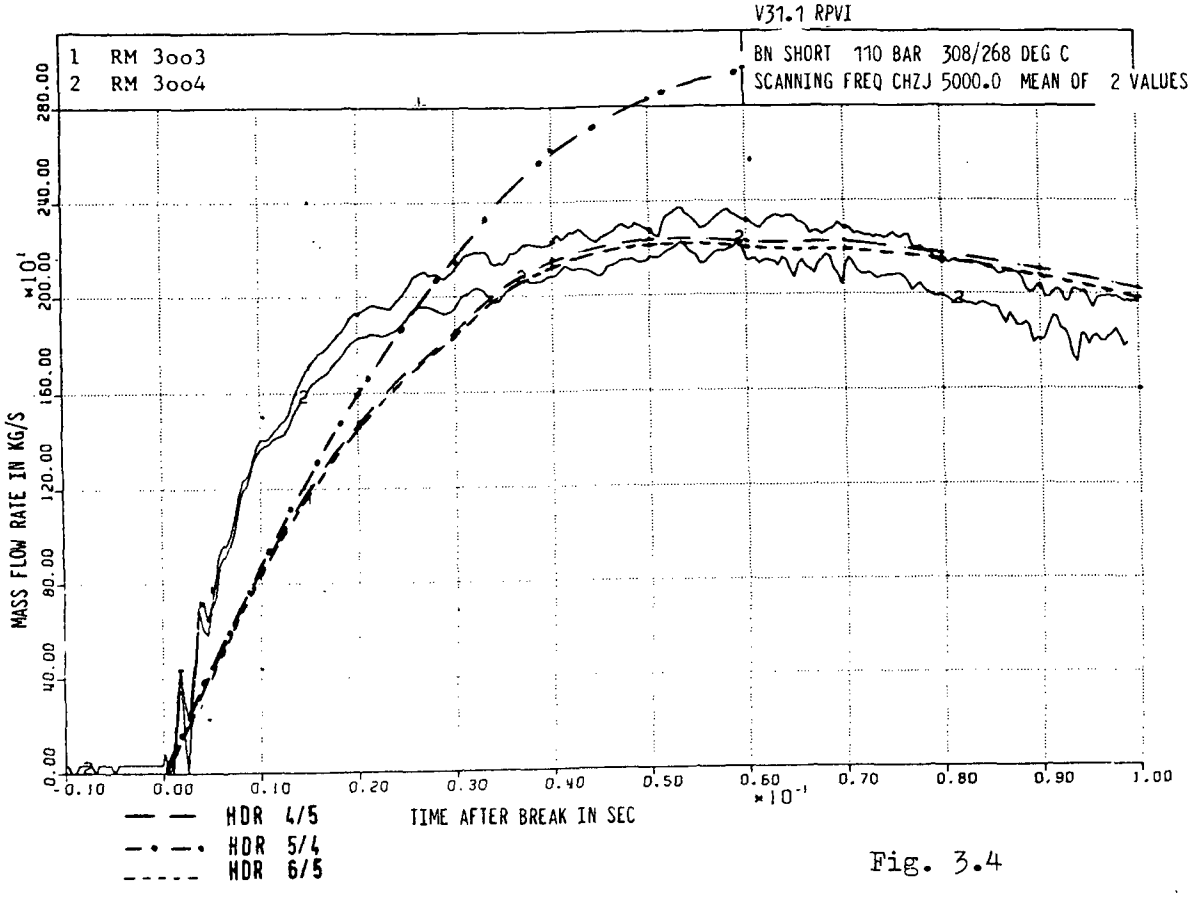
V31.1 RPVI
1 RM 3003
2 RM 3004
BN SHORT 110 BAR 308/268 DEG C
SCANNING FREQ CHZJ 5000.0 MEAN OF 2 VALUES
MASS FLOW RATE IN KG/S
×10¹
0.00
40.00
80.00
120.00
160.00
200.00
240.00
280.00
-0.10
0.00
0.10
0.20
0.30
0.40
0.50
0.60
0.70
0.80
0.90
1.00
×10⁻¹
TIME AFTER BREAK IN SEC
HDR 4/5
HDR 5/4
HDR 6/5

Fig. 3.4

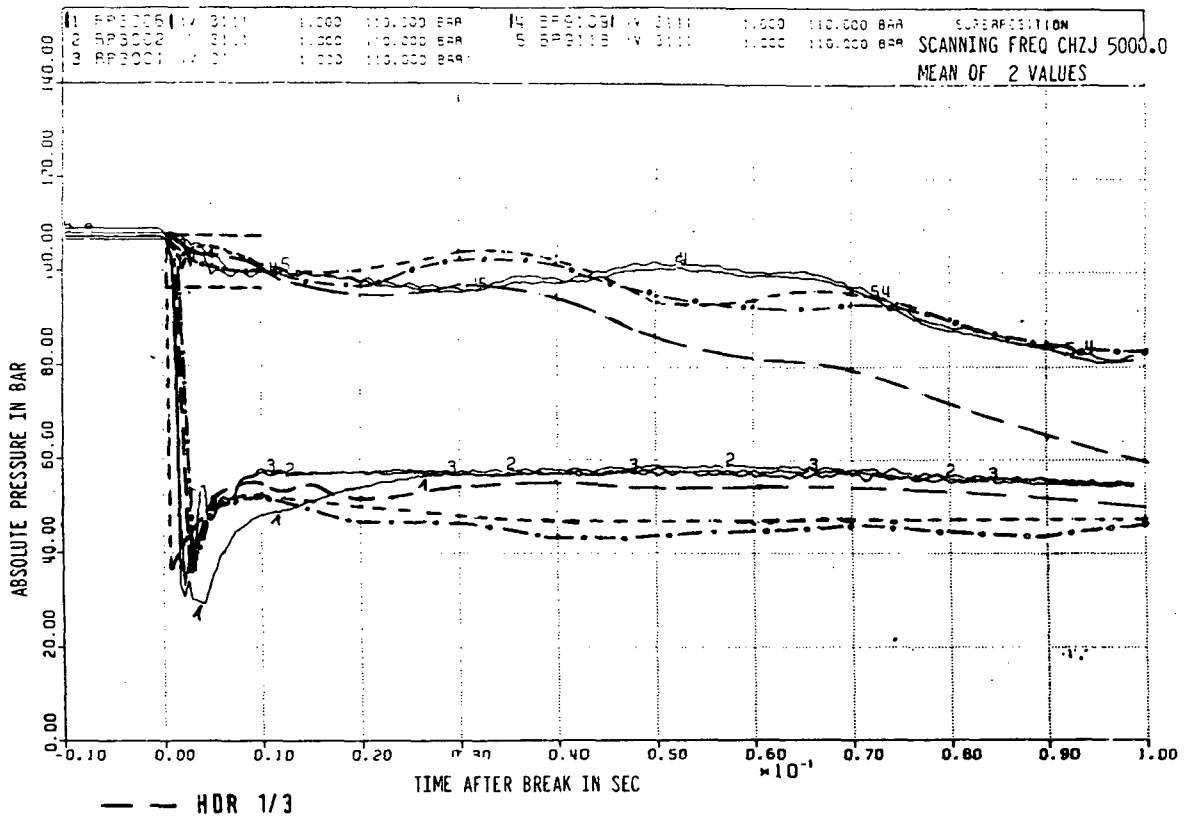
1 RP3006 IV 3111 1.000 110.000 BAR
2 RP3002 IV 3111 1.000 110.000 BAR
3 RP3001 IV 3111 1.000 110.000 BAR
4 BP9109 IV 3111 1.000 110.000 BAR
5 BP9118 IV 3111 1.000 110.000 BAR
SUPERPOSITION
SCANNING FREQ CHZJ 5000.0
MEAN OF 2 VALUES
ABSOLUTE PRESSURE IN BAR
TIME AFTER BREAK IN SEC
×10⁻¹
HDR 1/3
HDR 2/3
HDR 3/3

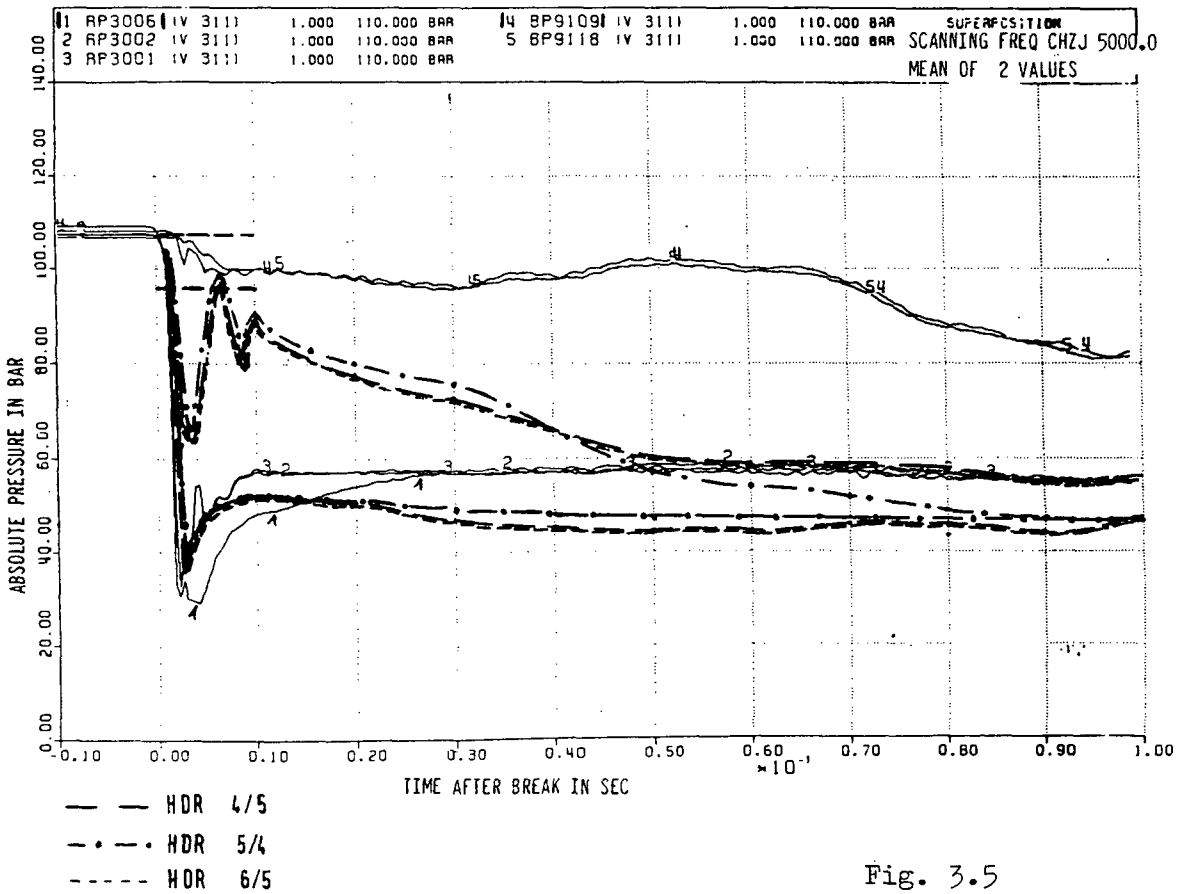
1 RP3006 IV 3111 1.000 110.000 BAR
2 RP3002 IV 3111 1.000 110.000 BAR
3 RP3001 IV 3111 1.000 110.000 BAR
4 BP9109 IV 3111 1.000 110.000 BAR
5 BP9118 IV 3111 1.000 110.000 BAR
SUPERPOSITION
SCANNING FREQ CHZJ 5000.0
MEAN OF 2 VALUES
ABSOLUTE PRESSURE IN BAR
TIME AFTER BREAK IN SEC
×10⁻¹
HDR 4/5
HDR 5/4
HDR 6/5

Fig. 3.5

3.1 HDR1/3 Initial Test Calculation

The results of this calculation form the basis for an assessment of the effectiveness of the measures subsequently implemented. The pressure and mass flow rate curves determined are compared with those resulting from the HDR tests; no absolute agreement is to be expected here; nevertheless, the same qualitative behaviour should be observed. Fig. 3.1 shows the entire set-up of the HDR experiment. In this model, only the RPV and nozzle A1 are pictured. Fig. 3.2 provides an overview of the RPV internals and the corresponding geometrical dimensions. The model pertaining to this calculation is pictured in Fig. 3.6. The REACTOR PRESSURE VESSEL is subdivided into 4 levels, each of which consists of 2 radial annuli and 4 azimuthal segments, so that each level comprises 8 zones. The blowdown nozzle is connected to zone 5 in level 4. It consists of 2 pipes (PIPE1 and PIPE2). Fig. 3.3 shows the exact discretization. The surroundings are represented by a BREAK (pressure boundary condition). A pressure drop to 1 bar within 2 ms is specified as the boundary condition. The locations of the measuring points for the pressures and flow rates are also indicated in Fig. 3.3. Figs. 3.4 and 3.5 feature the corresponding measurement curves. For easier comparison, the mathematical results obtained from the 6 calculations are also listed in these figures.

Furthermore, the most important mathematical results are plotted in Figs. 3.7 to 3.10. These are pressure, steam quality and flow rate.

A comparison of the calculated mass flow rate (Fig. 3.8) in PIPE2 CELL5 (measuring point RM 3003/3004) with the measurement curve (Fig. 3.4) makes readily apparent that in this case the outflow rate is calculated as being more than twice as high at 0.1 s. This is due to the vessel connection. The actual outflow losses are not covered by this model; this implies an excessive outflow velocity and a correspondingly high outflow rate. This results in a faster pressure loss in the RPV, which has nearly reached the pressure within the pipe after 0.1 s (Fig. 3.5).

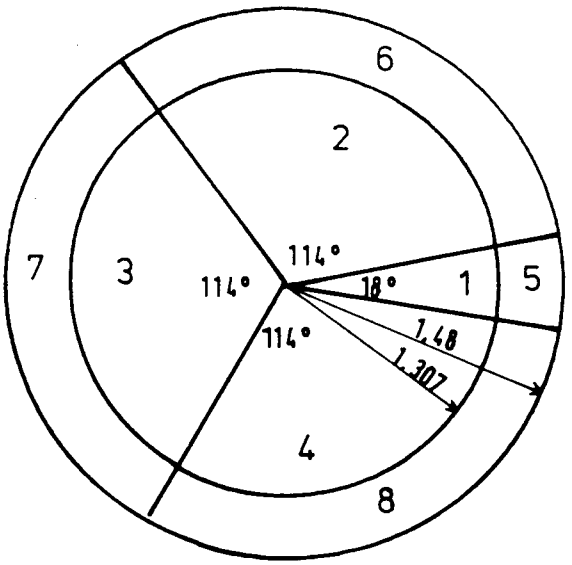

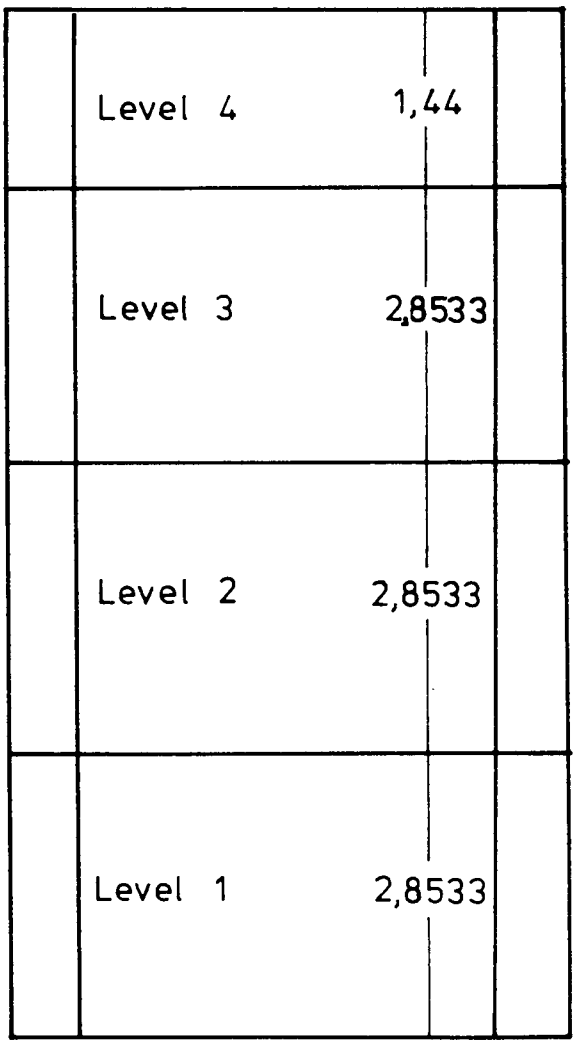

VESSEL 3

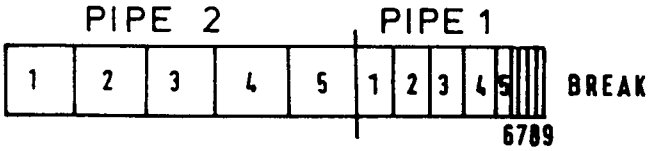

HDR 1/3

Fig. 3.6

KWU TRAC-PD2
EFFECT OF VARIOUS PARAMETERS ON THE OUTFLOW RATE
CHECK OF THE HDR TESTS WITH VESSEL COMPONENT

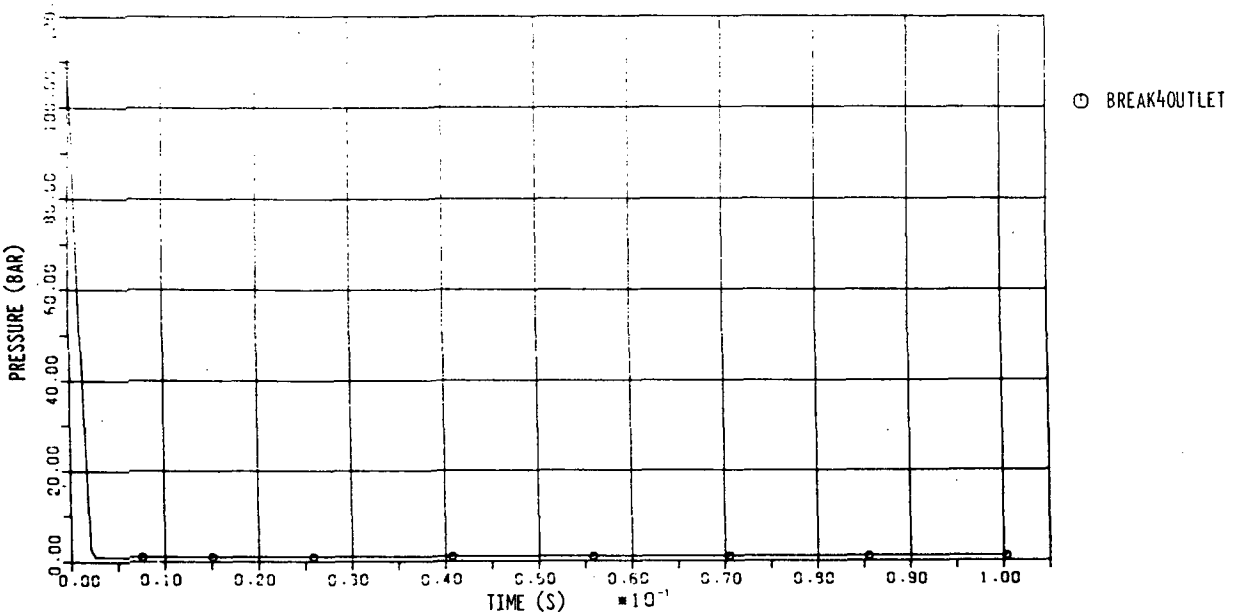

PIPE 2 - SEMI-IMPLICIT / VESSEL VERSION 3
PRESSURE

KWU TRAC-PD2
EFFECT OF VARIOUS PARAMETERS ON THE OUTFLOW RATE
CHECK OF THE HDR TESTS WITH VESSEL COMPONENT

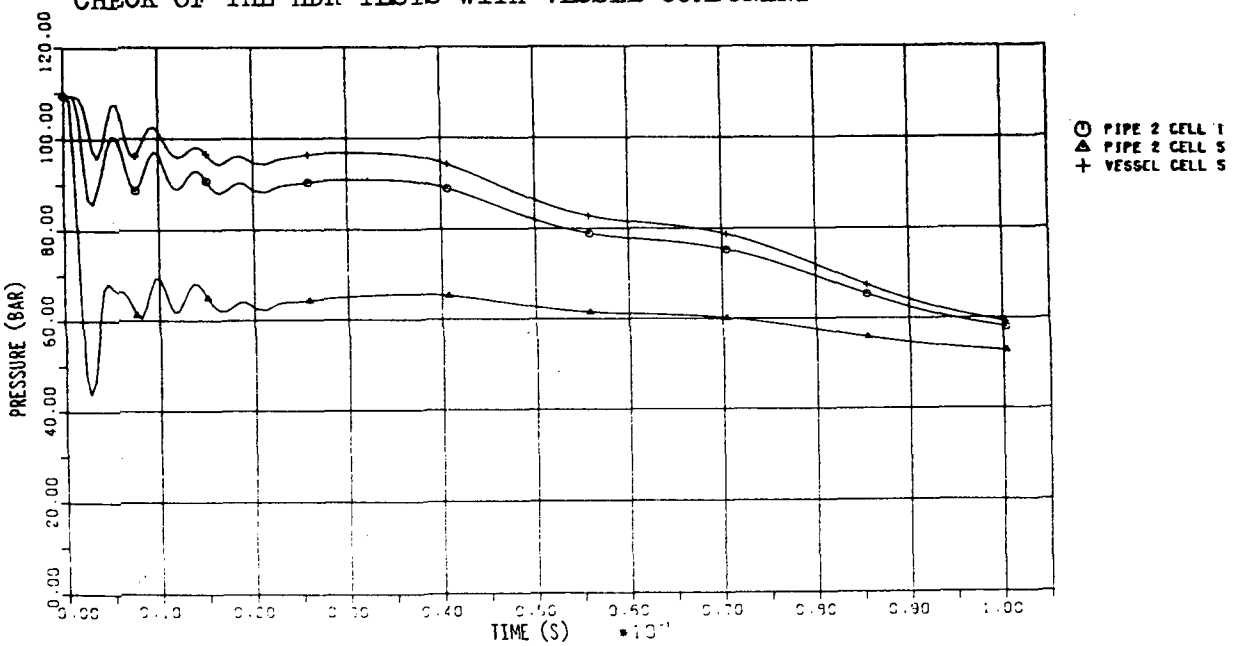

PIPE 2 - SEMI-IMPLICIT / VESSEL VERSION 3
PRESSURE

Fig. 3.7

KWU TRAC-PD2

EFFECT OF VARIOUS PARAMETERS ON THE OUTFLOW RATE

CHECK OF THE HDR TESTS WITH VESSEL COMPONENT

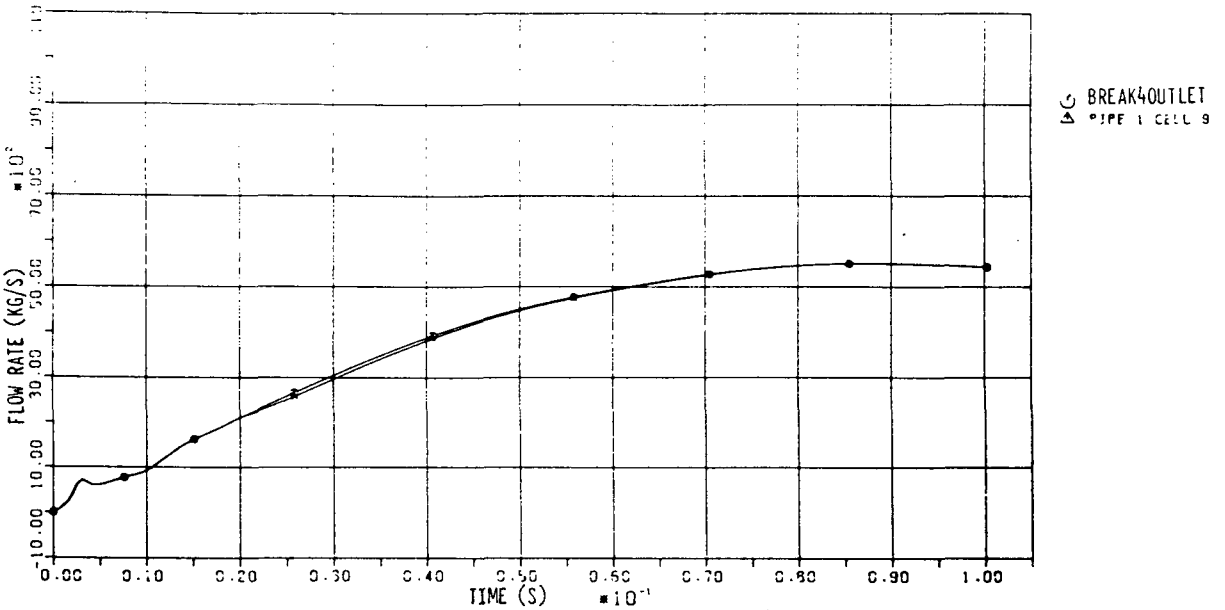

PIPE 2 - SEMI-IMPLICIT / VESSEL VERSION 3

FLOW RATE

KWU TRAC-PD2

EFFECT OF VARIOUS PARAMETERS ON THE OUTFLOW RATE

CHECK OF THE HDR TESTS WITH VESSEL COMPONENT

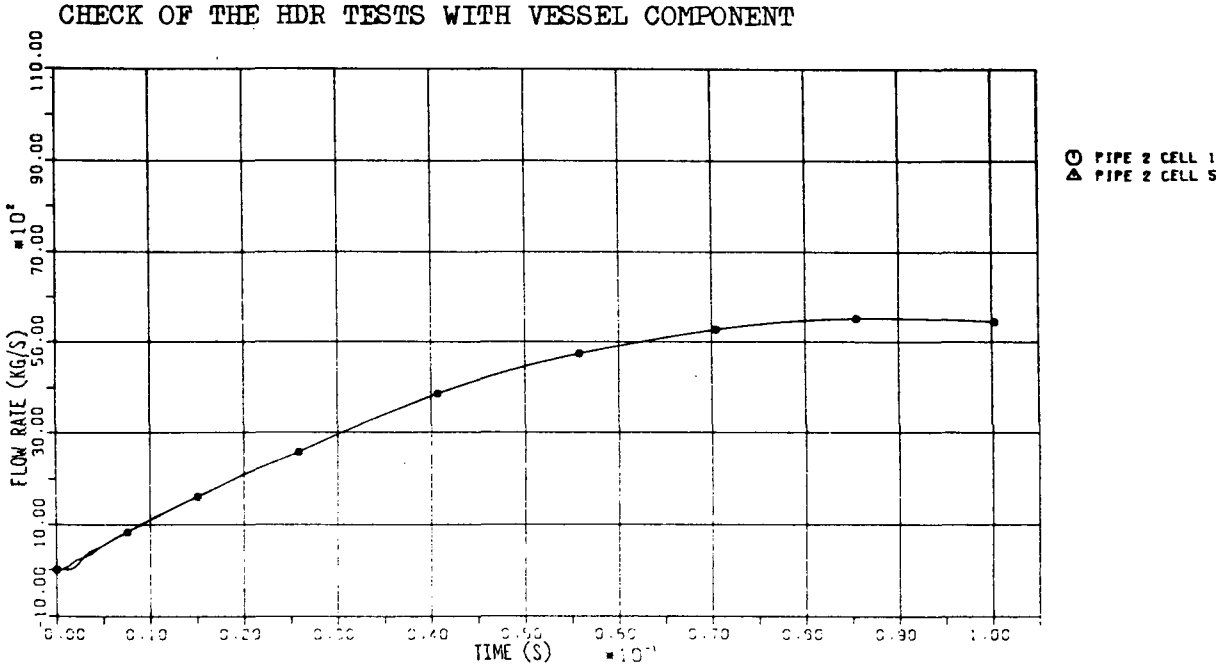

PIPE 2 - SEMI-IMPLICIT / VESSEL VERSION 3

FLOW RATE

Fig. 3.8

KWU TRAC-PD2

EFFECT OF VARIOUS PARAMETERS ON THE OUTFLOW RATE

CHECK OF THE HDR TESTS WITH VESSEL COMPONENT

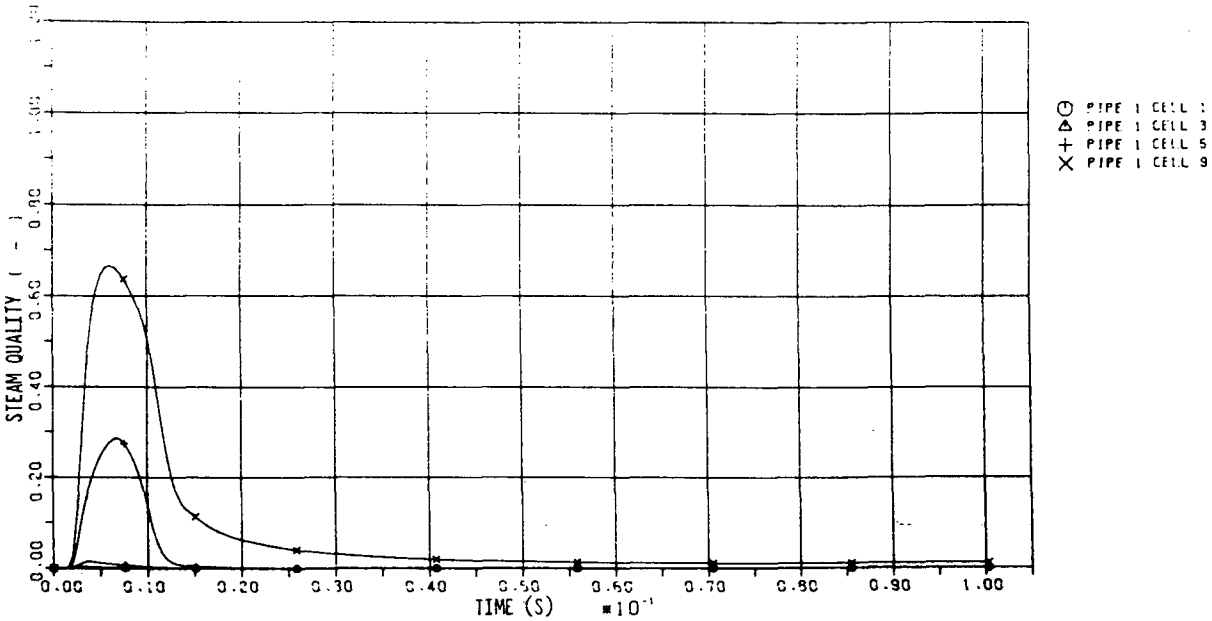

PIPE 2 - SEMI-IMPLICIT / VESSEL VERSION 3

STEAM QUALITY

KWU TRAC-PD2

EFFECT OF VARIOUS PARAMETERS ON THE OUTFLOW RATE

CHECK OF THE HDR TESTS WITH VESSEL COMPONENT

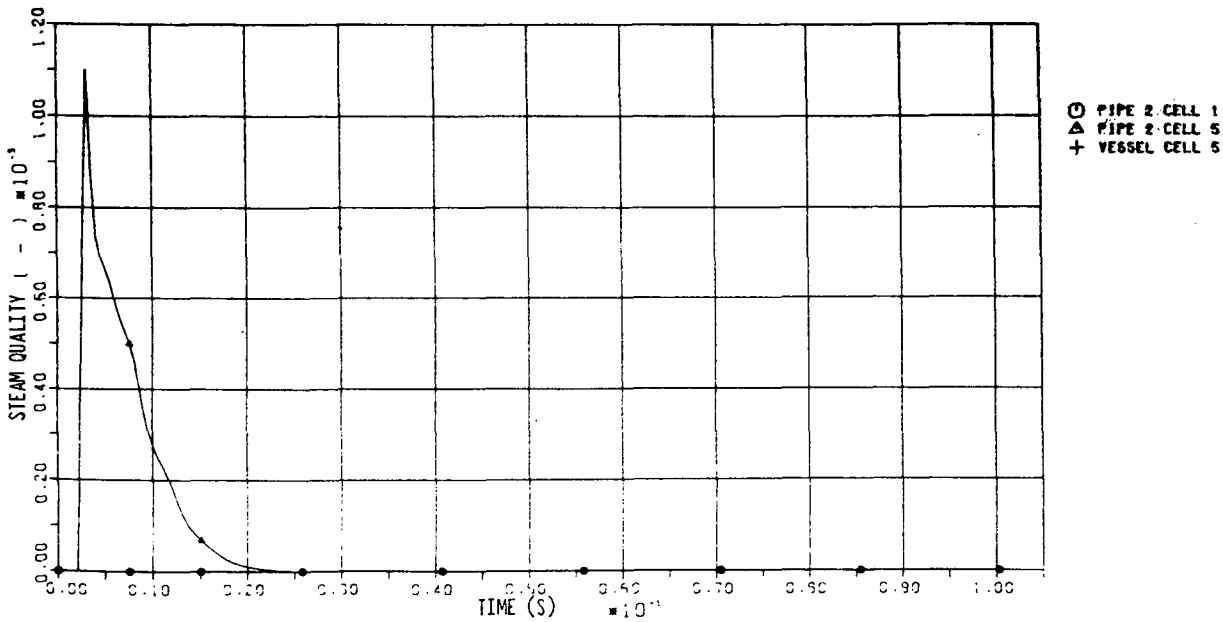

PIPE 2 - SEMI-IMPLICIT / VESSEL VERSION 3

STEAM QUALITY

Fig. 3.9

KWU TRAC-PD2

EFFECT OF VARIOUS PARAMETERS ON THE OUTFLOW RATE

CHECK OF THE HDR TESTS WITH VESSEL COMPONENT

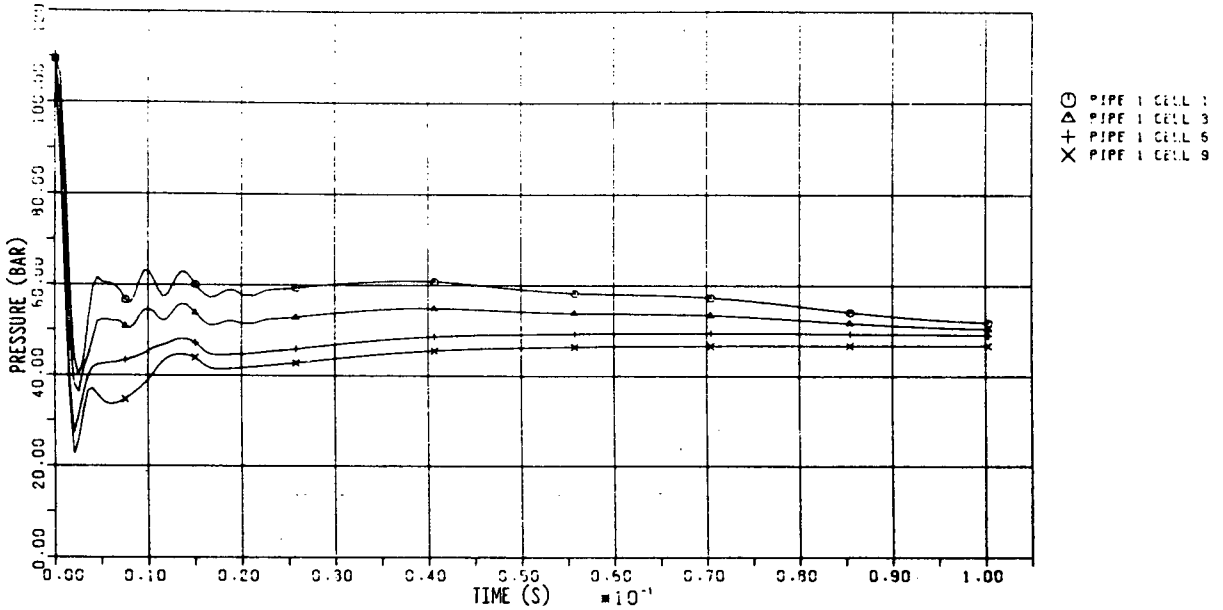

PIPE 2 - SEMI-IMPLICIT / VESSEL VERSION 3

PRESSURE

KWU TRAC-PD2

EFFECT OF VARIOUS PARAMETERS ON THE OUTFLOW RATE

CHECK OF THE HDR TESTS WITH VESSEL COMPONENT

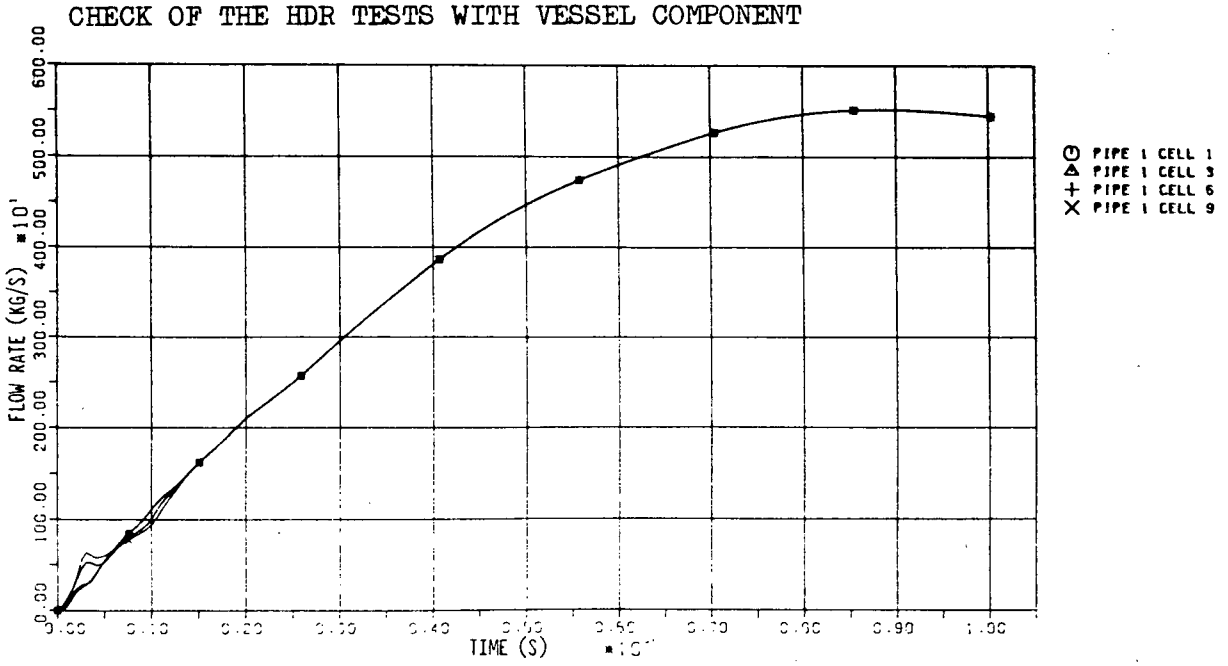

PIPE 2 - SEMI-IMPLICIT / VESSEL VERSION 3

FLOW RATE

Fig. 3.10

3.2 HDR2/3 Automatic Vessel Junction

In the following paragraphs, the various possible vessel junctions and their effects on the outflow rate as well as the pressure curve are discussed.

In this model (Fig. 3.11), the pressure loss occurring due to the contraction and turbulence of the flow upon leaving the vessel, is taken into account within the pipe.
This is effected by reducing the vessel junction area within the first two zones of the cross sectional area of the blowdown pipe. The pressure loss resulting from the contraction is thus automatically calculated with NFF = -4, in accordance with the equations in Chapter 1. Fig. 3.4 shows a relatively good agreement of the measured and the calculated curves of the outflow rates.

The agreement in the pressure curve for the RPV is similarly extensive, whereas in the blowdown nozzle the value of approx. 10 bar remains below the measured curve. This is certainly due to the outflow losses through the pipe and into the open being insufficiently considered (Figs. 3.12 to 3.15).

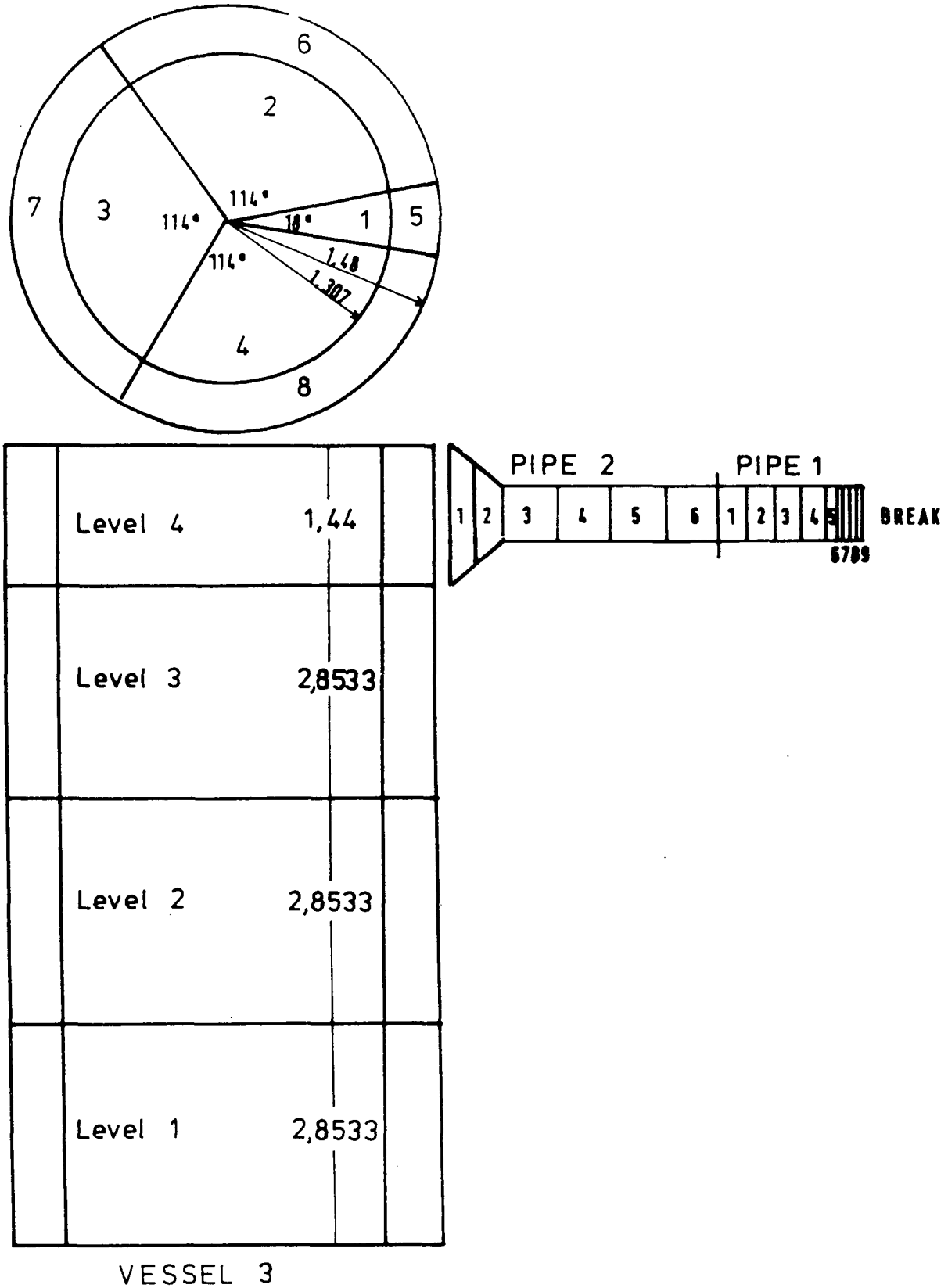

HDR 2/3

Fig. 3.11

KWU TRAC-PD2

EFFECT OF VARIOUS PARAMETERS ON THE OUTFLOW RATE

CHECK OF THE HDR TESTS WITH VESSEL COMPONENT

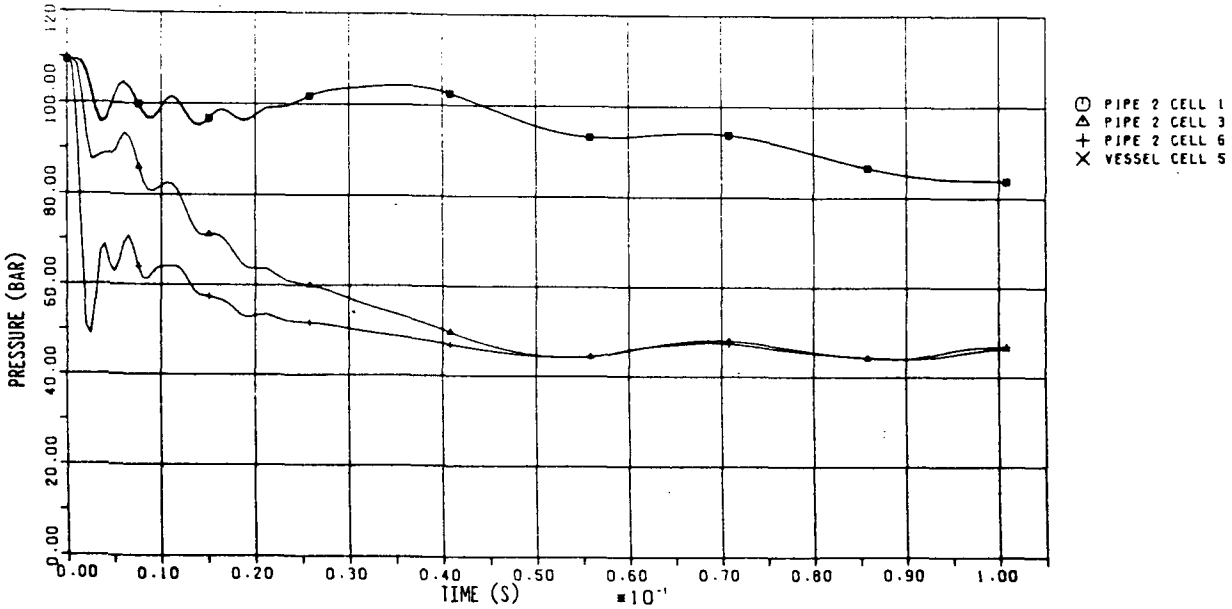

PIPE 2 - FI/VESSEL VERSION 3/AUTOMATIC VESSEL JUNCTION PRESSURE

KWU TRAC-PD2

EFFECT OF VARIOUS PARAMETERS ON THE OUTFLOW RATE

CHECK OF THE HDR TESTS WITH VESSEL COMPONENT

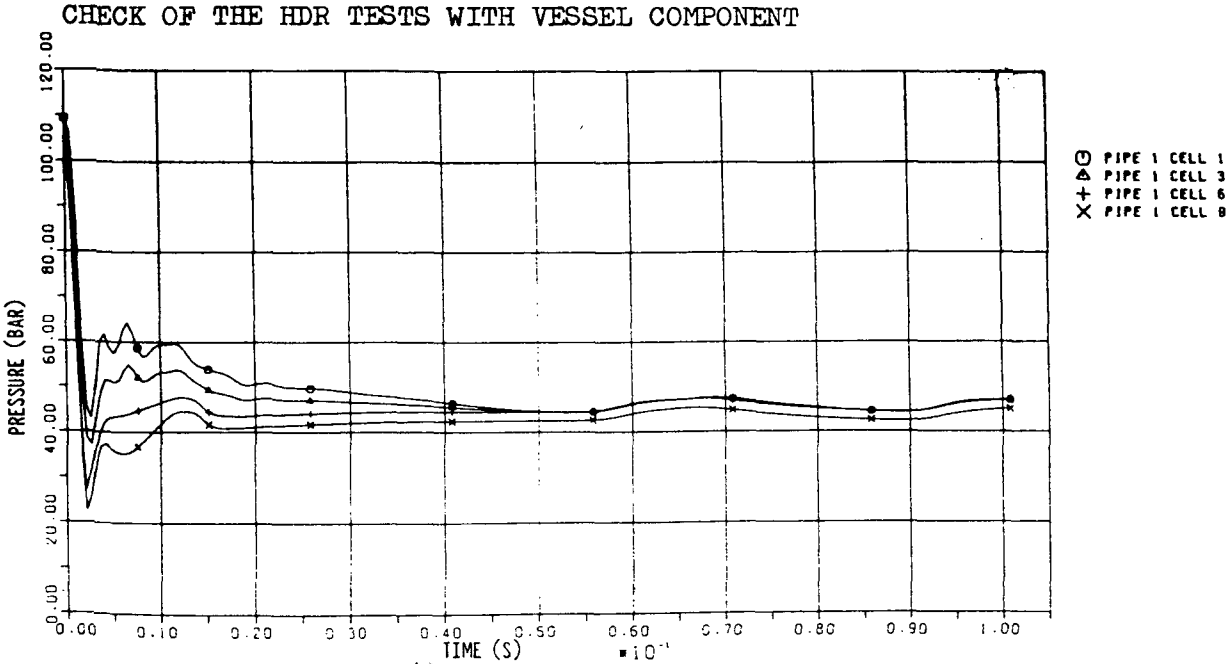

PIPE 2 - FI/VESSEL VERSION 3/AUTOMATIC VESSEL JUNCTION PRESSURE

Fig. 3.12

KWU TRAC-PD2

EFFECT OF VARIOUS PARAMETERS ON THE OUTFLOW RATE

CHECK OF THE HDR TESTS WITH VESSEL COMPONENT

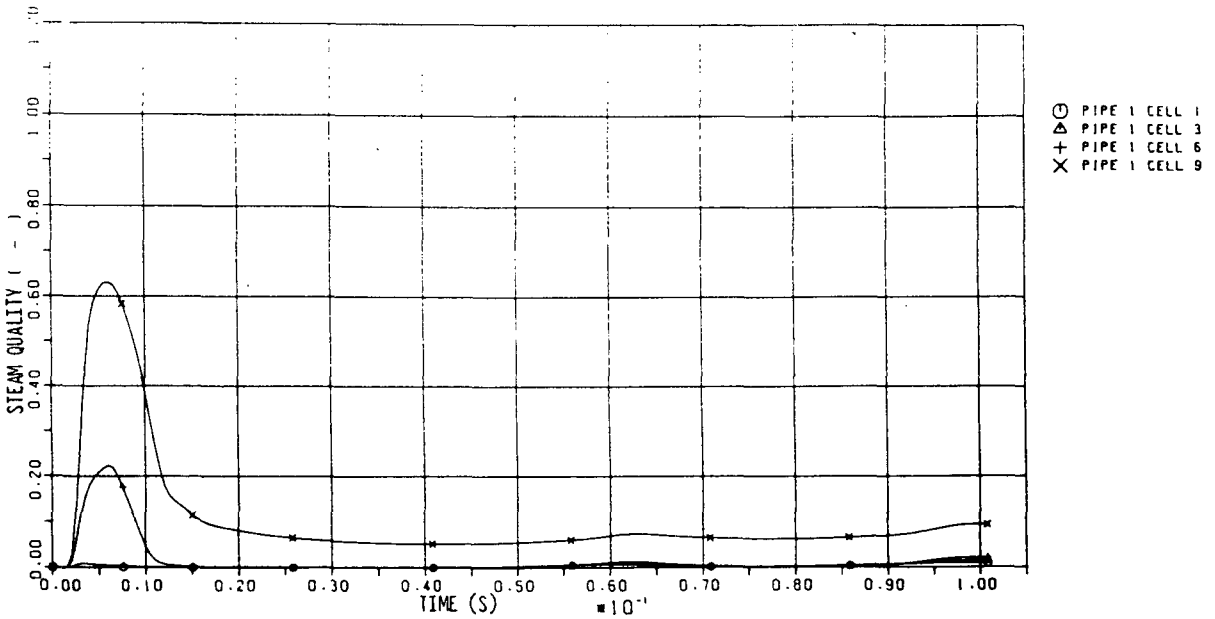

PIPE 2 - FI/VESSEL VERSION 3/AUTOMATIC VESSEL JUNCTION

STEAM QUALITY

KWU TRAC-PD2

EFFECT OF VARIOUS PARAMETERS ON THE OUTFLOW RATE

CHECK OF THE HDR TESTS WITH VESSEL COMPONENT

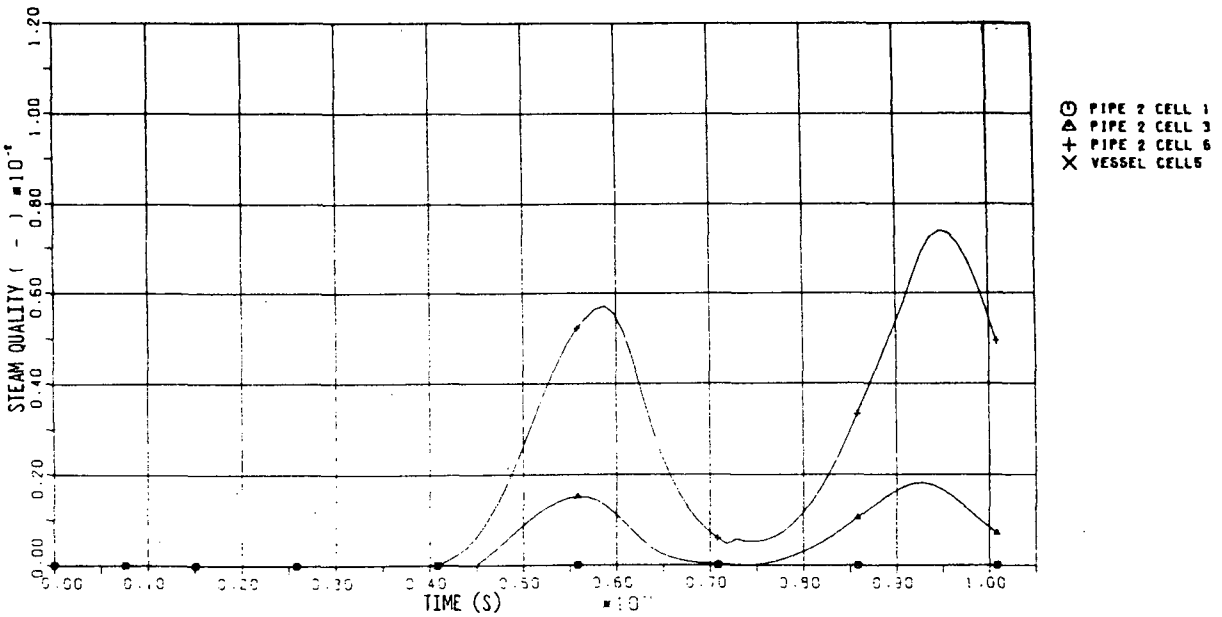

PIPE 2 - FI/VESSEL VERSION 3/AUTOMATIC VESSEL JUNCTION

STEAM QUALITY

Fig. 3.13

KWU TRAC-PD2

EFFECT OF VARIOUS PARAMETERS ON THE OUTFLOW RATE

CHECK OF THE HDR TESTS WITH VESSEL COMPONENT

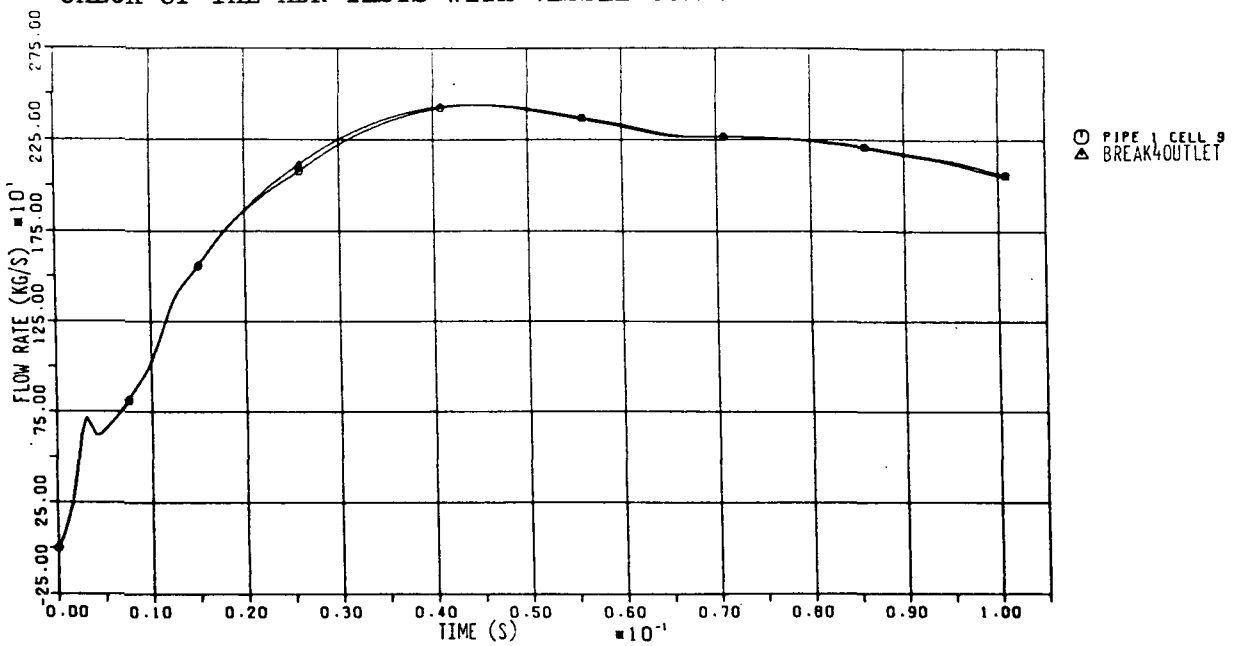

PIPE 2 - FI/VESSEL VERSION 3/AUTOMATIC VESSEL JUNCTION

FLOW RATE

KWU TRAC-PD2

EFFECT OF VARIOUS PARAMETERS ON THE OUTFLOW RATE

CHECK OF THE HDR TESTS WITH VESSEL COMPONENT

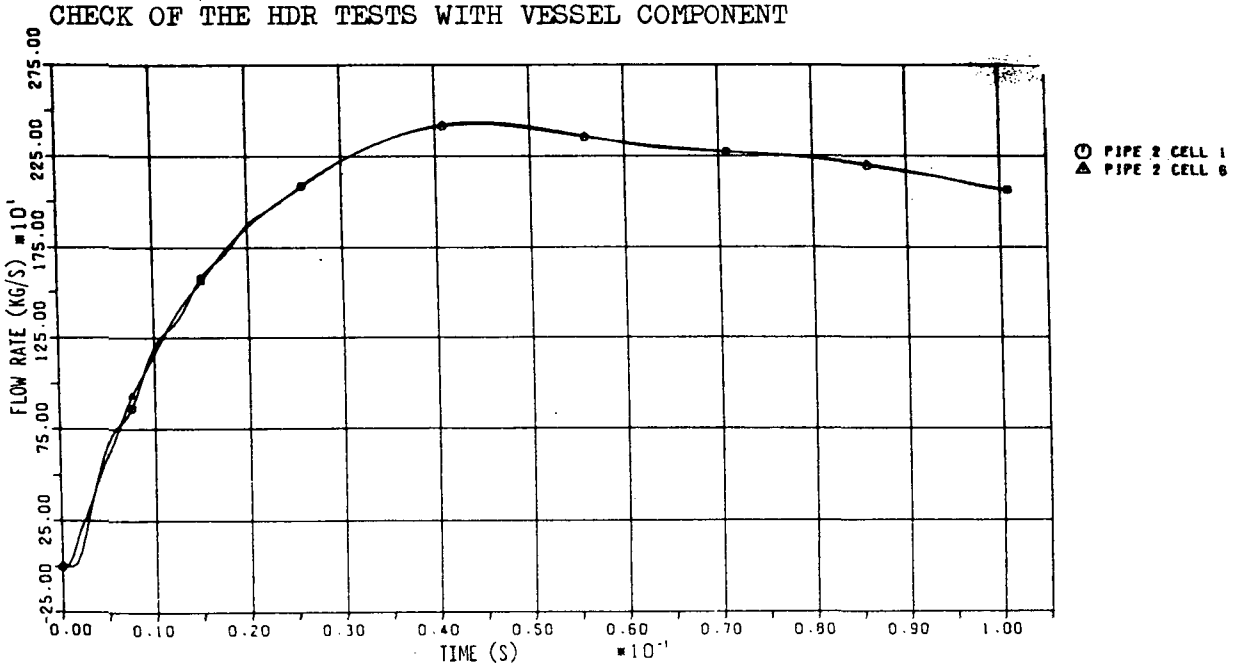

PIPE 2 - FI/VESSEL VERSION 3/AUTOMATIC VESSEL JUNCTION

FLOW RATE

Fig. 3.14

KWU TRAC-PD2

EFFECT OF VARIOUS PARAMETERS ON THE OUTFLOW RATE

CHECK OF THE HDR TESTS WITH VESSEL COMPONENT

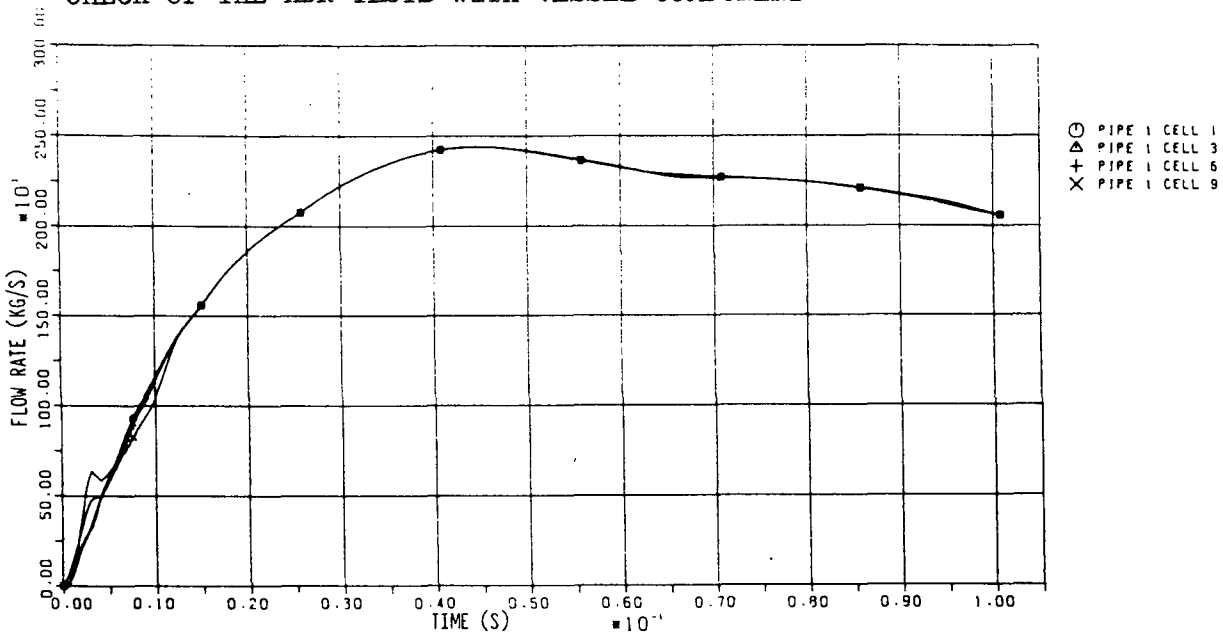

PIPE 2 - FI/VESSEL VERSION 3/AUTOMATIC VESSEL JUNCTION

FLOW RATE

Fig. 3.15

3.3 HDR3/3 Automatic Vessel Junction with Nozzle

This model (Fig. 3.16) is intended to serve for a more detailed examination of the effect of the boundary conditions on the computation results. Here, a continuous transition from the system state to the environment (BREAK) occurs, whereas in all other calculations a pressure discontinuity function is employed, which drops linearly from system pressure to 1 bar within 2 ms. For this purpose, a nozzle with an opening angle of 30° is positioned between the BREAK boundary condition and the blowdown pipe. In order to prevent the possibility of a water slug acting as a delay element in the nozzle, the nozzle is filled with steam. However, this implies that for programming reasons, an instantaneous pressure drop to 1 bar must be calculated. The time-based pressure curve thus displays a more rapid drop to saturation pressure during the first few milliseconds than in the measurement, which can be clearly seen in Fig. 3.5. On the whole, the calculated results agree best with the measured results. Firstly, due to the increased outflow velocity (in spite of an increase in steam formation), the outflow rate features an even smaller deviation from the measured value than in the case of HDR2/3; secondly, the pressure level in the blowdown nozzle is slightly raised, so that the pressure in the steady state agrees better with the measurement curve.

This is due to the realistic simulation of the free jet. Normally, this effect should be covered by the boundary conditions. In any case, the program must take these outflow conditions into account, provided these are exactly defined in physical terms. In a first approximation, a diffusor with an opening angle of 30° can be used for this purpose.

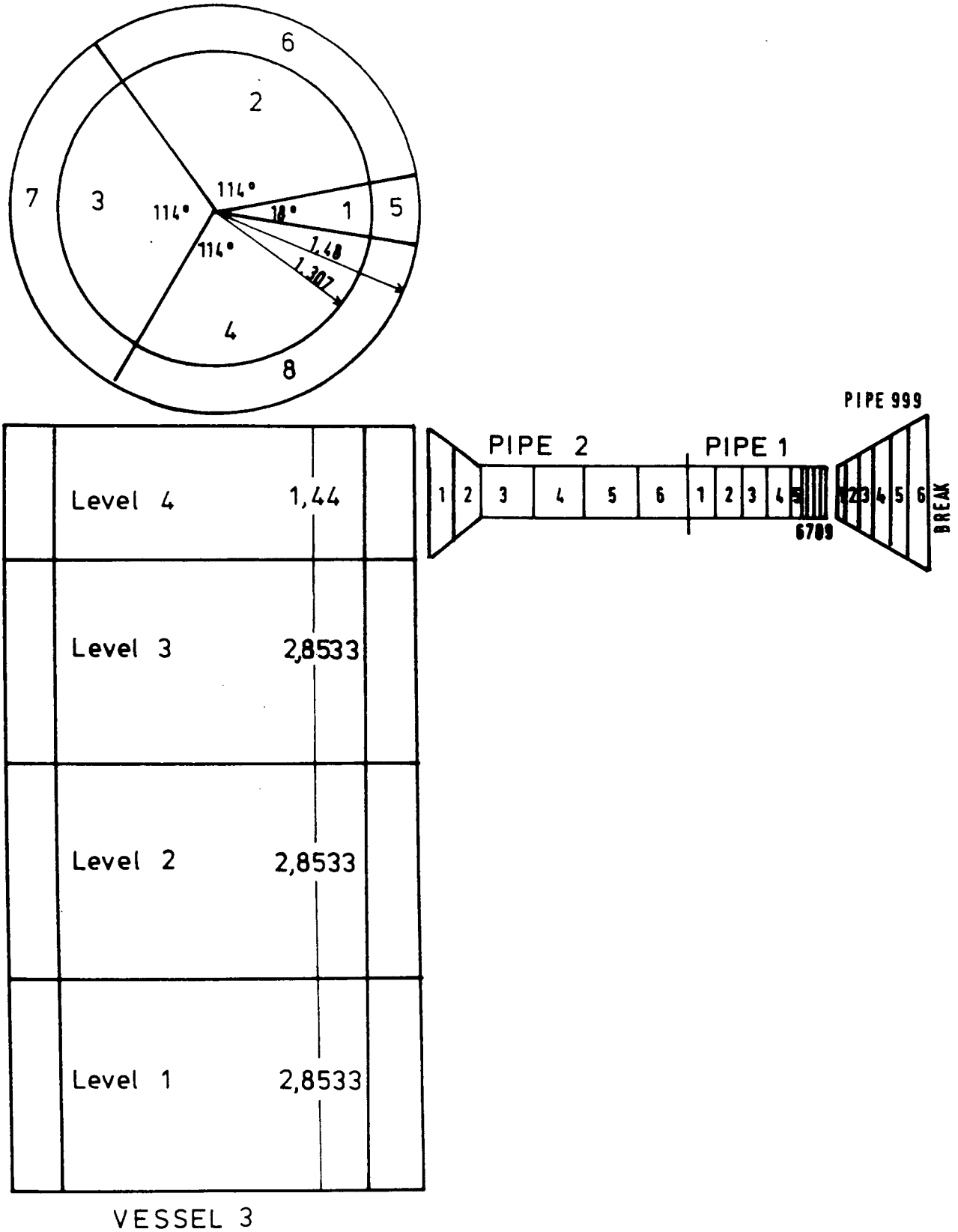

HDR 3/3

Fig. 3.16

KWU TRAC-PD2
EFFECT OF VARIOUS PARAMETERS ON THE OUTFLOW RATE
CHECK OF THE HDR TESTS WITH VESSEL COMPONENT

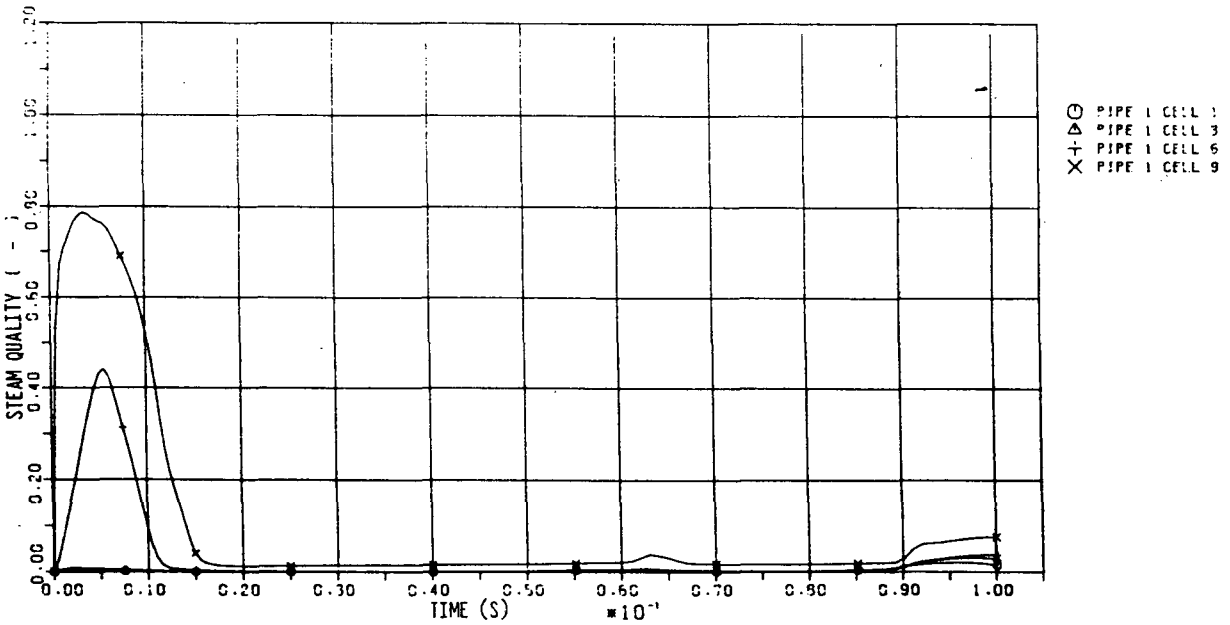

PIPE 2 - FI/VESSEL VERSION 3/AUTOMATIC VESSEL JUNCTION WITH NOZZLE
STEAM QUALITY

KWU TRAC-PD2
EFFECT OF VARIOUS PARAMETERS ON THE OUTFLOW RATE
CHECK OF THE HDR TESTS WITH COMPONENT

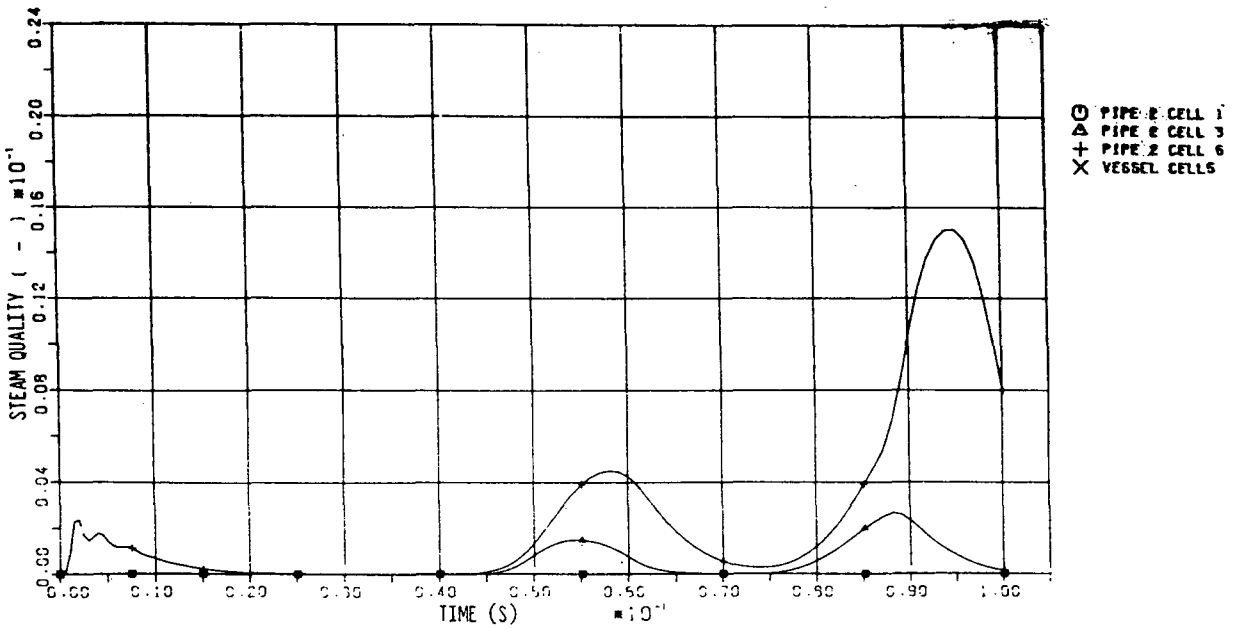

PIPE 2 - FI/VESSEL VERSION 3/AUTOMATIC VESSEL JUNCTION WITH NOZZLE
STEAM QUALITY

Fig. 3.17

KWU TRAC-PD2

EFFECT OF VARIOUS PARAMETERS ON THE OUTFLOW RATE

CHECK OF THE HDR TESTS WITH VESSEL COMPONENT

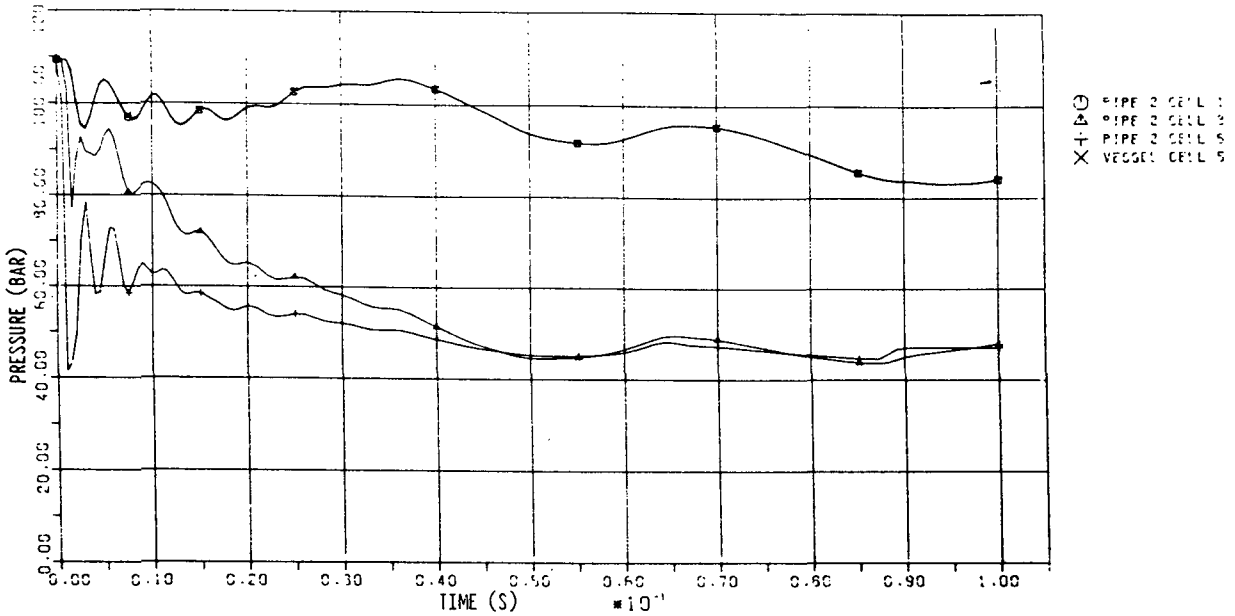

PIPE 2 - FI/VESSEL VERSION 3/AUTOMATIC VESSEL JUNCTION WITH NOZZLE PRESSURE

KWU TRAC-PD2

EFFECT OF VARIOUS PARAMETERS ON THE OUTFLOW RATE

CHECK OF THE HDR TESTS WITH VESSEL COMPONENT

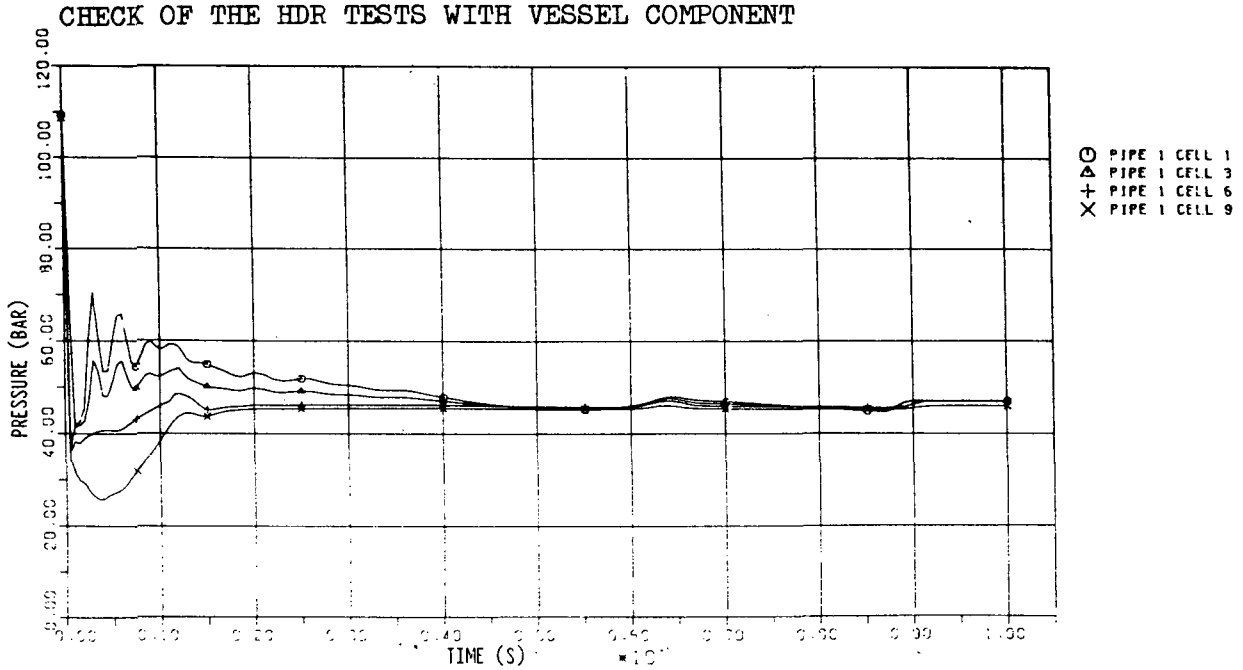

PIPE 2 - FI/VESSEL VERSION 3/AUTOMATIC VESSEL JUNCTION WITH NOZZLE PRESSURE

Fig. 3.18

KWU TRAC-PD2
EFFECT OF VARIOUS PARAMETERS ON THE OUTFLOW RATE
CHECK OF THE HDR TESTS WITH VESSEL COMPONENT

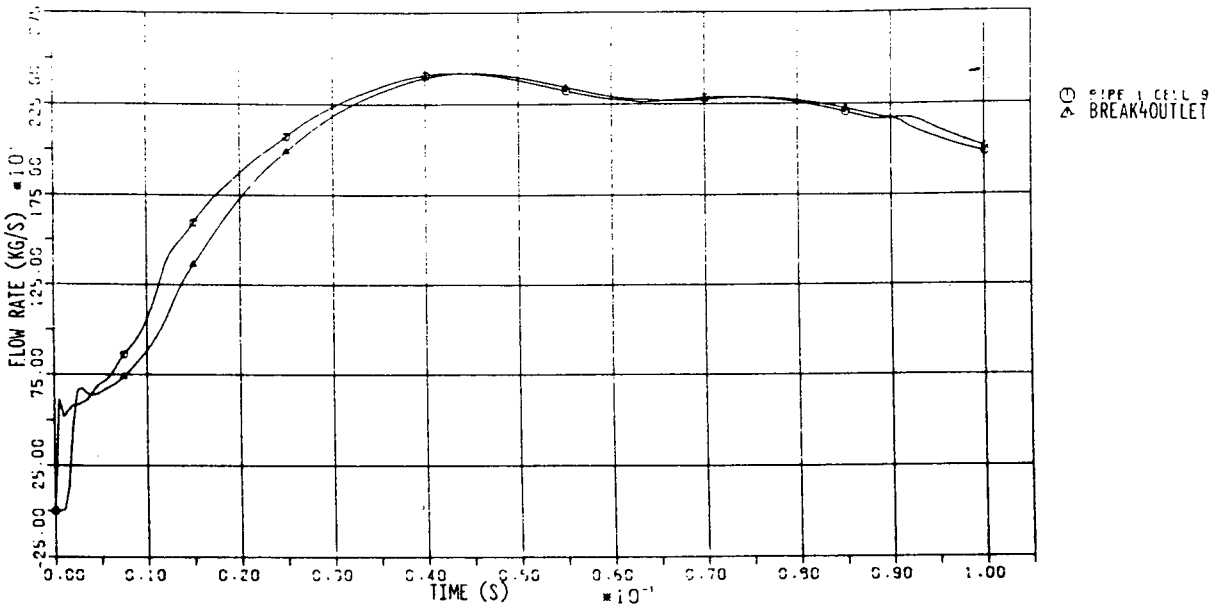

PIPE 2 - FI/VESSEL VERSION 3/AUTOMATIC VESSEL JUNCTION WITH NOZZLE
FLOW RATE

KWU TRAC-PD2
EFFECT OF VARIOUS PARAMETERS ON THE OUTFLOW RATE
CHECK OF THE HDR TESTS WITH VESSEL COMPONENT

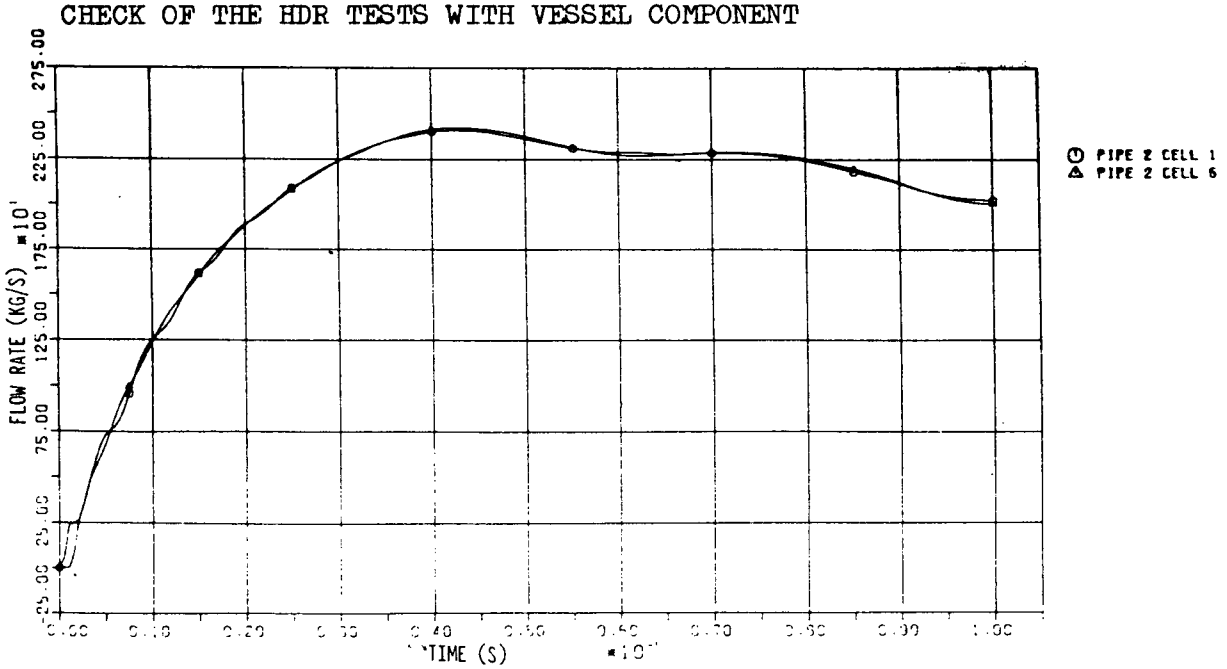

PIPE 2 - FI/VESSEL VERSION 3/AUTOMATIC VESSEL JUNCTION WITH NOZZLE
FLOW RATE

Fig. 3.19

KWU TRAC-PD2

EFFECT OF VARIOUS PARAMETERS ON THE OUTFLOW RATE

CHECK OF THE HDR TESTS WITH VESSEL COMPONENT

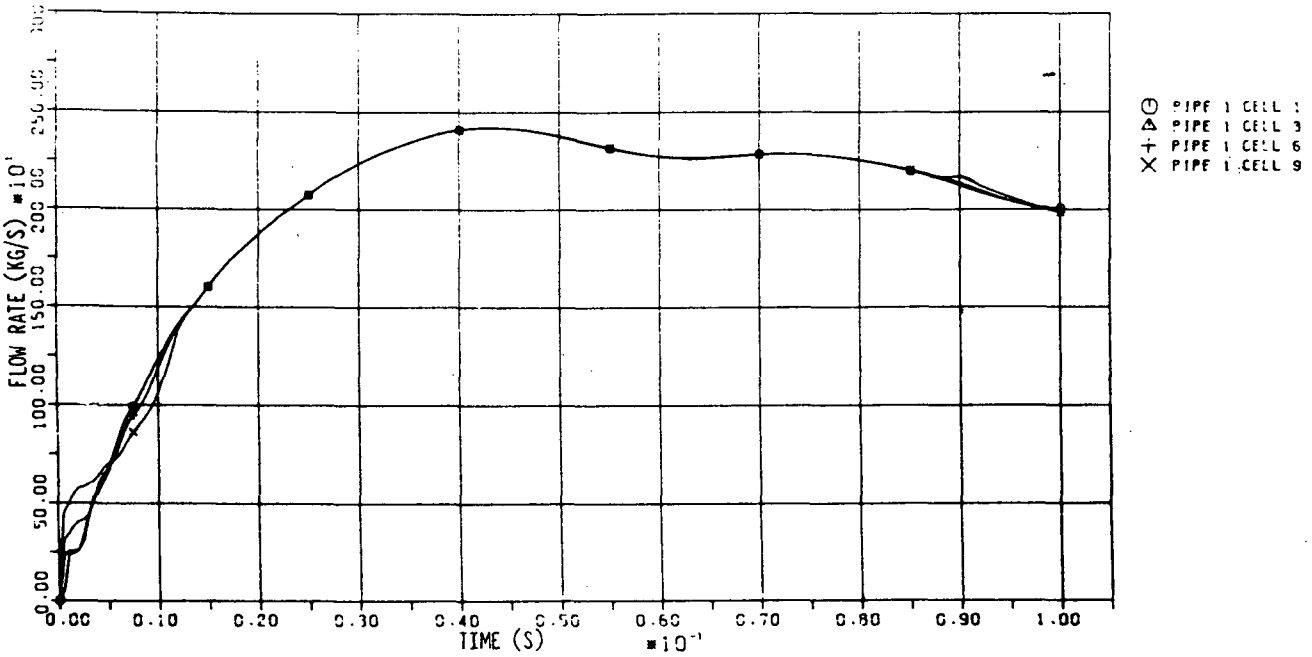

PIPE 2 - FI/VESSEL VERSION 3/AUTOMATIC VESSEL JUNCTION WITH NOZZLE FLOW RATE

Fig. 3.20

3.4 HDR4/5 Vessel Junction Area = Pipe Cross Sectional Area with Loss Coefficient

An additional vessel junction option is provided by the discretization of the vessel junction area (Fig. 3.21), so that it is in exact agreement with the pipe cross sectional area. However, this requires a great deal of discretization, which in the case of a complex installation can hardly be implemented, as the capacity of the computer is rapidly exhausted by the significant increase in the number of celles in the vessel. Furthermore, the outflow process from the RPV into the pipe is a three-dimensional flow for which a model must be produced which also represents the flow within the pipe. Within the RPV, as has already been mentioned, this is only possible with considerable difficulty; however, calculations within the pipe must always be one-dimensional, so that it is impossible to produce a complex model of the three-dimensional flow in the vessel nozzle with this program. Furthermore, due to the crude azimuthal subdivision of the RPV, the measured value obtained from the test does not coincide with the mathematical location in the program, so that a direct comparison of the curves is only possible to a limited extent.

A comparison of the curves in Figs. 3.4 and 3.5 shows that due to the increased pressure loss within the first few milliseconds, the flow curve remains below the experimental curve due to the increase in steam formation. In this case, the transition equal in area does not lead to an improvement in the result, since the loss for the outflow is not taken into consideration to a sufficient degree, in spite of ζ being given as 0.5.

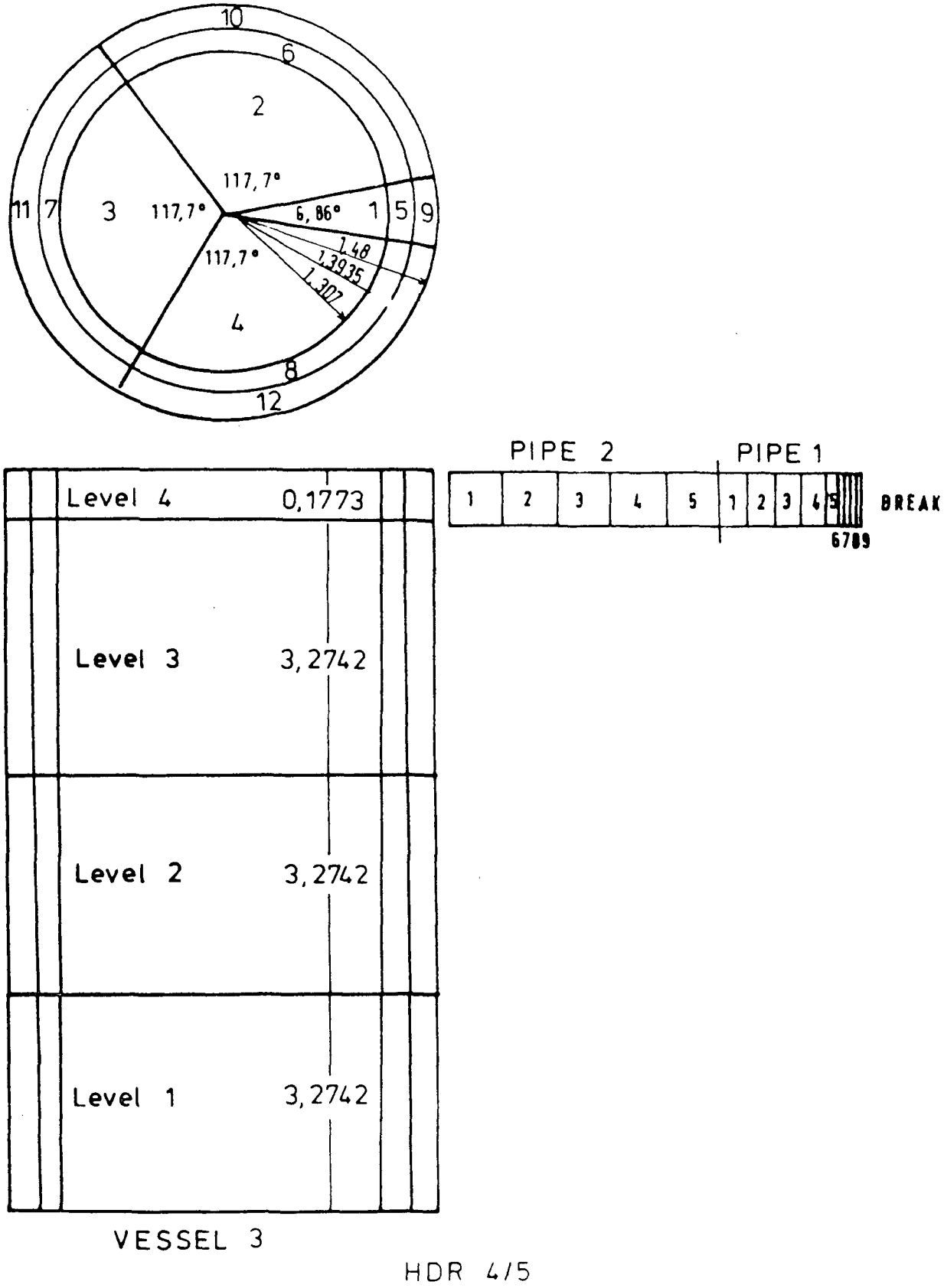

HDR 4/5

Fig. 3.21

KWU TRAC-PD2

EFFECT OF VARIOUS PARAMETERS ON THE OUTFLOW RATE

CHECK OF THE HDR TESTS WITH VESSEL COMPONENT

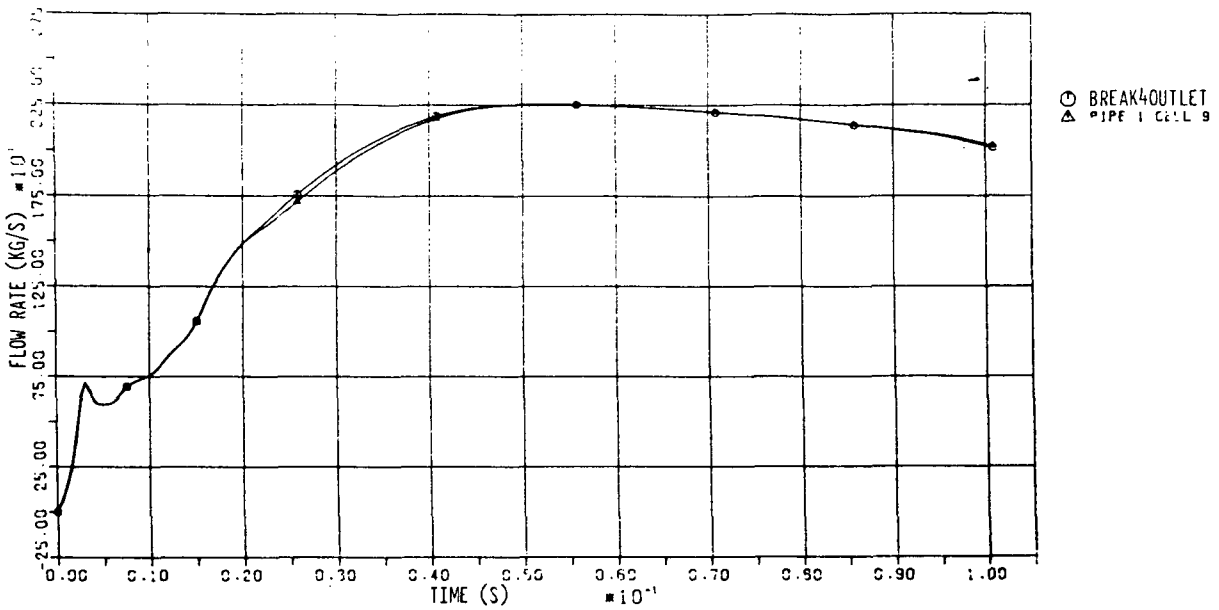

PIPE 2 - SI/VESSEL VERSION 5/ZETA (VESSEL OFF) = 0.5

FLOW RATE

KWU TRAC-PD2

EFFECT OF VARIOUS PARAMETERS ON THE OUTFLOW RATE

CHECK OF THE HDR TESTS WITH VESSEL COMPONENT

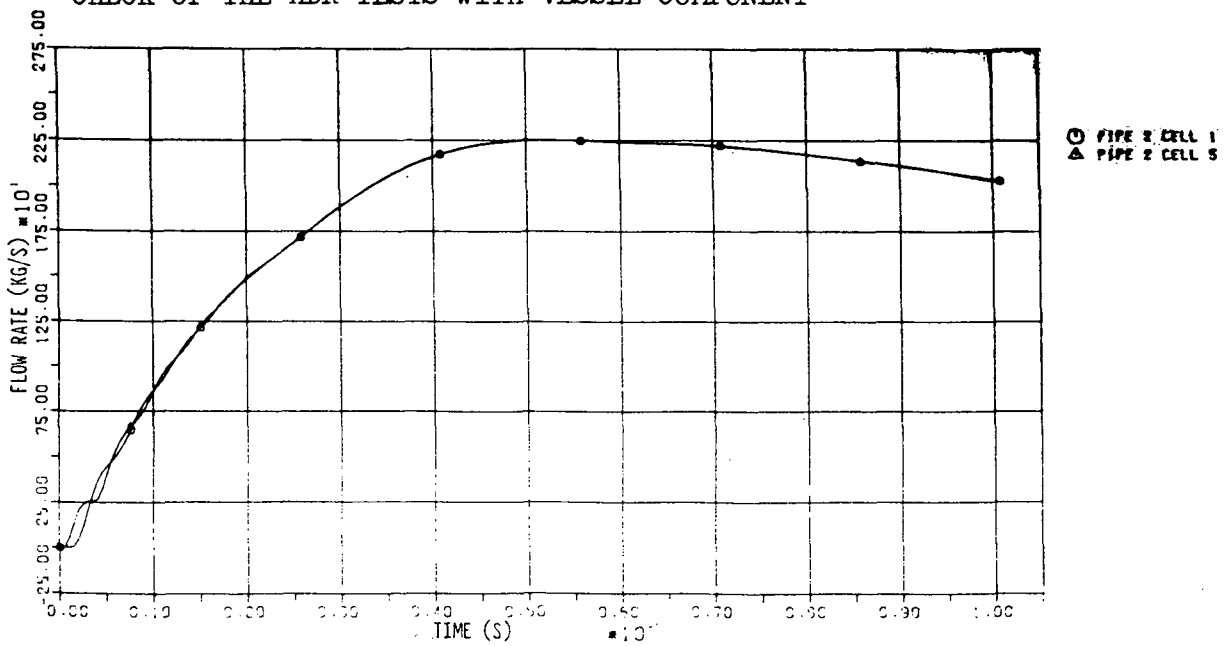

PIPE 2 - SI/VESSEL VERSION 5/ZETA (VESSEL OFF) = 0.5

FLOW RATE

Fig. 3.22

KWU TRAC-PD2

EFFECT OF VARIOUS PARAMETERS ON THE OUTFLOW RATE

CHECK OF THE HDR TESTS WITH VESSEL COMPONENT

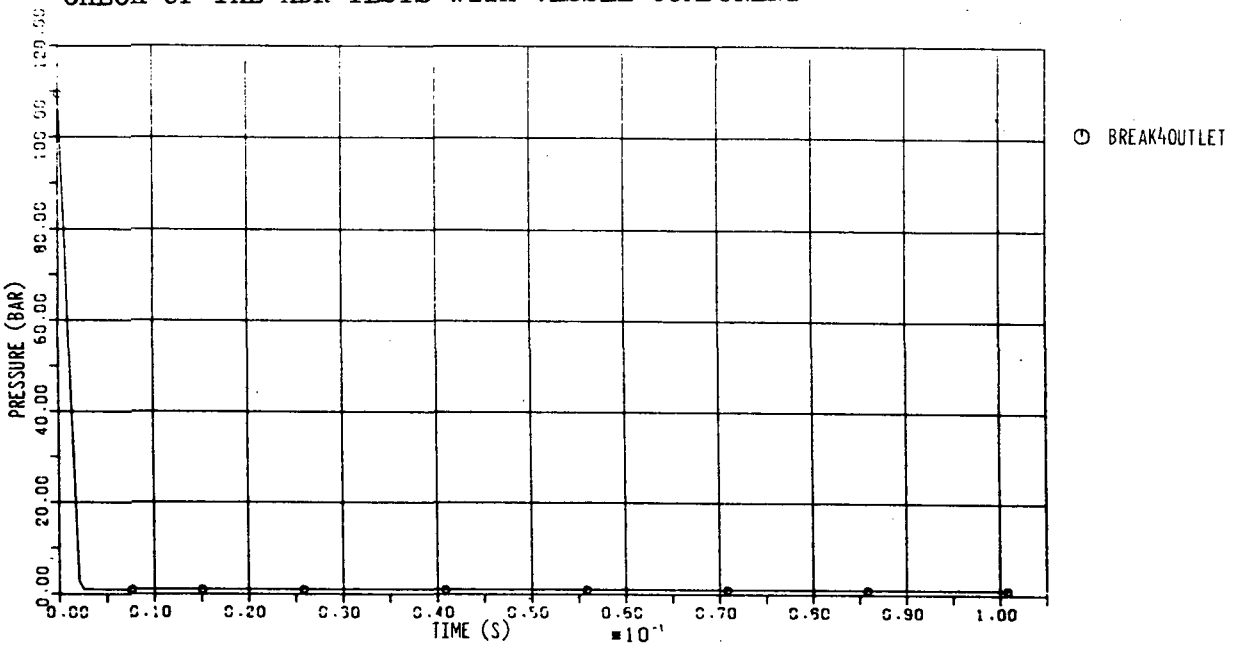

PIPE 2 - SI/VESSEL VERSION 5/ZETA (VESSEL OFF) = 0.5

PRESSURE

KWU TRAC-PD2

EFFECT OF VARIOUS PARAMETERS ON THE OUTFLOW RATE

CHECK OF THE HDR TESTS WITH VESSEL COMPONENT

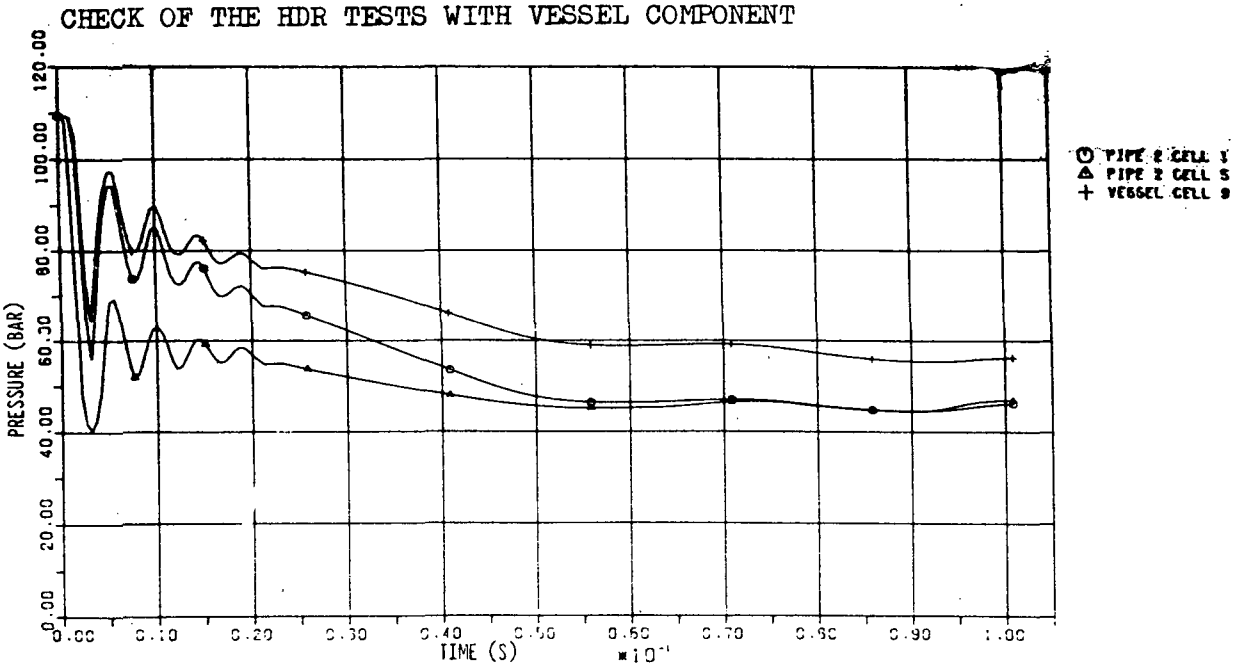

PIPE 2 - SI/VESSEL VERSION 5/ZETA (VESSEL OFF) = 0.5

PRESSURE

Fig. 2.23

KWU TRAC-PD2

EFFECT OF VARIOUS PARAMETERS ON THE OUTFLOW RATE

CHECK OF THE HDR TESTS WITH VESSEL COMPONENT

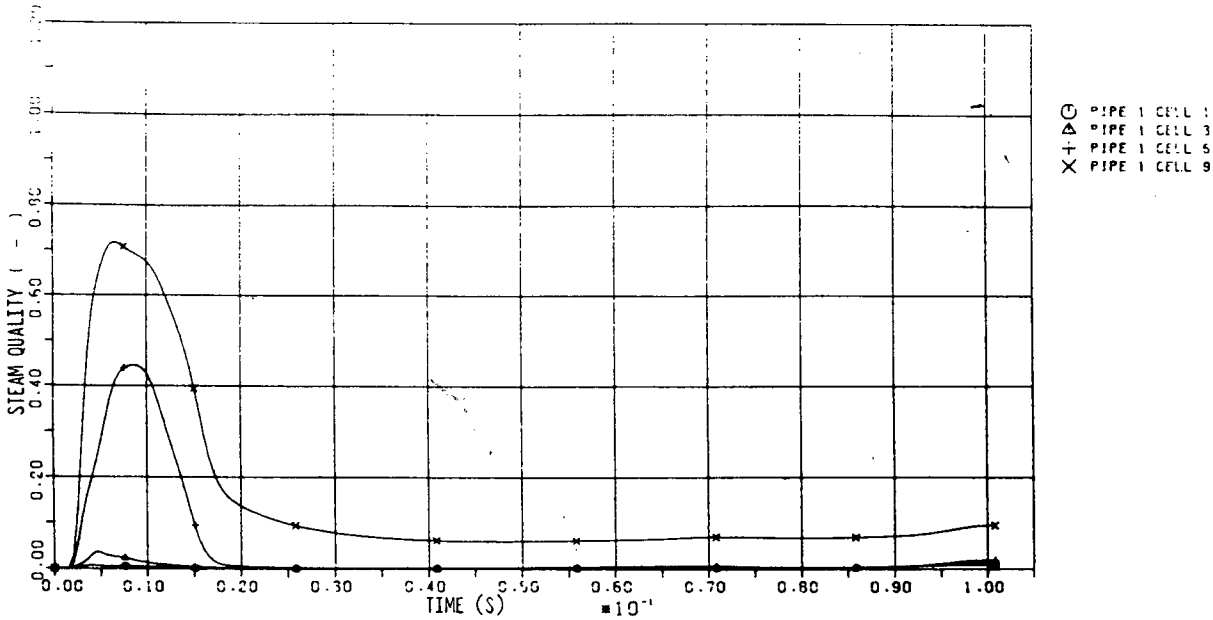

PIPE 2 - SI/VESSEL VERSION 5/ZETA (VESSEL OFF) = 0.5

STEAM QUALITY

KWU TRAC-PD2

EFFECT OF VARIOUS PARAMETERS ON THE OUTFLOW RATE

CHECK OF THE HDR TESTS WITH VESSEL COMPONENT

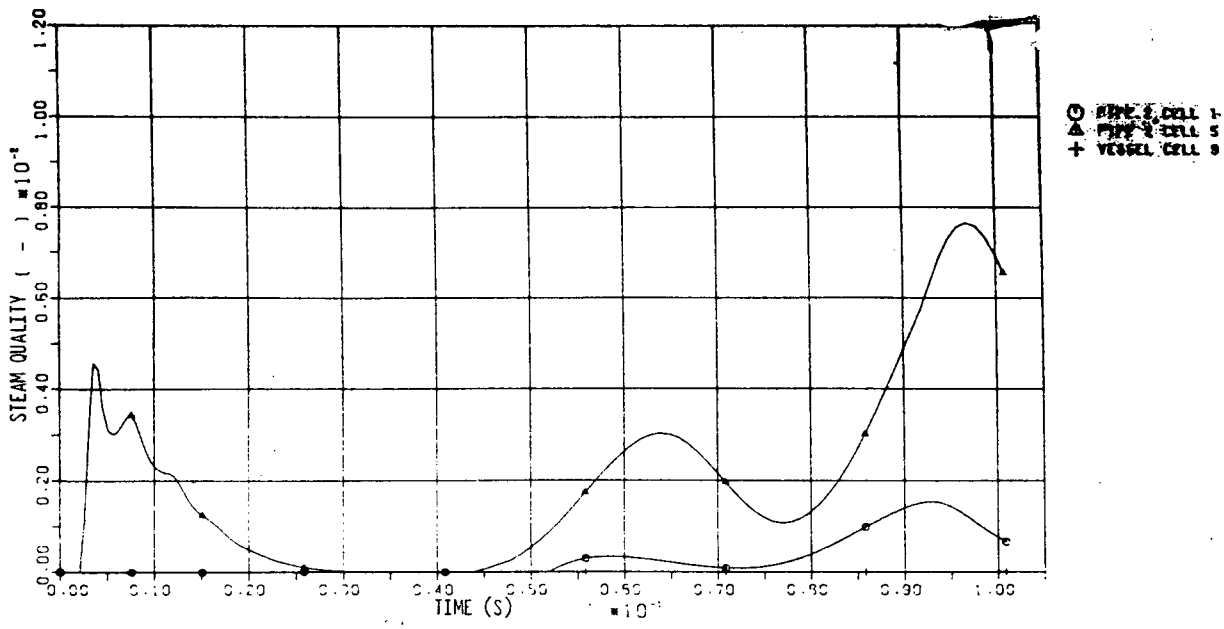

PIPE 2 - SI/VESSEL VERSION 5/ZETA (VESSEL OFF) = 0.5

STEAM QUALITY

Fig. 3.24

KWU TRAC-PD2

EFFECT OF VARIOUS PARAMETERS ON THE OUTFLOW RATE

CHECK OF THE HDR TESTS WITH VESSEL COMPONENT

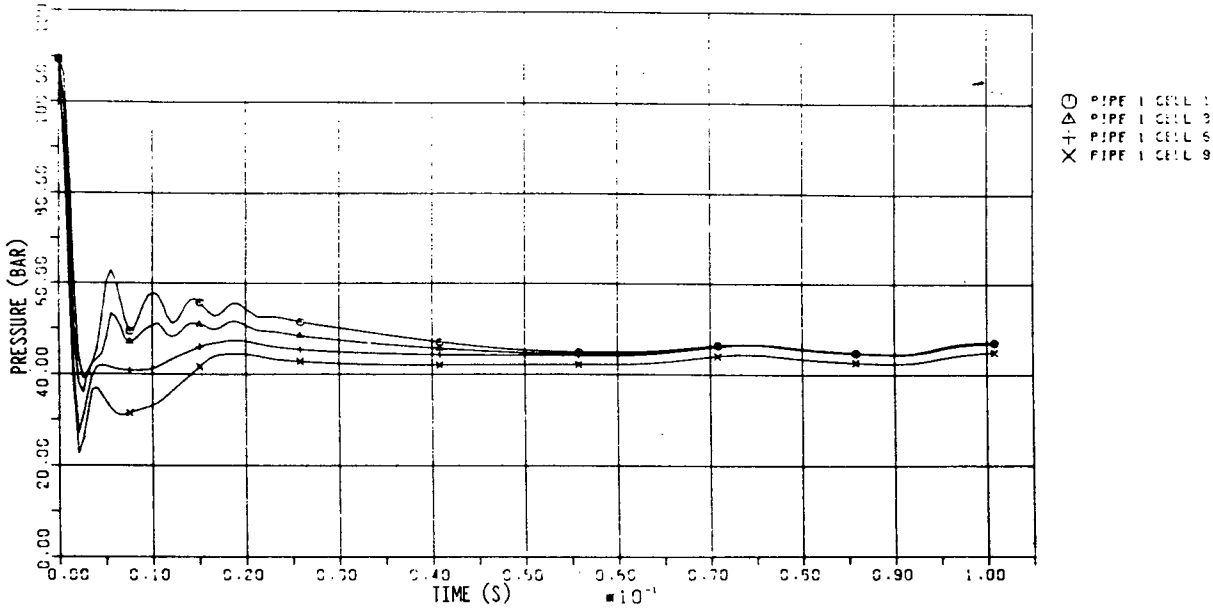

PIPE 2 - SI/VESSEL VERSION 5/ZETA (VESSEL OFF) = 0.5

PRESSURE

KWU TRAC-PD2

EFFECT OF VARIOUS PARAMETERS ON THE OUTFLOW RATE

CHECK OF THE HDR TESTS WITH VESSEL COMPONENT

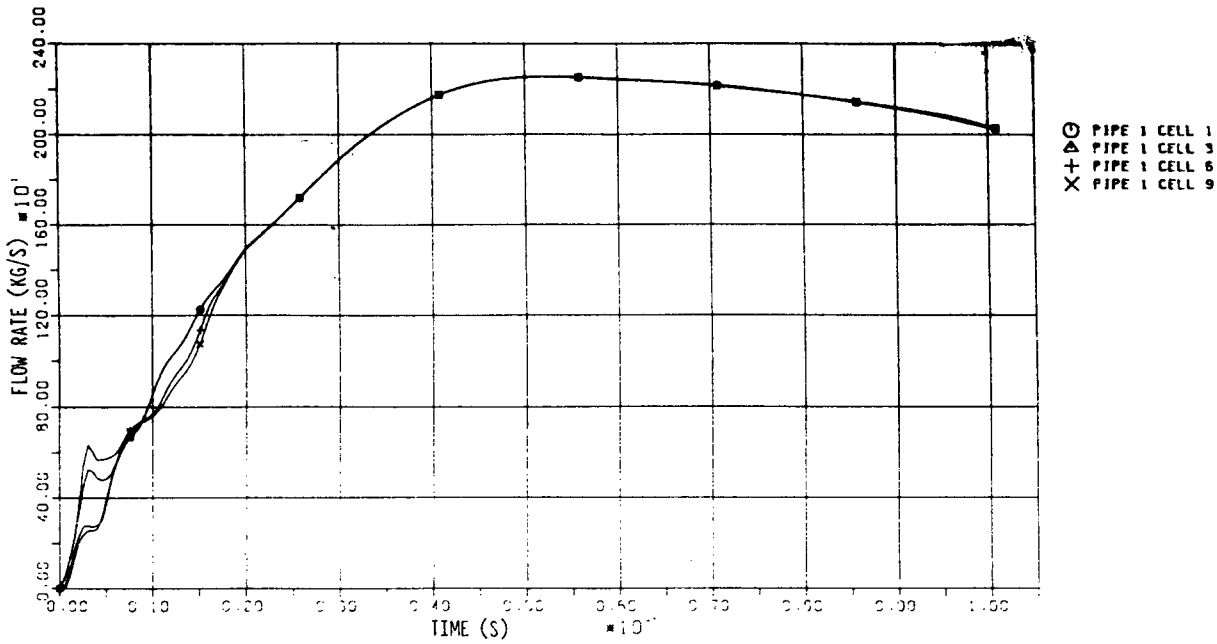

PIPE 2 - SI/VESSEL VERSION 5/ZETA (VESSEL OFF) = 0.5

FLOW RATE

Fig. 3.25

3.5 HDR5/4 HDR4/5 without ζ

The difference between this calculation and the last calculation in subsection 3.4 lies in the reduced model of the downcomer, consisting of a single annulus compared to 2 annuli in the HDR4/5 and HDR6/5 calculations. It can be seen from Fig. 3.4 that the calculated time-based mass flow curve deviates by more than 40 % from the measurement. This calculation shows quite clearly that this discretization leads to a different pressure profile and thus also to a different velocity profile in the downcomer, which in turn effects a higher outflow rate. It is thus evident that with an increasing number of annuli in the RPV downcomer and equal surface area ratios in the nozzle area, closer agreement of the mathematical results with the measurements is achieved.

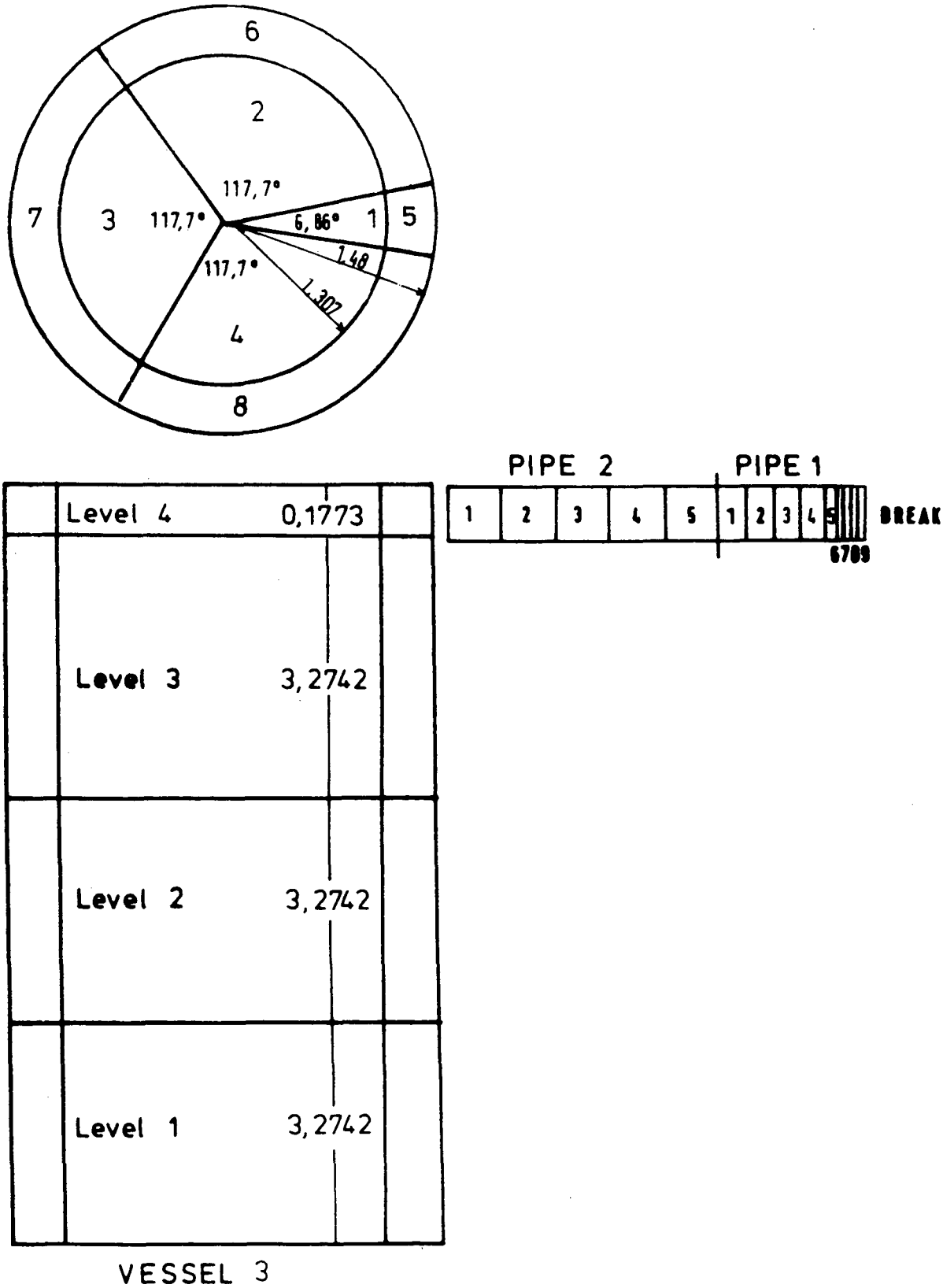

HDR 5/4

Fig. 3.26

KWU TRAC-PD2

EFFECT OF VARIOUS PARAMETERS ON THE OUTFLOW RATE

CHECK OF THE HDR TESTS WITH VESSEL COMPONENT

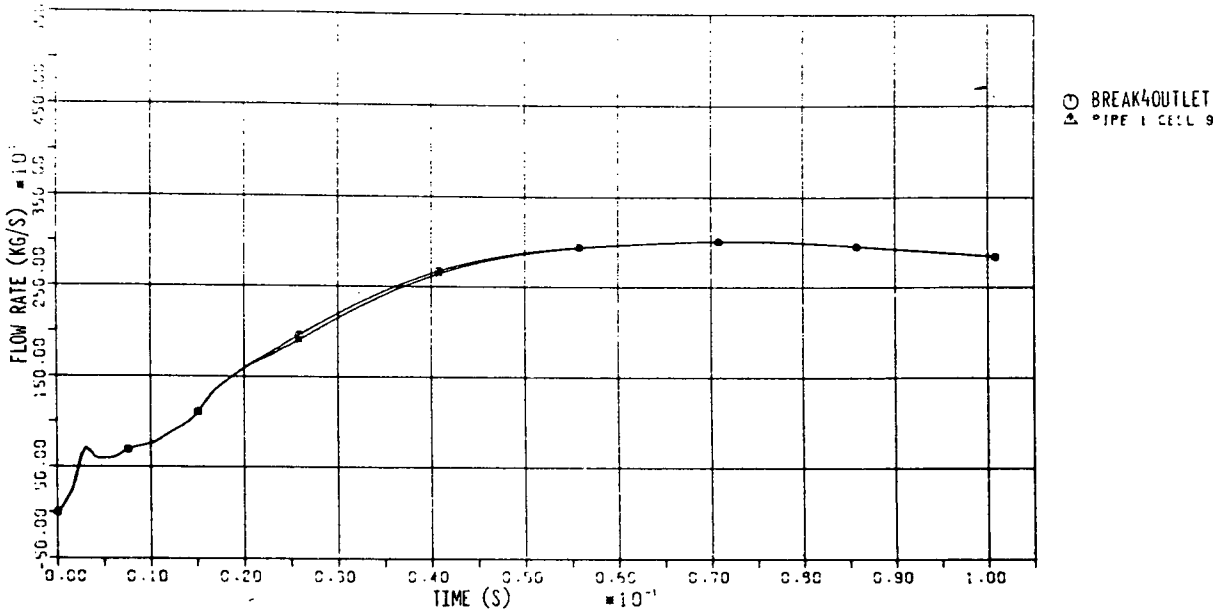

PIPE 2 - SEMI-IMPLICIT/VESSEL VERSION 4

FLOW RATE

KWU TRAC-PD2

EFFECT OF VARIOUS PARAMETERS ON THE OUTFLOW RATE

CHECK OF THE HDR TESTS WITH VESSEL COMPONENT

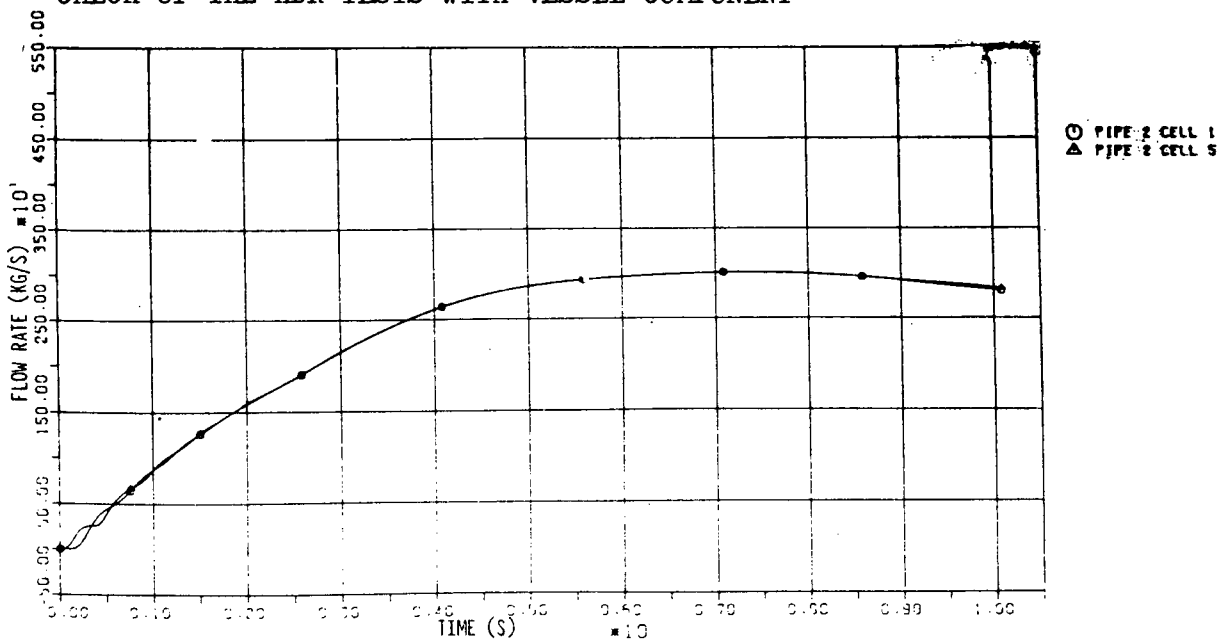

PIPE 2 - SEMI-IMPLICIT/VESSEL VERSION 4

FLOW RATE

Fig. 3.27

KWU TRAC-PD2
EFFECT OF VARIOUS PARAMETERS ON THE OUTFLOW RATE
CHECK OF THE HDR TESTS WITH VESSEL COMPONENT

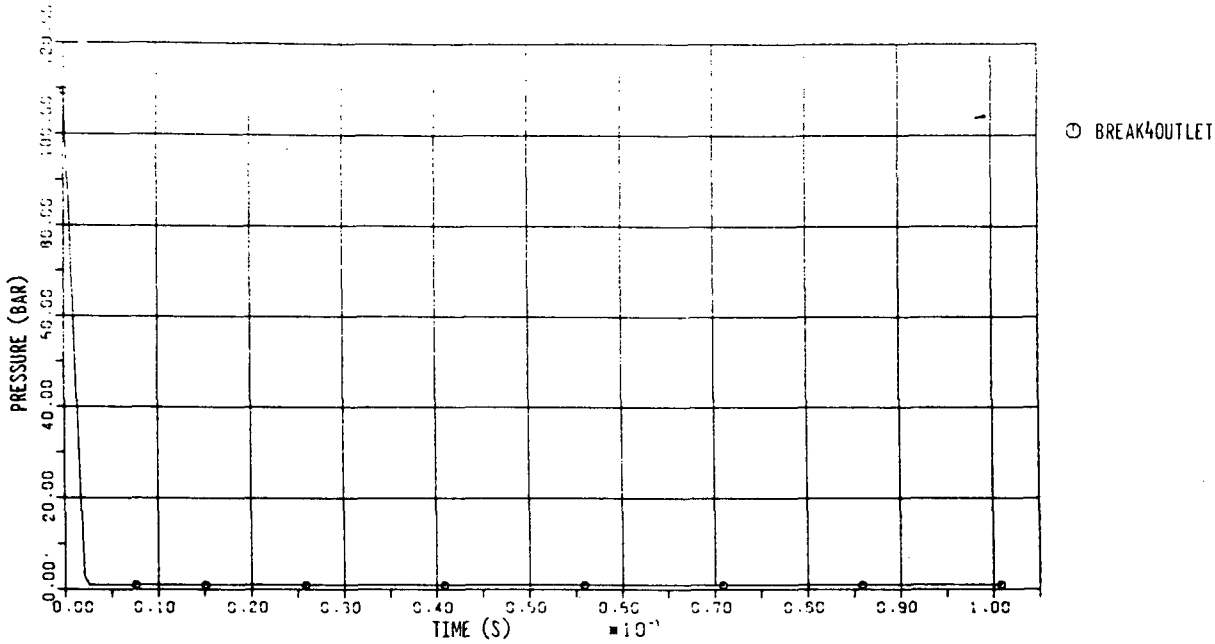

PIPE 2 - SEMI-IMPLICIT/VESSEL VERSION 4
PRESSURE

KWU TRAC-PD2
EFFECT OF VARIOUS PARAMETERS ON THE OUTFLOW RATE
CHECK OF THE HDR TESTS WITH VESSEL COMPONENT

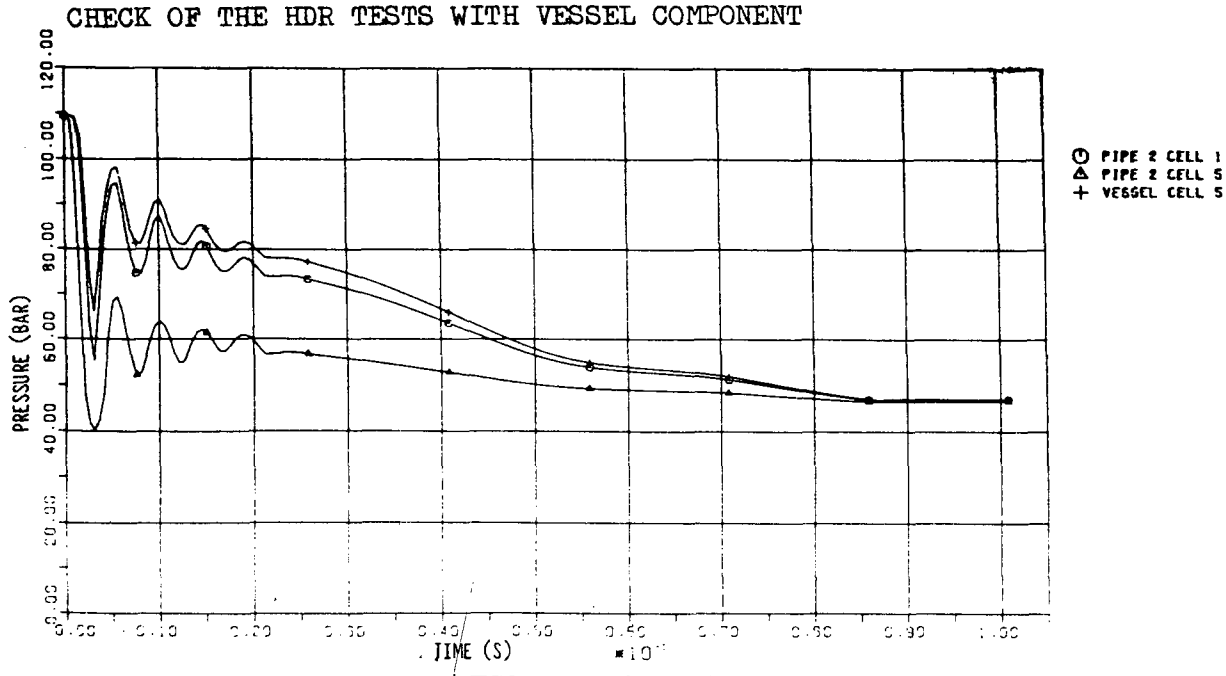

PIPE 2 - SEMI-IMPLICIT/VESSEL VERSION 4
PRESSURE

Fig. 3.28

KWU TRAC-PD2
EFFECT OF VARIOUS PARAMETERS ON THE OUTFLOW RATE
CHECK OF THE HDR TESTS WITH VESSEL COMPONENT

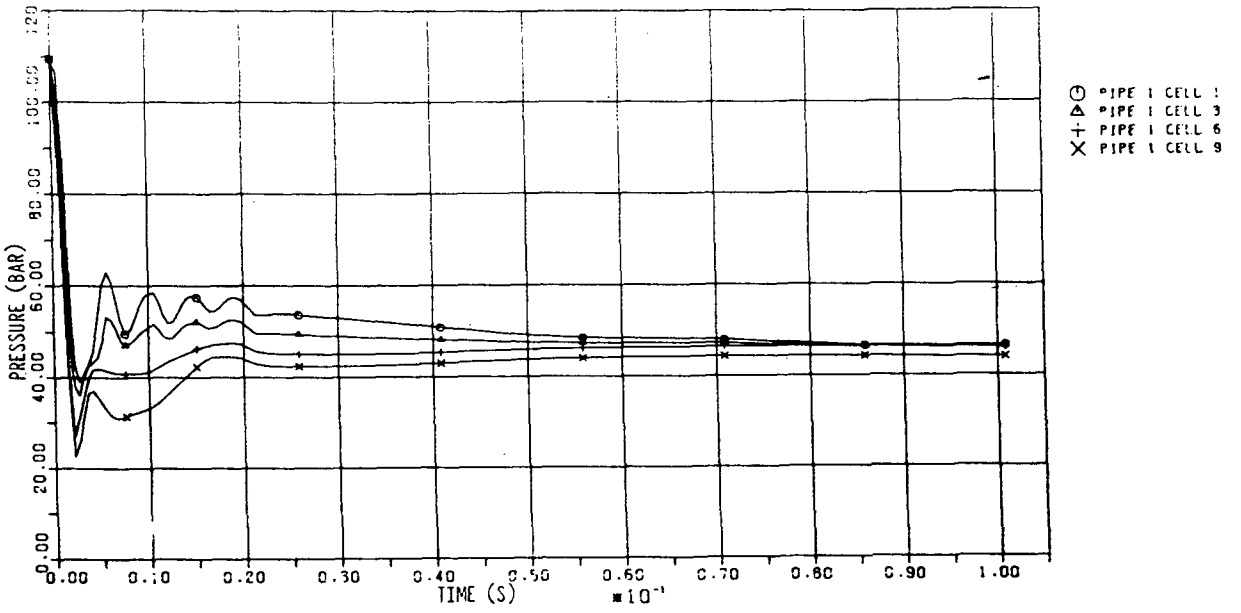

PIPE 2 - SEMI-IMPLICIT/VESSEL VERSION 4
PRESSURE

KWU TRAC-PD2
EFFECT OF VARIOUS PARAMETERS ON THE OUTFLOW RATE
CHECK OF THE HDR TESTS WITH VESSEL COMPONENT

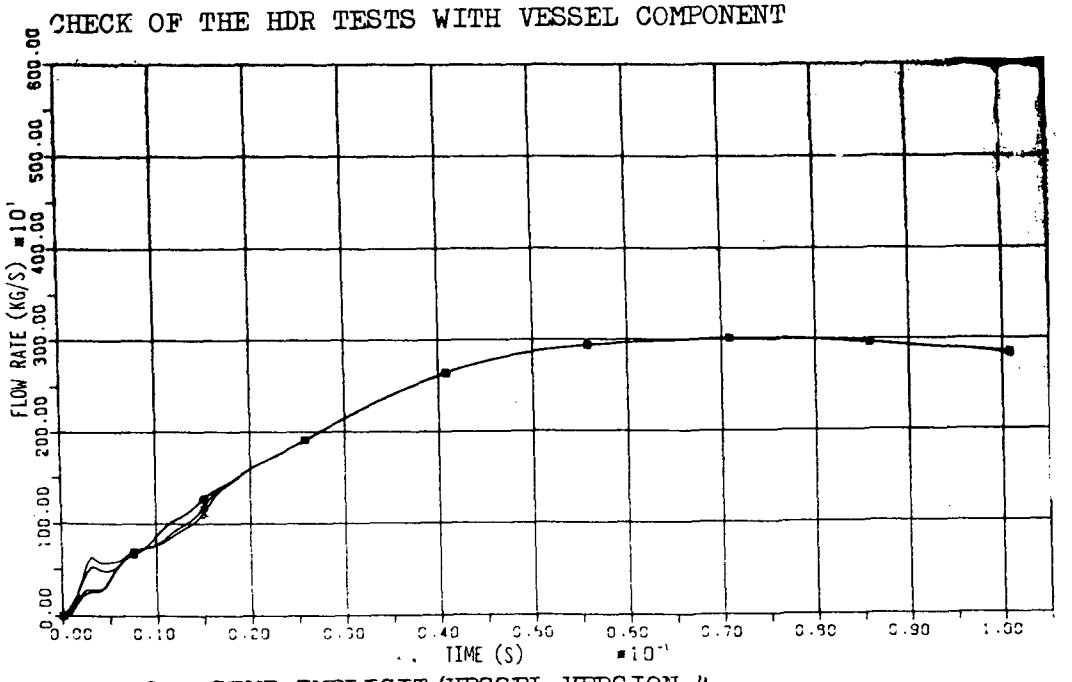

PIPE 2 - SEMI-IMPLICIT/VESSEL VERSION 4
FLOW RATE

Fig. 3.29

KWU TRAC-PD2
EFFECT OF VARIOUS PARAMETERS ON THE OUTFLOW RATE
CHECK OF THE HDR TESTS WITH VESSEL COMPONENT

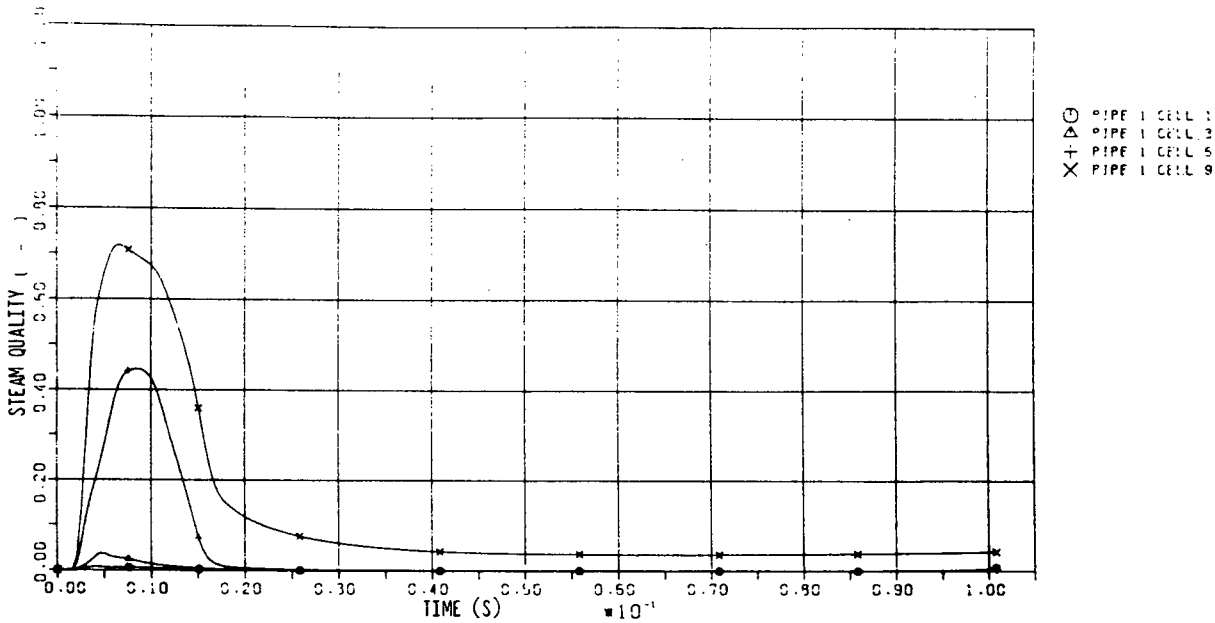

PIPE 2 - SEMI-IMPLICIT/VESSEL VERSION 4
STEAM QUALITY

KWU TRAC-PD2
EFFECT OF VARIOUS PARAMETERS ON THE OUTFLOW RATE
CHECK OF THE HDR TESTS WITH VESSEL COMPONENT

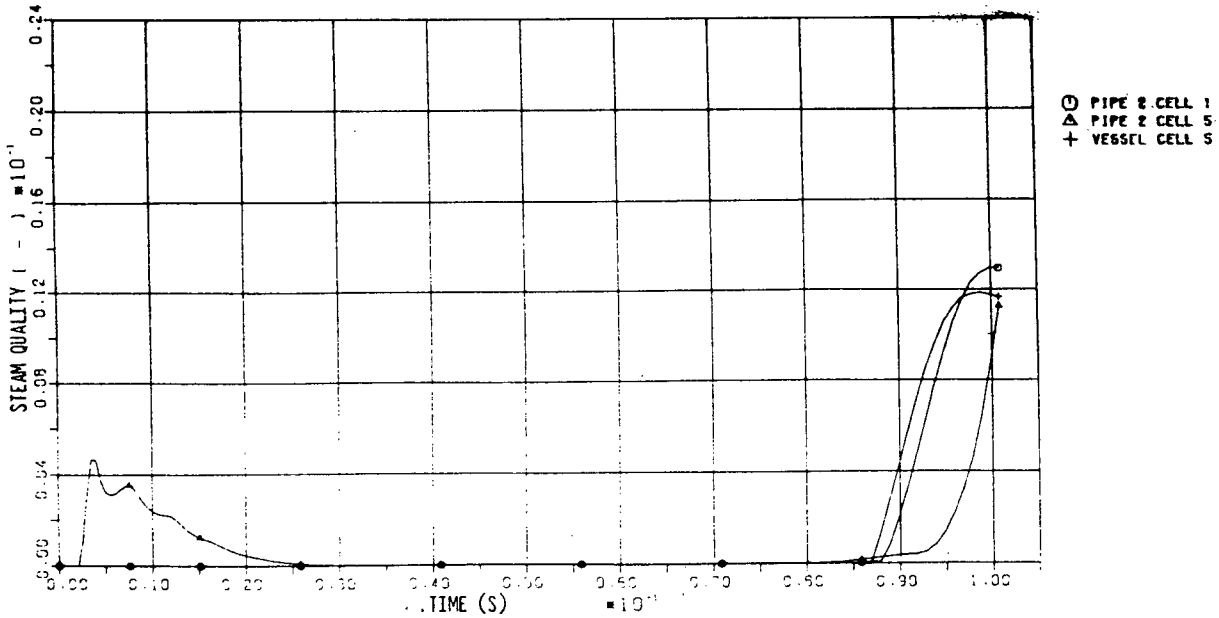

PIPE 2 - SEMI-IMPLICIT/VESSEL VERSION 4
STEAM QUALITY

Fig. 3.30

3.6 HDR6/5 HDR4/5 with Bypass in Blowdown Nozzle

This calculation is basically identical with HDR4/5. However, in this case, the bypass to the blowdown nozzle is modelled, which is used in the experimental set-up for setting a uniform temperature distribution within the nozzle.
In view of the measurement curves, the question remained as to whether the liquid present in the bypass might prevent flashing in the nozzle within the initial 10 to 20 ms, thus increasing the outflow rate. This assumption could be confirmed by the calculation as a trend; however, the effect on the mathematical results is marginal. It was assumed, however, that the valve in the bypass is closed, so that only liquid from the dead end can flow into the blowdown nozzle.

The drop of the outflow rate to zero after 3 ms can be clearly seen in Fig. 3.4. None of the post-test-calculations has produced results which have even approximated this behaviour. This is probably due to the rupture opening not being included with a sufficient degree of accuracy. After the rupture disc has been destroyed, a certain amount of time is required to blow it out of the pipe. During this time, however, the first decompression wave is reflected from the HDR inlet and hits the disc still located in the pipe.

The outflow rate is thus reduced to zero and subsequently rises again with an increased gradient. This process could be clarified, by using for instance the PISCES-2DELK-program.

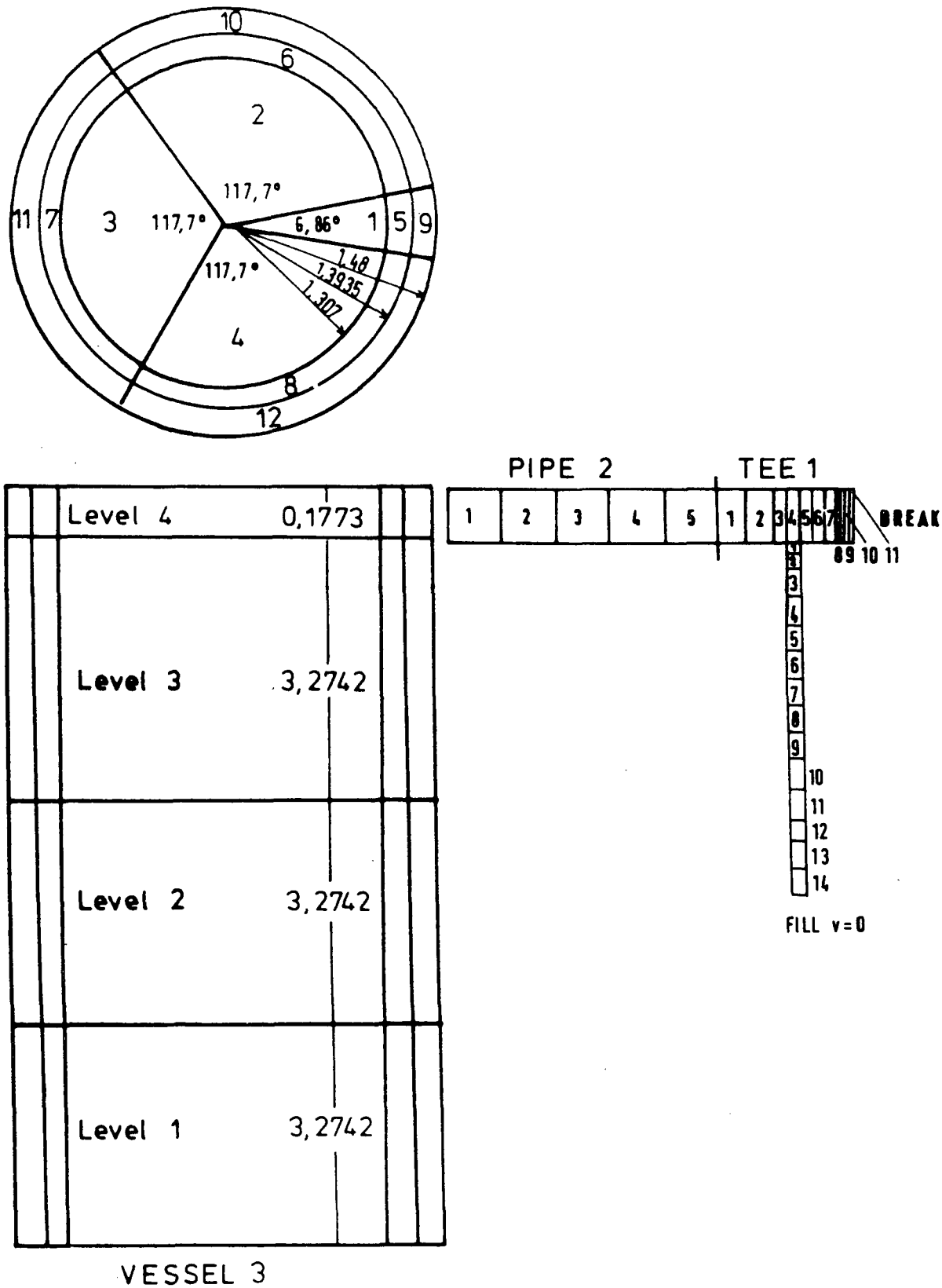
10
6
2
117,7°
11
7
3
117,7°
6,86°
1
5
9
117,7°
1,48
1,3935
1,307
4
8
12
PIPE 2
TEE 1
Level 4
0,1773
1
2
3
4
5
1
2
3
4
5
6
7
BREAK
8 9 10 11
Level 3
3,2742
3
4
5
6
7
8
9
10
11
12
13
14
Level 2
3,2742
FILL v=0
Level 1
3,2742
VESSEL 3
HDR 6/5

Fig. 3.31

KWU TRAC-PD2
EFFECT OF VARIOUS PARAMETERS ON THE OUTFLOW RATE
CHECK OF THE HDR TESTS WITH VESSEL COMPONENT

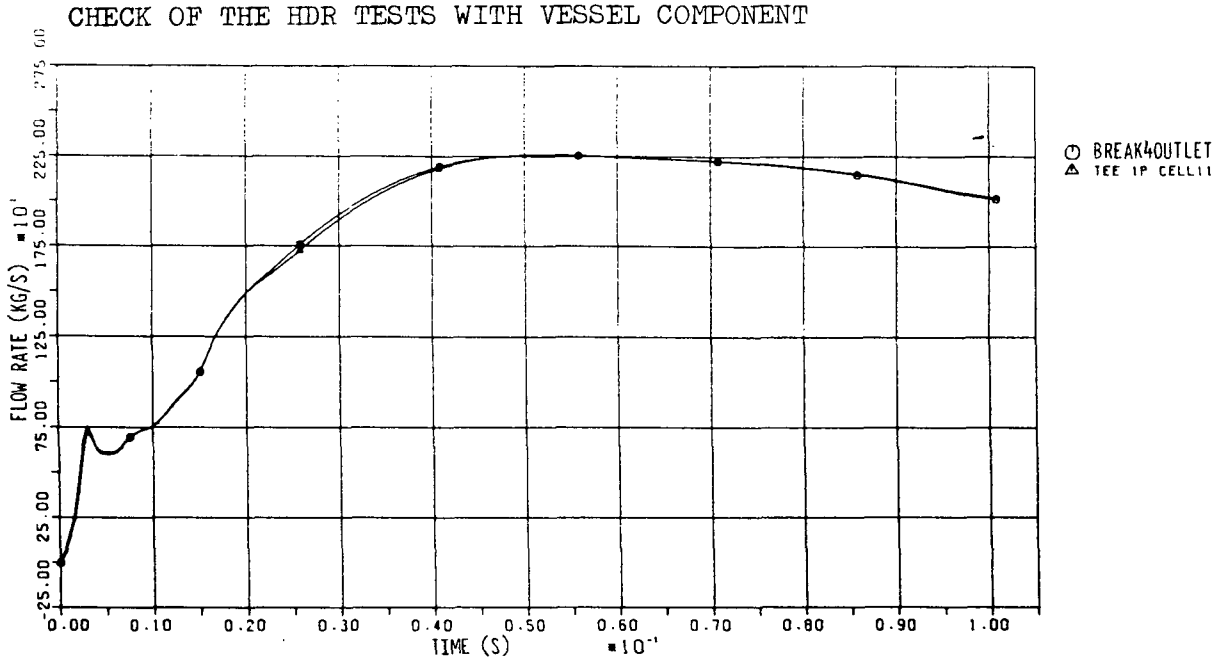

PIPE 2 - SI/VESSEL VERSION 5/ZETA (VESSEL OFF) = 0.5 WITH BYPASS FLOW RATE

KWU TRAC-PD2
EFFECT OF VARIOUS PARAMETERS ON THE OUTFLOW RATE
CHECK OF THE HDR TESTS WITH VESSEL COMPONENT

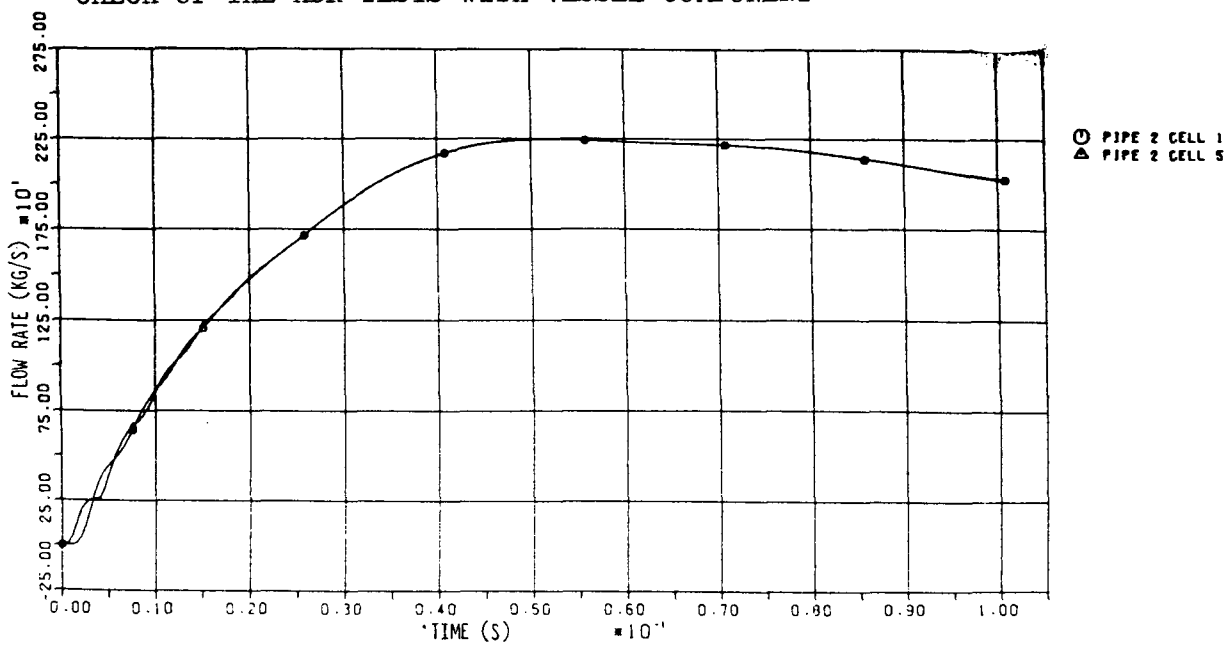

PIPE 2 - SI/VESSEL VERSION 5/ZETA (VESSEL OFF) = 0.5 WITH BYPASS FLOW RATE

Fig. 3.32

KWU TRAC-PD2
EFFECT OF VARIOUS PARAMETERS ON THE OUTFLOW RATE
CHECK OF THE HDR TESTS WITH VESSEL COMPONENT

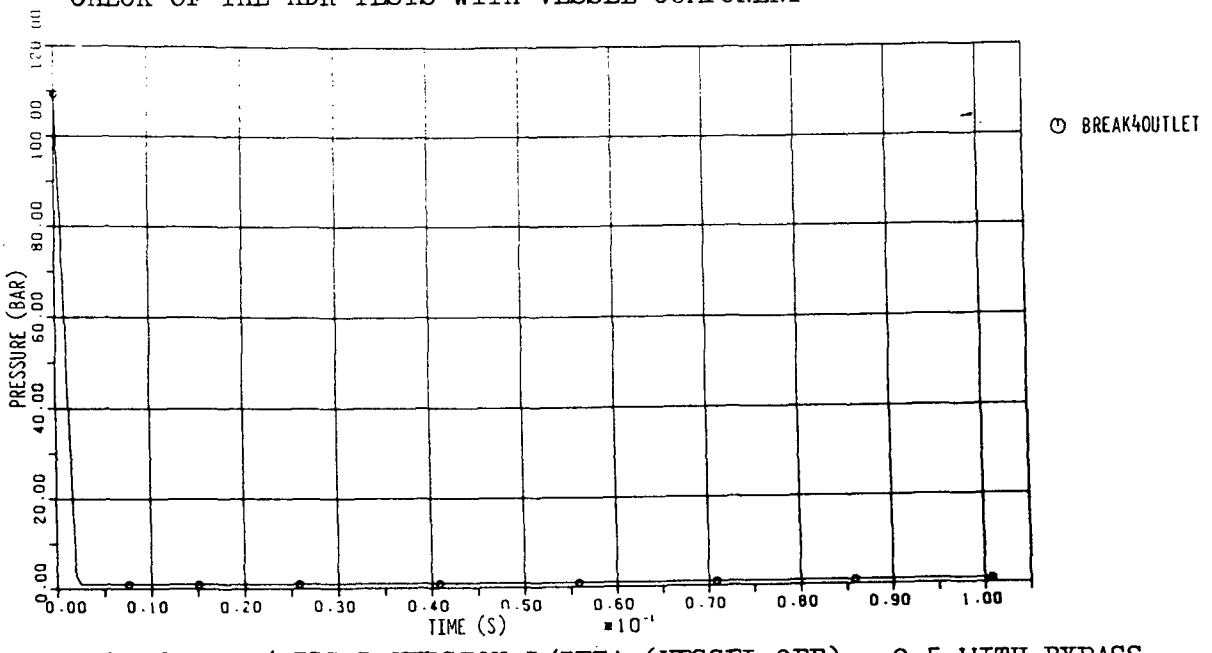

PIPE 2 - SI/VESSEL VERSION 5/ZETA (VESSEL OFF) = 0.5 WITH BYPASS
PRESSURE

KWU TRAC-PD2
EFFECT OF VARIOUS PARAMETERS ON THE OUTFLOW RATE
CHECK OF THE HDR TESTS WITH VESSEL COMPONENT

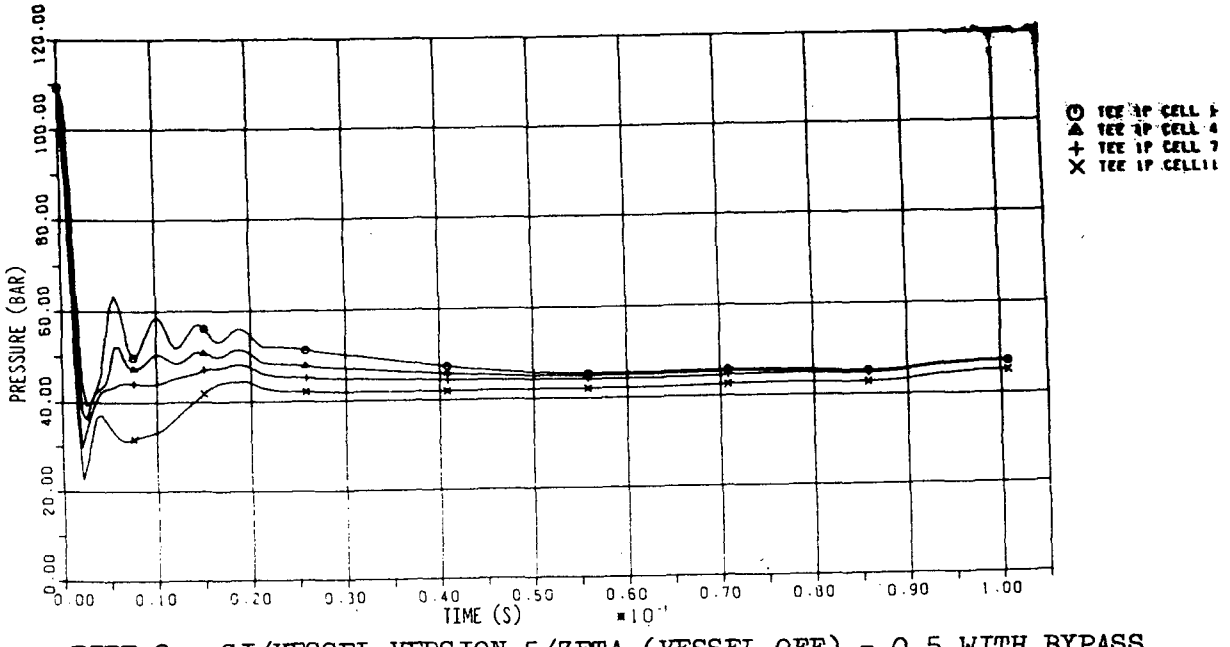

PIPE 2 - SI/VESSEL VERSION 5/ZETA (VESSEL OFF) = 0.5 WITH BYPASS
PRESSURE

Fig. 3.33

KWU TRAC-PD2

EFFECT OF VARIOUS PARAMETERS ON THE OUTFLOW RATE

CHECK OF THE HDR TESTS WITH VESSEL COMPONENT

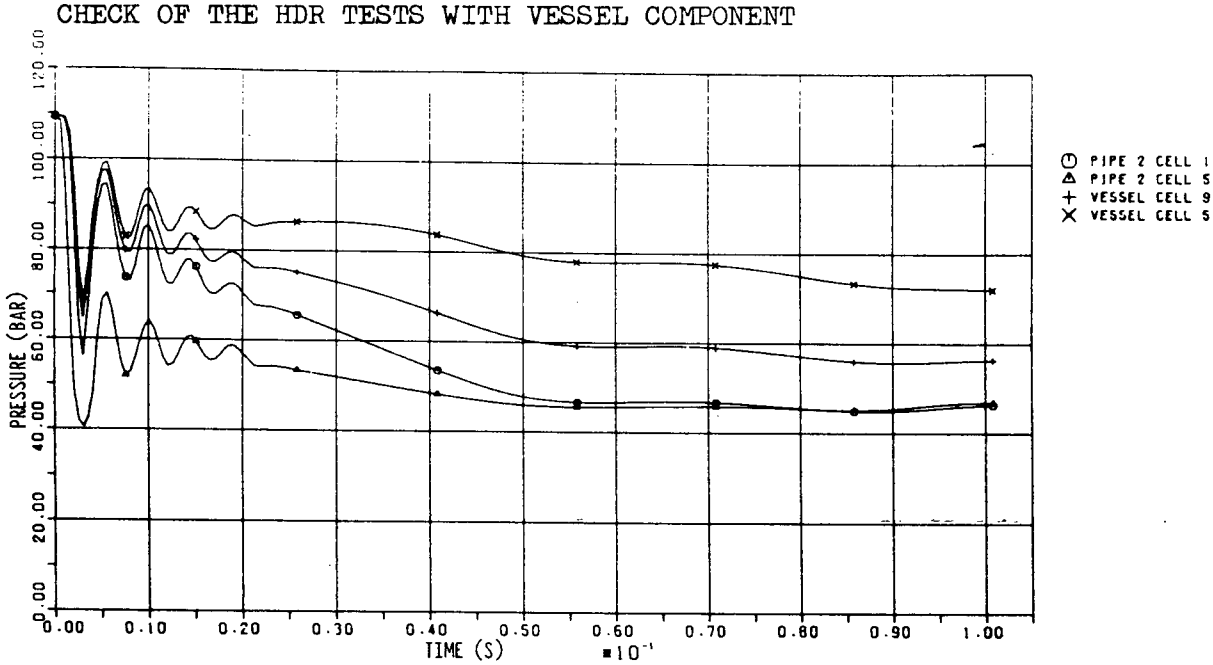

PIPE 2 - SI/VESSEL VERSION 5/ZETA (VESSEL OFF) = 0.5 WITH BYPASS

PRESSURE

KWU TRAC-PD2

EFFECT OF VARIOUS PARAMETERS ON THE OUTFLOW RATE

CHECK OF THE HDR TESTS WITH VESSEL COMPONENT

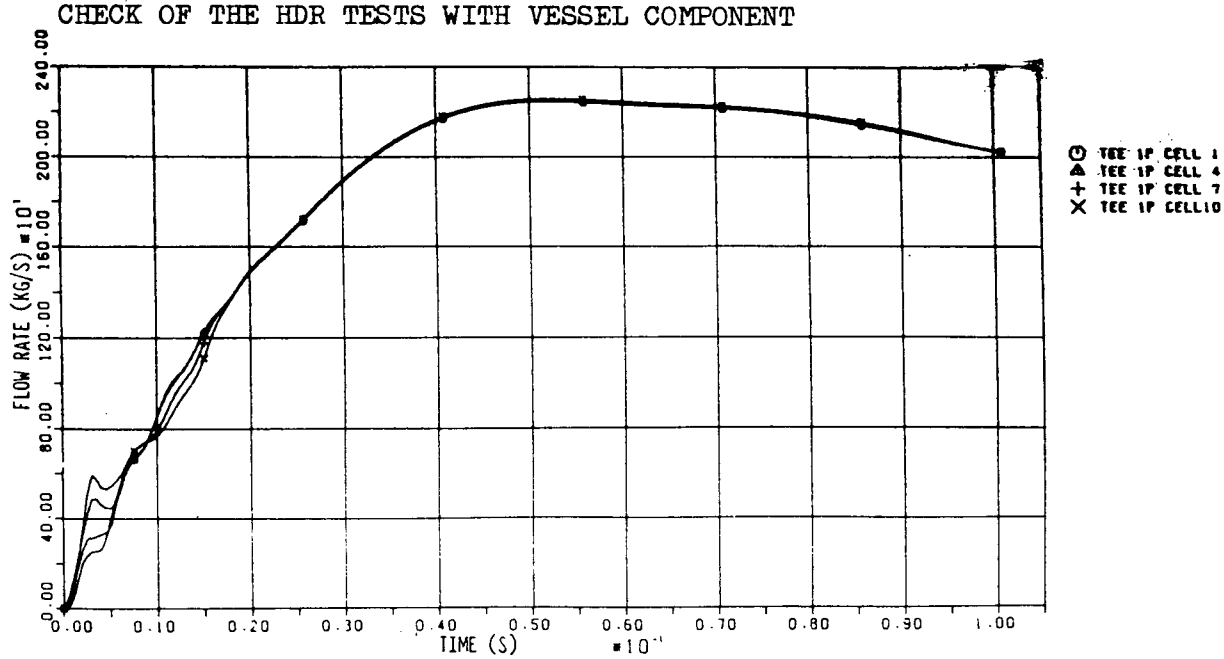

PIPE 2 - SI/VESSEL VERSION 5/ZETA (VESSEL OFF) = 0.5 WITH BYPASS

FLOW RATE

Fig. 3.34

KWU TRAC-PD2

EFFECT OF VARIOUS PARAMETERS ON THE OUTFLOW RATE

CHECK OF THE HDR TESTS WITH VESSEL COMPONENT

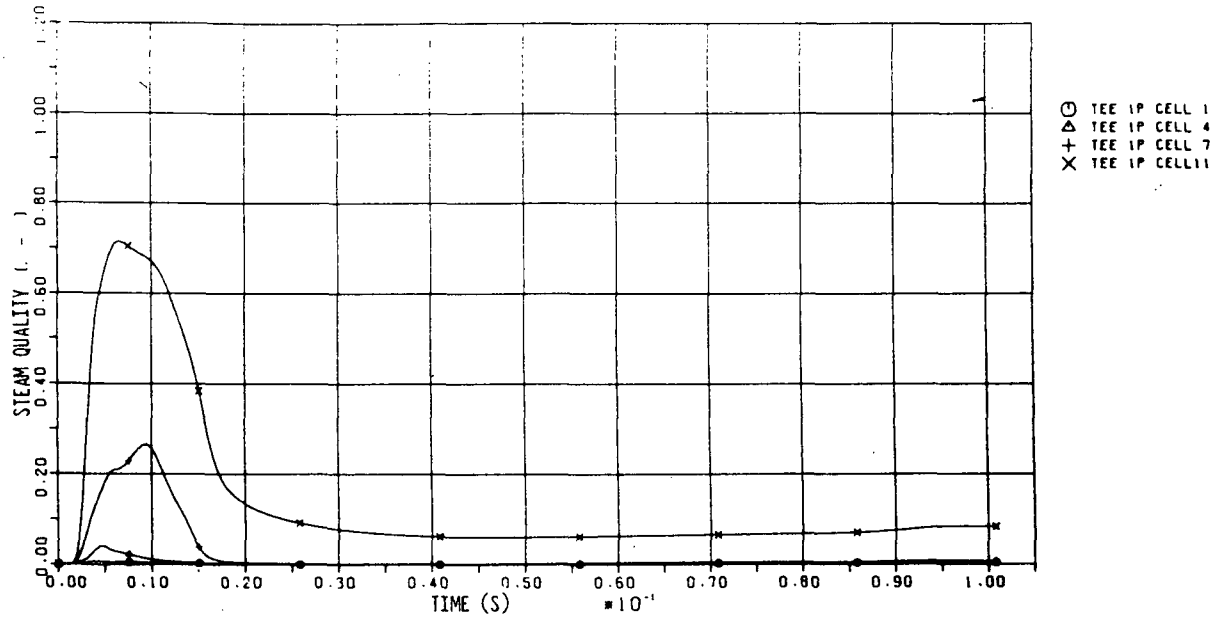

PIPE 2 - SI/VESSEL VERSION 5/ZETA (VESSEL OFF) = 0.5 WITH BYPASS

STEAM QUALITY

KWU TRAC-PD2

EFFECT OF VARIOUS PARAMETERS ON THE OUTFLOW RATE

CHECK OF THE HDR TESTS WITH VESSEL COMPONENT

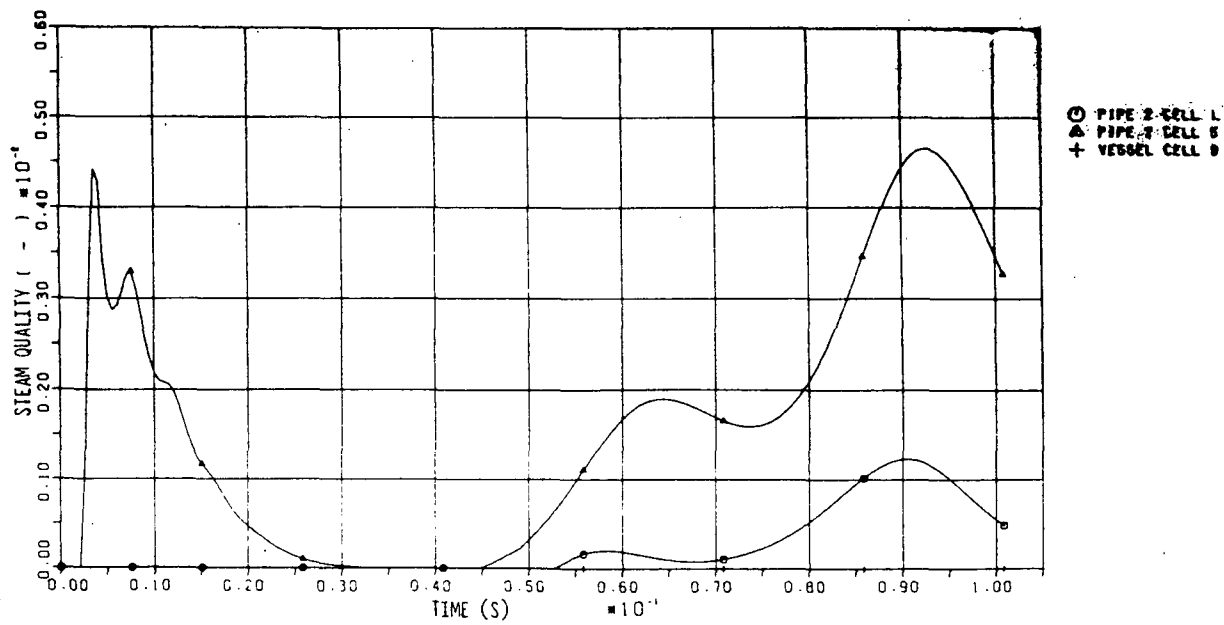

PIPE 2 - SI/VESSEL VERSION 5/ZETA (VESSEL OFF) = 0.5 WITH BYPASS

STEAM QUALITY

Fig. 3.35

3.7 Summary of the Results from HDR Computations

Comparing the pressure and mass flow curves for the various computations plotted in Figs. 3.4 and 3.5, it can be stated with a high degree of certainty that the computations HDR2/3 and 3/3 yield by far the best results. In these two models, the pressure loss due to outflow from the RPV is calculated relatively well, so that very close agreement of the pressure curves as well as the mass flow curves with the measurements is obtained. The HDR2/3 computation is to be given preference over the others here, as the transition from the system state to the ambient state is modelled with physical exactness with the aid of the nozzle, thus forcing the program to take these conditions into account in the calculations.

4 TRAC Components

This chapter contains several hints which have resulted from the work done so far with the TRAC program. However, there are plans to establish a systematic card file of all TRAC users so as to profit from the experience of others.

4.1 TRIP-DATA

When restarting with TRIP cards, the following possibilities exist: Firstly, the TRIP-data cards can again be placed into the input. This leads to the TRIP being reinitialized and restarted. In most cases, however, the TRIP is to be continued with the restart. In this case, a card with a negative number and a blank card must be placed behind the Main Control Cards, so that the TRIP's are read in from the restart file. This is the only way to continue an already started TRIP in the restart mode.

4.2 BREAK

This instruction is based on several test calculations regarding the arrangement of components having a BREAK at the inlet and the outlet.

In this case, so high a pressure difference is obtained that the flow velocities in the components may be far greater than the speed of sound. For this reason, no useful results can be obtained with this calculation; in principle, this arrangement is therefore not advisable. As an alternative, either a large vessel or a large-volume pipe can be employed for the pressure boundary condition.

4.3 TEE

This component allows the modelling of branches in a network.

The following conditions should be fulfilled: A minimum of 2 celles should exist between the junction celles of the side tube and the pipe end of the primary tube, as otherwise numerical instabilities must be expected.

Fig. 4.3.1 shows an obstructed rupture with a TEE; the geometrical data are represented as a function of pipe diameter.

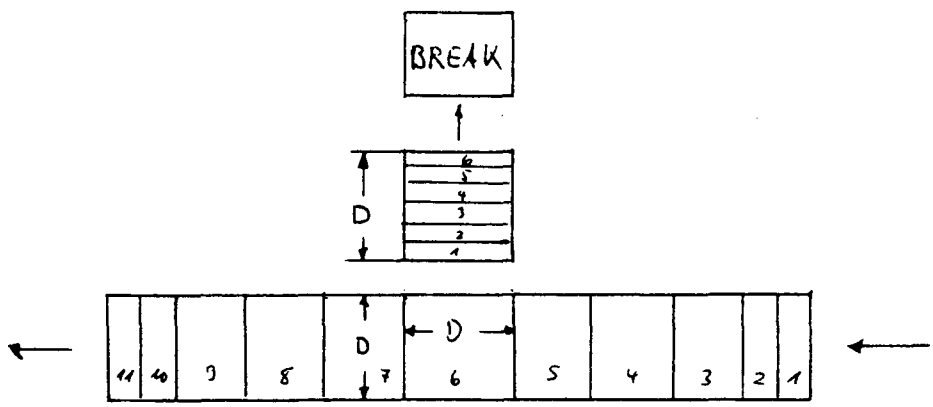

Fig. 4.3.1

This model has generally proven to be reliable. Furthermore, it is important to reduce the celle length in the rupture opening to 1 cm, so as to keep the time interval at the high outflow velocities as small as possible.

4.4 STEAM GENERATOR

The great advantage of the TRAC program is the modular arrangement of complex installations. For this reason, realistic modeling is possible with all components. The only exception is the steam generator, since only the flow in the inner shroud is calculated. The secondary side of the steam generator thus only acts as a heat sink. This fact barely has any relevance for the pressure wave analysis in the primary circuit, so that no negative effect results from this. Nevertheless, an improved steam generator component is to be employed in subsequent TRAC versions. For the steam generator component in this TRAC version, two items of information are required for the feed-water inlet on the secondary side. These are inlet velocity and inlet temperature. The respective values are determined by the following calculating operation:

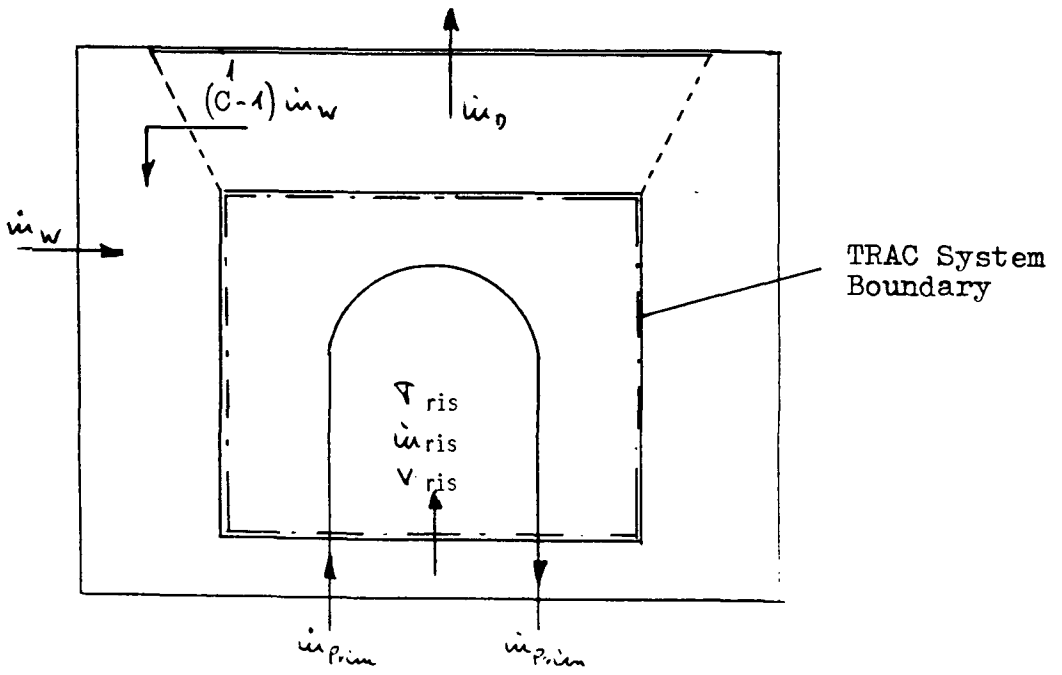

Fig. 4.4

During steady-state operation, $\dot{m}_W = \dot{m}_S$. Hence:

$$\dot{Q}_{SG} = \dot{m}_W \, (h'' - h_W) \qquad \text{Eqn. 4.1}$$

for the steam generator $\hat{=}$ SG

This equation allows us to calculate the inlet water mass flow:

$$\dot{m}_W = \frac{\dot{Q}_{SG}}{h'' - h_W} \qquad \text{Eqn. 4.2}$$

Furthermore, the following equation applies to the riser:

$$\dot{m}_{ris} \, h_{ris} = \dot{m}_W \, h_W + (C - 1) \, \dot{m}_W \, h' \qquad \text{Eqn. 4.3}$$

C $\hat{=}$ number of cycles

With the mass flow rate in the riser given as

$$\dot{m}_{ris} = C \cdot \dot{m}_W \qquad \text{Eqn. 4.4}$$

we obtain the following expression for the enthalpy in the riser:

$$h_{ris} = \frac{\dot{m}_W \, h_W + (C - 1) \, \dot{m}_W \cdot h}{\dot{m}_{ris}} \qquad \text{Eqn. 4.5}$$

With the enthalpy obtained from Equation 4.5 and with the aid of the steam table, the temperature of the water in the riser space and hence the inlet temperature in the FILL on the secondary side of the steam generator can be calculated.

Furthermore, the specific volume at that temperature and system pressure can be determined from the steam table.
Hence it follows from Equation 4.6 that

$$\overset{m^3}{\dot{m}_{ris}} \left| \frac{m^3}{s} \right| = \overset{kg}{\dot{m}_{ris}} \left| \frac{kg}{s} \right| \cdot v \qquad \text{Eqn. 4.6}$$

Given the flow area on the secondary side, the inlet velocity into the riser can be calculated using Equation 4.7:

$$V_{ris} = \frac{\overset{m^3}{\dot{m}}_{ris}}{F_{SG,\ sec}} \qquad \text{Eqn. 4.7}$$

Thus all the input parameters required for the FILL on the secondary side of the steam generator are known.

4.5 VESSEL

As a matter of principle, only one PIPE component may be connected to the VESSEL component. If it should be necessary to initialize a pressure loss in the junction area of the PIPE component by stating a ξ value, the pressure loss is given by Eqn.4.5.1

$$\Delta p = \xi_{PIPE} \cdot \frac{1}{2} \rho v^2_{PIPE,\ End} \qquad \text{Eqn. 4.5.1}$$

The corresponding $FRIC_{PIPE}$ value, which is entered as an input parameter, follows from Equation 4.5.2:

$$FRIC_{PIPE} = \frac{\xi_{PIPE} \cdot H_{D,PIPE}}{(\Delta x_1 + \Delta r_1)} \qquad \text{Eqn. 4.5.2}$$

The individual items of Equation 4.5.2 are depicted in Figure 4.5.1.

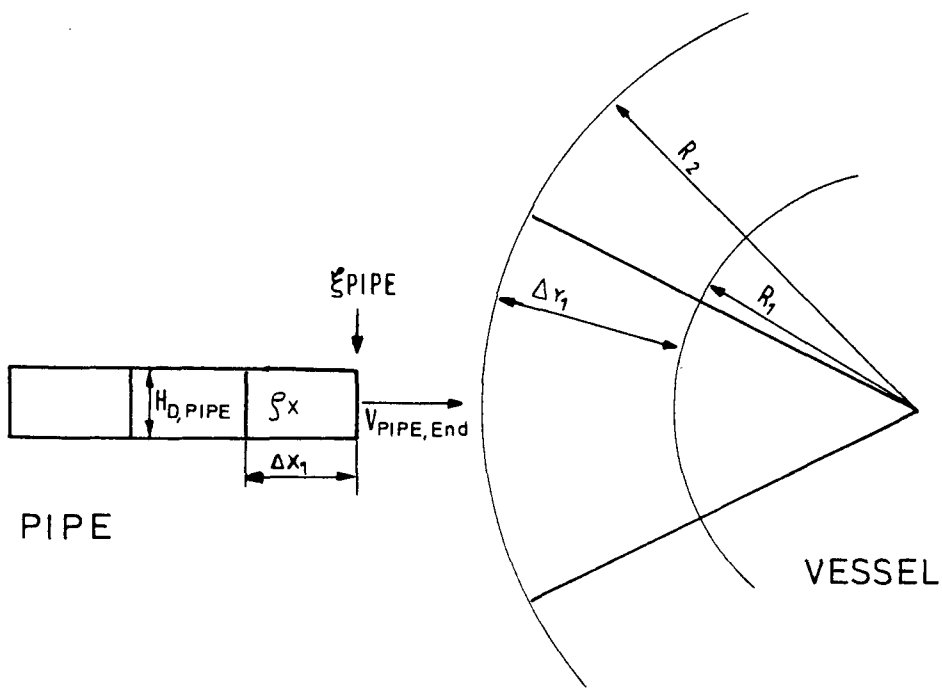

Fig. 4.5.1

Equation 4.5.2 also applies in cases where the PIPE component is connected to one of the inner cylinder surfaces of the vessel component; of course, a different Δr must be employed. Furthermore, it is possible to state ξ values inside the vessel component so as to take for instance the pressure loss upon flowing through a cooling channel into account. In this case, the loss coefficient ξ between two axially superimposed celles is determined and enters as CFZ input. Its numerical value is obtained from Equation 4.5.3:

$$CFZ = \frac{\xi_{AXIAL}}{2h_{1,2}} \qquad \text{Eqn. 4.5.3}$$

with Fig. 4.5.2 explaining the geometric parameter $h_{1,2}$.

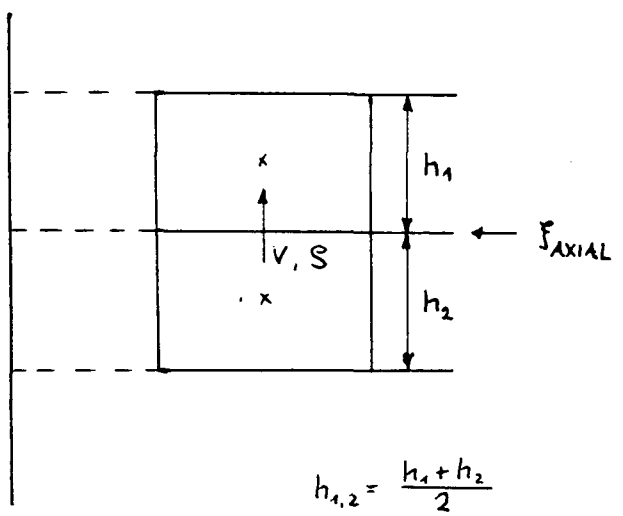

Fig. 4.5.3

If a ξ coefficient is to be inserted between two radial celles, Equation 4.5.4 applies:

$$CFR = \frac{\xi\ RADIAL}{2\Delta r_{1,2}} \qquad \text{Eqn. 4.5.4}$$

$\Delta r_{1,2}$ being given in Fig. 4.5.3.

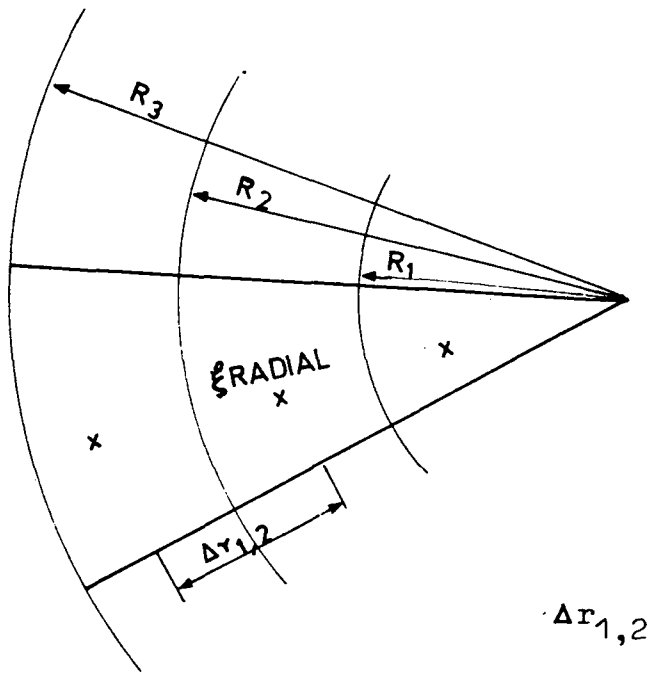

$$\Delta r_{1,2} = \frac{R_3 - R_2}{2} + \frac{R_2 - R_1}{2}$$

Fig. 4.5.3

4.6 PUMP

a

The pump is an important aid for the exact setting of the steady state solution. In complex model configurations, it is the only effective means of influencing the steady state setting. Such a model consists, for example, of a RPV and two closed loops, so that no boundary conditions, neither BREAK's nor FILL's, which determine the state of the installation, exist. The pump determines both the flow rate (i.e. the mixture velocity) and the pressure increase in the loop. The required data are included in the input of the pump.

1. Rated head $/\frac{m^2}{s^2}/$
2. Rated torque /Nm/
3. Rated flow $/\frac{m^3}{s}/$
4. Rated density $/\frac{kg}{m^3}/$
5. Rated pump speed /rpm/

The input information of the rated head consists of the head of the pump multiplied by the gravitational constant g. This can be expressed as follows:

$$RH = H \cdot g \qquad \text{Eqn. 4.6.1}$$

RH = Rated head $/\frac{m^2}{s^2}/$

H = Discharge head of the pump (manufacturer's specification) /m/

g = Gravitational constant $/\frac{m}{s^2}/$

The specific rated speed is given by the following equation:

$$nq = \frac{n \cdot \sqrt{Q}}{H^{3/4}} \qquad \text{Eqn. 4.6.2}$$

nq = Specific rated speed /rpm/

n = Speed /rpm/

H = Head /m/
Q = Flow rate $/\frac{m^3}{s}/$

The relationship between the pressure increase Δp and the rated head is given by the following equation:

Eqn. 4.6.3

p = Pressure increase in the pump /bar/
ϱ = Rated density $/\frac{kg}{m^3}/$

With the aid of the last two equations, 4.6.2 and 4.6.3, the flow rate and the pressure increase in the pump can be set within a certain bandwidth. The procedure is as follows:

The manufacturer's pump data are used in the first mathematical operation for the steady state setting. The specific rated speed nq is given by Equation 4.6.2. The current values for each of the boundary conditions then result from the TRAC computation. If the calculated values do not sufficiently correspond with the intended setting, the input data are corrected in a new computation. If, for example, the flow rate through the pump and the loop is insufficient, the specific rated speed nq is to be increased in accordance with Equation 4.6.2. If furthermore the pressure increase achieved by means of the pump is insufficient, RH (Equation 4.6.1) would also have to be increased. This in turn has an effect on the specific rated speed nq, which therefore must also be changed. This is evidently an iterative process, which must be continued until the values calculated by means of TRAC correspond with the stipulated setting. This method has been tried and tested in practice by setting each of the circuits individually and only then linking the component systems to the RPV.

5 General TRAC Instructions

In the following paragraphs, several facts or items of experience are briefly outlined.

Due to its state equations, the TRAC program can only compute up to a pressure of 190 bar.

Since the error messages are not always very informative and a direct cause may not be indicated, the input should be checked very thoroughly. All errors that hitherto appeared to be inexplicable were input errors.

In order to accomplish an optimal setting of a steady state solution, the components should be tested individually and only then be combined to form a system. This may mean having to put up with more extensive paperwork, since it is not possible to combine several restart files. However, there are plans to provide for such an operation.

In pressure wave analyses, DELT = 1. E-5 should be employed in the calculation during the first 10 to 20 ms in order to accurately calculate the initial phase of the decompression wave.

References

/1/ TRAC-PD2
An Advanced Best Estimate Computer Program for PWR LOCA Analysis, LOS ALAMOS Scientific Laboratory
NUREG/CR-2054

/2/ HDR Versuchsprogramm

/3/ G. Hughes
TRAC-P1A
Inbetriebnahme auf der CYBER 176
KWU-Arbeitsbericht R 11/2113/79

/4/ J. Herterich
Diplomarbeit KWU
Verifikationsrechnungen für das Programmsystem TRAC-PD2 anhand einiger meßtechnisch erfaßter, bzw. analytisch berechenbarer Versuche
Bochum/Erlangen 1981 a

NRC FORM 335 (2-84) NRCM 1102, 3201, 3202

U.S. NUCLEAR REGULATORY COMMISSION

BIBLIOGRAPHIC DATA SHEET

SEE INSTRUCTIONS ON THE REVERSE.

1. REPORT NUMBER (Assigned by TIDC, add Vol. No., if any)

NUREG/IA-0001

2. TITLE AND SUBTITLE

Assessment of TRAC-PD2 Using SUPER CANNON and HDR Experimental Data

3. LEAVE BLANK

4. DATE REPORT COMPLETED

MONTH	YEAR

5. AUTHOR(S)

U. Neumann

6. DATE REPORT ISSUED

MONTH	YEAR
August	1986

7. PERFORMING ORGANIZATION NAME AND MAILING ADDRESS (Include Zip Code)

Kraftwerk Union
Hammerbacherstr. 12+14
Postfach 3220
8520 Erlangen, The Federal Republic of Germany

8. PROJECT/TASK/WORK UNIT NUMBER

9. FIN OR GRANT NUMBER

10. SPONSORING ORGANIZATION NAME AND MAILING ADDRESS (Include Zip Code)

Office of Nuclear Regulatory Research
U.S. Nuclear Regulatory Commission
Washington, DC 20555

11a. TYPE OF REPORT

Technical Report

b. PERIOD COVERED (Inclusive dates)

12. SUPPLEMENTARY NOTES

13. ABSTRACT (200 words or less)

This report assesses the predictive capabilities of the Transient Reactor Analysis Code (TRAC-PD2) using data from the SUPER CANON and HEISS DAMPF REACTOR (HDR) experimental facilities. The report is divided into three parts. Part I is the TRAC-PD2 assessment using the SUPER CANON data. Part II is the TRAC-PD2 assessment using HDR data. Part III provides recommendations for the user using the combined assessment results. In general, it is shown that the TRAC-PD2 predictions were in good agreement with the actual test pressures and mass flow rates for both these tests. TRAC-PD2 provided considerably better results than TRAC-P1A. This was particularly true with regard to sound velocity predictions which play a signifcant role whenever the speed of pressure relief waves must be determined.

14. DOCUMENT ANALYSIS – a. KEYWORDS/DESCRIPTORS

TRAC-PD2, Super Canon, and HDR

b. IDENTIFIERS/OPEN-ENDED TERMS

15. AVAILABILITY STATEMENT

Unlimited

16. SECURITY CLASSIFICATION

(This page) Unclassified

(This report) Unclassified

17. NUMBER OF PAGES

18. PRICE

UNITED STATES
NUCLEAR REGULATORY COMMISSION
WASHINGTON, D.C. 20555

OFFICIAL BUSINESS
PENALTY FOR PRIVATE USE, $300

SPECIAL FOURTH-CLASS RATE
POSTAGE & FEES PAID
USNRC
WASH. D.C.
PERMIT No. G-67